Effects of Environment on Creep Behavior of Two Oxide-Oxide Ceramic Matrix Composites at 1200°C

THESIS

Pavlos A. Koutsoukos, Captain, Hellenic Air Force

AFIT/GAE/ENY/06-S05 GAE 06S

DEPARTMENT OF THE AIR FORCE
AIR UNIVERSITY

AIR FORCE INSTITUTE OF TECHNOLOGY

Wright-Patterson Air Force Base, Ohio

The views expressed in this thesis are those of the author and do not reflect the official policy or position of the United States Air Force, Department of Defense, or the United States Government.

AFIT/GAE/ENY/06-S05

Effects of Environment on Creep Behavior of Two Oxide-Oxide Ceramic Matrix Composites at 1200°C

THESIS

Presented to the Faculty

Department of Aeronautics and Astronautics

Graduate School of Engineering and Management

Air Force Institute of Technology

Air University

Air Education and Training Command

In Partial Fulfillment of the Requirements for the

Degree of Master of Science in Aeronautical Engineering

Pavlos A. Koutsoukos

Captain, HAF

September 2006

AFIT/GAE/ENY/06-S05

Effects of Environment on Creep Behavior of Two Oxide-Oxide Ceramic Matrix Composites at 1200°C

Pavlos A. Koutsoukos
Captain, HAF

Approved:

Dr. Marina Ruggles-Wrenn (Chair)	date
Dr. Som Soni (Member)	date
Dr. Robert Canfield (Member)	date

AFIT/GAE/ENY/06-S05

Abstract

Aerospace engine components require structural materials that exhibit superior long-term mechanical properties under severe environmental conditions, such as ultra-high temperature, high pressure, or water vapor. Ceramic-matrix composites (CMCs), capable of maintaining excellent strength and fracture toughness at high temperatures continue to attract attention as candidate materials for aerospace turbine engine applications. Advanced reusable space launch vehicles will likely incorporate fiber-reinforced CMCs in critical propulsion components. In these applications, CMCs will be subjected to mechanical loading in complex environments. Before ceramic matrix composites can be widely used in high-temperature aerospace engine applications, their structural integrity and long-term environmental durability must be assured. Characterization of the mechanical behavior of the candidate CMCs in relevant engine environments is required for design of structural components.

Previous studies by the advisor and graduate students examined creep behavior of the Nextel720/Alumina CMC in air and in 100% steam environments at 1200 and 1330°C. Results showed that while this oxide/oxide system exhibits an exceptionally high fatigue limit at 1200°C it also experiences substantial strain accumulation under sustained loading conditions. Furthermore, these earlier investigations revealed a significant degrading effect of 100%-steam environment on material performance under both static and cyclic loadings. The present effort will investigate creep rupture behavior of

Nextel720/Alumina composite in the inert gas environment. In addition, creep rupture behavior of Nextel720/Aluminosilicate CMC will be investigated in both inert gas and in 100% steam environments. Combined with existing data, results of this research will fully reveal effects of progressively more oxidizing environment on creep resistance of these CMCs. In addition, degradation of Nextel720 fibers under load in oxidizing environments will be assessed. The study will follow a systematic plan. Baseline tensile tests will be performed to verify the at-temperature basic properties and to guide selection of the creep stress levels. Creep-rupture tests will be carried out at different stress levels at 1200°C. In order to examine combined effects of temperature and exposure to oxidizing environment on the creep response, creep-rupture tests will be performed in the inert gas and in 100% steam environments. For selected creep stress levels, creep tests in laboratory air will be performed as well. As a result of this effort creep-rupture curves, as well as families of creep curves will be established. Degradation of creep resistance due to increasing moisture exposure will be assessed. Composite microstructure, as well as damage and failure mechanisms will be examined. The results will establish the boundaries of mechanical behavior and determine the suitability as well as limitations of these materials for use in aerospace applications. The test results will contribute to the basis for future material development and processing.

Acknowledgments

I would like to thank my faculty advisor, Dr. Marina Ruggles-Wrenn, for her support , her guidance and help throughout my work. I would like also to thank Dr. Seungsu Baek for sharing his experience and for helping me with the microscopy examinations. Lastly I would like to thank my readers Dr. Som Soni and Dr. Robert Canfield and the sponsors of my thesis research Dr. Ruth Sikorski and Dr. Joseph Zelina.

Pavlos Koutsoukos

Table of Contents

List of Figures

List of Tables

EFFECTS OF ENVIRONMENT ON CREEP BEHAVIOR OF TWO OXIDE-OXIDE CERAMIC MATRIX COMPOSITES AT 1200°C

I. Introduction

Several thousands of years have passed since the Iron Age and still even in nowadays the use of metals and especially of steel and aluminum has a dominant role in high performance applications.

But beginning from the second half of the 20th century, a new trend is taking over and this trend is the usage of composite materials. “The first fiberglass boat was made in 1942, accompanied by the use of reinforced plastics in aircraft and electrical components. Filament winding was invented in 1946 followed by missile applications in the 1950s. The first boron and high-strength carbon fibers were introduced in the early 1960s, followed by applications of advanced composites to aircraft components in 1968” [4:2]

The research for developing composite materials was driven and still is by the need for improved performance in applications such as aerospace, automotive, armor compared to the usage of metals.

About 40% of the structural weight of Eurofighter is carbon fiber reinforced composite material [6]. Boeing is using composite materials weighting about 20% of the structural weight of the 777 aircraft while the upcoming 787 is going to consist by about 50% from composites.

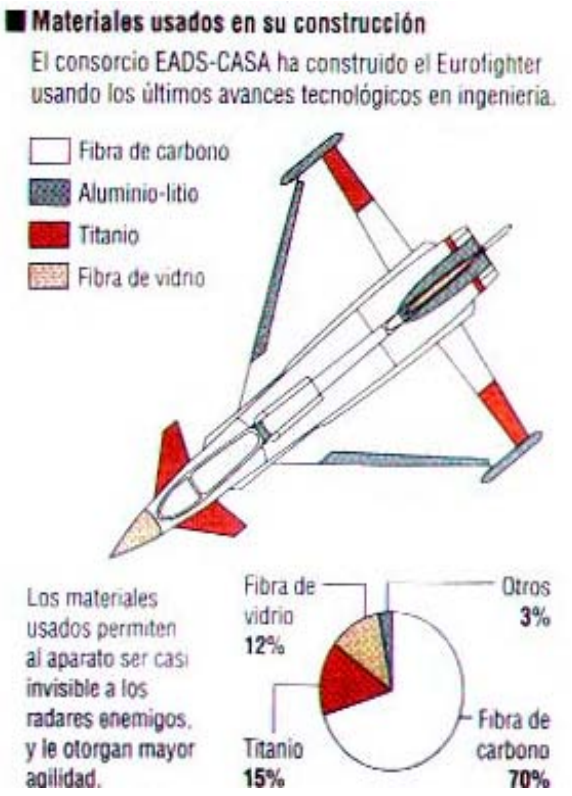

Figure 1. Materials used in Eurofighter [7]

Recent efforts [7,8] investigated the mechanical behavior of the N720/alumina $0/90^0$ and $+45/-45^0$ composite at 1200°C in laboratory air and steam environments. Harlan [7] reported on the effect of air and steam on creep resistance for a $0/90^0$, while Siegert [8] reported on the effect of environment on creep resistance for a $+45/-45^0$. The purpose of the present research is to investigate the effect of environment on creep resistance on the N720/aluminosilicate $0/90^0$ layered CMC and of argon environment on the N720/alumina $0/90^0$ layered.

II. Background

2.1 Ceramic Matrix Composites

"A structural composite is a material system consisting of two or more phases on a macroscopic scale, whose mechanical performance and properties are designed to be superior to those of the constituent materials acting independently"[4:1]

In particular interest for airspace applications is ceramic matrix composites. Like other Olympic Games athletes, aerospace companies are continuously competing for "Citius, Altius, Fortious"- faster, higher, stronger, and ceramic matrix composites seems to be the perfect "athletes". Ceramics have some very desirable properties like high-stiffness, high-strength and low density as seen in figure 2, for use in both military and civilian aircraft.

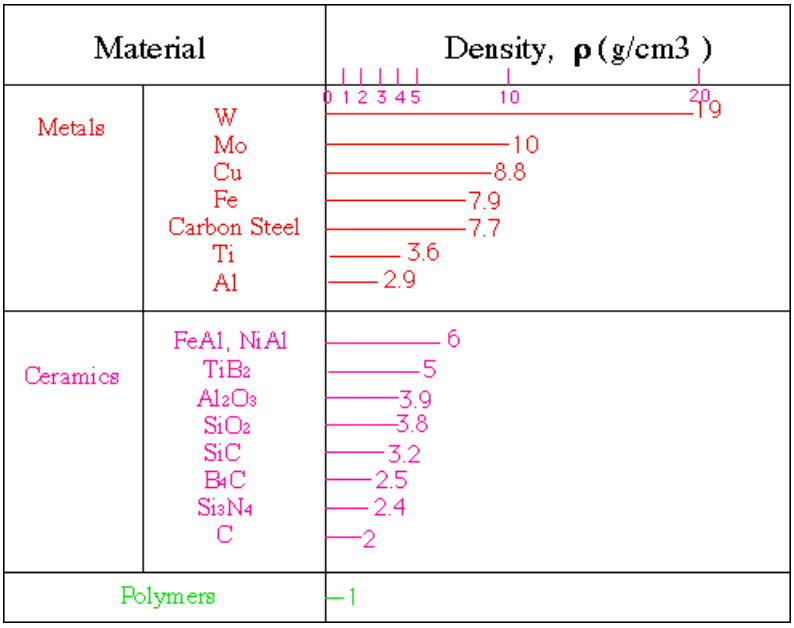

Figure 2. Density properties of important materials

But it is their high temperature strength that made ceramic materials candidates for use in the aerospace industry, since they are the only material that can perform in temperatures above 1000^0C.

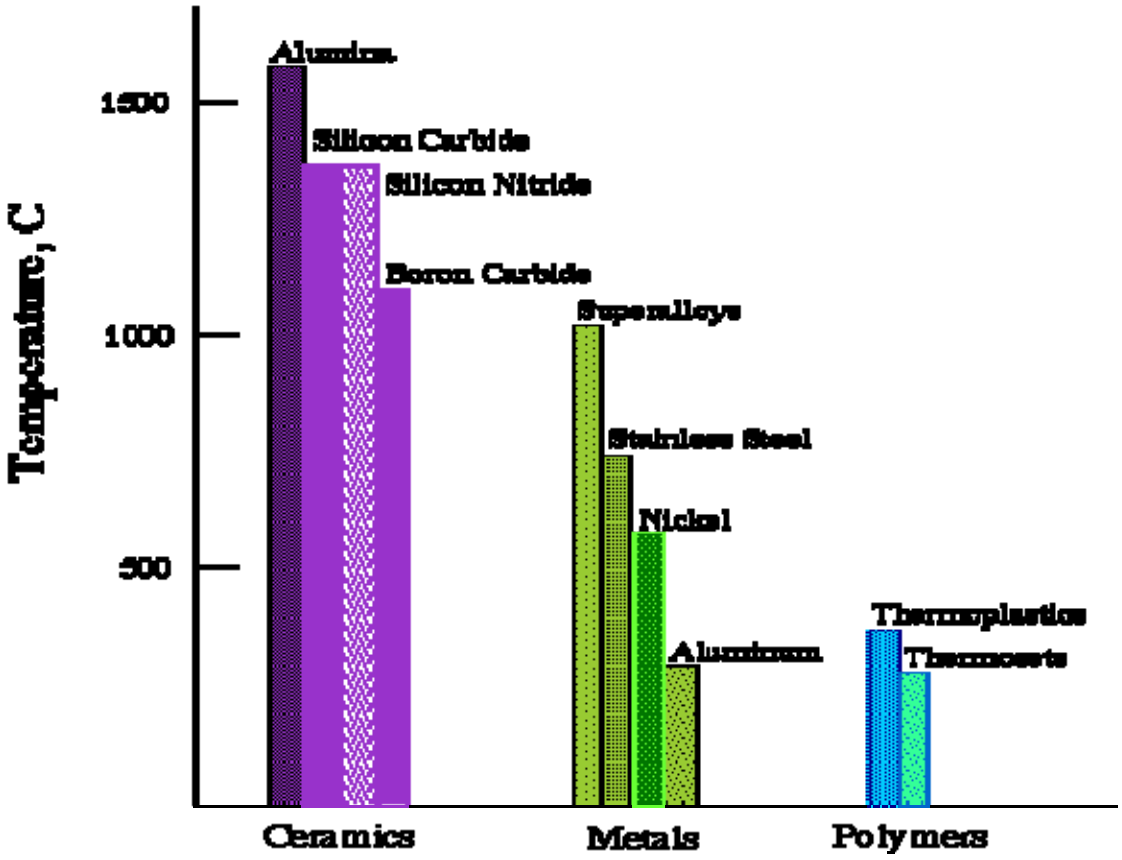

Figure 3. Maximum Operating Temperatures of Important Materials

The downside though of ceramics is that they are brittle, so unusable in the aerospace environment. That is the gap that Ceramic matrix composites were manufactured to fill. To use the advantages of ceramics, without their disadvantage -that is their brittleness.

Ceramic matrix composites (CMCs) combine reinforcing ceramic phases with a ceramic matrix to create materials with new and superior properties. In ceramic matrix composites, the primary goal of the ceramic reinforcement is to provide toughness to an otherwise brittle ceramic matrix [5]. Figure 4 illustrates the stress vs. strain curve of a CMC vs. a monolithic ceramic.

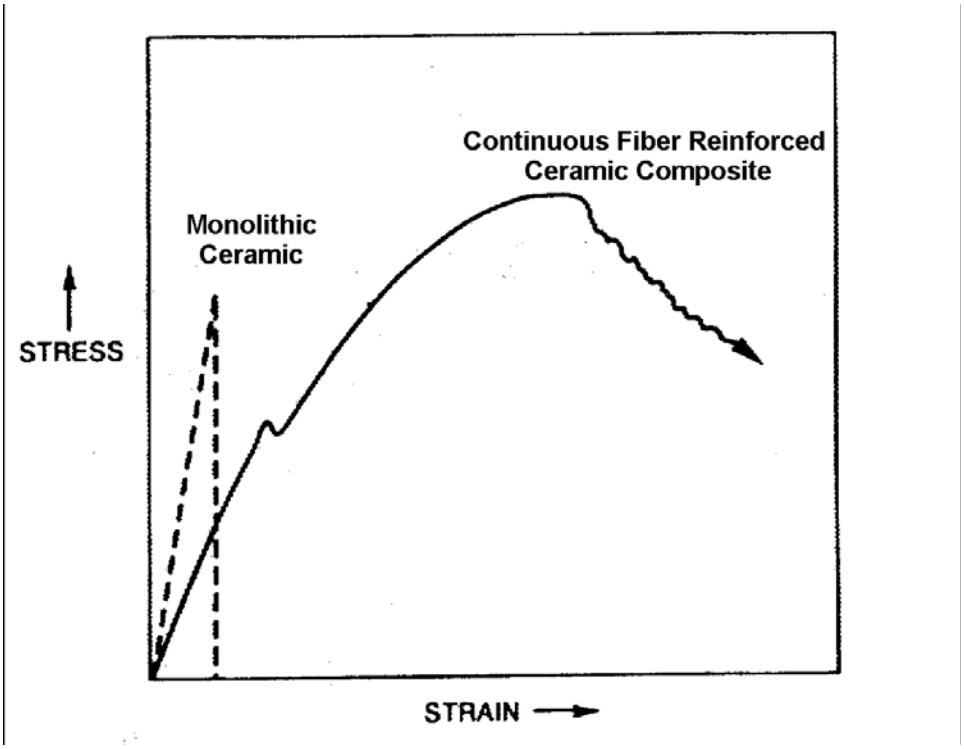

Figure 4. CMC and Monolithic Ceramics Stress vs. Strain Chart

The desirable characteristics of CMCs include high-temperature stability, high thermal shock resistance, high hardness, high corrosion resistance and light weight.

2.2. Matrix

The role of the matrix is to provide support for the fibers, to protect them from the environment and to transfer local stress from one fiber to another

Depending on the category of the matrix, a CMC can be categorized as a non-oxide or oxide. “Common oxide matrices include alumina, silica, mullite, and barium aluminosilicate. Of these alumina and mullite have been the most widely used because of their in service thermal and chemical stability and their compatibility with common reinforcements” [4].

2.3.Fibers

Fibers in a composite material play the role of the reinforcement. They determine the composites stiffness and strength.

Early ceramic composites used discontinuous fibers like whiskers, platelets and particulates. Nowadays continuous fibers are the trend as a composite reinforcement since they provide better properties.

Another characterization of fibers is whether they are from oxide or non-oxide material. Oxide fibers are usually alumina (Al_2O_3) or mullite ($3\ Al_2O_3\ \ 2SiO_2$). Non-oxide fibers are usually silicon carbide (SiC).

2.4. Oxide-oxide CMC

The main purpose for researching oxide/oxide composites is their resistance to degradation when the material is used in applications were oxidizing environments like steam or air and high temperatures exists. Environments like these described are met in aerospace applications, so this is the reason why oxide/oxide CMC's are of particular interest.

Non-oxide CMC's have relatively highest UTS than oxide CMC's but when used in oxidizing environments their mechanical properties degrade severely.

In particular interest in an oxide/oxide CMC is the interface between the matrix and the fiber. As described above, the purpose of the matrix is to matrix is to provide support for the fibers, to protect them from the environment and to transfer local stress from one fiber to another. In the early days of oxide/oxide CMC's in order for the cracks to propagate around the fibers, the fibers were coated in order to create a waek matrix/fiber interface. This method had disadvantages as the coating was not stable in oxidizing environments and the fiber coating process added cost and complexity [11]. The new method that was proposed was the replacement of the weak matrix/fiber interface with a stronger one. The difference in this new suggestion has to do with the nature of the matrix which now has pores in order to help the propagation of cracks. "Studies have shown that a matrix with a high porosity (≈35-40%) exhibits extensive fiber pullout after failure, indicative of random fiber failure, resulting in high strength and fracture toughness. When the matrix density was increased, fiber failures became more correlated, producing more planar fracture surfaces resulting in a dramatic loss in strength and fracture toughness" [12]

III. Material and Test Specimen

3.1. Material description

The Composite Matrix Materials used in this research consisted of Nextel 720 fibers inside an aluminosilicate matrix in the case of N720/AS specimens and inside an alumina matrix for the N720/A specimen.

The fiber used in the material was manufactured by the Minnesota Mining and Manufacturing Company (3M). The fiber consists of 85% alumina (Al_2O_3) and 15% silica (SiO_2) in the form of mullite. The mechanical properties of the fiber can be seen at figure 5[1] “Nextel 720 fiber was developed for load-bearing applications at temperatures in excess of 1000^0C.The superior high temperature creep performance of N720 fiber results from a high content of mullite, which has much better creep resistance than alumina. Additionally, Nextel 720 fiber consists of 0.5 μm globular grains of mullite; this is five times larger than grains in Nextel 610 fiber. In fine-grained oxides, creep rate is inversely proportional to grain size, so the larger grain size of Nextel 720 fiber reduces creep. Lastly, the presence of acicular and globular grains of mullite and alumina reduces grain boundary sliding. However, these microstructural factors that improve creep represent a tradeoff with respect to strength. High strength fibers should preferably have a fine and uniform grain size and high contents of alumina, which has higher fracture toughness than mullite.” [7]

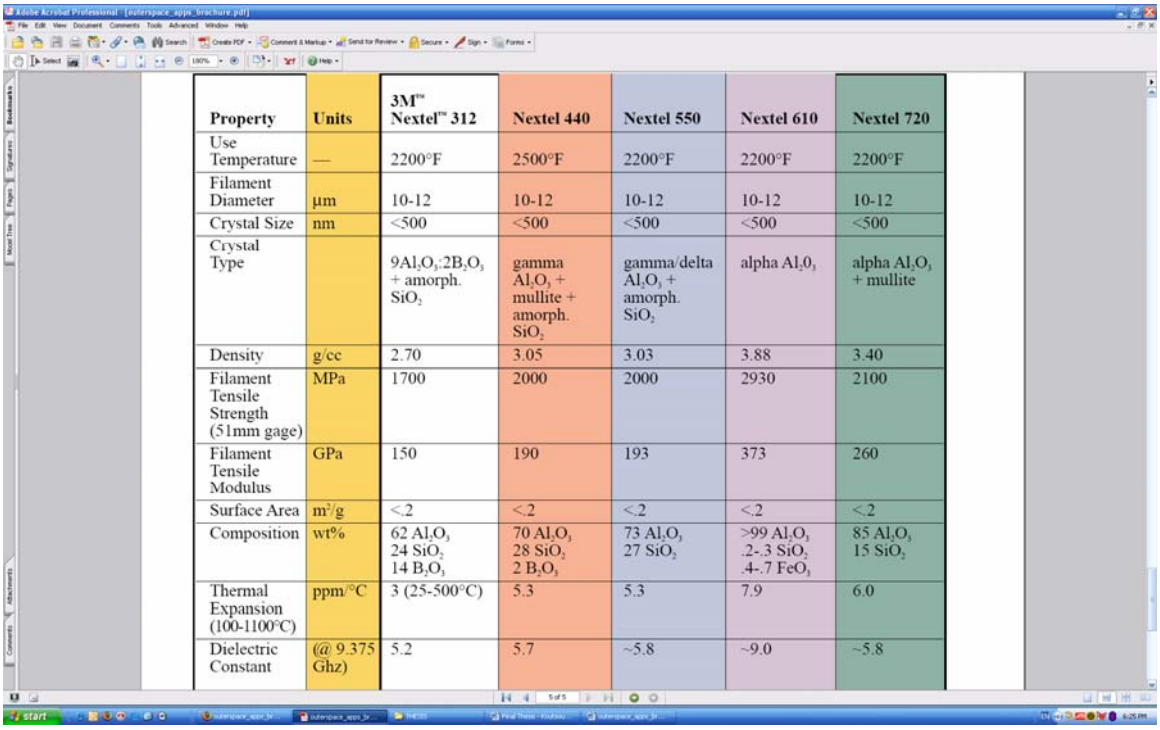

Property	Units	3M™ Nextel™ 312	Nextel 440	Nextel 550	Nextel 610	Nextel 720
Use Temperature	—	2200°F	2500°F	2200°F	2200°F	2200°F
Filament Diameter	µm	10-12	10-12	10-12	10-12	10-12
Crystal Size	nm	<500	<500	<500	<500	<500
Crystal Type		$9Al_2O_3{:}2B_2O_3$ + amorph. SiO_2	gamma Al_2O_3 + mullite + amorph. SiO_2	gamma/delta Al_2O_3 + amorph. SiO_2	alpha Al_2O_3	alpha Al_2O_3 + mullite
Density	g/cc	2.70	3.05	3.03	3.88	3.40
Filament Tensile Strength (51mm gage)	MPa	1700	2000	2000	2930	2100
Filament Tensile Modulus	GPa	150	190	193	373	260
Surface Area	m^2/g	<.2	<.2	<.2	<.2	<.2
Composition	wt%	62 Al_2O_3 24 SiO_2 14 B_2O_3	70 Al_2O_3 28 SiO_2 2 B_2O_3	73 Al_2O_3 27 SiO_2	>99 Al_2O_3 .2-.3 SiO_2 .4-.7 FeO_3	85 Al_2O_3 15 SiO_2
Thermal Expansion (100-1100°C)	ppm/°C	3 (25-500°C)	5.3	5.3	7.9	6.0
Dielectric Constant	(@ 9.375 Ghz)	5.2	5.7	~5.8	~9.0	~5.8

Figure 5. N720 Fiber Properties

The matrix materials used in the specimens - that is the aluminosilicate and the alumina matrix - of this research as well as the CMC's were manufactured by Composite Optics Inc (COI). The composite panel consisted of 12 woven in eight harness satin weave (8HSW) N720 $0^0/90^0$ layers infiltrated into the matrix in a sol-gel process. Then under low temperature and low pressure, the composite was left to dry with a vacuum bag technique. After that CMC was pressure sintered.

Figure 6 show the surface microstructure of the as received N720/AS material. $0^0/90^0$ layers are clearly observable as well as micro- cracks in the matrix that are formed during the manufacturing process.

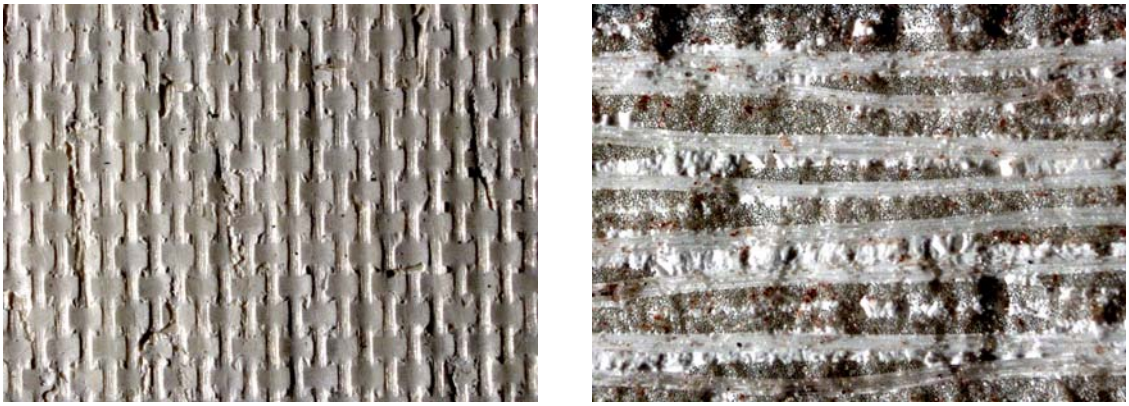

Figure 6. Surface Microstructure of as received Material N720/AS

3.2. Specimen Description

The materials were received in two 12” X 12” panels and they were cut using a water-jet machine in dog-bone specimens. That shape was chosen in order to weaken the middle portion of the specimens so that the failure would occur in that gage section. As can be seen at figure 7 the total length of the specimens were 152mm, the total width at the grip section 16mm, the gage section width 10mm and the specimen thickness 2.6mm. Figure 8 depicts an actual specimen.

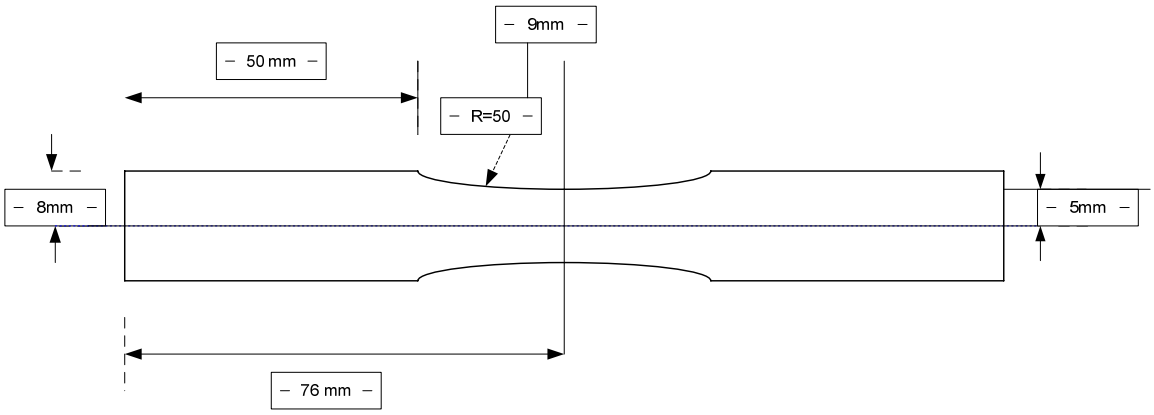

Figure 7. Dog-bone specimen

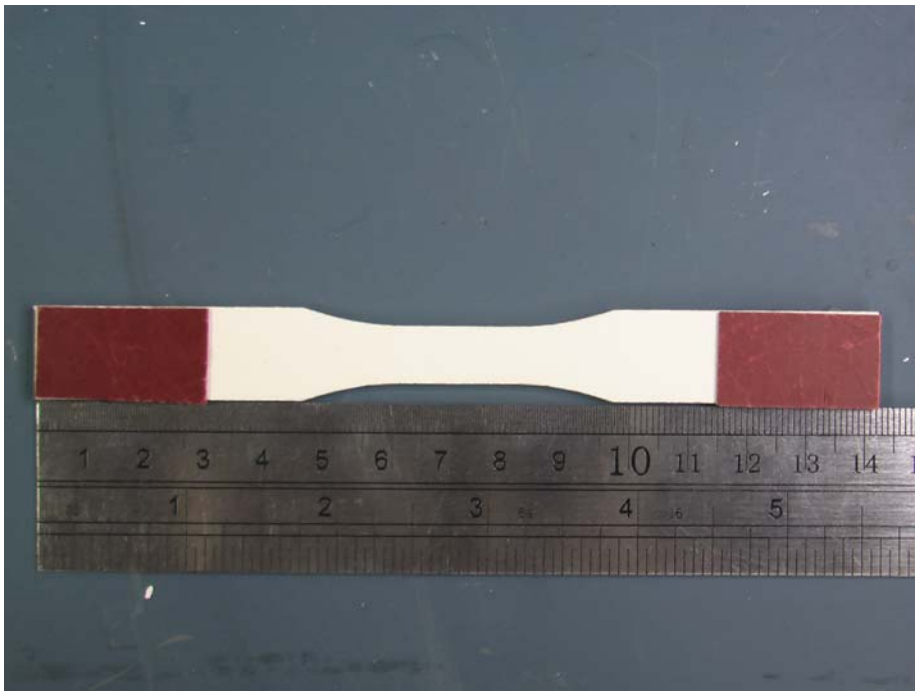

Figure 8. Dog- bone specimen with tabs

IV. Experimental Arrangements and Testing

4.1. Mechanical Testing

For the mechanical testing of the specimens two MTS (Material Test Systems) Corporations servo hydraulic machines (model 810) were used as seen in figure 9. One of those had a load capacity of 5.5 kip and on that machine the testing in air and steam environment was conducted while the other had a load capacity of 22 kip and the testing in argon environment was conducted.

Figure 9. MTS hydraulic testing machine

In order to secure the specimens in their place a grip force of about 8Mpa was used in the first machine whereas the later required a grip force of about 3 Mpa. The grips were MTS's model 647 water cooled hydraulic wedge with a surfalloy surface used to prevent slipping. For the water cooling a Neslab model HX-75 chiller was used, for circulating through the grips cold water in order to maintain a safe temperature.

For the measurement of strain a MTS uni-axial high-temperature extensometer (model 632.53E-14) as seen in figure 10 was used. The extensometer features two 6-inch alumina rods that are used for contacting the specimen with and at their end a spring was used for keeping them in contact with the specimen.

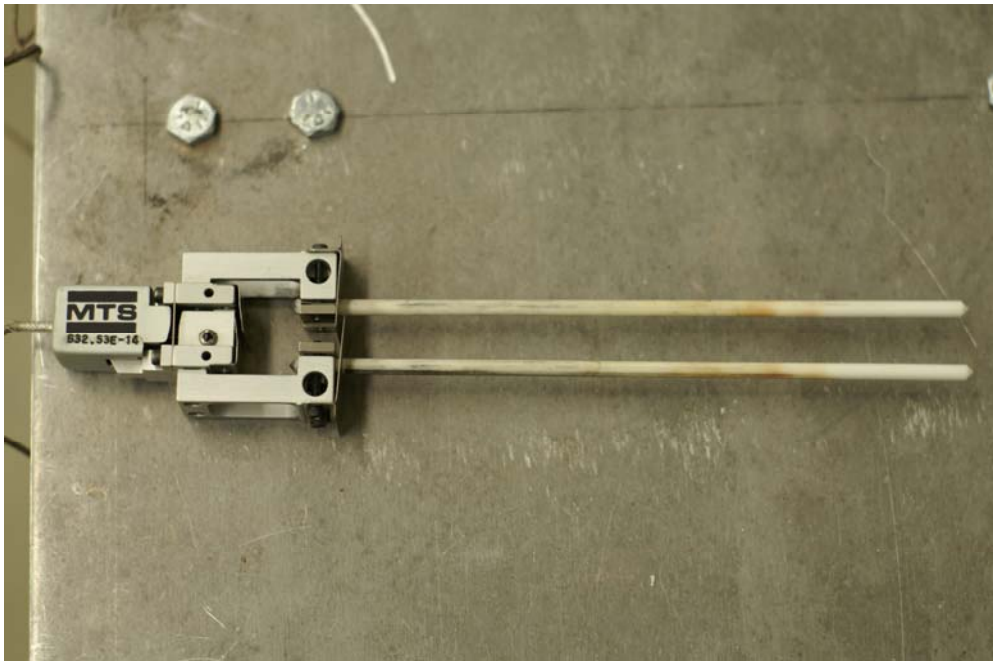

Figure 10. MTS uni-axial high-temperature extensometer

For the control of the machine, testing and data acquisition a MTS Test Star II controller was used in conjunction with MPT (Multi Purpose TestWare) which was used to program, execute and control the tests.

4.2.Environmental Equipment

The environmental equipment used for the testing was a furnace, an external temperature controller, a steam generator machine and a system for creating an argon-only environment.

The furnaces that were used were a two -zone Amteco Hot-Rail Furnace system for the 5kip machine and a two-zone MTS 653 High Temperature Furnace for the 22 kip machine. Both consisted of two chambers which were sliding on a rail towards each other

in order to enclose the specimen. Inside each chamber silicon carbide heating elements were positioned at the top and the bottom in order to achieve the required temperatures. Alumina pieces were fitted inside each one, leaving enough room just for the specimen in order to prevent heat loss. To achieve temperature monitor and control an S-type thermocouple was placed inside each chamber connected to the other end with a MTS model 409.83B temperature controller as seen in figure 11.

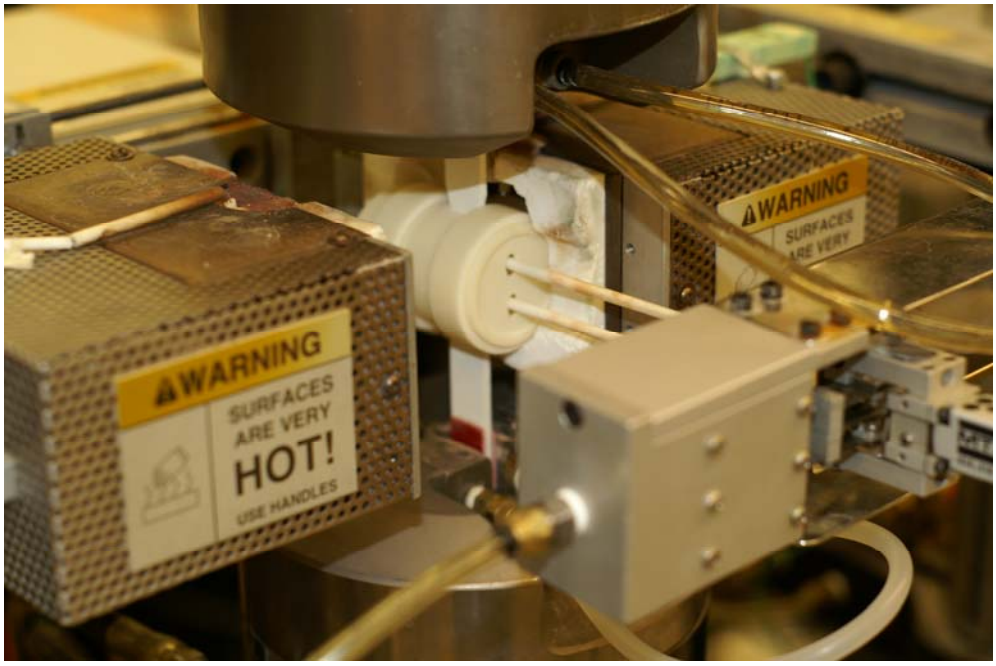

Figure 11. Amteco Hot-Rail Furnace

In order to create the argon and steam environment the specimens were enclosed in a cylindrical alumina susceptor. The susceptor had only two small holes in the front for the extensometer rods and one in the back were the steam or argon alumina provider tube was fitted. In that way air was forced out thus leaving the area surrounding the specimen in pure argon or steam environment.

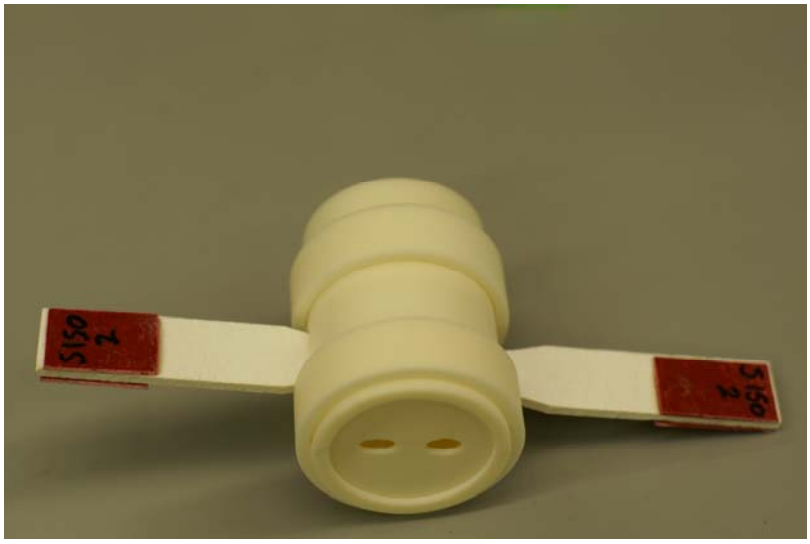

Figure 12. Alumina susceptor

The argon environment was created by using a high pressurized tank filled with high purity argon and an Omega Mass Flow Controller which was used in order to control the amount of argon that would flow into the susceptor. For the specific tests the flow was 41mL/min.

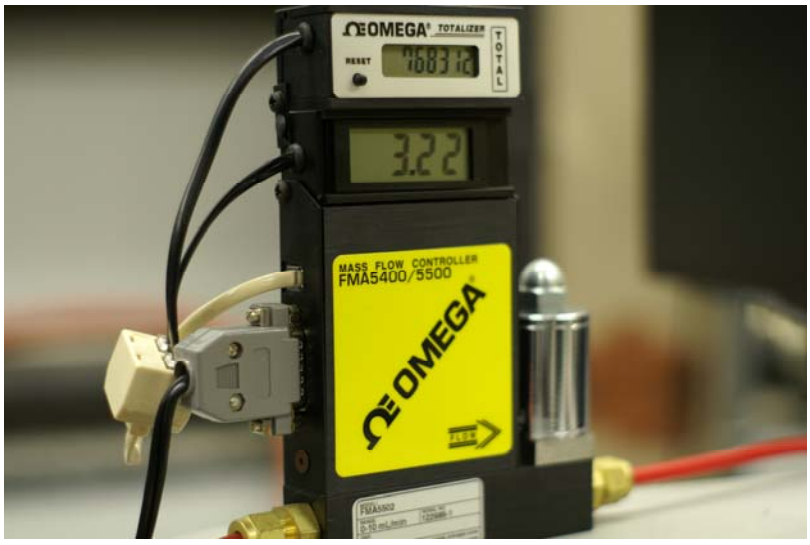

Figure 13. Omega Mass Flow Controller

The steam environment was created by using an AMTECO HRFS Steam Generator System. In the same manner after the steam was created in the generator by using de-ionized water, it was fed into the susceptor at a flow of 30mL/h.

Figure 14. MTS uni-axial high-temperature extensometer

4.3. Imaging Devices

For the analysis of the microstructure of the specimens optical microscopy as well as Scanning Electron Microscope (SEM) was used. Optical observations were made possible using a Zeiss Stemi SV II optical microscope. The optical microscope is shown in figure 15.

For higher magnification images a FEI FP 2011/11 Quanta 200 HV Scanning Electron Microscope which is shown in figure 16 was used.

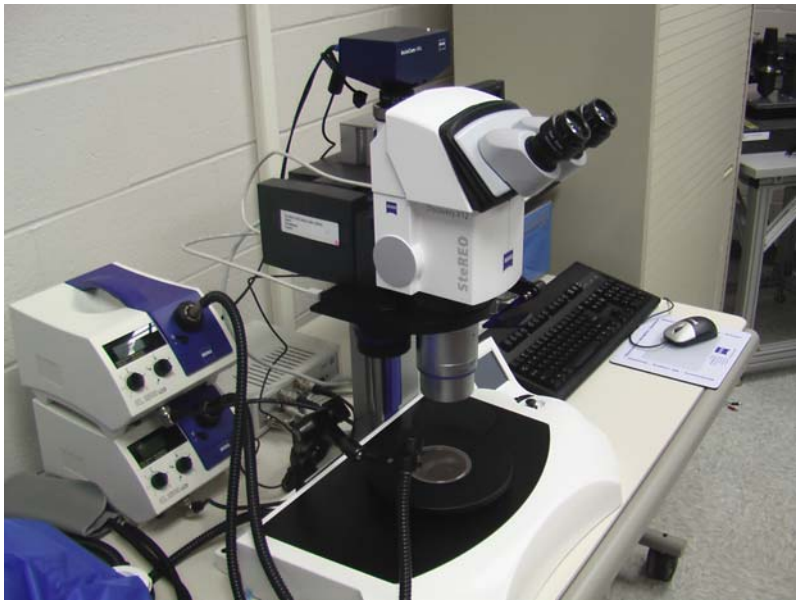

Figure 15. Zeiss Stemi SV II optical microscope

Figure 16. FEI FP 2011/11 Quanta 200 HV Scanning Electron Microscope

4.4.Test Procedures

4.4.1.Specimen Preparation

Prior to testing all specimens were cleaned into an ultrasonic cleaner with de-ionized water for 20 minutes. After that they were placed into an alcohol bath for another 20 minutes. Finally they were placed for 1 hour into an oven in order to dry.

After the cleaning, the width and the thickness of all specimens was measured at the cross section with a Mitutoyo Corporation Digital Micrometer- model NTD 12-6". The measurements were used to calculate the cross sectional area for each specimen.

In order to prevent damage and slippage from the hydraulic grips, fiberglass tabs were bonded at both sides on every specimen at the grip section, using M-Bond 200 adhesive.

4.4.2. Equipment Preparation

The servo hydraulic machine prior to testing was prepared by a procedure that calibrated the proportional, integral, differential and forward gains in order to make it stable for the specific material.

After that the temperature setting for the furnace was calibrated in order to achieve exactly 1200^{o} C at the surface of the specimen regardless the environment. For this to happen a specimen was prepared with two thermocouples bonded at each side of the cross sectional area with Zircon alumina cement.

The specimen was then gripped at the machine and each thermocouple was connected to an Omega Engineering OMNI CAL -8A-110 temperature sensor in order to monitor the temperature at the surface of the specimen. Closely monitoring the sensors, the furnace temperature was raised slowly until the required temperature was achieved. Then the furnace temperature was recorded.

Figure 17. Omega Engineering OMNI CAL -8A-110 temperature sensor

Prior to each testing the servo hydraulic machine was fed with a sinusoidal waveform from the MTS function generator with an amplitude of +- 0.1 inch for about 20 minutes. This procedure was performed in order for the hydraulic fluid to warm up.

V. Results and Discussion

5.1.Tensile Test

Monotonic tensile tests were conducted prior to creep-rupture tests in order to determine the ultimate tensile strength of the specimens under test, its elastic modulus and the strain to failure. The tests were conducted in displacement control with a displacement rate of 0.05mm/s in laboratory air at 1200^0C. The UTS determined by those tests for N720/AS CMC was 231 MPa as seen in figure 18, the elastic modulus 55Gpa and the strain to failure 0.44%. For N720/A Harlan [8] reported a UTS of 192Mpa, elastic modulus 75GPa and strain at failure 0.35%

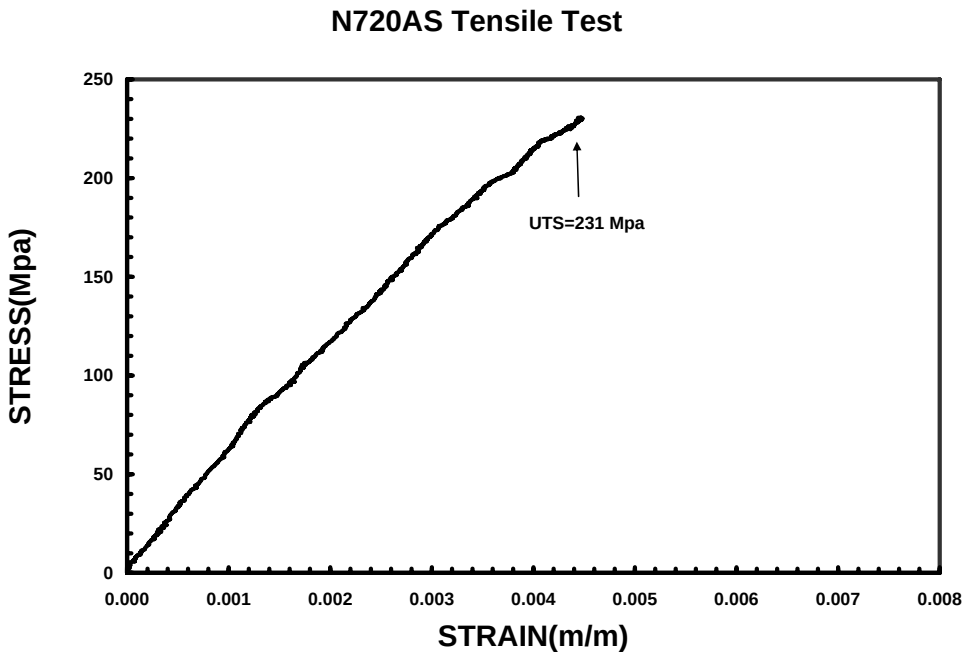

Figure 18. Tensile stress-strain curve for N720/AS at 1200^oC

5.2.Creep –Rupture Tests

Creep rupture tests were conducted in laboratory air, 100% steam environment and 100% argon environment for the N720/AS specimens and in 100% argon environment for the N720/A specimens. The stress levels were 150MPa, 125Mpa, 100MPa and 80MPa. Table 1 summarizes all the tests that were conducted.

Table 1 . Creep- Rupture Results Summary

Stress level-Environment	***Specimen Name***	***Temperature***	***Strain at Failure (m/m)***	***Time to Failure (h)***
N720 AS				
Air 150 Mpa	A150-3	1200 C	0.0034	11.23
Air 125 Mpa	A125	1200 C	0.0055	30.71
Air 95 Mpa	A95-2	1200C	0.0040	Run-out 100h
Air 95 Mpa	A95	1200 C	0.0112	52.99
Air 80 Mpa	A80	1200 C	0.0028	Run-out 100h
Steam 150 Mpa	S150	1200 C	Failure during Ramp-Up	
Steam 125 Mpa	S125	1200 C	0.0056	0.20
Steam 100 Mpa	S100	1200 C	0.0036	0.27
Steam 80 Mpa	S80	1200 C	0.0079	10.94
Argon 150 Mpa	AsAr150	1200 C	0.0064	1.51
Argon 125 Mpa	AsAr125	1200 C	0.0032	1.76
Argon 100 Mpa	AsAr100	1200 C	0.0196	Run-out 100h
Argon 80 Mpa	AsAr80	1200 C	0.0106	Run-out 100h
N720 A				
Argon 150 Mpa	AAr150	1200 C	0.0062	0.87
Argon 125 Mpa	AARr125	1200 C	0.0188	36.33
Argon 100 Mpa	AAr100	1200 C	0.0096	Run-out 100h
Argon 80 Mpa	AAr80	1200 C	0.0065	Run-out 100h

5.2.1. Creep –Rupture Tests in Air

As seen on the table 2 the specimen that was tested in 150MPa failed in only 11 hours in comparison with the one tested in 80Mpa that didn't failed even after 100 hours. In the time the tests were conducted the machine was serviced and calibrated by MTS technicians. During the first testing at 150 MPa, the specimen achieved a surprising 52 hours before rupture. A repeat at the same test resulted in an even more surprising 100h run-out. Investigating the settings of the machine, a huge offset of 55MPa was discovered, which explained the results as the specimens were loaded actually in 95 MPa and not 150MPa. Both results were used due to lack of further specimens as alternatives of the 100MPa test. The largest amount of creep was observed at 125MPa. Harlan [8]at his tests for the $0/90^{o}$ N720A in air and for the same stress conditions reported 0.03h at 154 Mpa, 4.25h at 125 MPa, 41h at 100Mpa and 254h at 80 Mpa. Comparing the results N720/AS material exhibited far better performance at 150 and 125 Mpa. Although the results don't seem consistent, lack of more specimens didn't allow a repeat at the tests for confirmation.

Table 2 .Creep-Rupture Results of N720/AS in Laboratory Air

Stress level-Environment	*Specimen Name*	*Temperature*	*Strain at Failure (m/m)*	*Time to Failure (h)*	*Residual Strength(Gpa)*
Air 150 Mpa	A150-3	1200 C	0.003446514	11.23610567	
Air 125 Mpa	A125	1200 C	0.005595709	30.71640158	
Air 95 Mpa	A95-2	1200C	0.004012875	Run-out 100h	97
Air 95 Mpa	A95	1200 C	0.01127139	52.99973403	
Air 80 Mpa	A80	1200 C	0.002880229	Run-out 100h	116

Figure 19 shows strain vs. time for all specimens. In figure 20 the time scale is truncated in order to show clearly the strain curves. It should be noted that all the

specimens exhibited both primary and secondary creep while specimen A95-2 had tertiary creep as well.

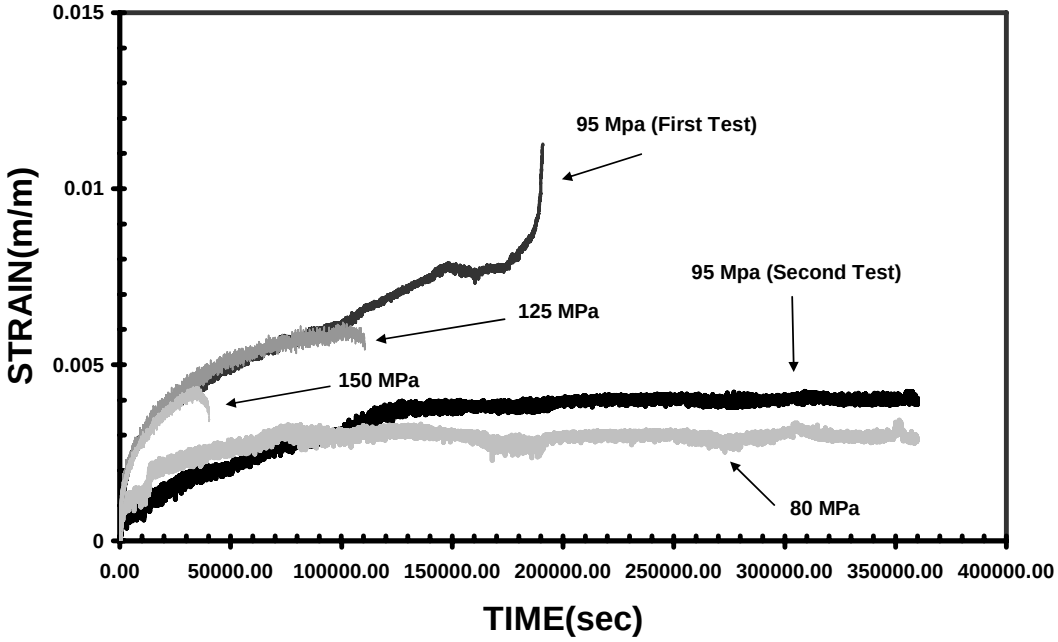

Figure 19. Creep Strain vs Time for N720/AS in air 1200^{o}C

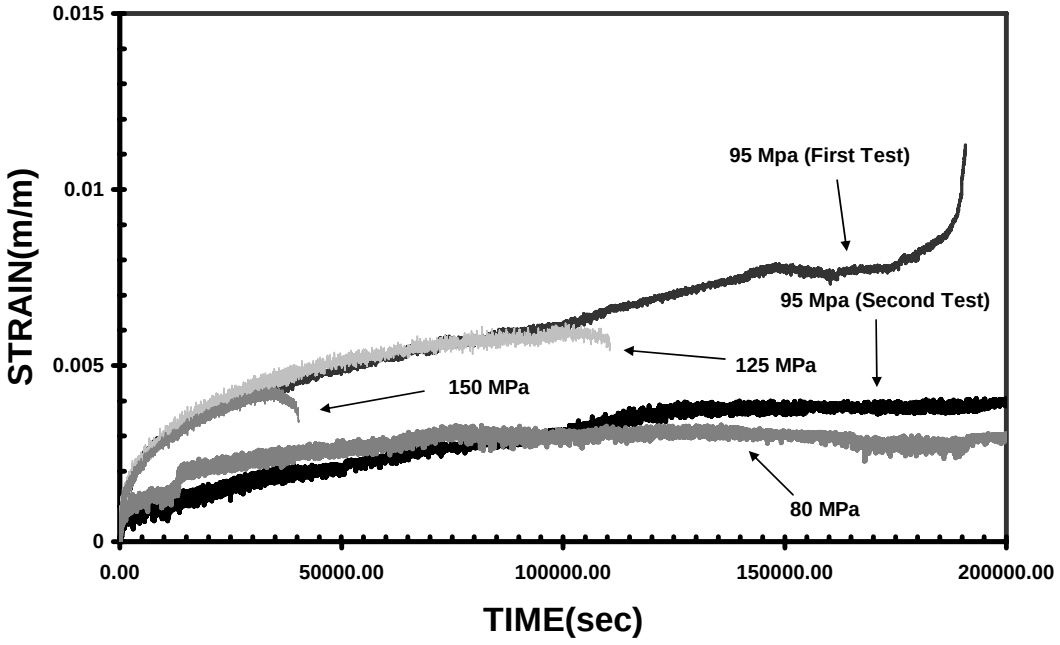

Figure 20. Creep Strain vs Time for N720/AS in air 1200^{o}C (Time Truncated)

5.2.2.Creep-Rupture in 100% Steam Environment

In table 3 results are summarized for the tests of N720/AS in 100% steam environment. It is worth mentioning that at 150MPa the test didn't even started as the specimen failed during ramping up at about 135Mpa. The same test was repeated and the specimen failed again during ramp-up at 130Mpa. To further investigate these results, a specimen was left for 12 hours at 1200^{o}C in 100% pure steam environment at zero load , prior to conducting a tensile test. The results of that test as seen in figure 21 showed a UTS of 83 Mpa. A comparison of this result to the UTS of 231MPa in air environment shows a severe degradation in the material properties of the composite as a result of the

environment, which explained why the specimens failed during ramp up for the 150Mpa. The steam environment resulted also in the depicted at table 3 failure times for the other stress levels, which compared to the air environment are significantly reduced. In contrast to the air environment the maximum strain was observed at the lowest stress level. Additionally at stress levels of 125MPa, 100MPa and 80Mpa primary creep was observed as well as secondary as can been seen in figures 22, 23.

Table 3 .Creep-Rupture Results of N720/AS in 100% Steam Environment

Stress level-Environment	*Specimen Name*	*Temperature*	*Strain at Failure (m/m)*	*Time to Failure (h)*
Steam 150 Mpa	S150	1200 C	Failure during Ramp-Up	
Steam 125 Mpa	S125	1200 C	0.005615808	0.2025
Steam 100 Mpa	S100	1200 C	0.003643548	0.271944444
Steam 80 Mpa	S80	1200 C	0.00794	10.94417311

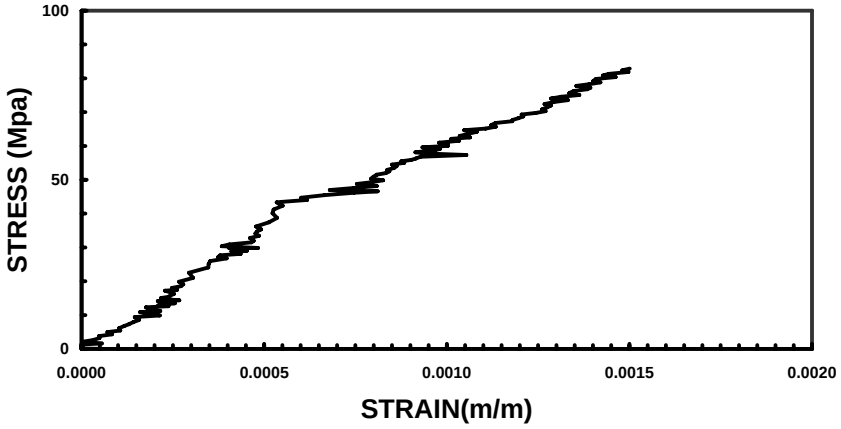

Figure 21. Tensile Test N720/AS Aged in steam 1200°C

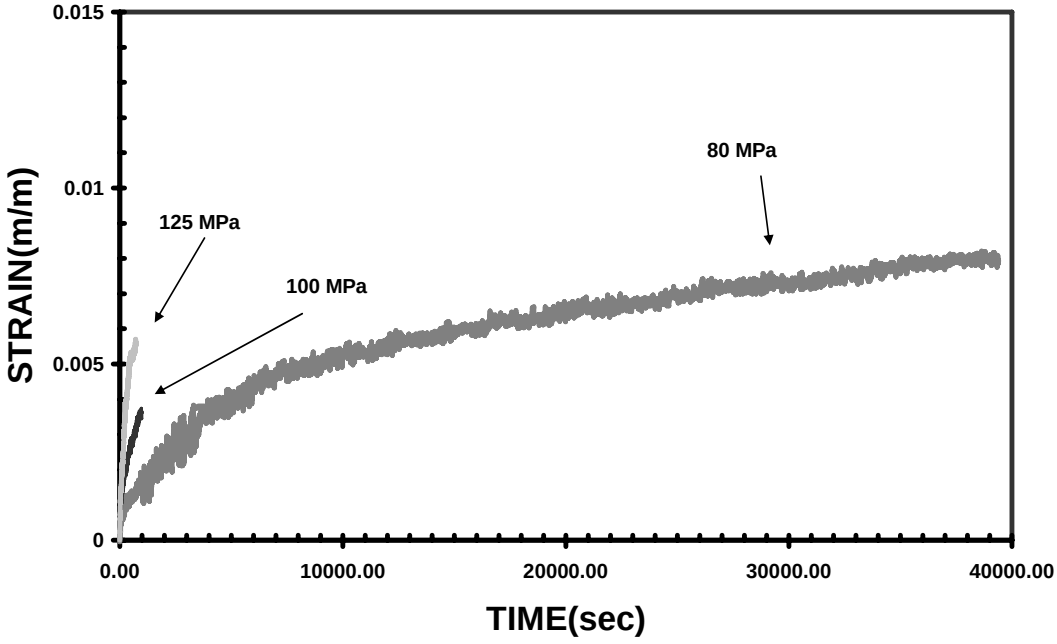

Figure 22. Creep Strain vs Time for N720/AS in steam 1200°C

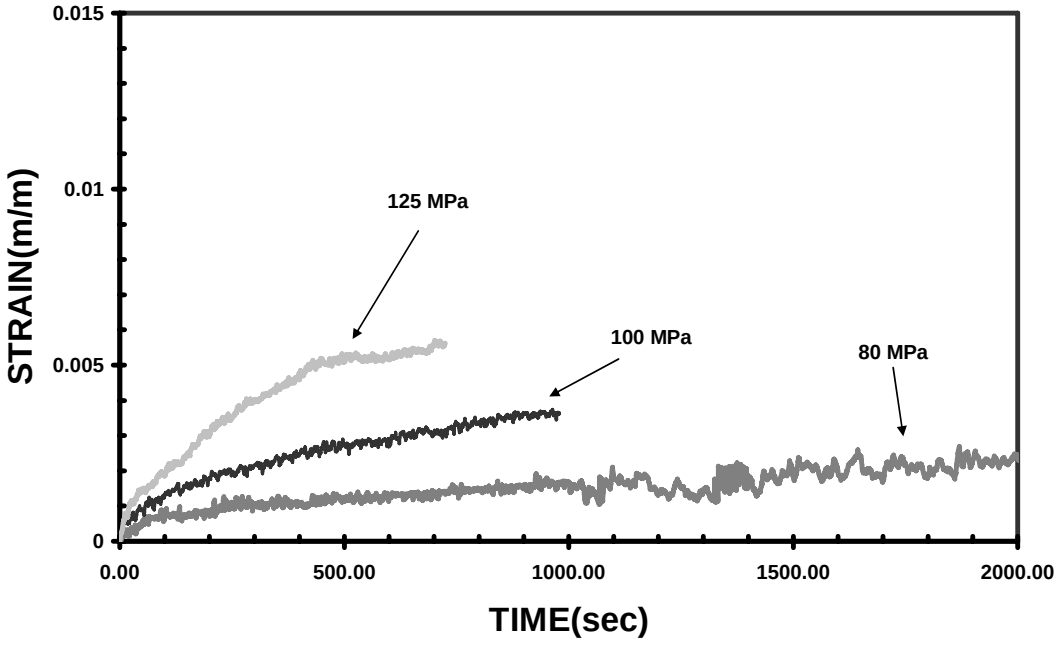

Figure 23. Creep Strain vs Time for N720/AS in steam 1200^{o}C (Time Truncated)

5.2.3.Creep- Rupture Tests in 100% Argon Environment for N720/AS

A summary of the results for Nextel 720AS specimens in argon are depicted at table 4. Specimens at stress levels of 100MPa and 80MPa withstand their loads for 100h, whereas the specimens loaded at 150 and 125 Mpa had a time to failure of 1.5 and 1.76. All specimens had both primary and secondary creep regions while the specimen loaded at 150 MPa had also a tertiary region. The maximum strain was obtained from the loading at 100MPa.

Table 4.Creep-Rupture Results for N720/AS in 100% Argon Environment

Stress level-Environment	*Specimen Name*	*Temperature*	*Strain at Failure (m/m)*	*Time to Failure (h)*	*Residual Strength(Gpa)*
Argon 150 Mpa	AsAr150	1200 C	0.006492506	1.515910639	
Argon 125 Mpa	AsAr125	1200 C	0.003256903	1.769172444	
Argon 100 Mpa	AsAr100	1200 C	0.019678945	Run-out 100h	105
Argon 80 Mpa	AsAr80	1200 C	0.010695516	Run-out 100h	87

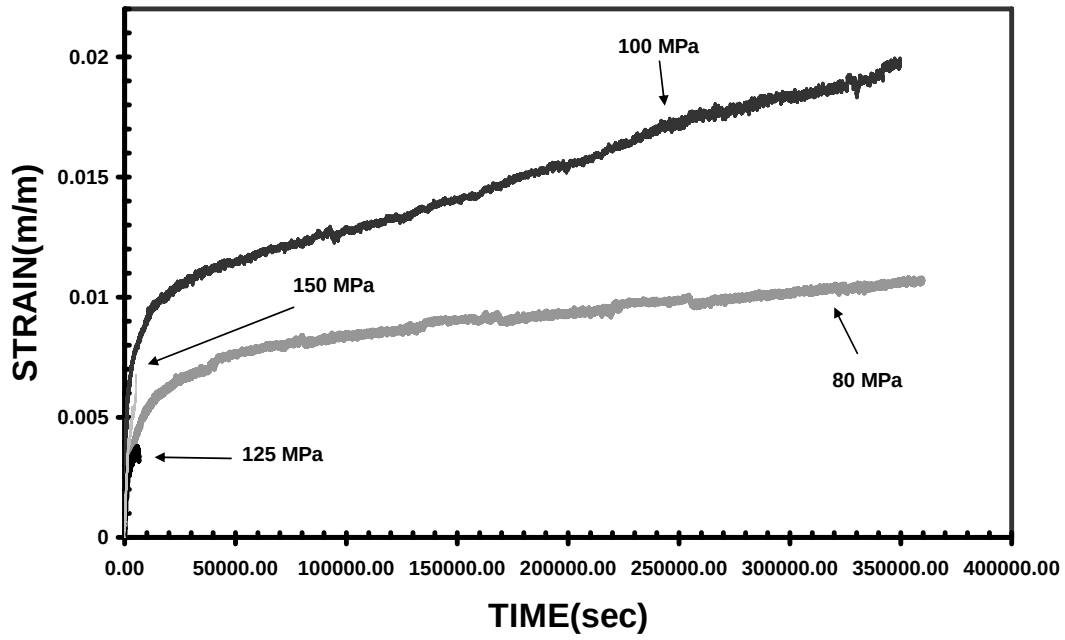

Figure 24. Creep Strain vs Time for N720/AS in argon 1200°C

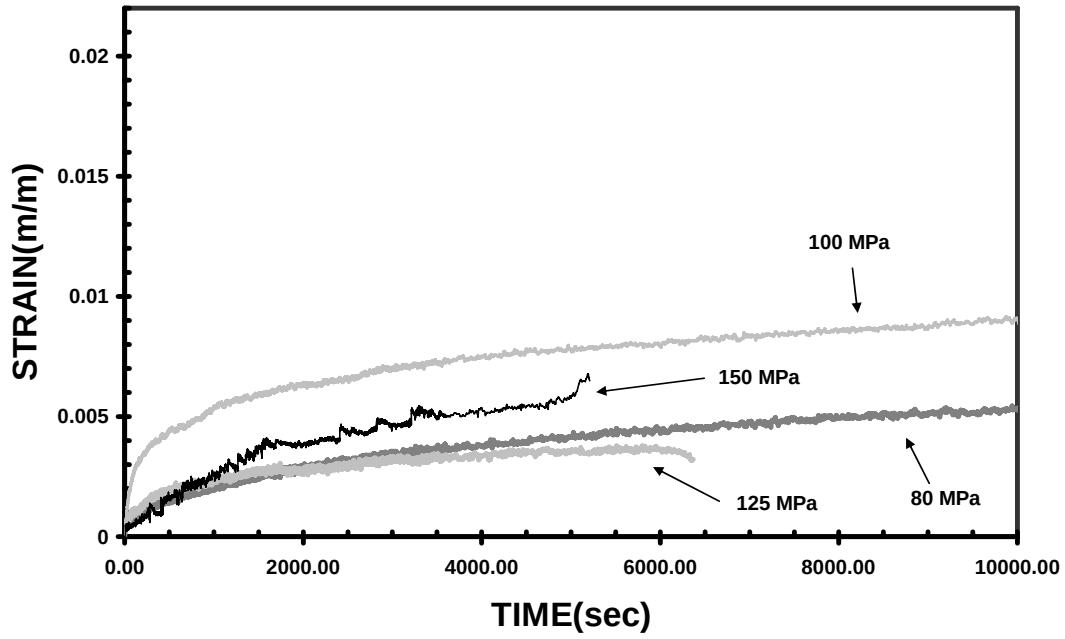

Figure 25. Creep Strain vs Time for N720/AS in argon 1200°C (Time Truncated)

5.2.4 Creep- Rupture Tests in 100% Argon Environment for N720/A

N720/A specimens tested in argon resulted as illustrated in table 5. Similarly to N720/AS tested in argon the tests at 100MPa and 80 MPa run for 100h without failing.

Table 5.Creep-Rupture Results for N720/A in 100% Argon Environment

Stress level-Environment	*Specimen Name*	*Temperature*	*Strain at Failure (m/m)*	*Time to Failure (h)*	*Residual Strength(Gpa)*
Argon 150 Mpa	AAr150	1200 C	0.006223945	0.87777778	
Argon 125 Mpa	AARr125	1200 C	0.01889297	36.33314958	
Argon 100 Mpa	AAr100	1200 C	0.009621264	Run-out 100h	160
Argon 80 Mpa	AAr80	1200 C	0.006556961	Run-out 100h	180

From figures 26 and 27 it is observable that all specimens had both a primary and a secondary creep curve as expected.

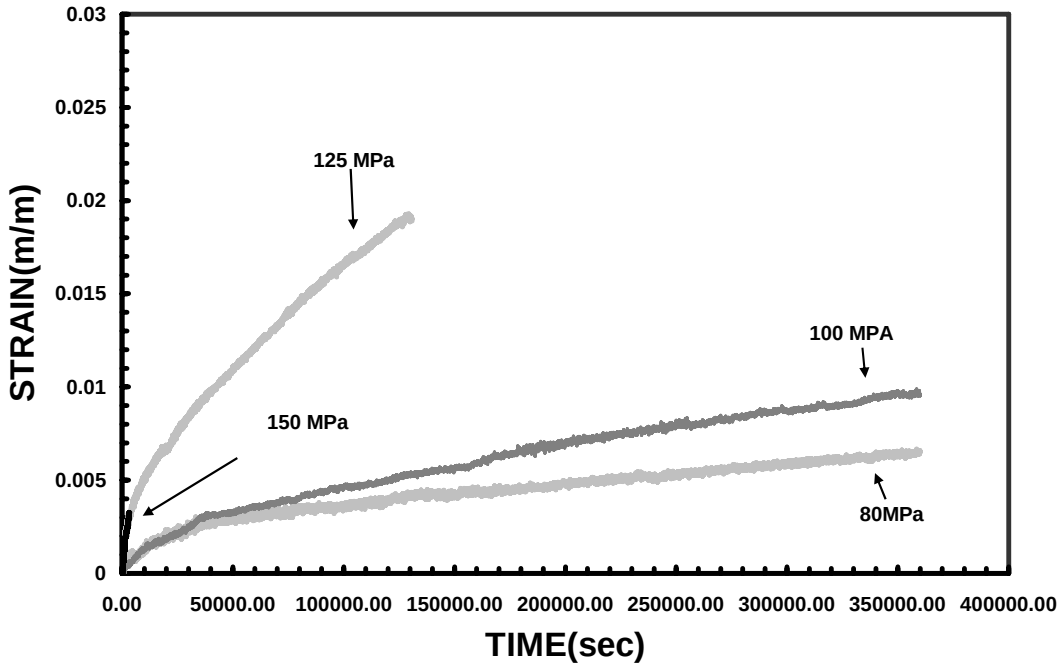

Figure 26. Creep Strain vs Time for N720/A in argon 1200^{o}C

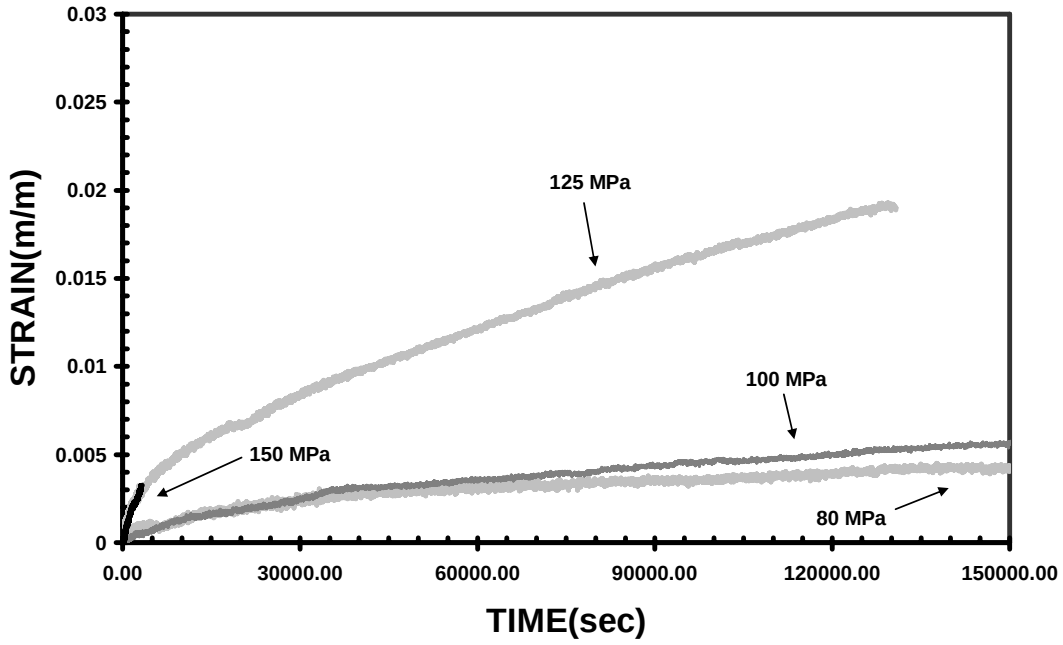

Figure 27. Creep Strain vs Time for N720/A in argon 1200^{o}C (Time Truncated)

5.2.6. Creep Rate

Creep strain rate of a material is very important factor since it is a key criterion when designing aerospace application. Table 6 summarizes the creep strain rates of all the specimens tested. It can be seen that the lowest creep rate was achieved by N720/A specimen tested in argon at 100MPa, while the highest was met by the specimen tested in steam at 125MPa. It should be noted that a comparison of N720/AS and N720/A materials tested in argon shows that at lower stress levels material N720/A had better creep rate by about one order of magnitude.

Table 6. Specimens Creep Rates

Stress level-Environment	*Specimen Name*	*Temperature*	*Strain at Failure (m/m)*	*Time to Failure (h)*	*Creep Rate (sec-1)*
N720 AS					
Air 150 Mpa	A150-3	1200 C	0.003446514	11.23610567	5.00E-08x + 1.98E-03
Air 125 Mpa	A125	1200 C	0.005595709	30.71640158	1.23E-08x + 4.64E-03
Air 95 Mpa	A95-2	1200C	0.004012875	Run-out 100h	5.18E-08x - 1.50E-02
Air 95 Mpa	A95	1200 C	0.01127139	52.99973403	1.12E-06x - 2.03E-01
Air 80 Mpa	A80	1200 C	0.002880229	Run-out 100h	7.61E-08x - 2.29E-02
Steam 150 Mpa	S150	1200 C	Failure during Ramp-Up		
Steam 125 Mpa	S125	1200 C	0.005615808	0.2025	6.68E-06x + 8.62E-04
Steam 100 Mpa	S100	1200 C	0.003643548	0.271944444	1.19E-06x + 2.50E-03
Steam 80 Mpa	S80	1200 C	0.00794	10.94417311	2.72E-07x - 2.64E-03
Argon 150 Mpa	AsAr150	1200 C	0.006492506	1.515910639	7.15E-07x + 2.27E-03
Argon 125 Mpa	AsAr125	1200 C	0.003256903	1.769172444	1.10E-07x + 3.01E-03
Argon 100 Mpa	AsAr100	1200 C	0.019678945	Run-Out	2.77E-08x + 1.01E-02
Argon 80 Mpa	AsAr80	1200 C	0.010695516	Run-Out	3.68E-08x - 2.52E-03
N720 A					
Argon 150 Mpa	AAr150	1200 C	0.006223945	0.877777778	2.18E-06x - 3.68E-03
Argon 125 Mpa	AARr125	1200 C	0.01889297	36.33314958	1.77E-07x - 3.60E-03
Argon 100 Mpa	AAr100	1200 C	0.009621264	Run-out 100h	9.92E-10x + 9.32E-03
Argon 80 Mpa	AAr80	1200 C	0.006556961	Run-out 100h	2.43E-09x + 5.61E-03

5.2.6.Cross Environment Comparisons

Figure 28 depicts a comparison of creep strain and time to rupture for all the specimens tested at 150 MPa. The specimen S150 is not listed as it failed during ramp-up. The results for the argon environments were as expected, but what seems weird is the rupture time for the specimen in air. As argon is an inert gas what was expected was the specimen in air to have worst performance than the one in argon. The fact that as described earlier the MTS machine that was used for the tests in air had a big offset, although the whole process and temperature was inspected thoroughly both before and after the test, raises questions about the credibility of the result in air.

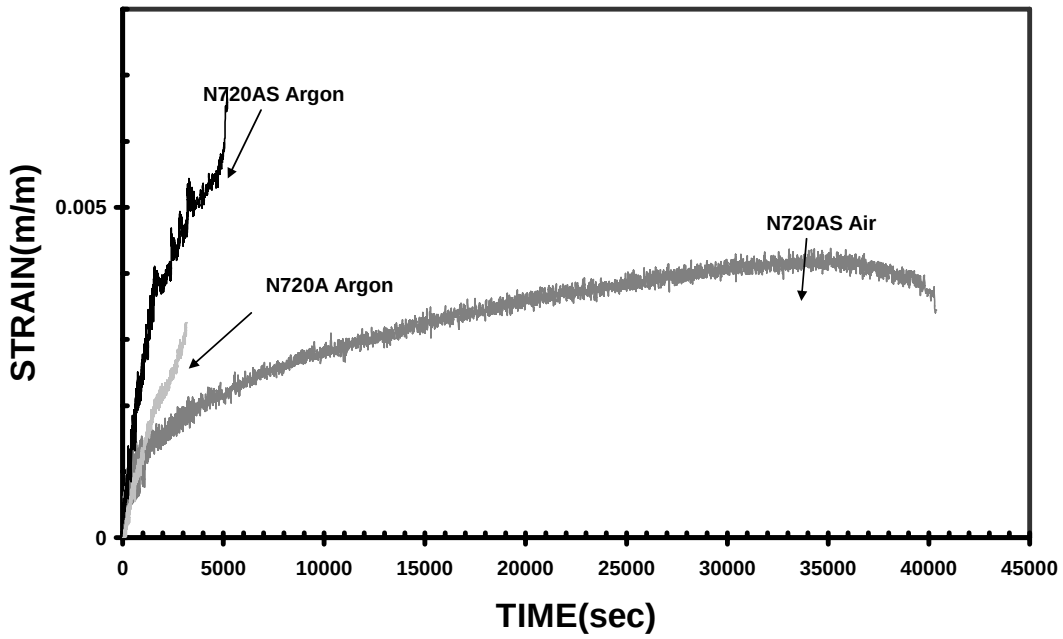

Figure 28. Creep Strain vs Time at 150 MPa in all environments at 1200^{o}C

Figures 29 and 30 demonstrate the specimens tested at 125MPa. It is clear here that N720A material performed far better than the N720AS specimens. It should be noted that although N720AS in argon failed early until its fracture, the accumulated strain had the same curvature as the N720A.

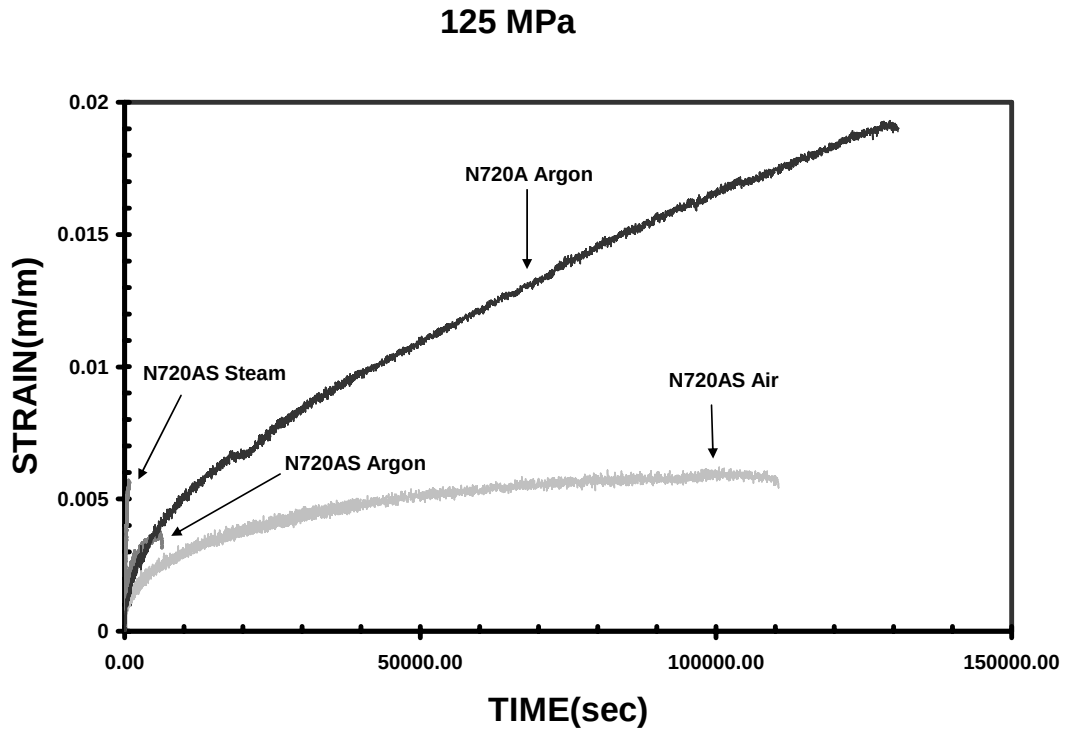

Figure 29. Creep Strain vs Time at 125 MPa in all environments at 1200^{o}C

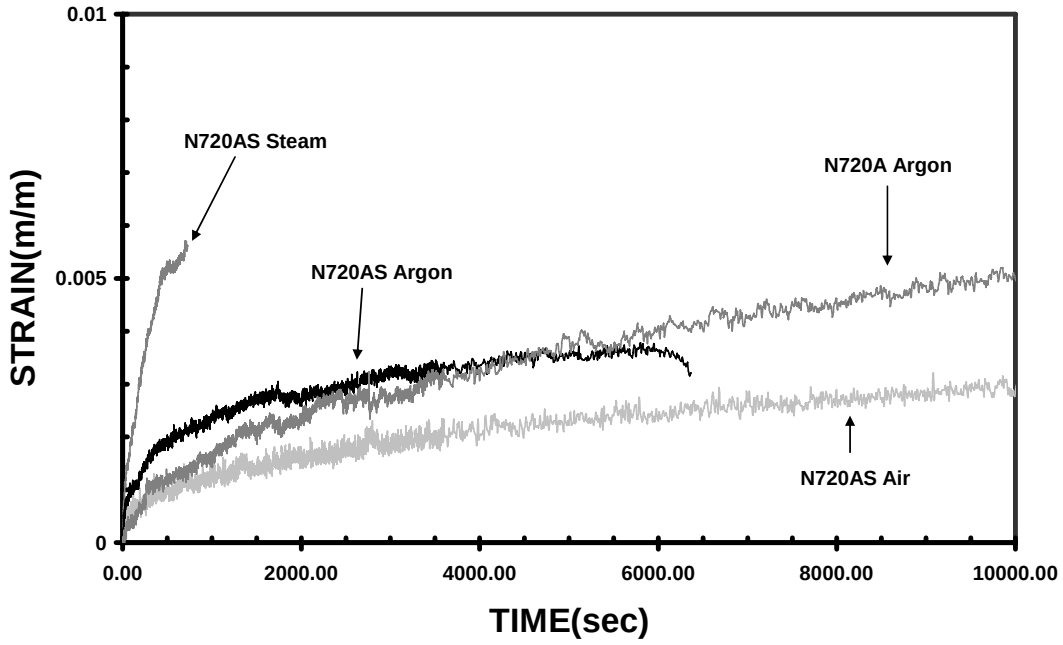

Figure 30. Creep Strain vs Time at 125 MPa in all environments at 1200^0(Time Truncated)

At 100MPa it can be also be observed that N720A material had the highest creep strain as it was also observed at 125Mpa, where it also easily observable that the specimen in steam environment failed much earlier than the others. The early failure in steam environment is depicted also at figures 31 and 32.

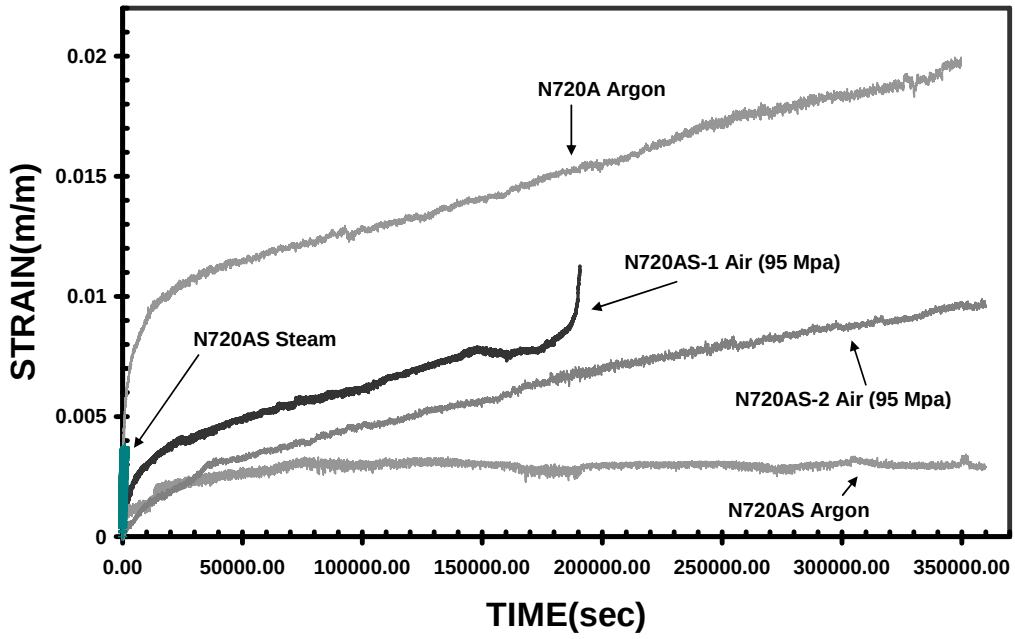

Figure 31. Creep Strain vs Time at 100 MPa in all environments at 1200^{o}C

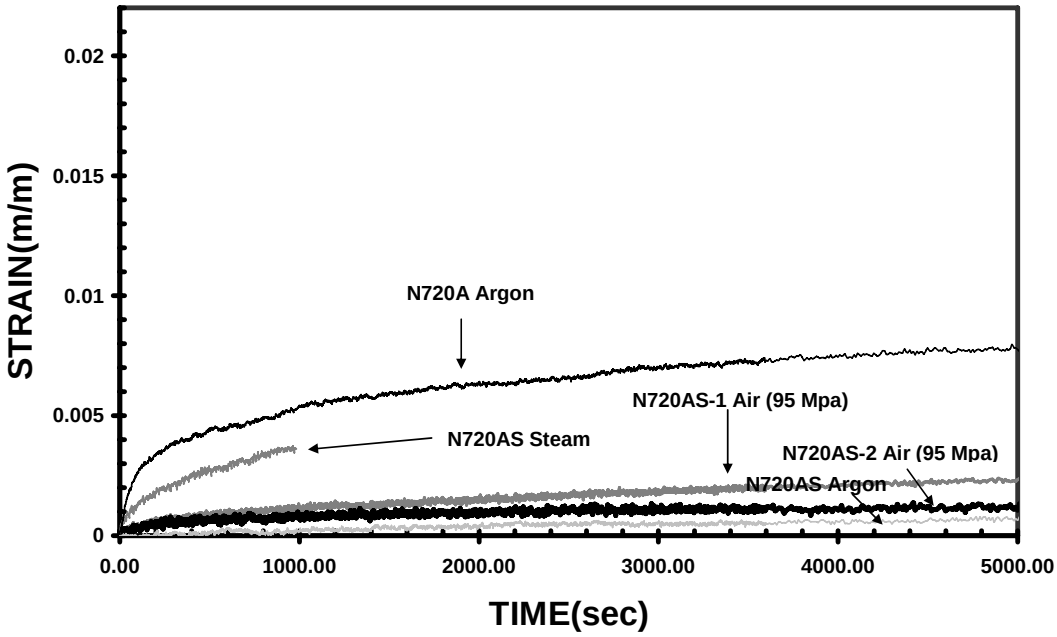

Figure 32 . Creep Strain vs Time at 100 MPa in all environments at 1200^0C(Time Truncated)

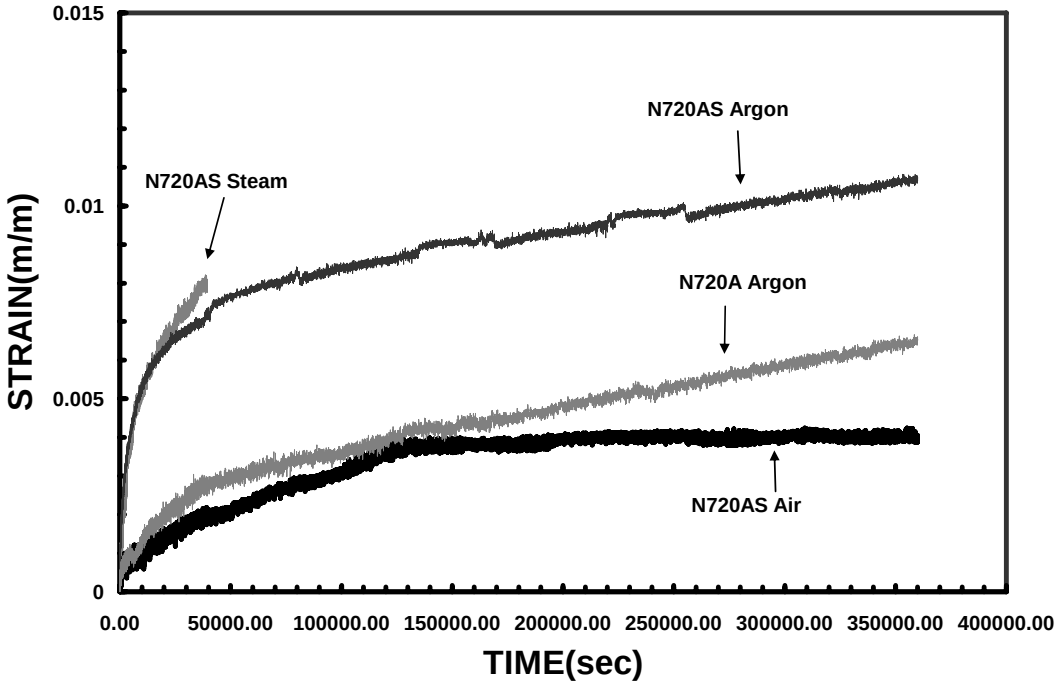

Figure 33. Creep Strain vs Time at 80 MPa in all environments at 1200^{o}

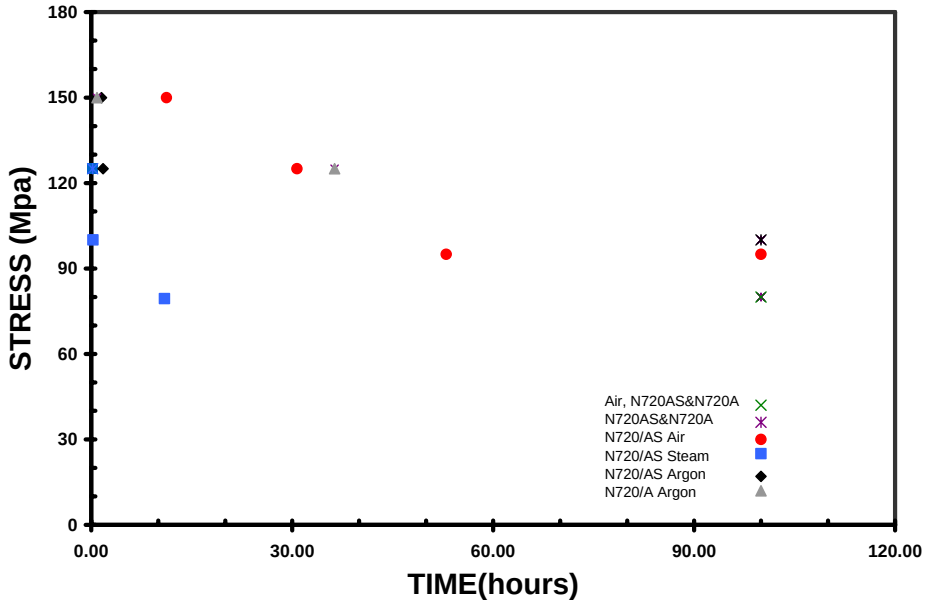

Figure 34. Applied stress vs time to failure summary

5.2.6. Retained Strength Testing

Retained strength testing as summarized in table 7 shows that specimens of N720/AS material that achieved 100 hours run out, have significantly reduced UTS, something that didn't happened at N720/A specimens. These results are another clue of the degrading effects of the prolonged stay in high temperatures, in the performance of N720/AS material.

Table 7 . Retained Strength Results

Stress level-Environment	***Specimen Name***	***Temperature***	***Strain at Failure (m/m)***	***Time to Failure (h)***	***Retained Strength (Gpa)***	***Strength Retention %***
N720 AS						
Air 95 Mpa	A95-2	1200C	0.004012875	Run-out 100h	97	41.9
Air 80 Mpa	A80	1200 C	0.002880229	Run-out 100h	116	50.2
Argon 100 Mpa	AsAr100	1200 C	0.019678945	Run-Out	105	45.5
Argon 80 Mpa	AsAr80	1200 C	0.010695516	Run-Out	87	37.6
N720 A						
Argon 100 Mpa	AAr100	1200 C	0.009621264	Run-out 100h	160	83.3
Argon 80 Mpa	AAr80	1200 C	0.006556961	Run-out 100h	180	93.2

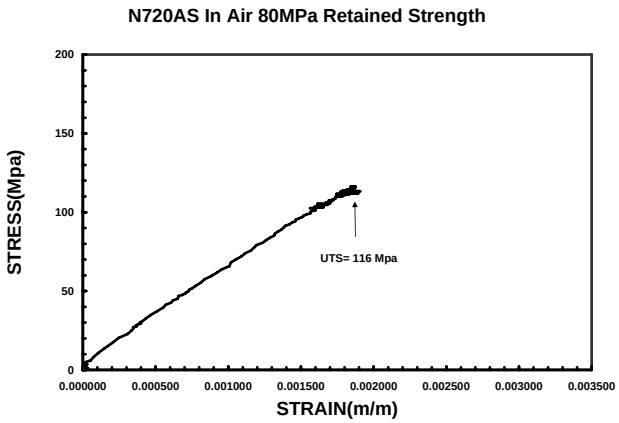

Figure 35. Retained strength of A80 specimen

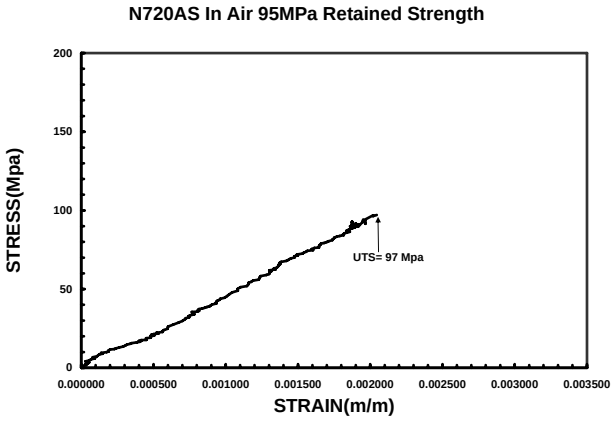

Figure 36. Retained strength of A95-2 specimen

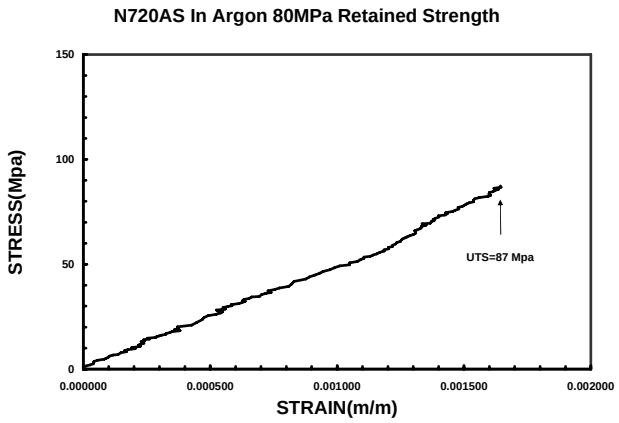

Figure 37. Retained strength of AsAr80 specimen

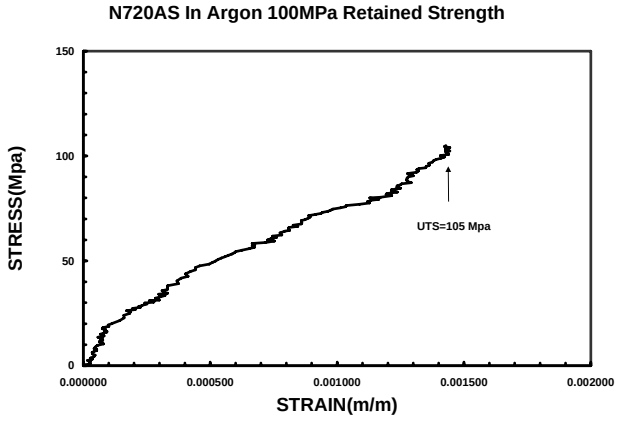

Figure 38. Retained strength of AsAr100 specimen

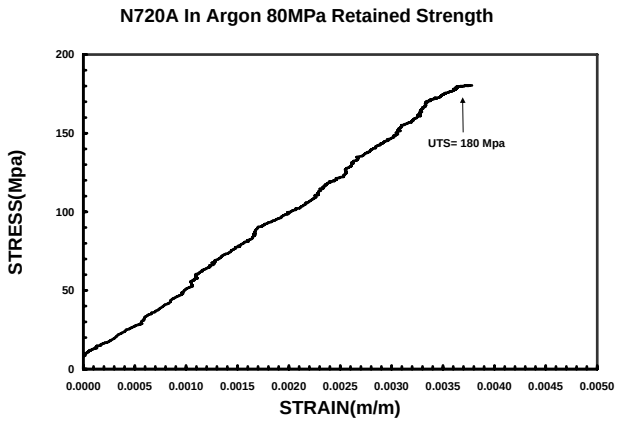

Figure 39. Retained strength of AAr80 specimen

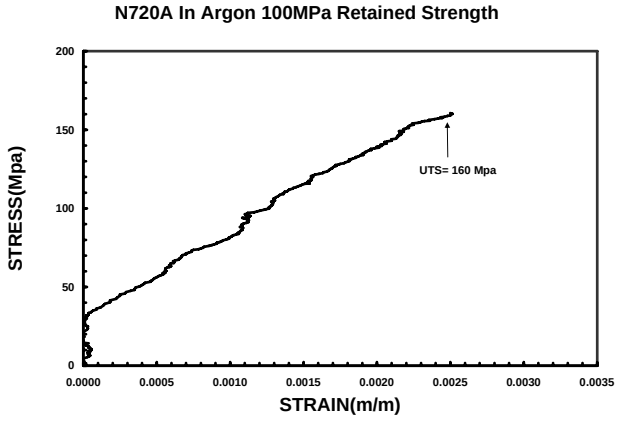

Figure 40. Retained strength of AAr100 specimen

5.3. Microstructure Analysis

After the completion of tests, the specimens were examined both at low magnification with the use of the optical microscopy and at high magnification with the use of the SEM.

The first step was to examine the fracture surface of the specimens at the optical microscopy. Cross-examining the photographs taken from all the specimens revealed a trend both for the load level as well as for the testing environment for the N720AS

material. As can be seen at figures 41,42,43 there is a trend from flat fracture surface at lower load levels to brush fracture surface at higher load levels at all three environments. It can also be observed by comparing the same load levels at the three environments that the specimens tested in steam had more flat fracture surface than specimens tested in air or argon.

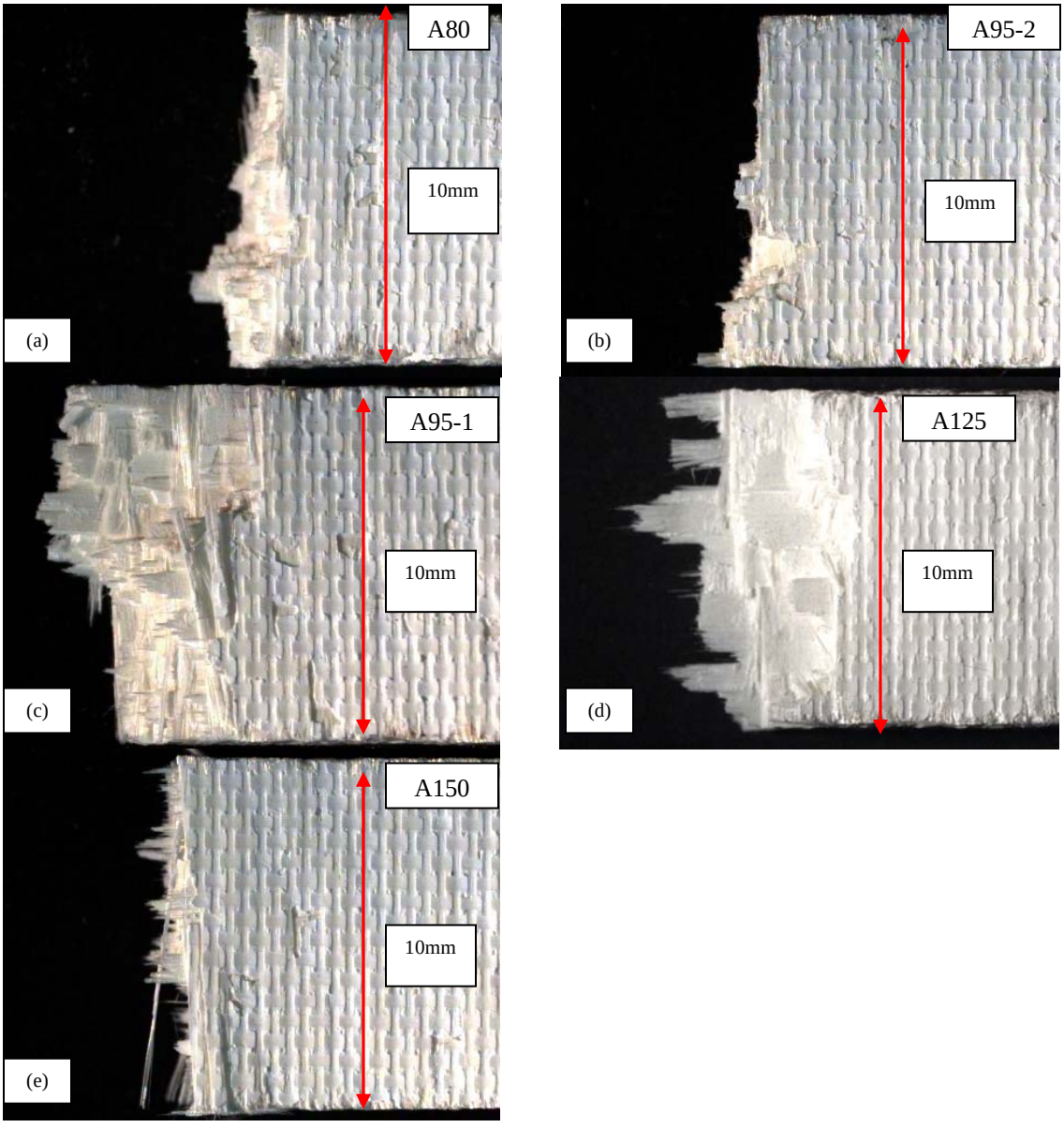

Figure 41.N720AS specimens fractured in air environment at 1200^0C

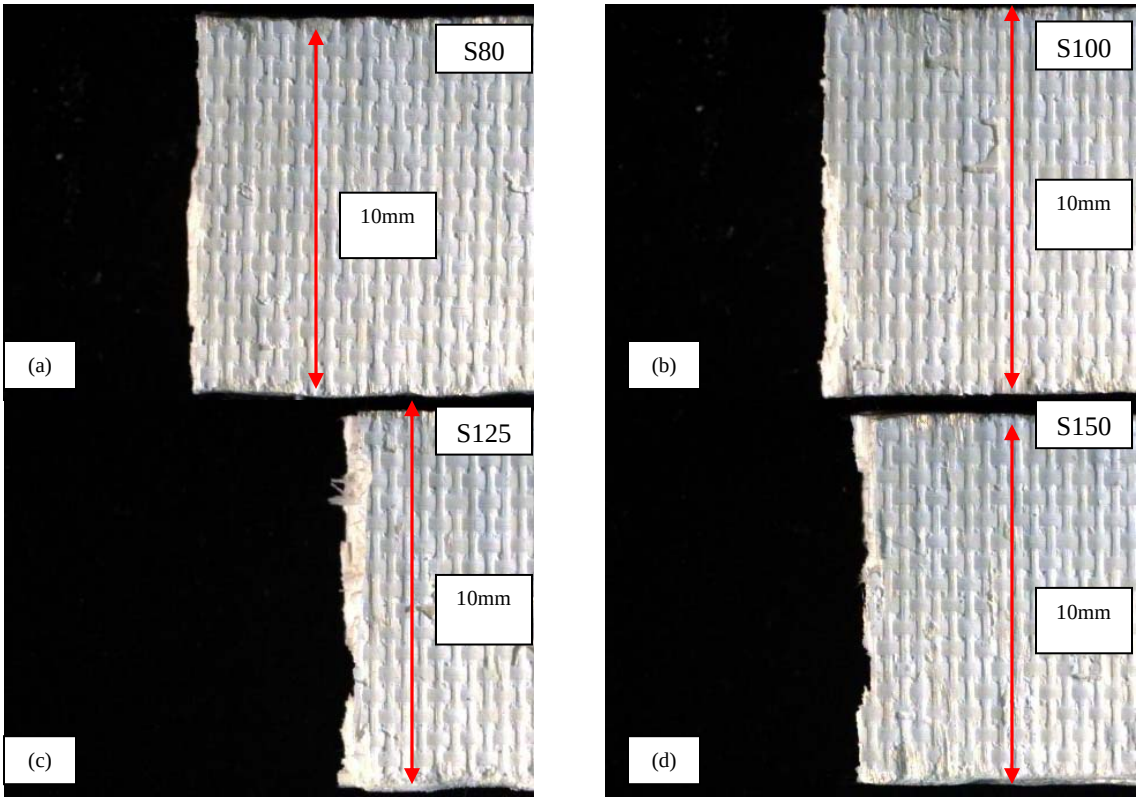

Figure 42.N720AS specimens fractured in 100% steam environment at 1200^{0}C

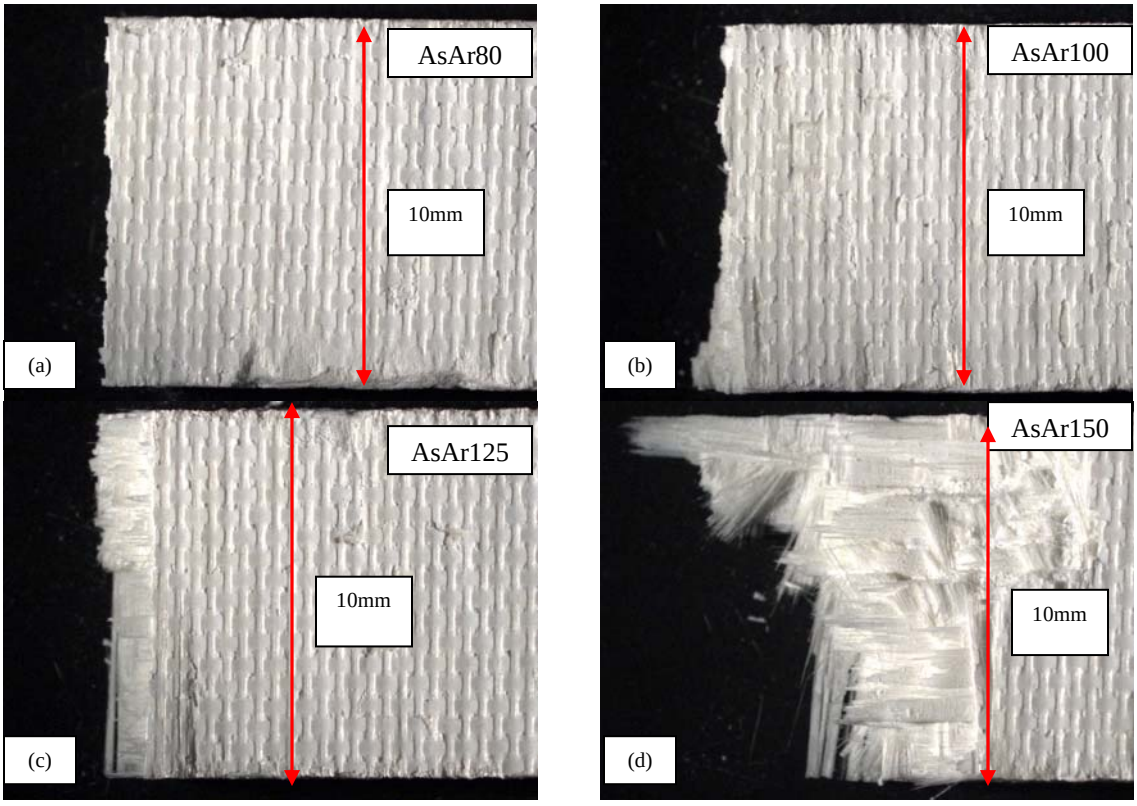

Figure 43.N720AS specimens fractured in 100% argon environment at 1200^{0}C

Consistent with what Harlan[8] reported for the fracture surfaces in air and steam environment for the N720A specimen, in argon there is no particular trend that can be related with the loading levels. Comparing though N720A fracture surfaces seen in figure 44 with N720AS fracture surfaces seen in figure 43 it is easily observable that N720A specimens had brushier fracture surfaces at the same load levels.

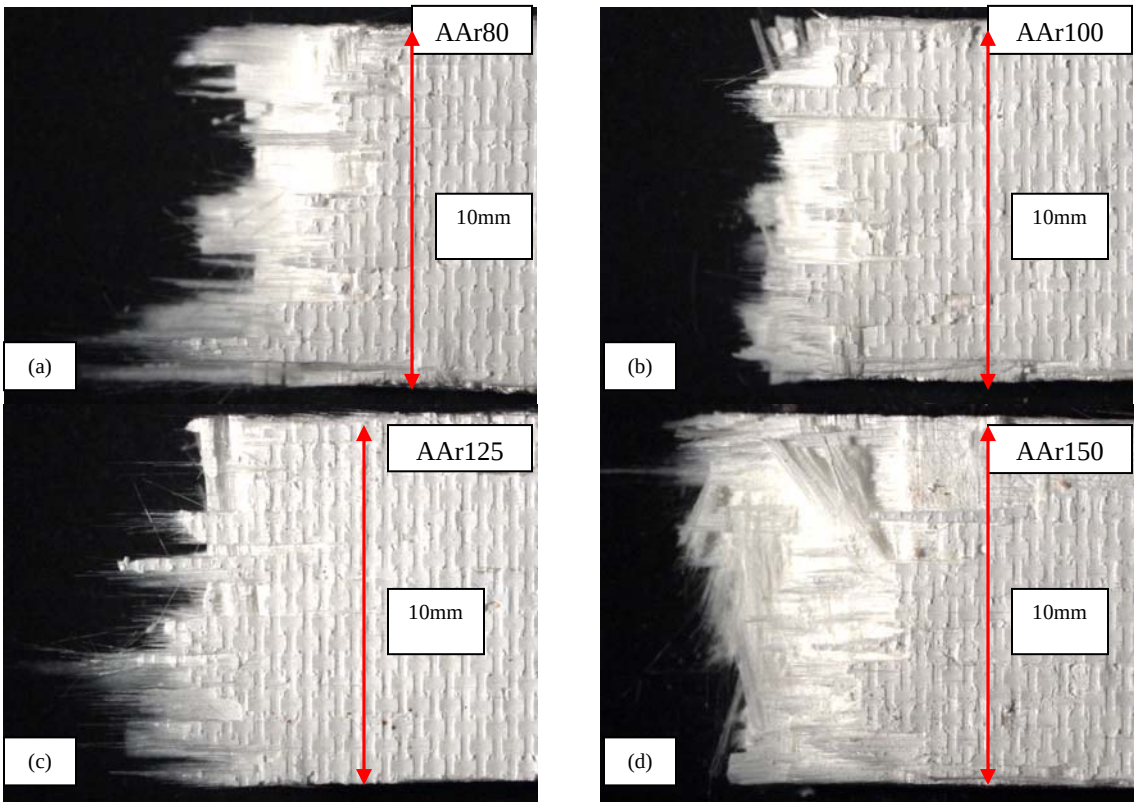

Figure 44.N720A specimens fractured in 100% argon environment at 1200^{0}C

Figure 45 illustrates the fracture surfaces of the N720AS CMC after tensile test for a specimen aged in 100% steam environment for 12 hours in 1200^{0}C (a) and for a specimen tested in tensile after heating up up to 1200^{0}C in air (b). It can be seen that the fracture surface of (a) follow the pattern of the surfaces of specimens tested for creep in steam as depicted in figure 41. Specimen (b) has brush fracture surface much like the specimens tested in air or argon for creep at high load levels.

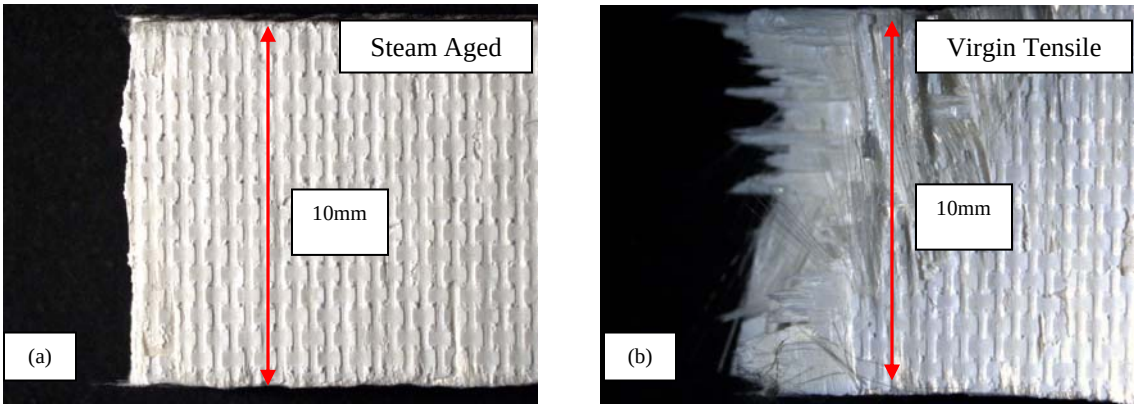

Figure 45.N720AS specimens fractured in tensile test in 100 % steam environment (a) and in air environment (b) at 1200^{0}C

Following the optical microscopy observations, the specimens were prepared and observed at the Scanning Electronic Microscope. Figures 46,47,48 and 49 illustrates the fracture surfaces of the specimens at 40x magnification. This magnification was chosen as the whole width of the specimen can be observed. From the analysis of the fracture surfaces the trend that was discussed earlier for N720AS CMC seems even more obvious. The lowest the load level of the specimen, the more flat its fracture surface is. And again the specimens tested in steam are more flat than the specimens tested in air or argon at the same load level.

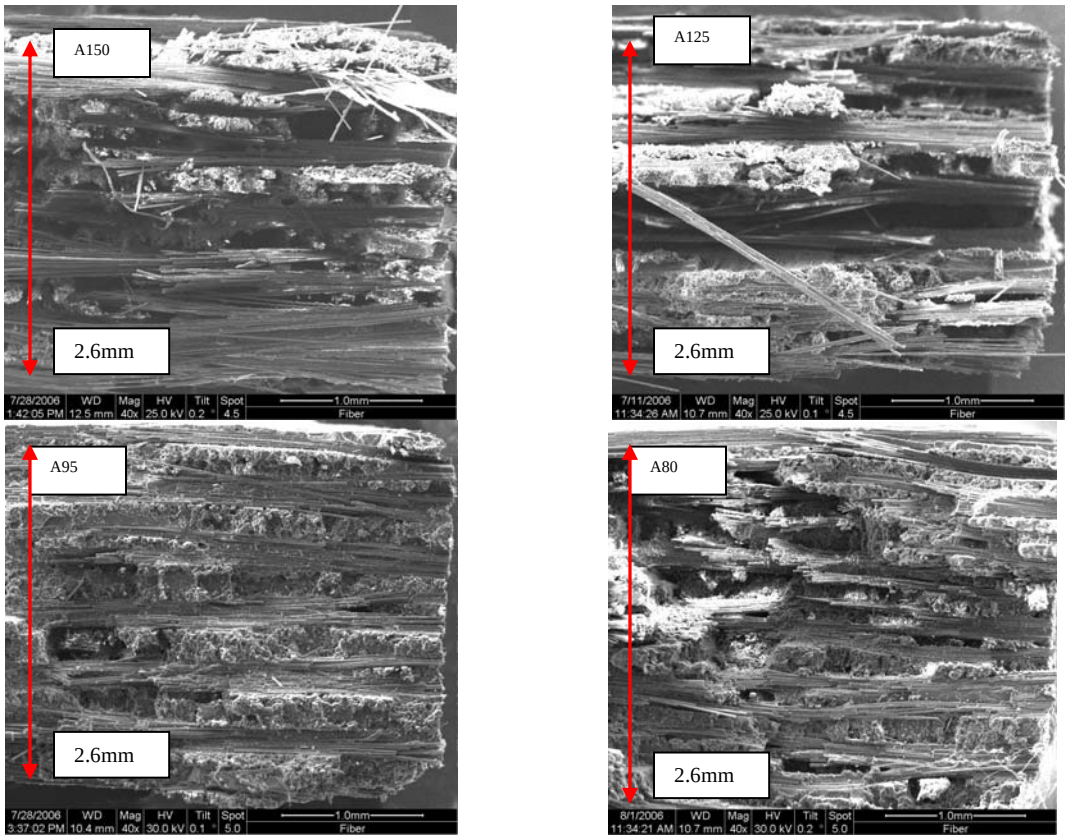

Figure 46. N720/AS Specimens at Air – 40x Magnification

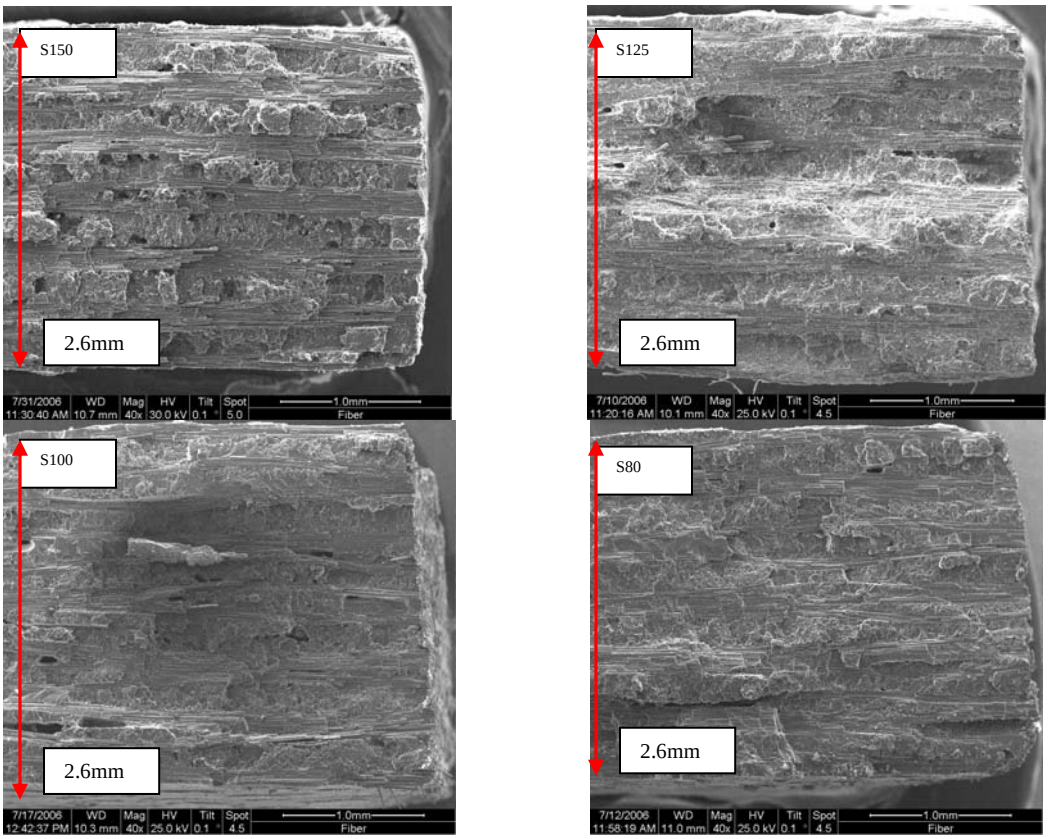

Figure 47. N720/AS Specimens at Steam – 40x Magnification

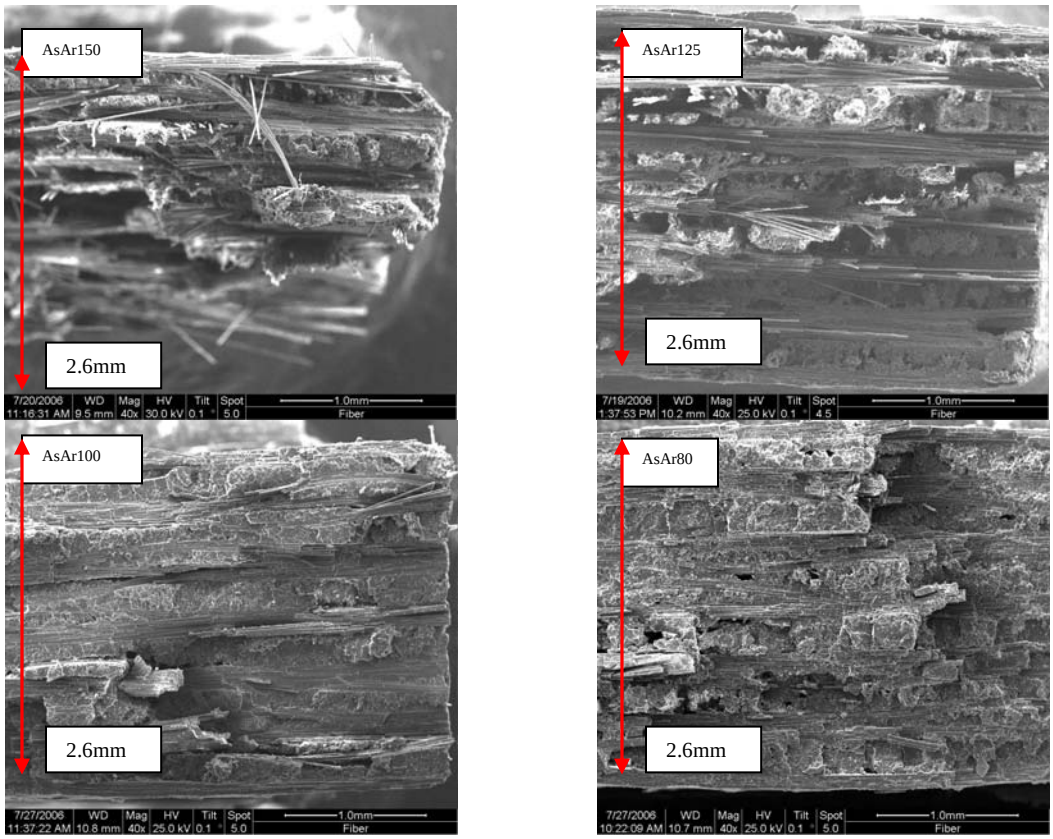

Figure 48. N720/AS Specimens at Argon – 40x Magnification

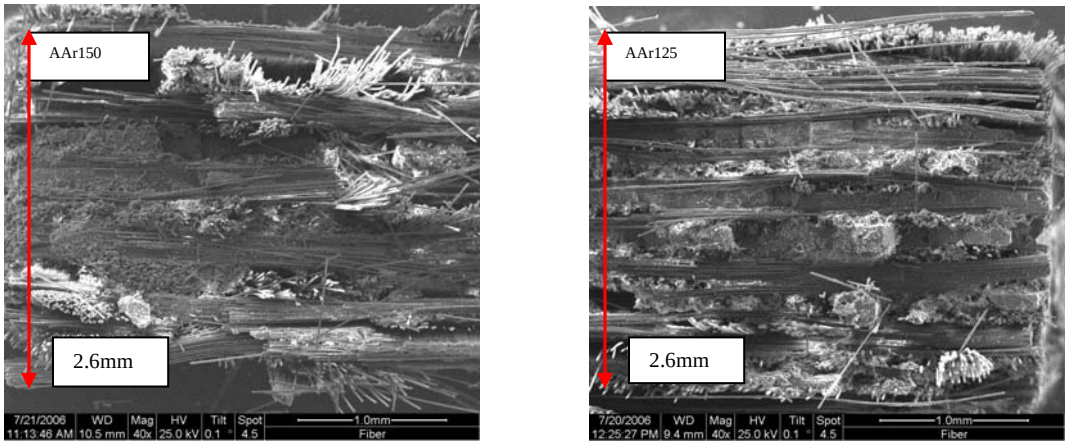

Figure 49. N720/A Specimens at Argon – 40x Magnification

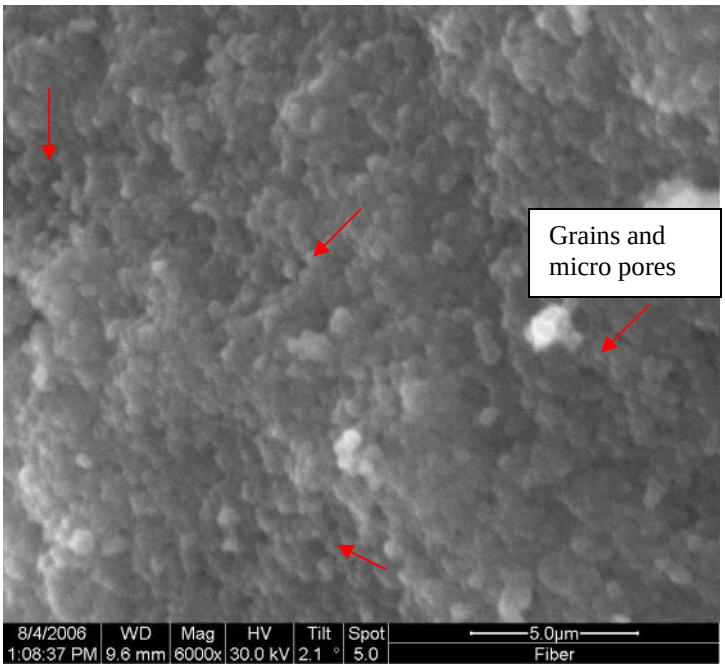

Figure 50. Virgin N720/AS -6000x

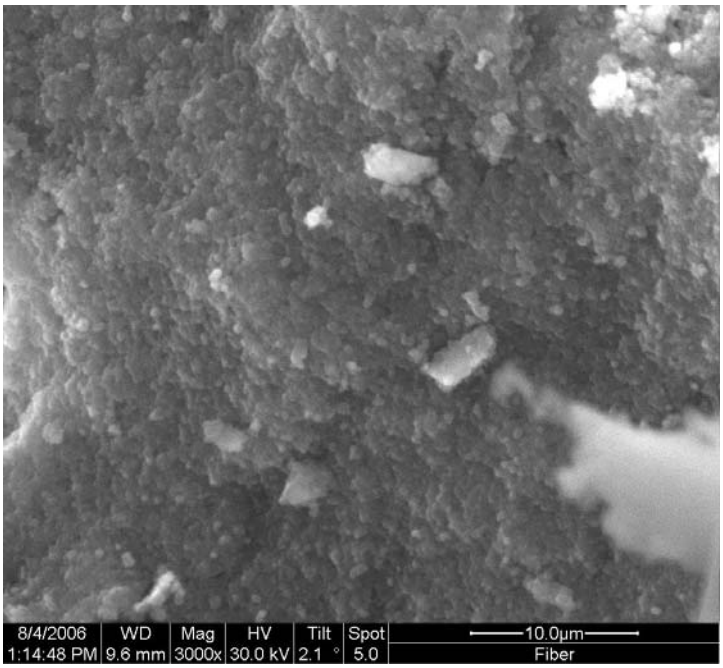

Figure 51. Virgin N720/AS - 3000x

Figures 50, 51 illustrate N720/AS material as received at a magnification of 6000x. It was used for comparison reasons. The grains of the matrix material as well as the micro-cracks and the pores are clearly observable. Figure 52 and 53 are pictures of the matrix of the Steam Aged specimen. It seems that after 12 hours at 1200^0C in steam environment with zero loading the matrix material started "morphing" or densified as pores are not observable as in figures 50, 51. Jurf and Butner [10] tested the same material and observed a decrease of 70% in strength after 1000h at 1100^0C. Their suggestion was that the lost in strength was due to densification of the matrix. Antii, Lara-Curzio and Warren [2] reported that exposure of N720AS CMC for 100h at 1100^0C led to a combination of matrix densification and increased fiber/matrix bonding. They also reported a partial change of phase of the matrix material as the silica in the matrix from an amorphous state crystallized to cristobalite.

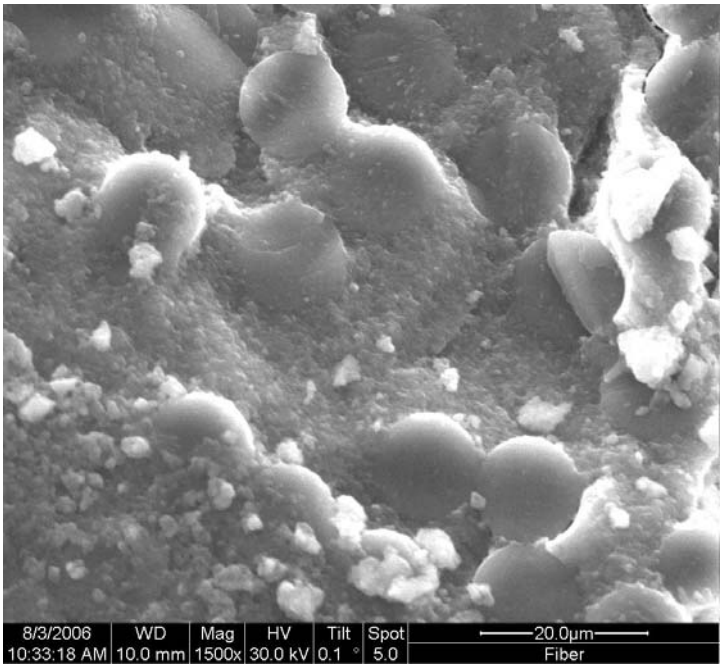

Figure 52. Specimen Steam Aged - 1500x

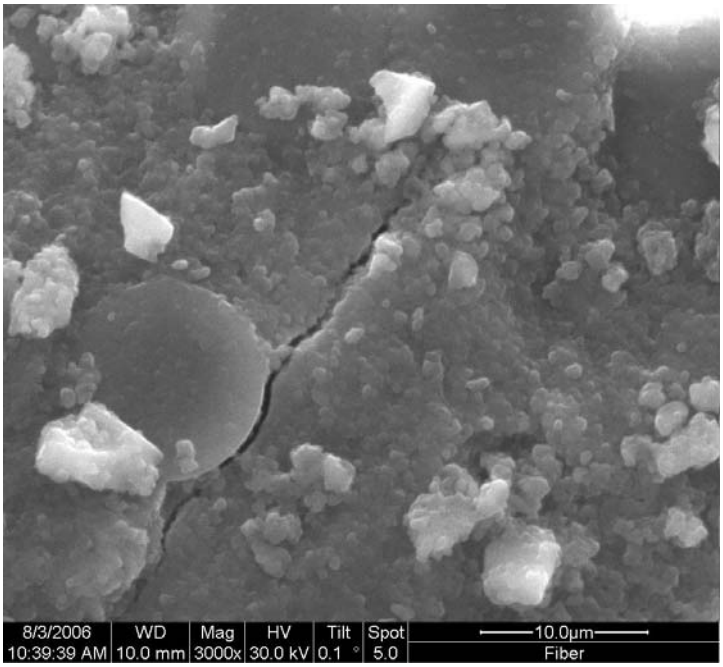

Figure 53. Specimen Steam Aged - 3000x

Further examination of the specimens at the SEM, revealed spots at the fractured surfaces where matrix material seemed as it was “melted” or “liquified” during the test. This pattern can be seen at figures 54, 55, 56, 57. It should be noted that this ‘melted” phase of the matrix material was observed only in specimens that where tested in lower load levels- that is the specimens that stayed longer at 1200^0C. The fact that this phase is present at specimen S100 that fractured after only .27h signifies that the steam environment “accelerated” this transformation of the matrix.

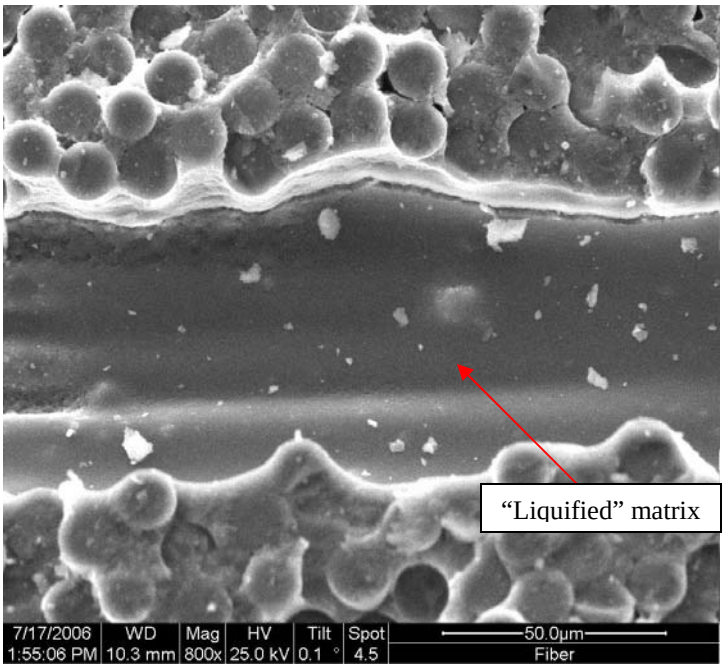

Figure 54. Specimen S100- 800x

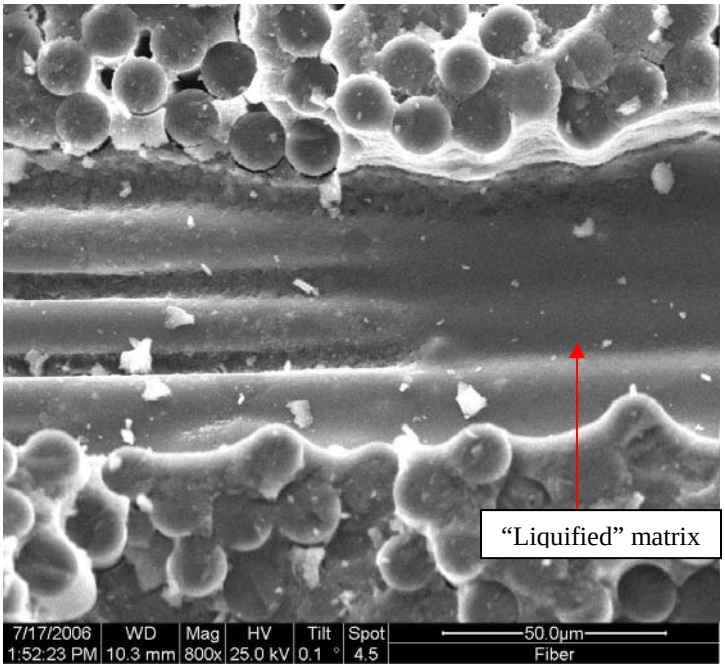

Figure 55. Specimen S100- 800x

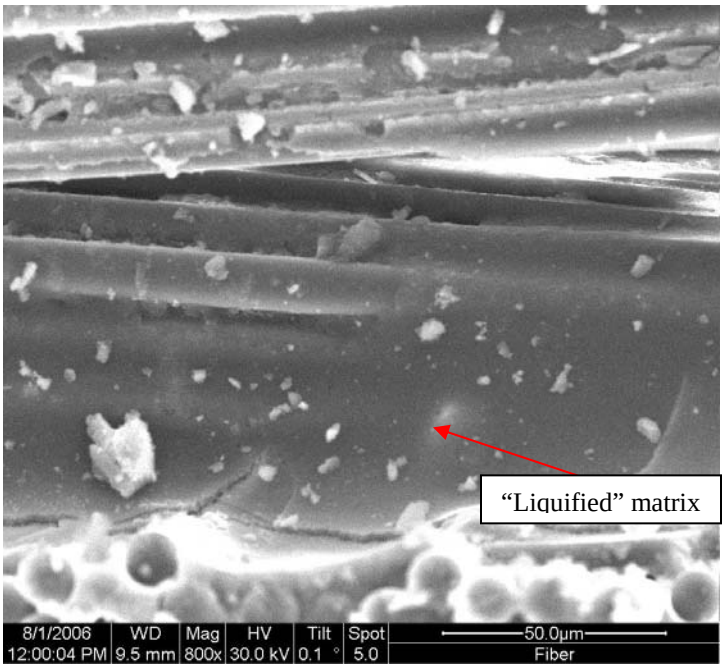

Figure 56. Specimen A80- 800x

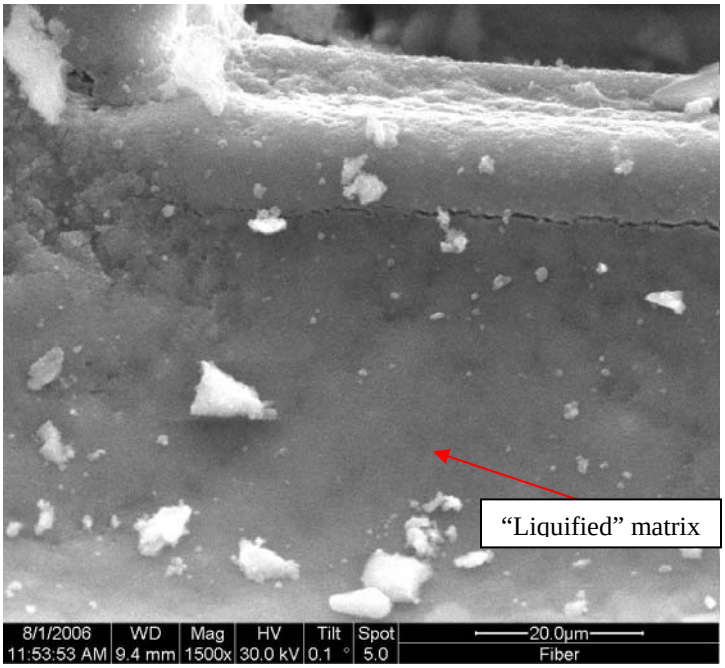

Figure 57. Specimen A80- 1500x

Comparing the fracture surfaces of the specimens tested in steam, the trend that was observed was that the lower the load level, the denser the matrix material was. This is particularly apparent by observing the propagation of the cracks at figures 59, 60, 61, 62. At a grainy matrix as N720/AS has, the cracks should propagate around the grains and these grains should be observable like the crack depicted at figure 58, something that wasn't observed at figures 59, 60, 61, 62 where the crack propagated in a straight line and no grains are observable.

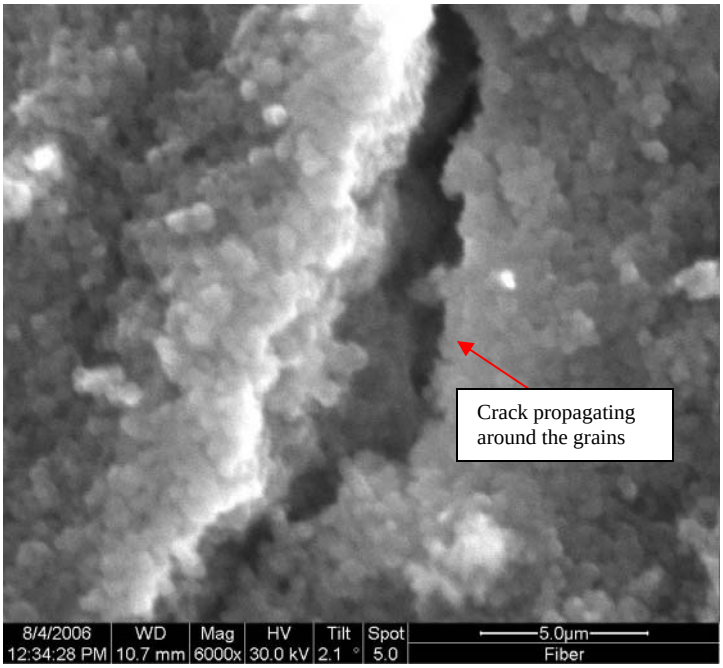

Figure 58. Specimen Virgin A - 6000x

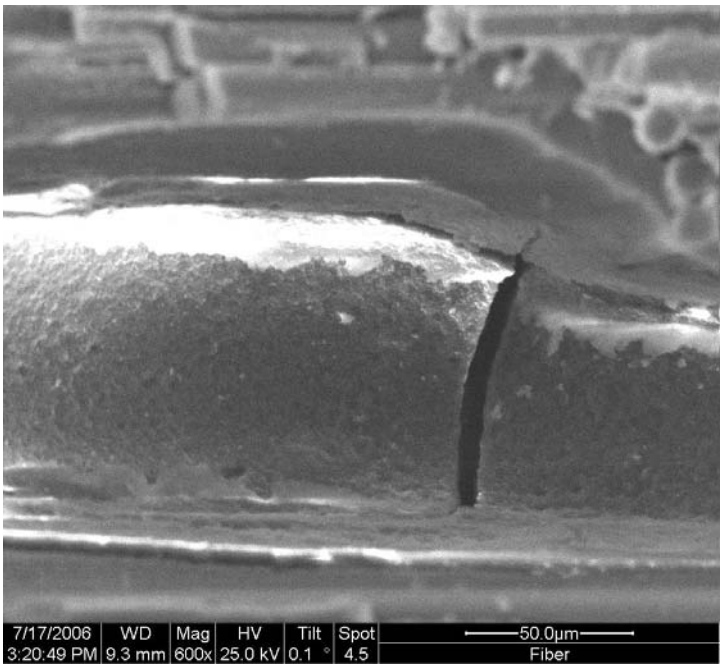

Figure 59. Specimen S80- 600x

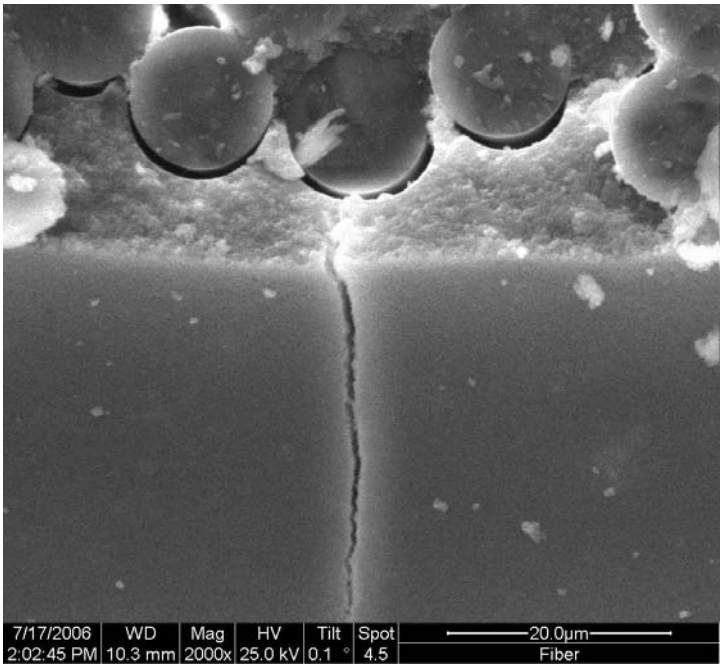

Figure 60. Specimen S100- 2000x

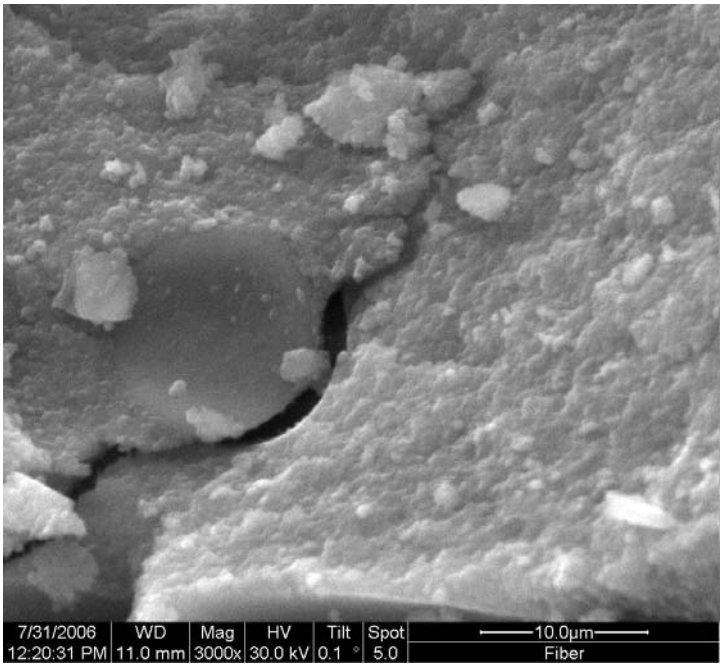

Figure 61. Specimen S125- 3000x

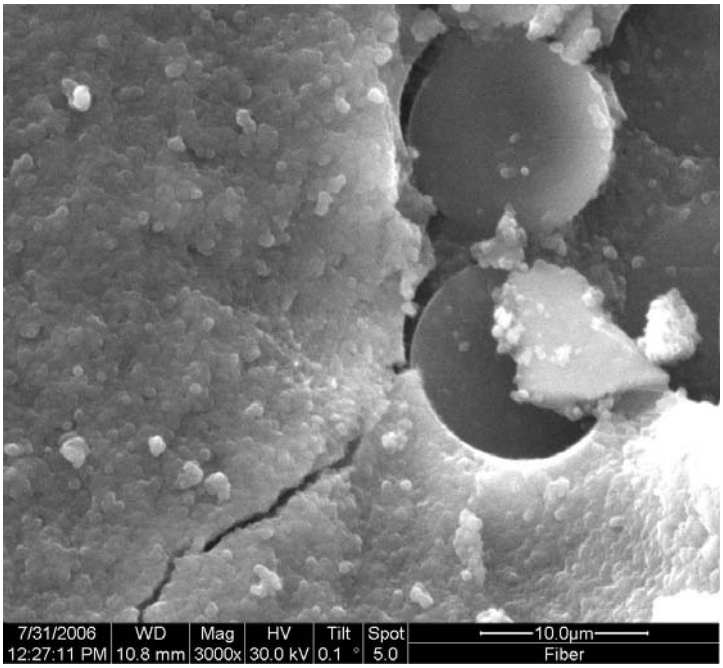

Figure 62. Specimen S150- 3000x

The same trend of matrix densifying the longer the longer the specimen remained at 1200^0C was observed for the specimens tested in air and argon environment for N720/AS CMC as can be seen at figures 63-69. The densification of the matrix can be used to explain the reason why the fracture surfaces appeared so flat, since a denser matrix would formatted a stronger fiber-matrix interface, thus not allowing crack to propagate around the fibers and fibers to pull out, leading to a CMC acting like a monolithic material.

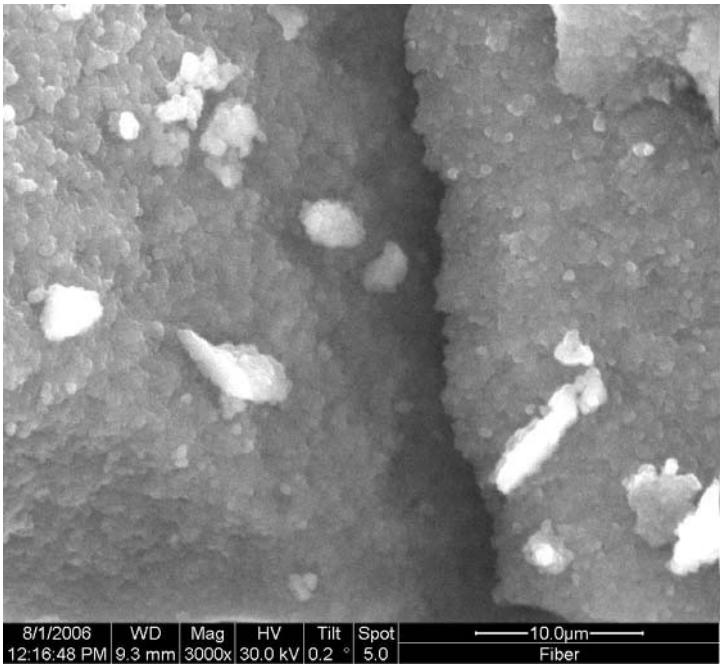

Figure 63. Specimen A80- 3000x

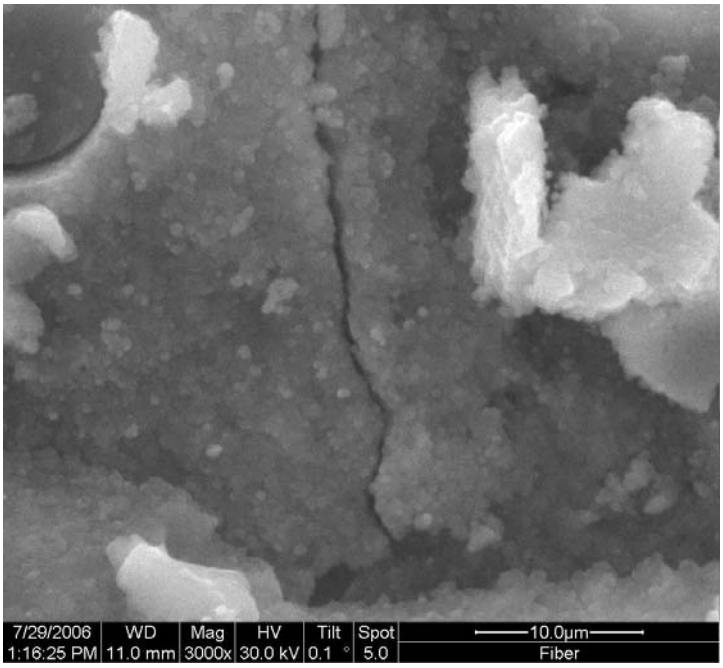

Figure 64. Specimen A95- 3000x

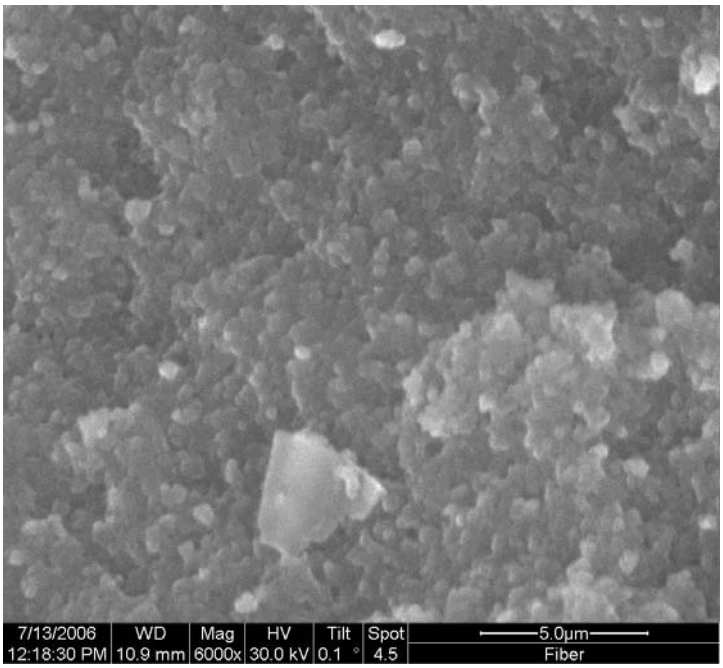

Figure 65. Specimen A125- 6000x

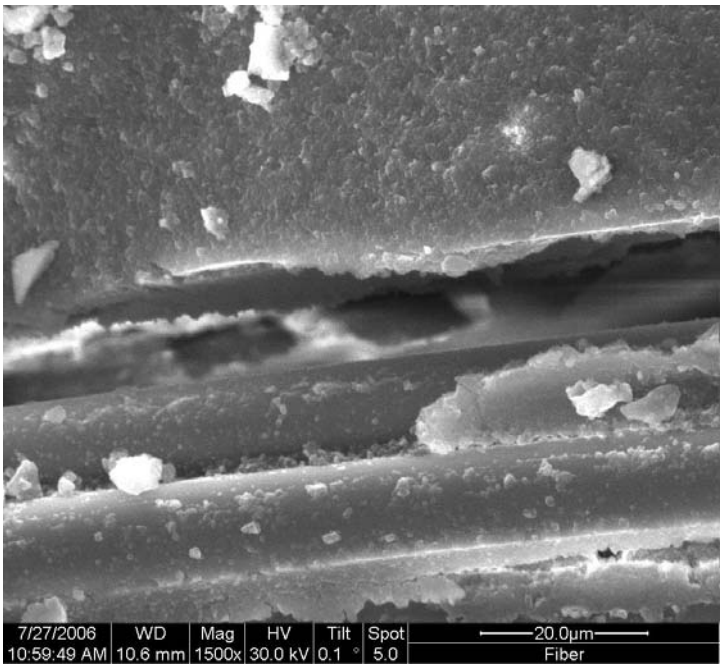

Figure 66. Specimen AsAr80- 1500x

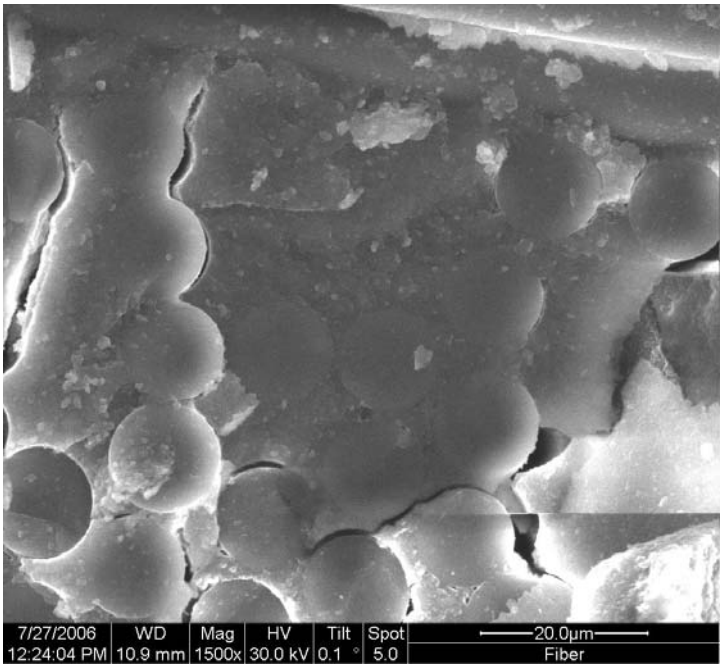

Figure 67. Specimen AsAr100- 1500x

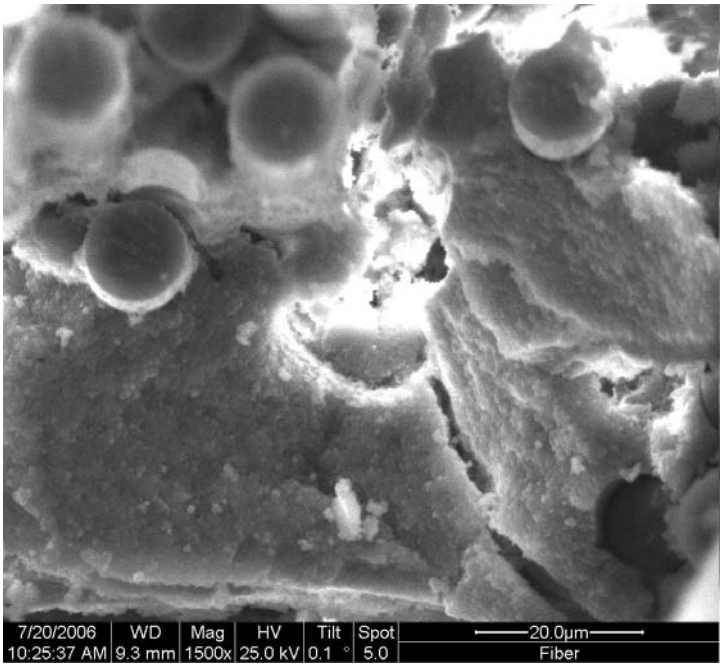

Figure 68. Specimen AsAr125-1500x

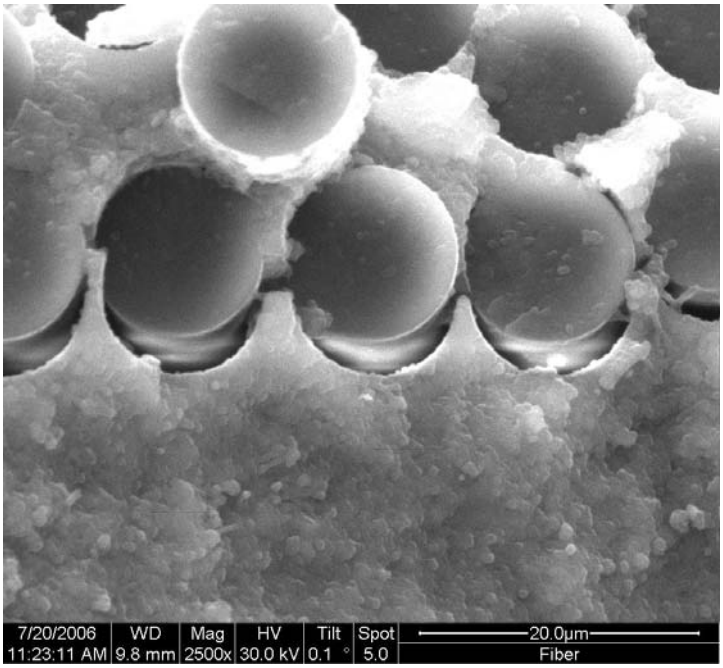

Figure 69. Specimen AsAr150-2500x

Examining the fracture surfaces of the N720/A CMC revealed that the matrix material maintained its properties that are the grains and the micro-pores as can be seen in figures 70, 71.

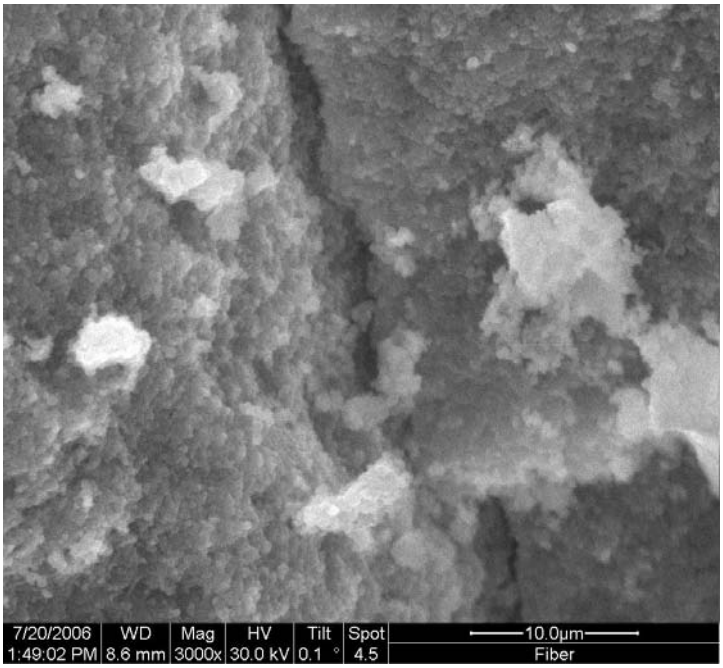

Figure 70. Specimen AAr125-3000x

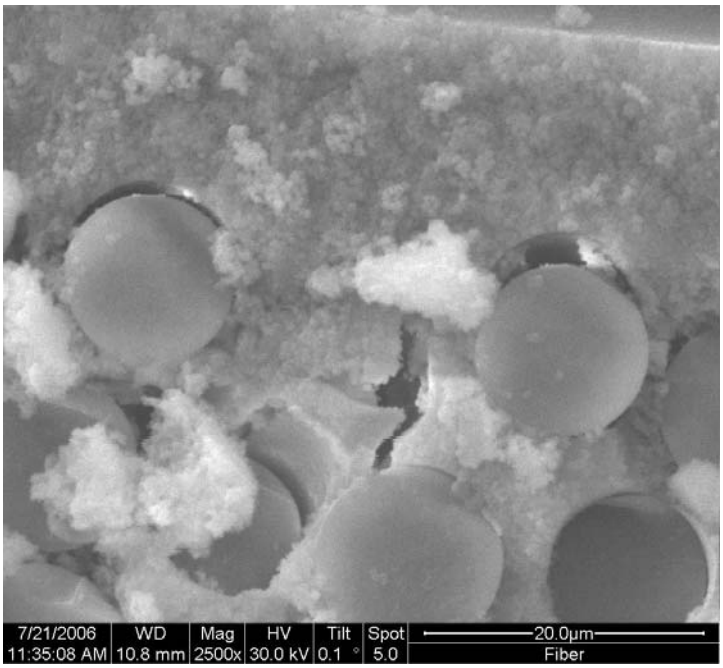

Figure 71. Specimen AAr150-2500x

V. Conclusion and Recommendations

6.1. Conclusions

6.1.1. Mechanical Testing

Prior to creep-rupture tests, monotonic tensile tests were performed at 1200^0C in laboratory air environment for the N720/AS CMC. The ultimate tensile test recorded was 231 MPa, the modulus of elasticity 55Gpa and the failure strain 0.44%. For N720/A material Harlan [8] reported UTS of 192 MPa, modulus of elasticity 75 GPa and failure strain 0.38%.

For N720/AS CMC creep-rupture tests were conducted at stress levels of 80,100, 125 and 150 MPa, in laboratory air, 100% steam and 100% argon environment.

Comparing the results between the different environments led to the conclusion that the shorter creep life at the same stress levels was recorded by the specimens tested in steam.

Specimen tested in steam at 150 MPa didn't reach the required stress level and failed during ramp up at 131 MPa.

Additional tensile test was performed in a specimen that was left for 12 hours at 1200^0C in steam environment. The UTS was 83 MPa, modulus of elasticity 48 GPa and failure strain 0.15%.

Tests in air and argon at 80 and 100MPa reached 100 hours without failing.

Specimens of N720/A material tested in argon had larger rupture times than those reported for the same material by Harlan [8] in steam and air, and fron N720/AS specimen tested in argon.

Comparing the results in steam of N720/AS with those reported by Harlan [8] for N720/A indicates that N720/AS has worst creep performance. The above comparisons indicate that alumina matrix has better mechanical characteristics.

6.1.2. Microstructure Analysis

Examination of the fractured specimens in optical microscopy revealed a trend at N720/AS CMC.

The specimens tested in steam environment were flatter than those tested in air and the specimens in air were flatter than the ones tested in argon.

In all environments it was observed that the lower the stress level, the flatter the fracture surface was.

No such trend was reported by Harlan [8] for N720/A CMC tested in air and steam or was observed in tested specimens in argon.

The SEM examination of the specimens in lower magnification revealed again the same trend. Examination in higher magnification showed that matrix degradation was the main cause for the fracture of the specimens. Aluminosilicate matrix “densified”, as less micro-pores were observed compared to the as received material. Areas were found in lower stress levels at air and steam environments, were matrix appeared “melted” or “liquified”. Denser matrix led to a stronger fiber-matrix interface, thus not allowing crack to propagate around the fibers and fibers to pull out. Matrix material in argon environment appeared less dense than in air or steam.

Matrix in specimens of N720/A material tested in argon were grainier and with more micro- pores compared to the N720/AS matrix material.

6.2. Recommendations

The current research together with Harlan's [8] report concluded the evaluation of N720/A and N720/AS specimens of $0/90^0$ fiber orientation. Further research should be done in $+\text{-}45^0$ fiber orientation N720/AS CMC, so that the additional results would give the whole evaluation of these oxide/oxide materials.

Additional research could be done on the aging under high temperature aspect of aluminosilicate matrix and how the matrix is affected by the environment. This kind of research could focus on the "phase" change of the matrix and its change of density and micro-porosity. For this research to be carried out, a more advanced electron microscope should be used, the Transmission Electron Microscope (TEM), which is capable of far better analysis than SEM.

D.M.Wilson [6] reported on new high temperature oxide fibers that have superior creep performance than N720 fiber. The results of a CMC made with that fiber would be very interesting to compare with the available ones.

Appendix: Additional SEM Pictures

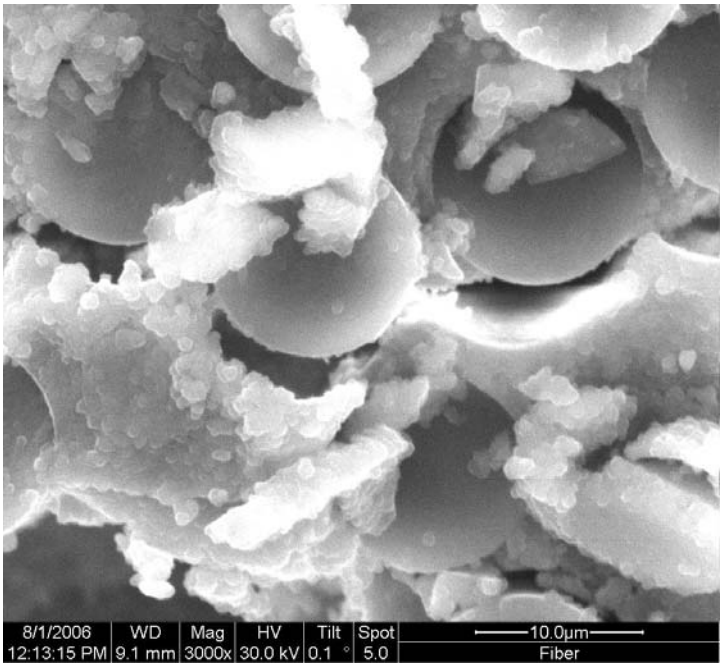

Figure 72. Specimen A80- 3000x

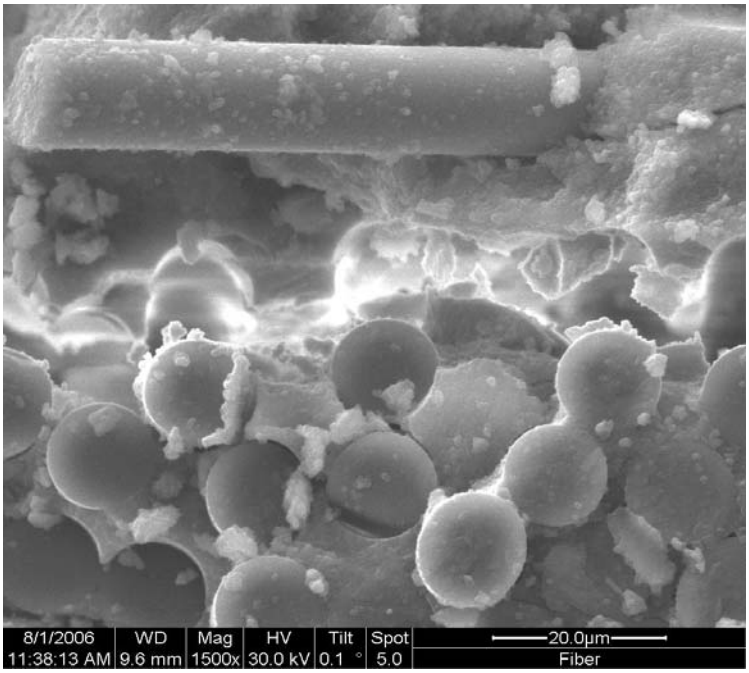

Figure 73. Specimen A80- 1500x

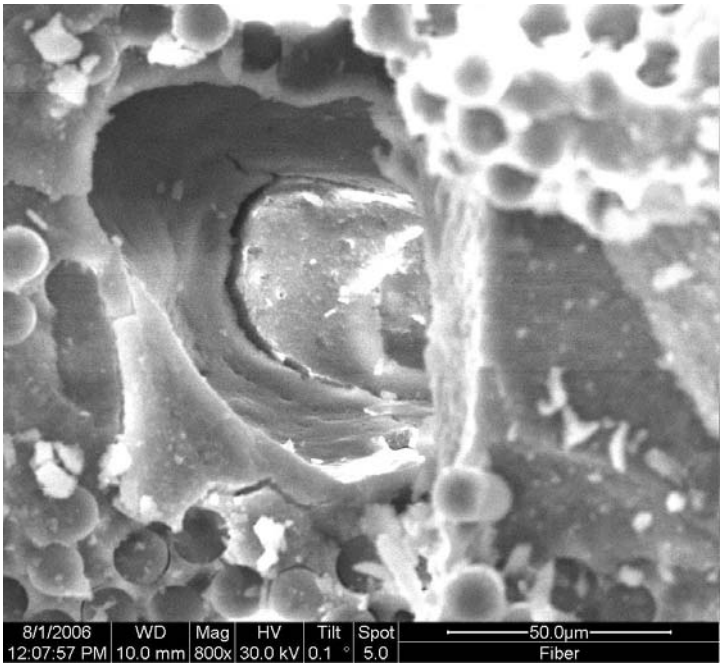

Figure 74. Specimen A80- 800x

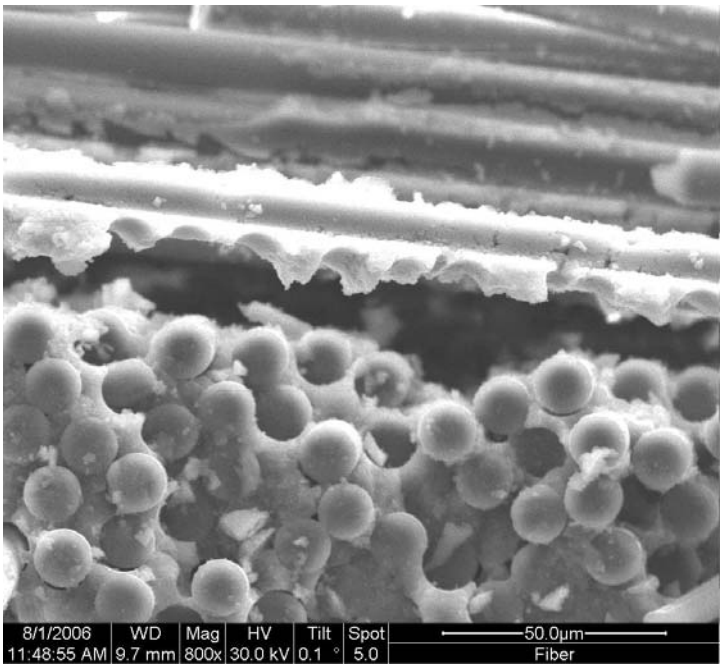

Figure 75. Specimen A80- 800x

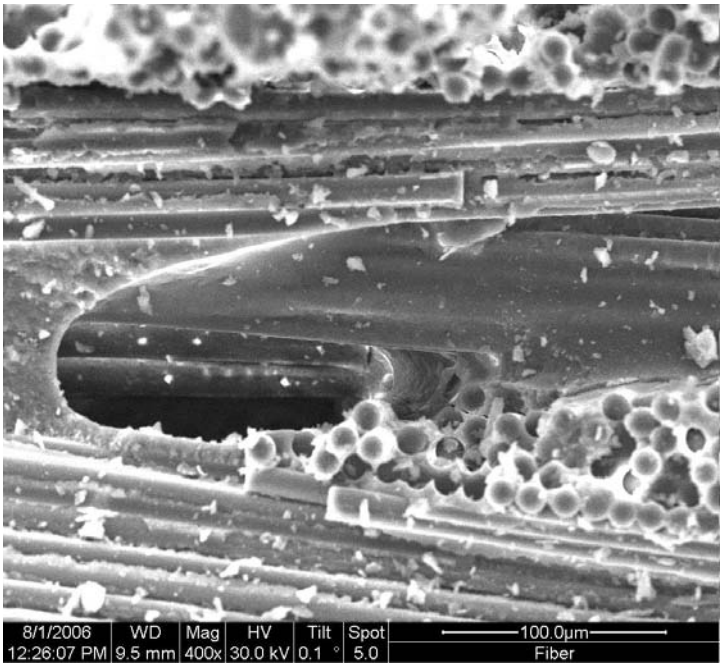

Figure 76. Specimen A80- 400x

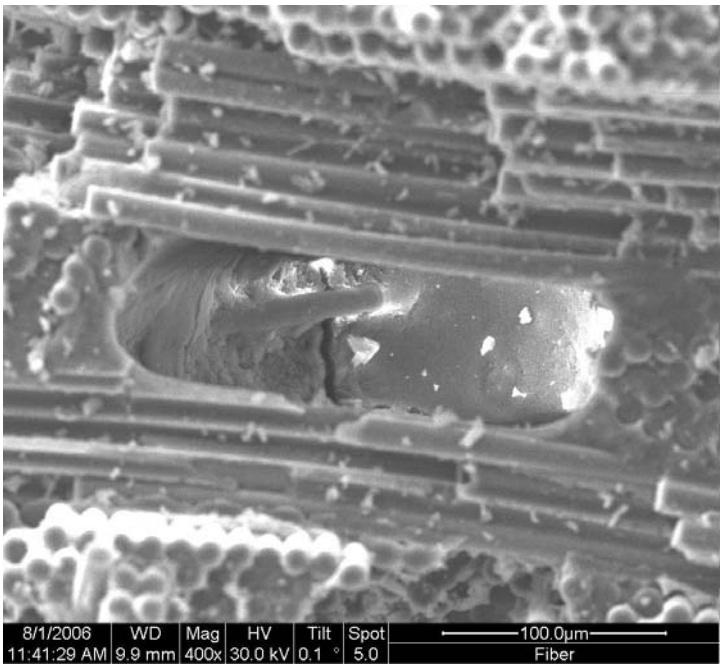

Figure 77. Specimen A80- 400x

Figure 78. Specimen A80- 200x

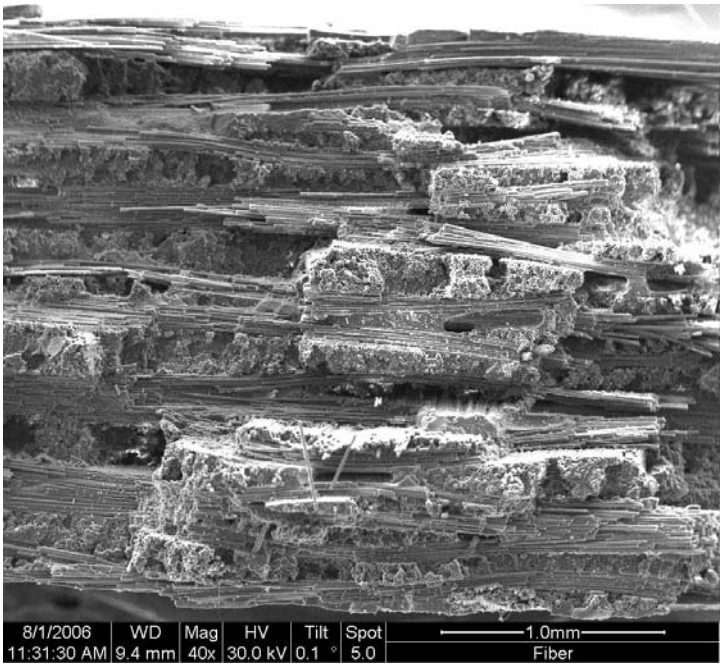

Figure 79. Specimen A80- 40x

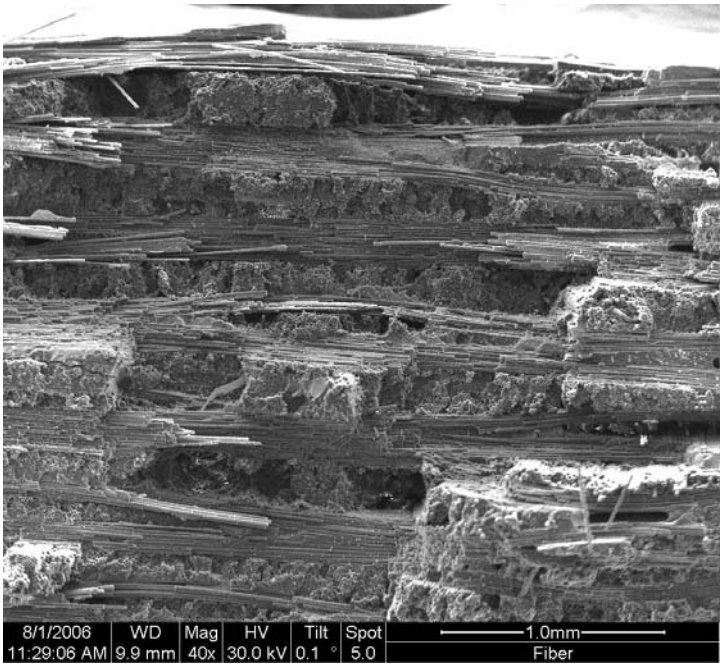

Figure 80. Specimen A80- 40x

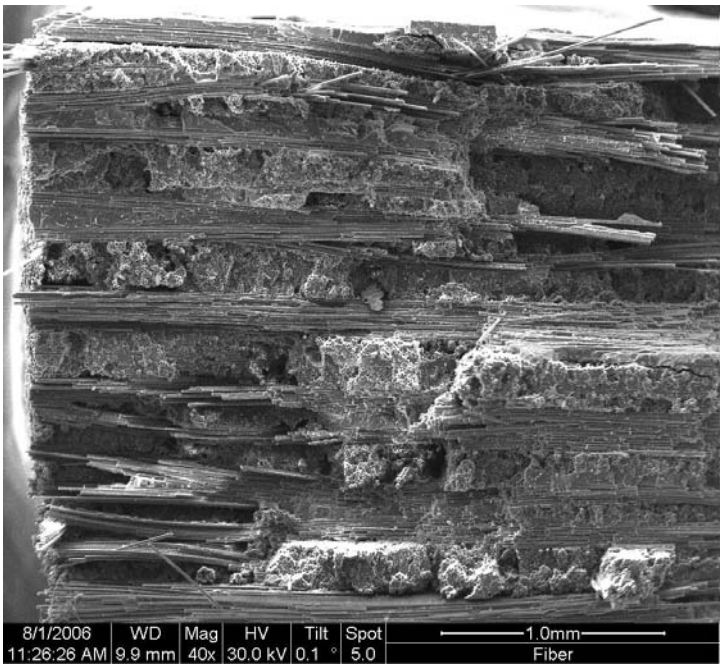

Figure 81. Specimen A80- 40x

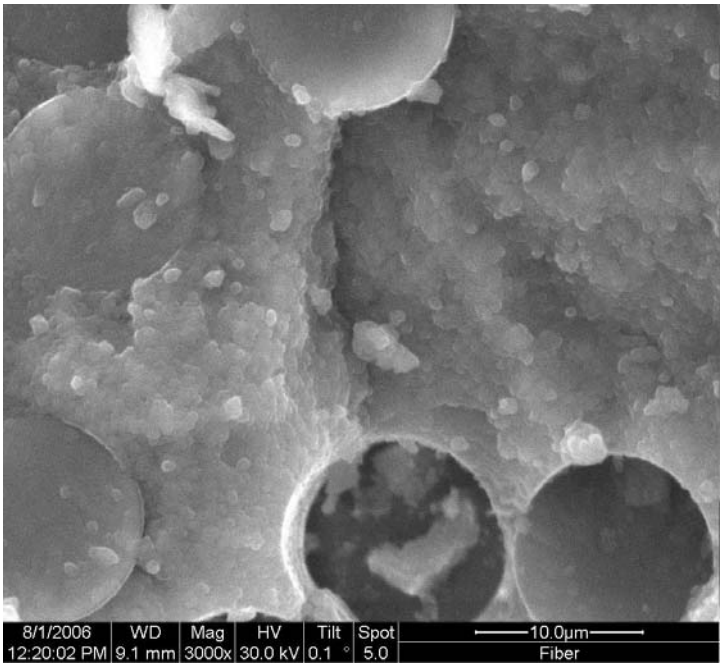

Figure 82. Specimen A80- 3000x

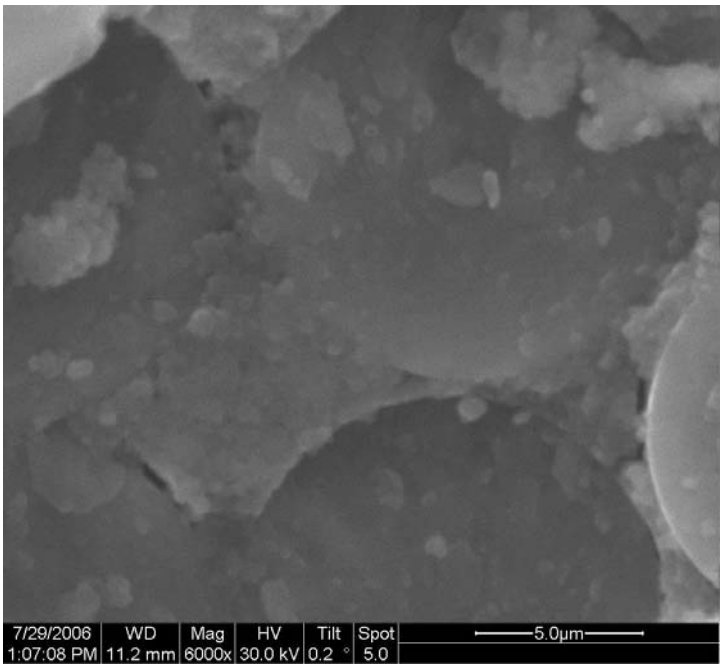

Figure 83. Specimen A95- 6000x

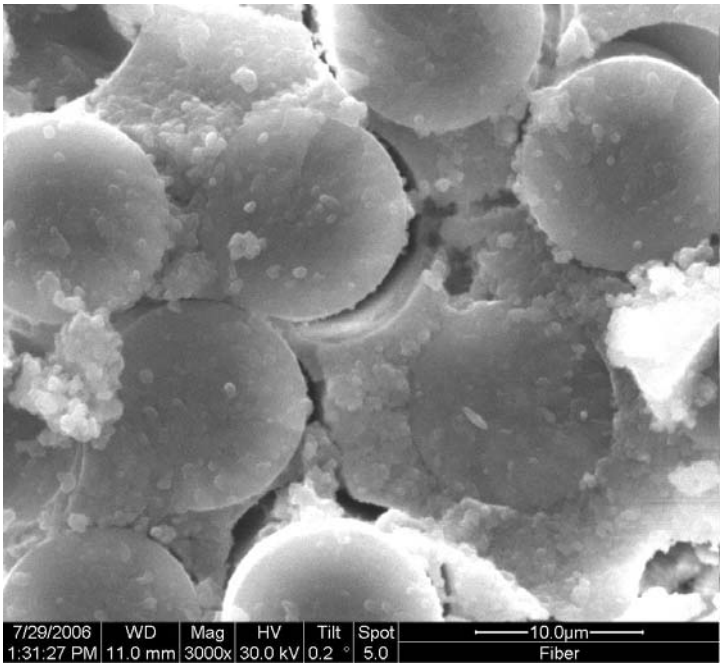

Figure 84. Specimen A95- 3000x

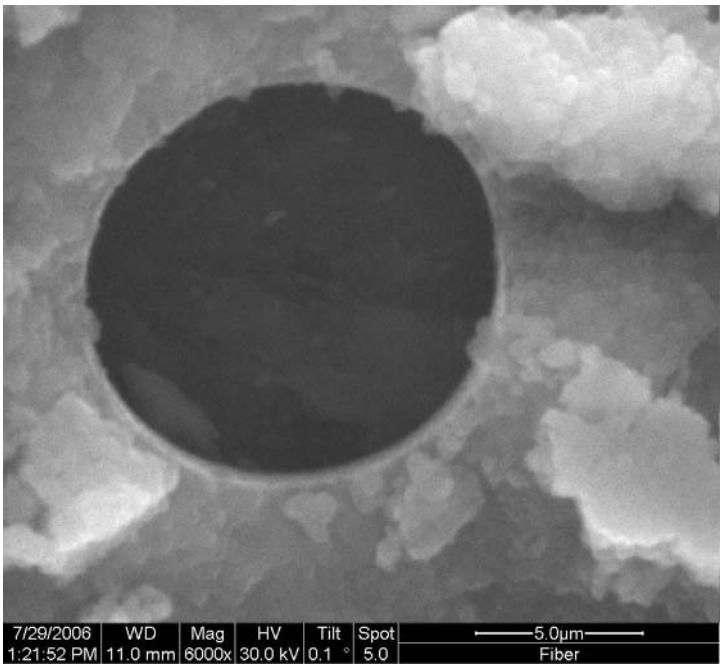

Figure 85. Specimen A95- 6000x

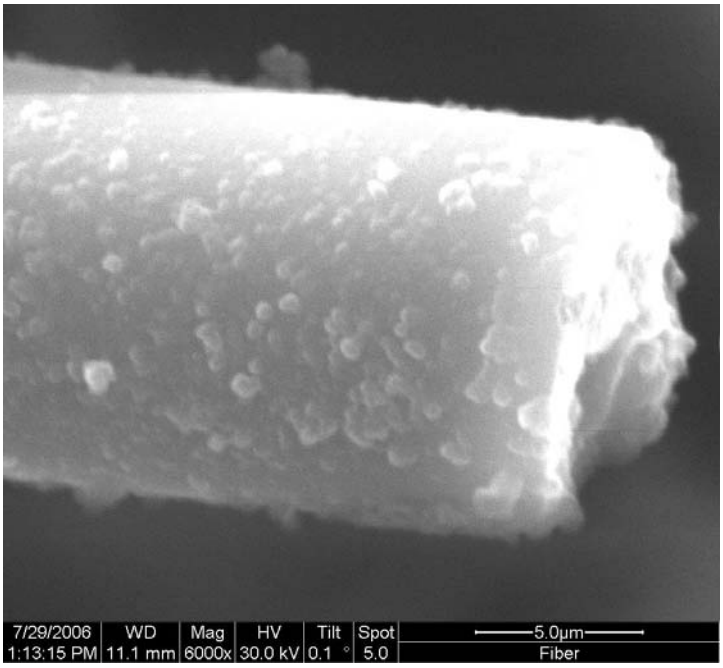

Figure 86. Specimen A95- 6000x

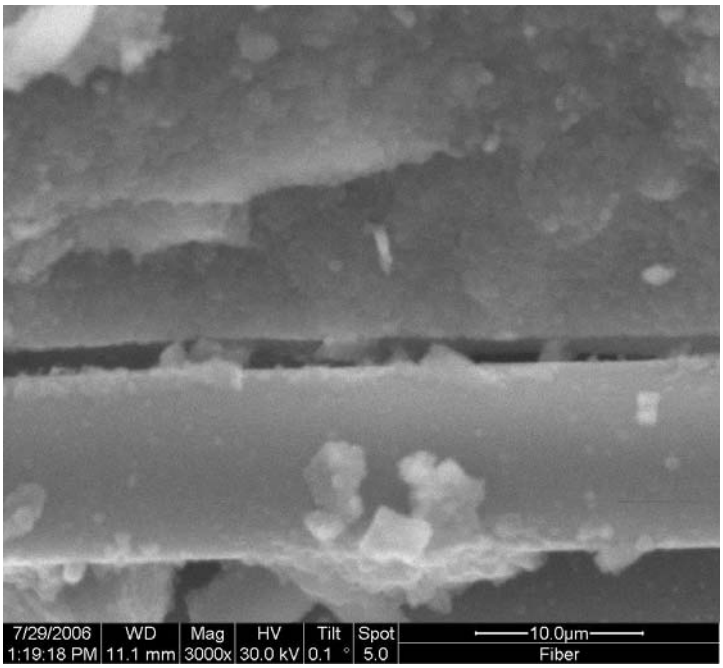

Figure 87. Specimen A95- 3000x

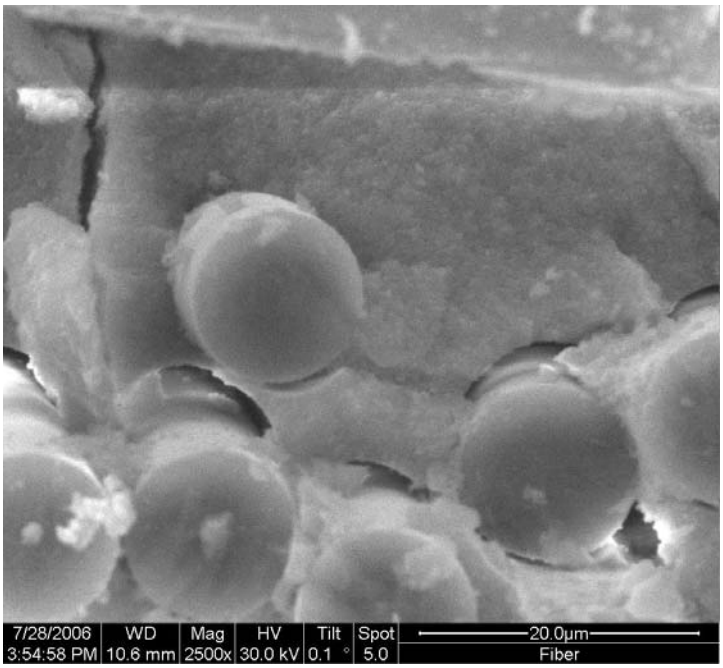

Figure 88. Specimen A95- 2500x

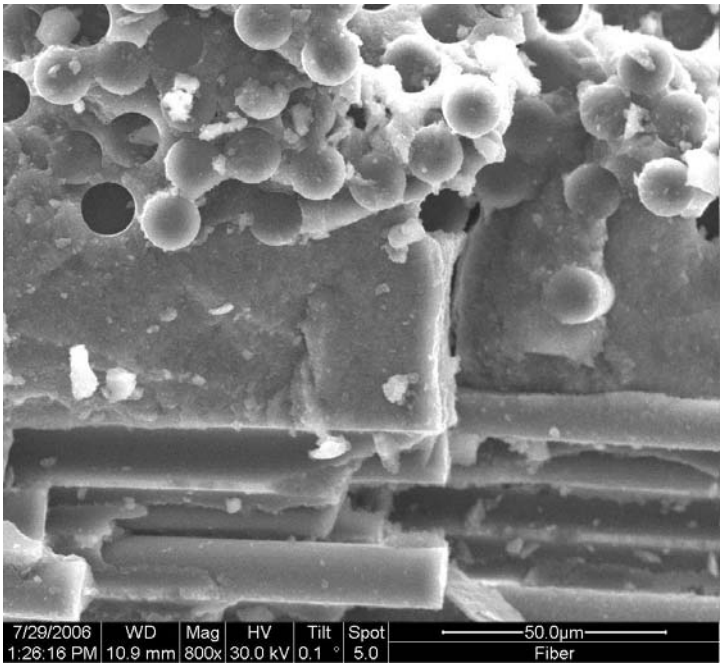

Figure 89. Specimen A95- 800x

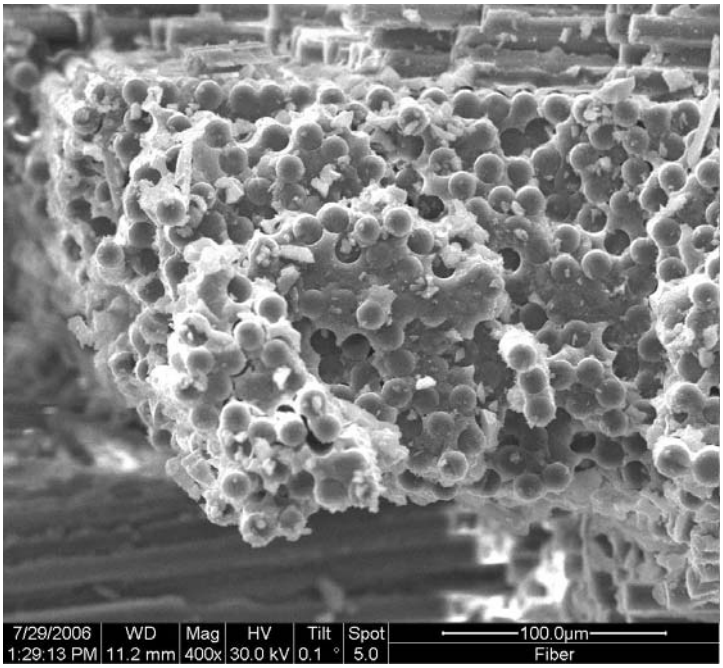

Figure 90. Specimen A95- 400x

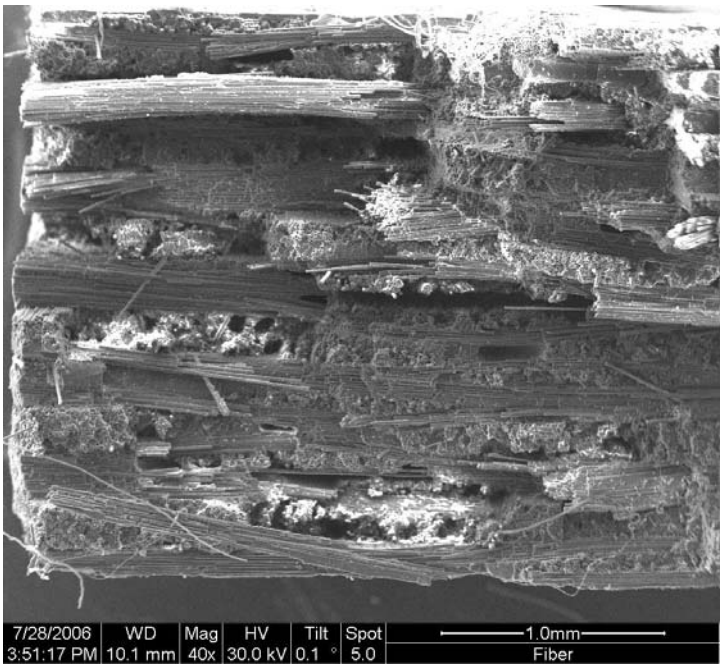

Figure 91. Specimen A95- 40x

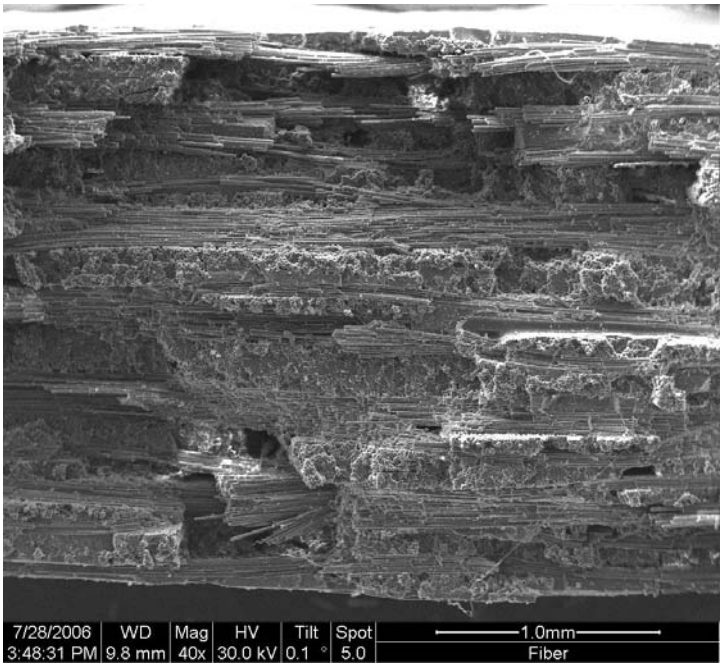

Figure 92. Specimen A95- 40x

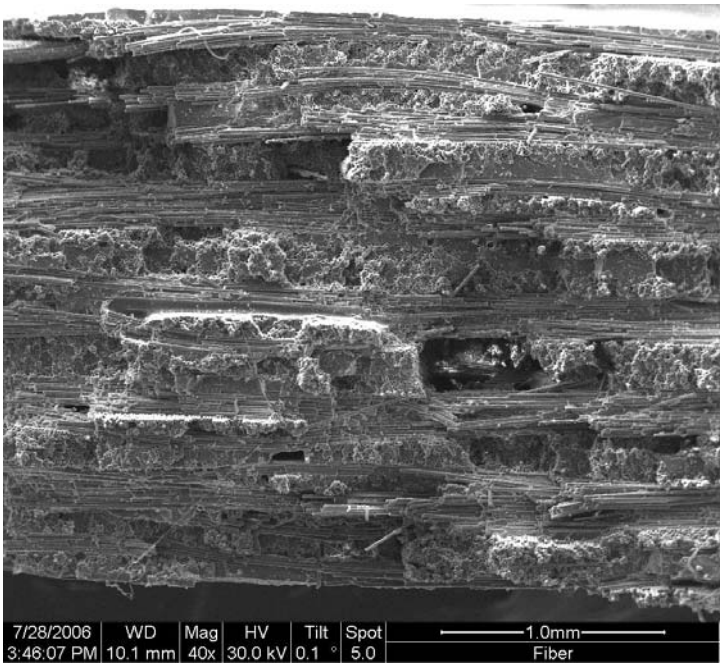

Figure 93. Specimen A95- 40x

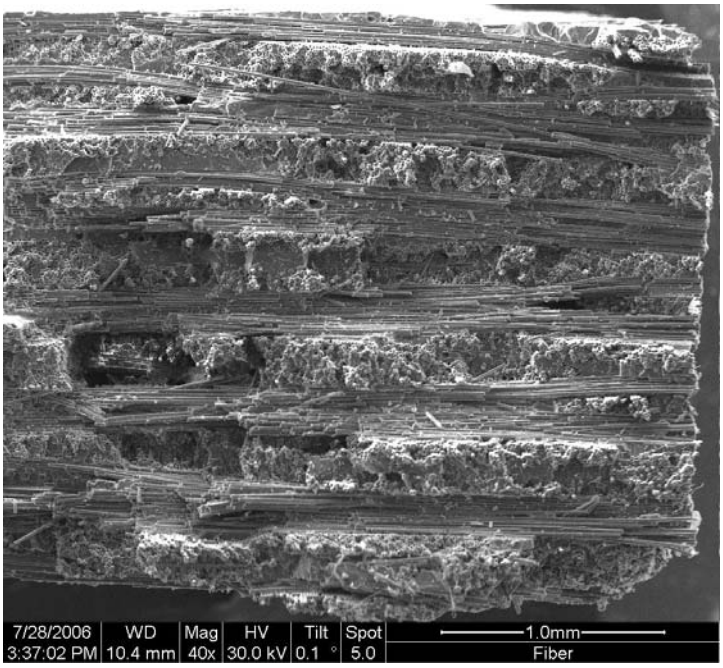

Figure 94. Specimen A95- 40x

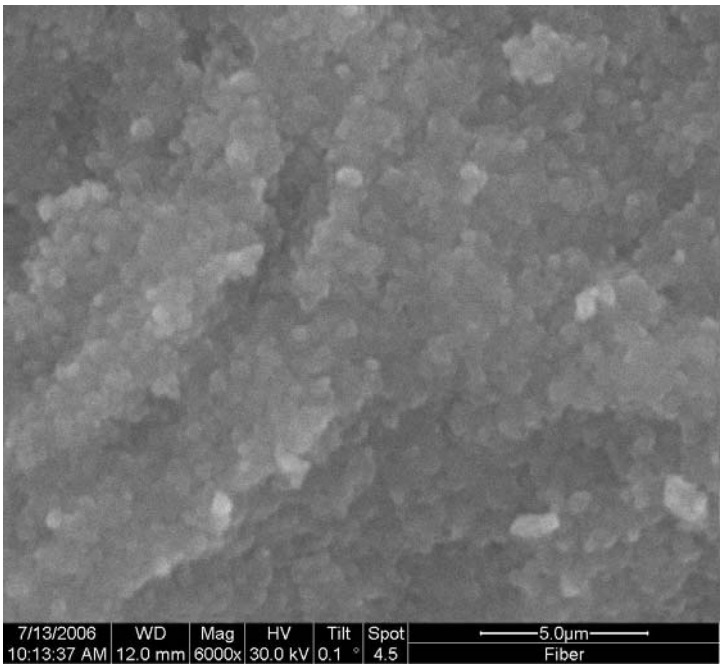

Figure 95. Specimen A125- 6000x

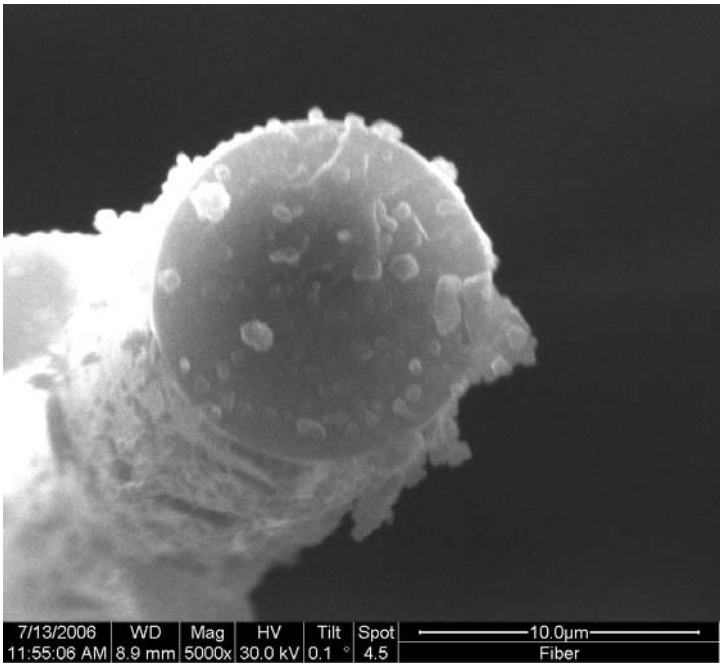

Figure 96. Specimen A125 -5000x

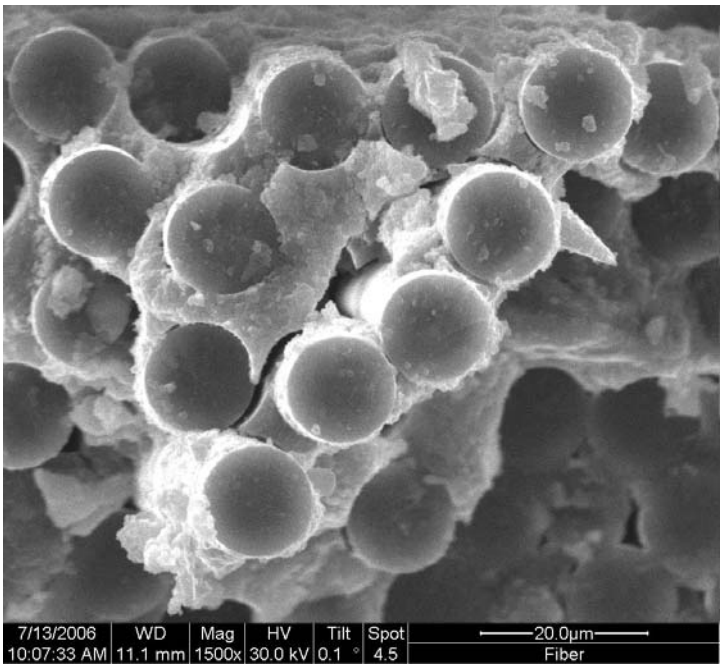

Figure 97. Specimen A125- 1500x

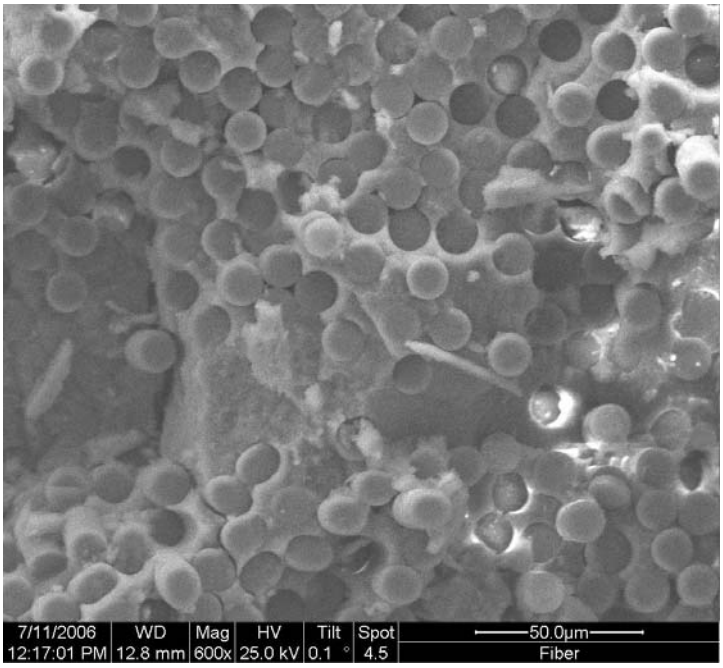

Figure 98. Specimen A125- 600x

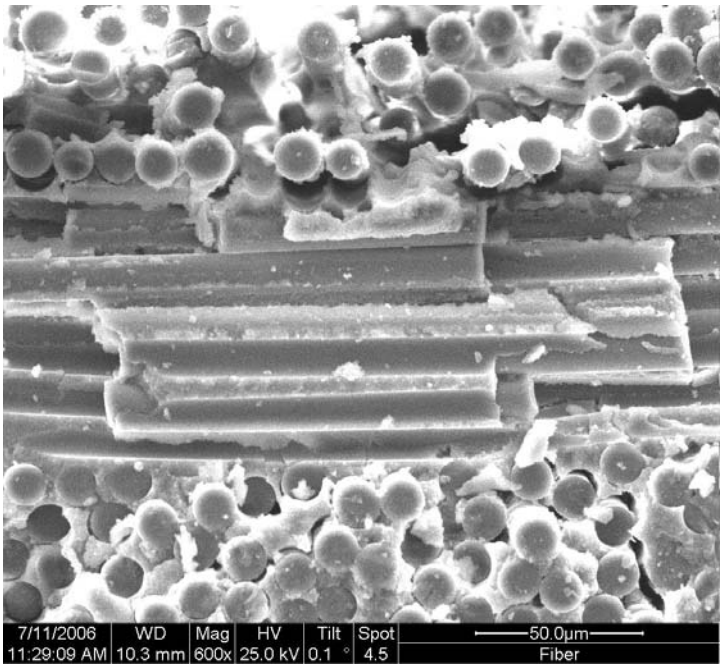

Figure 99. Specimen A125- 600x

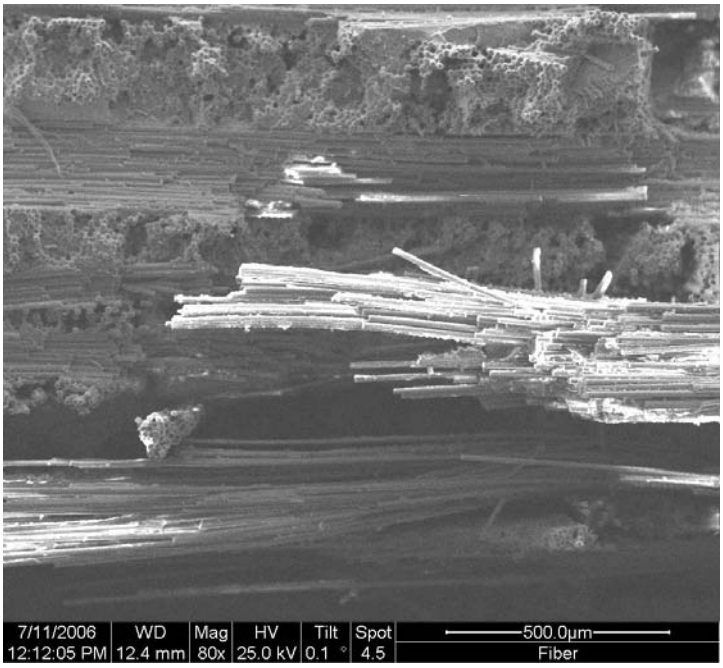

Figure 100. Specimen A125- 80x

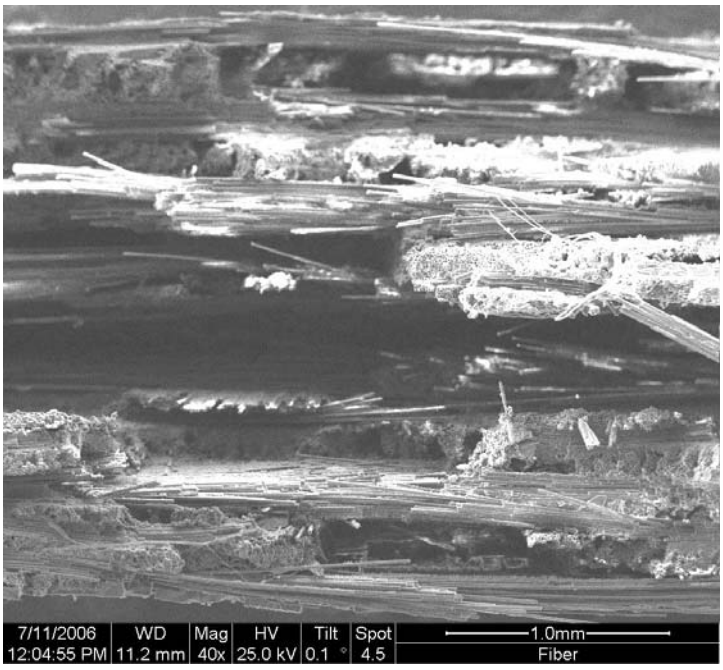

Figure 101. Specimen A125- 40x

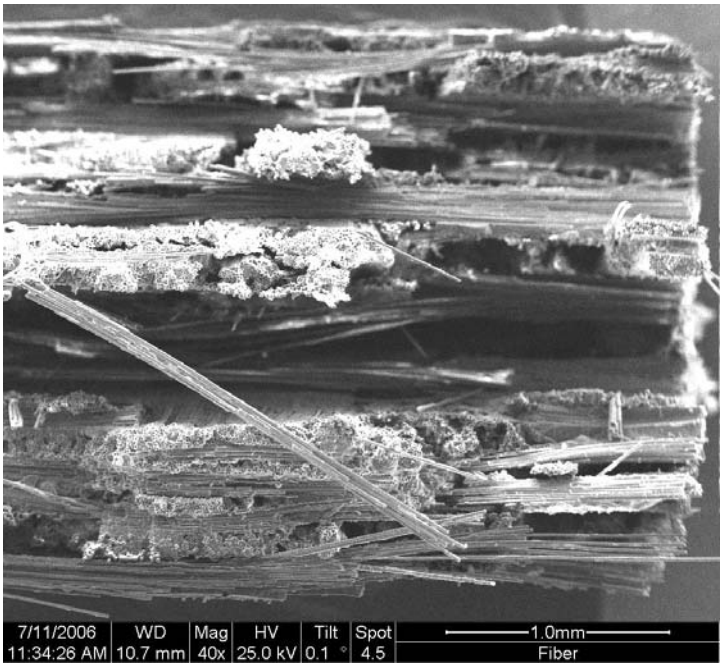

Figure 102. Specimen A125- 40x

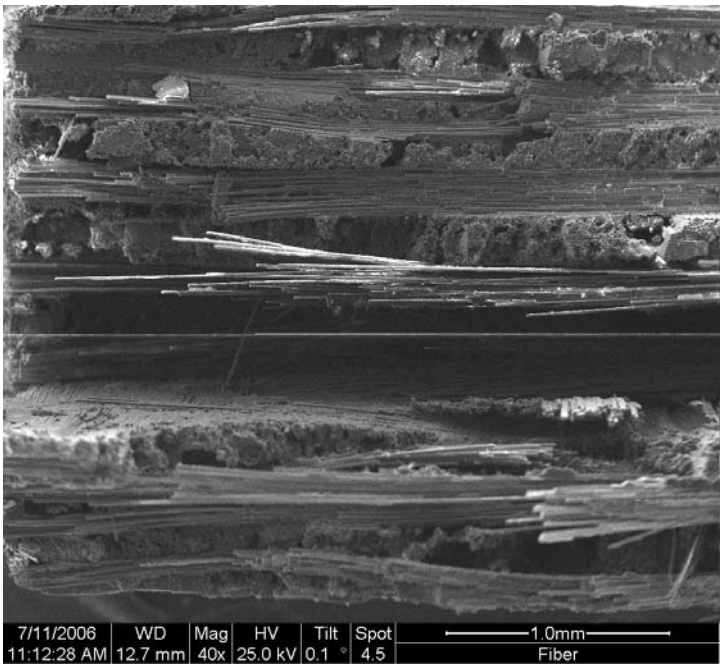

Figure 103. Specimen A125- 40x

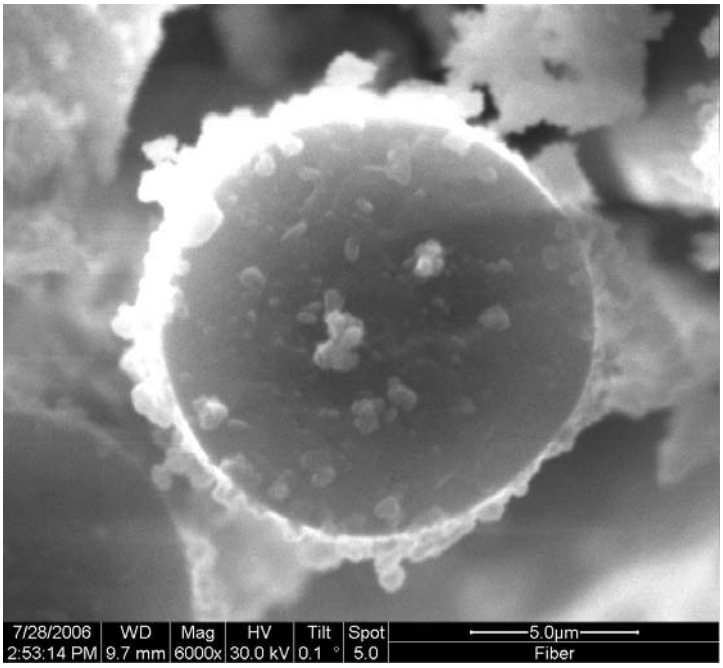

Figure 104. Specimen A150- 6000x

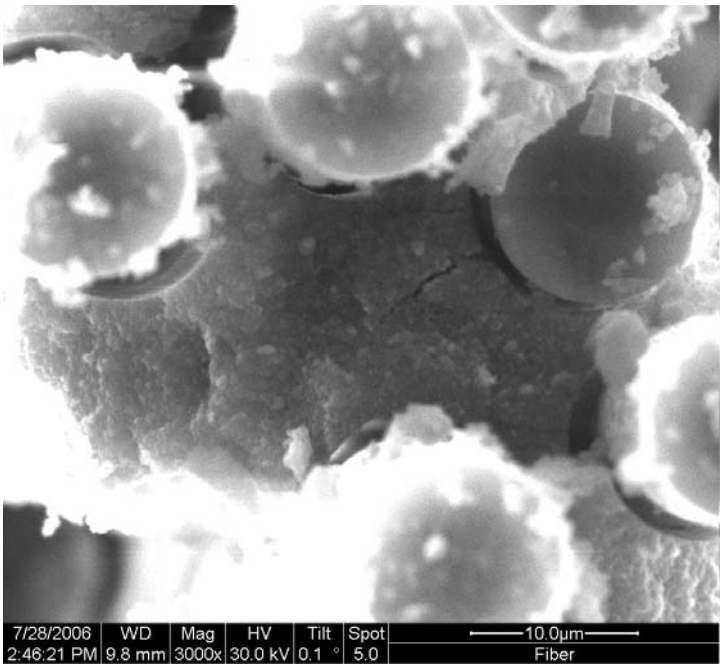

Figure 105. Specimen A150- 3000x

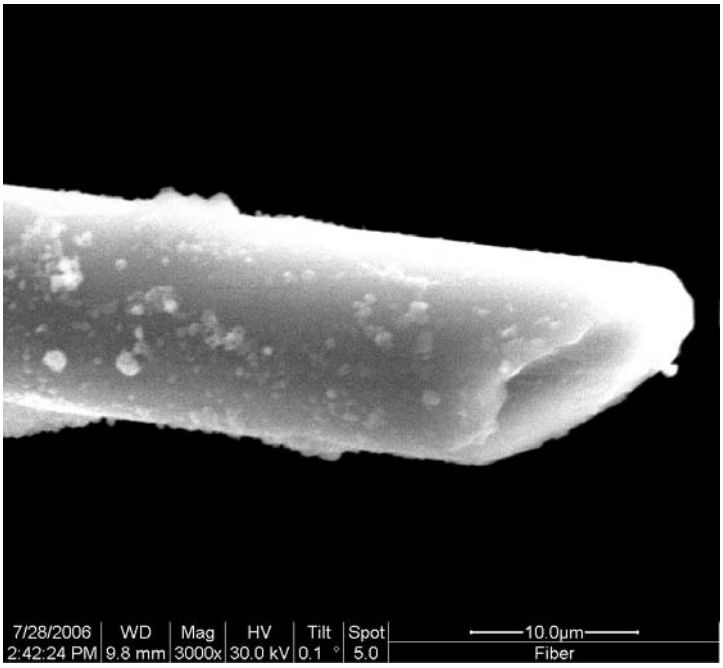

Figure 106. Specimen A150- 3000x

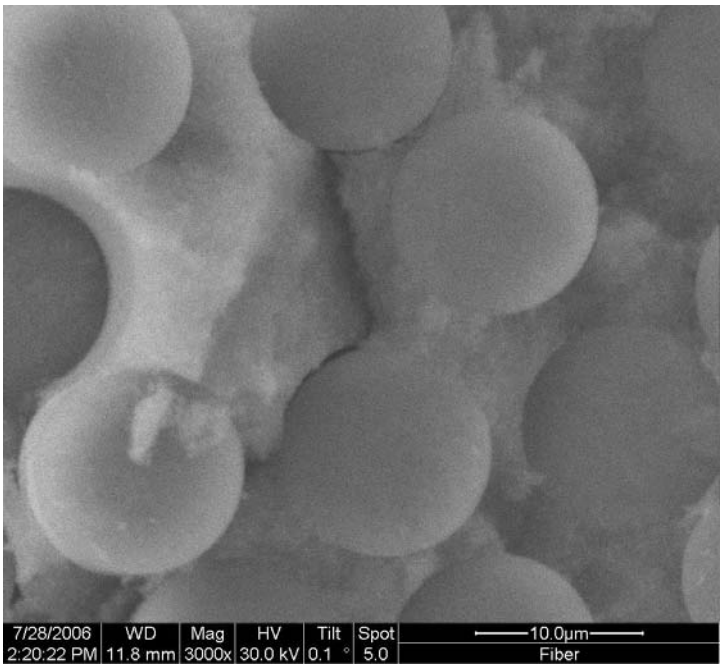

Figure 107. Specimen A150- 3000x

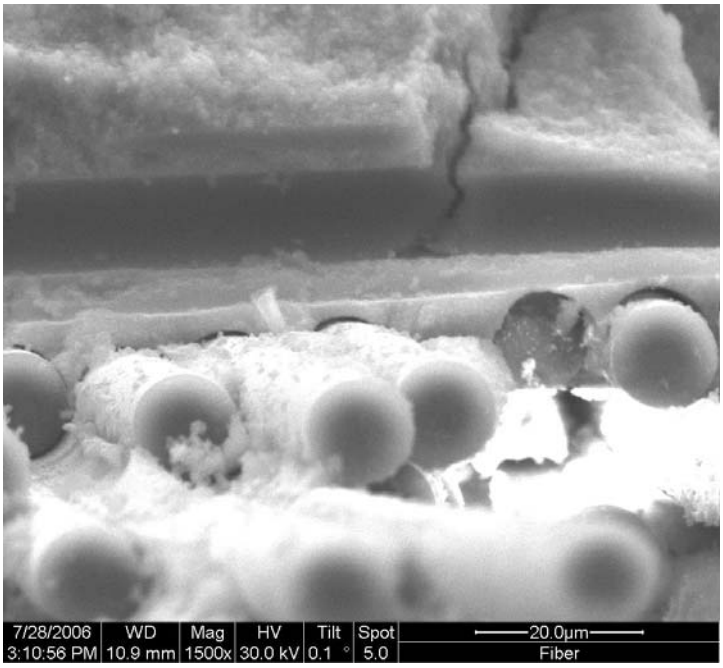

Figure 108. Specimen A150- 1500x

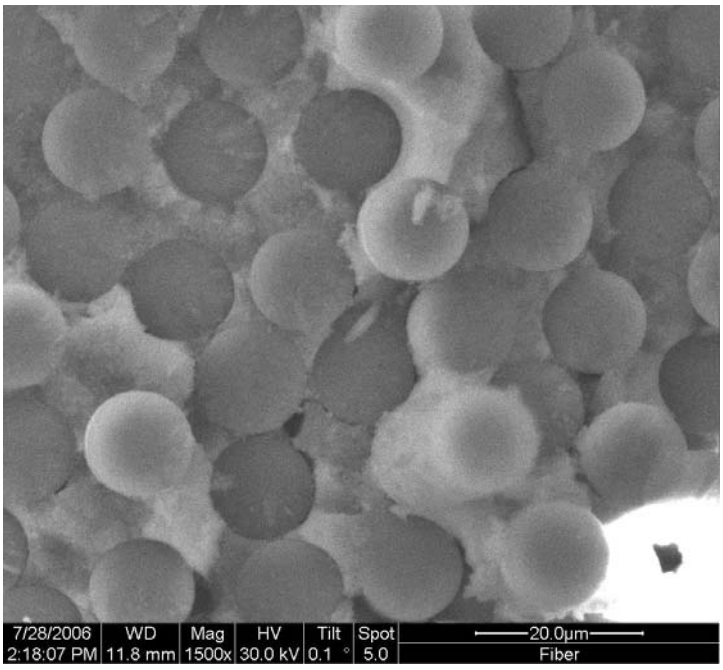

Figure 109. Specimen A150- 1500x

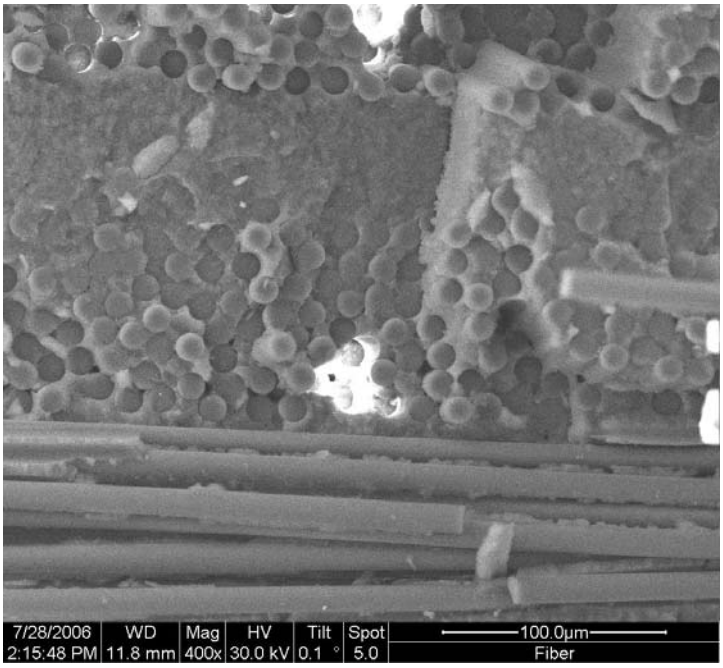

Figure 110. Specimen A150- 400x

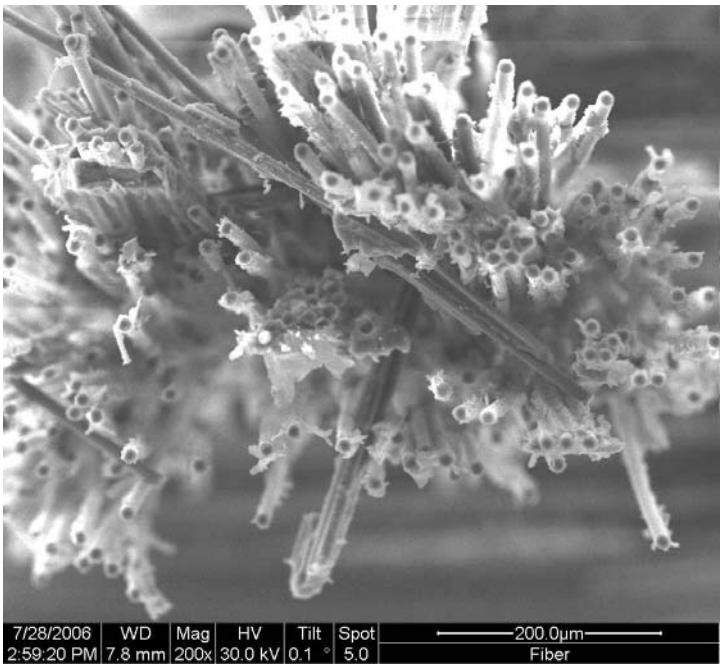

Figure 111. Specimen A150- 200x

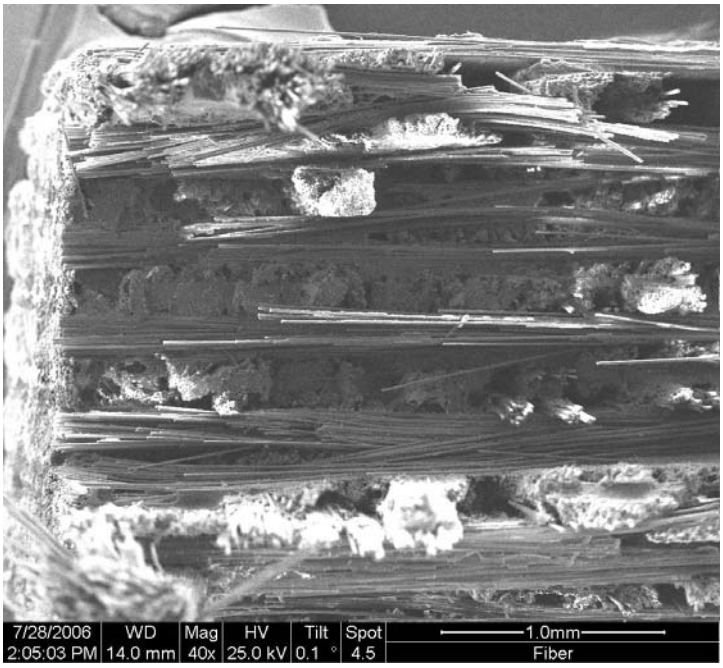

Figure 112. Specimen A150- 40x

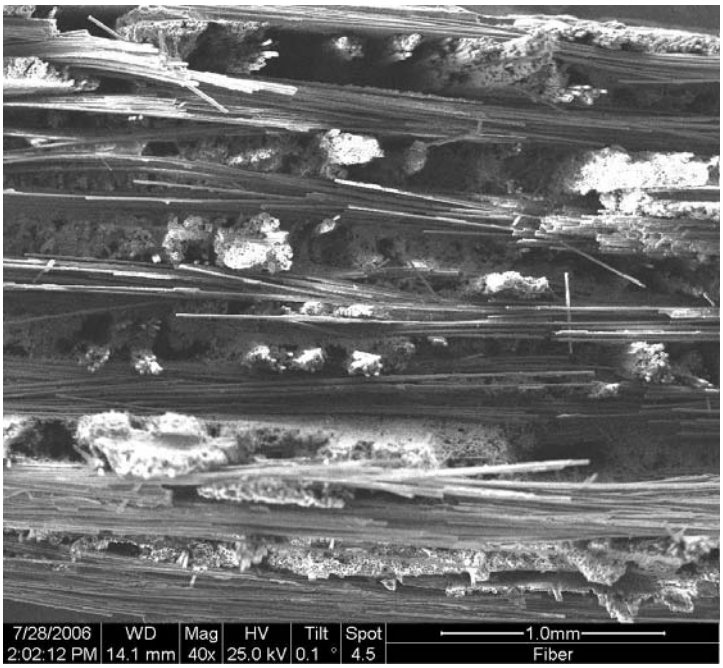

Figure 113. Specimen A150- 40x

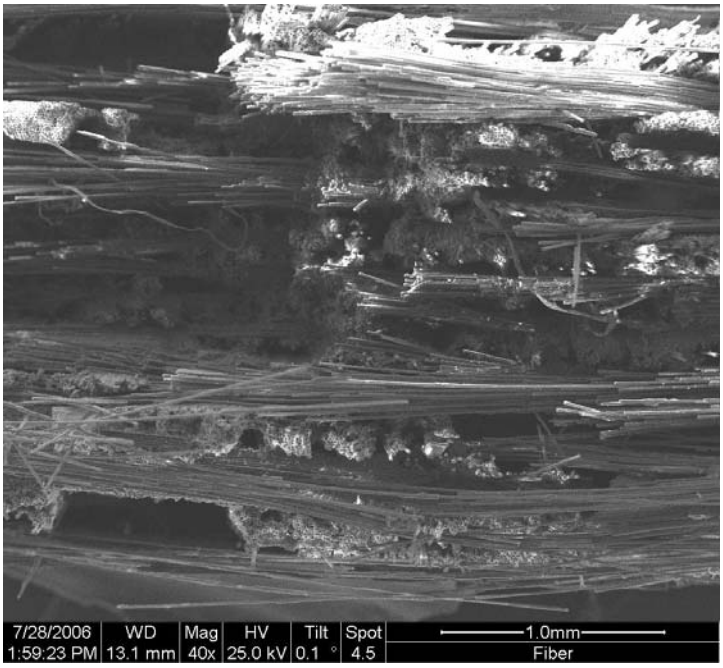

Figure 114. Specimen A150- 40x

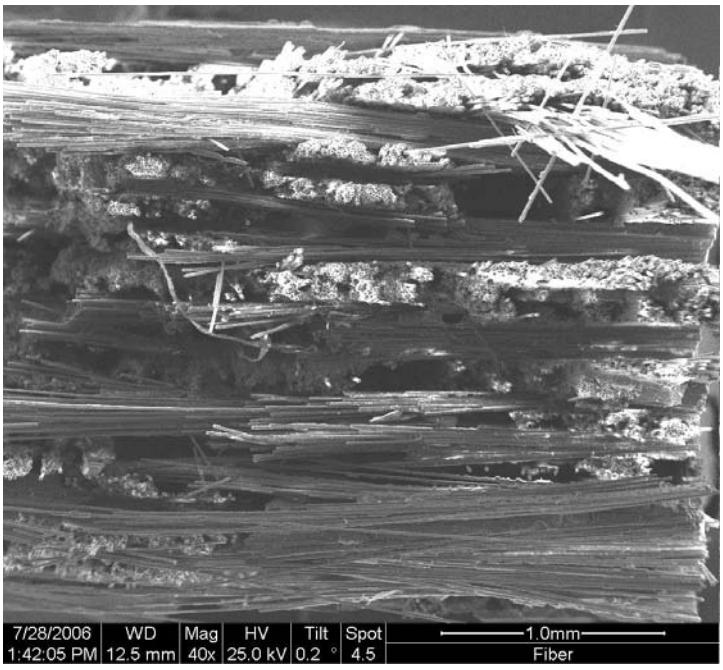

Figure 115. Specimen A150- 40x

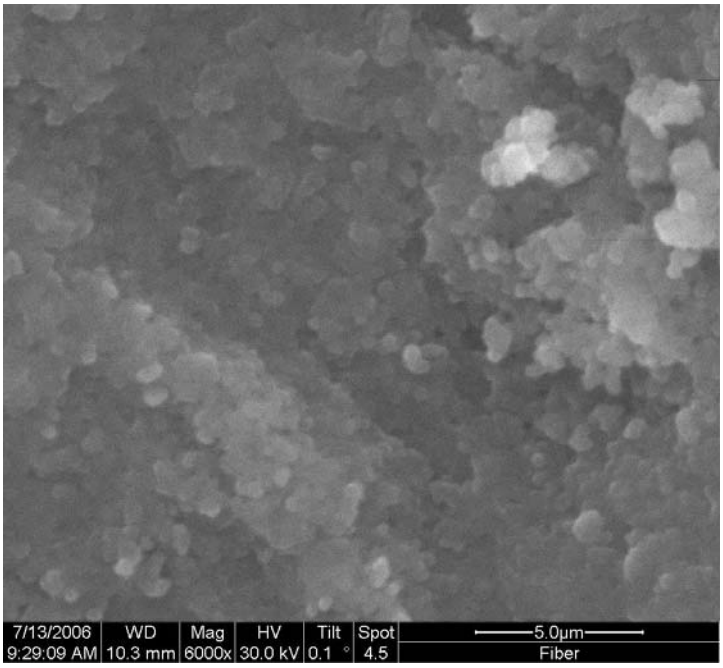

Figure 116. Specimen S80- 6000x

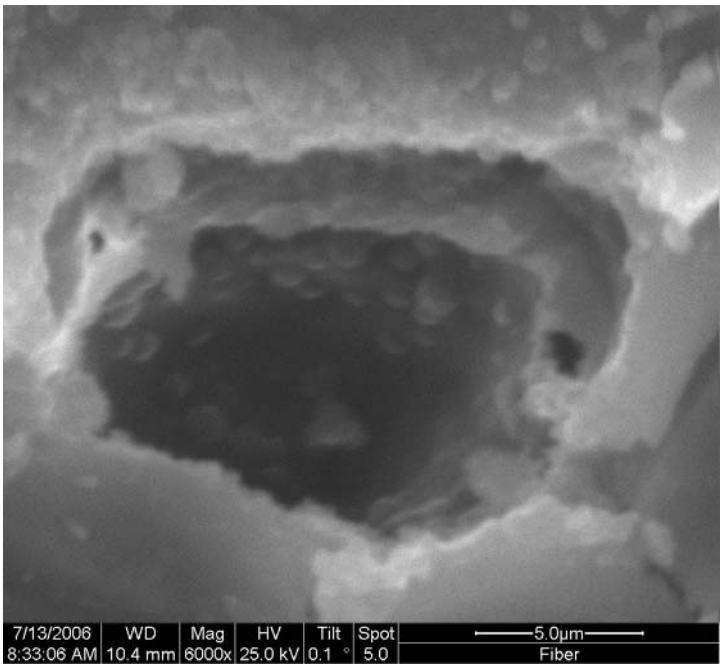

Figure 117. Specimen S80- 6000x

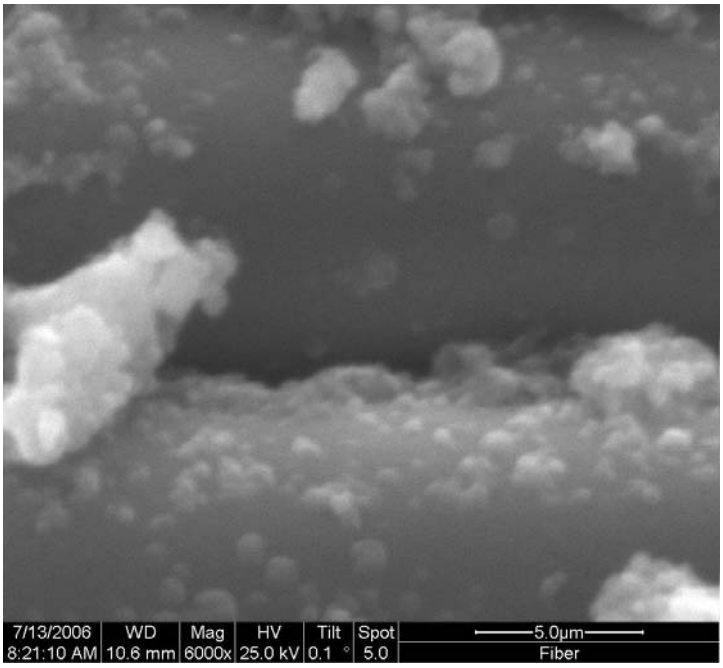

Figure 118. Specimen S80- 6000x

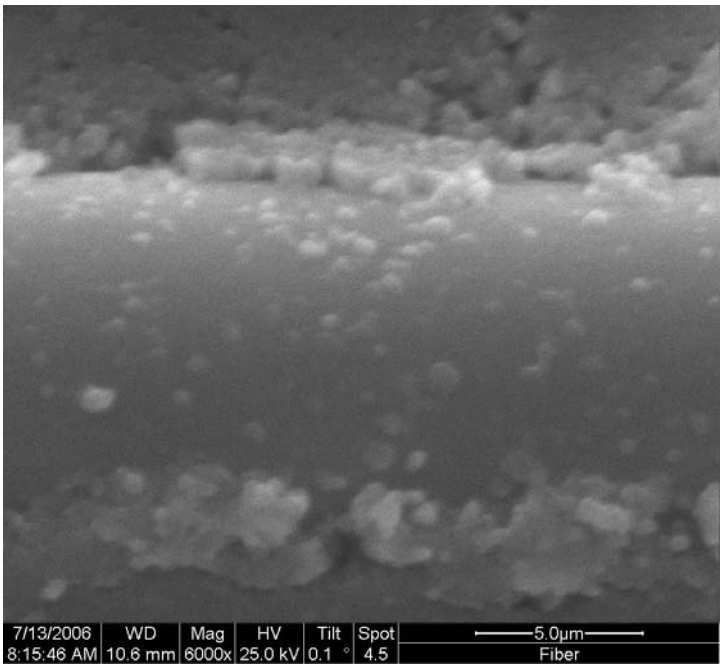

Figure 119. Specimen S80- 6000x

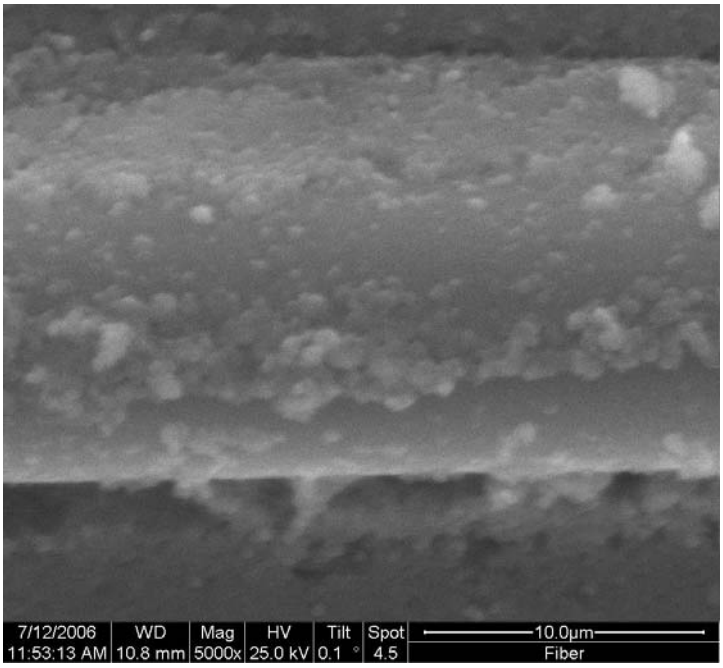

Figure 120. Specimen S80- 5000x

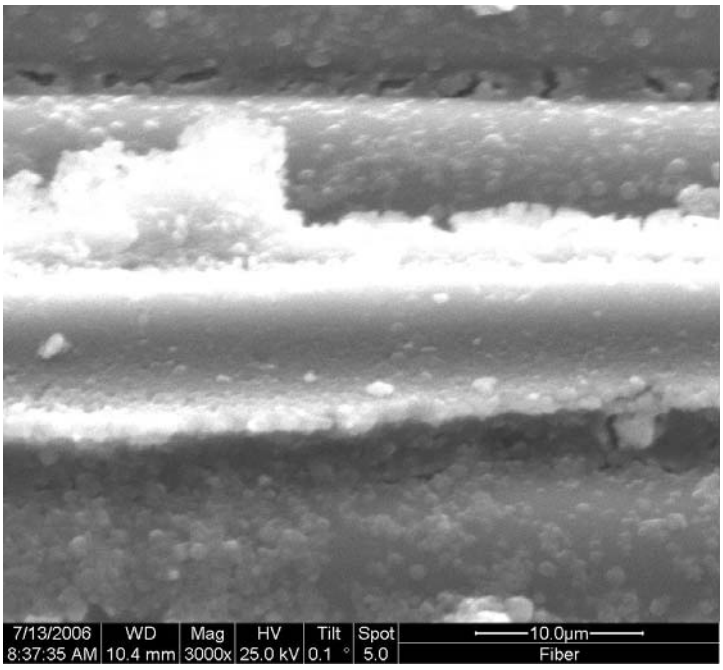

Figure 121. Specimen S80- 3000x

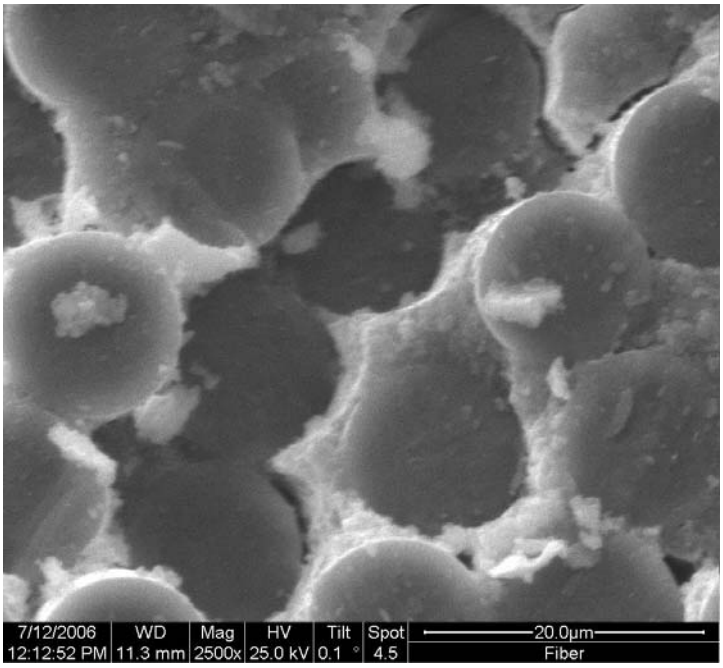

Figure 122. Specimen S80- 2500x

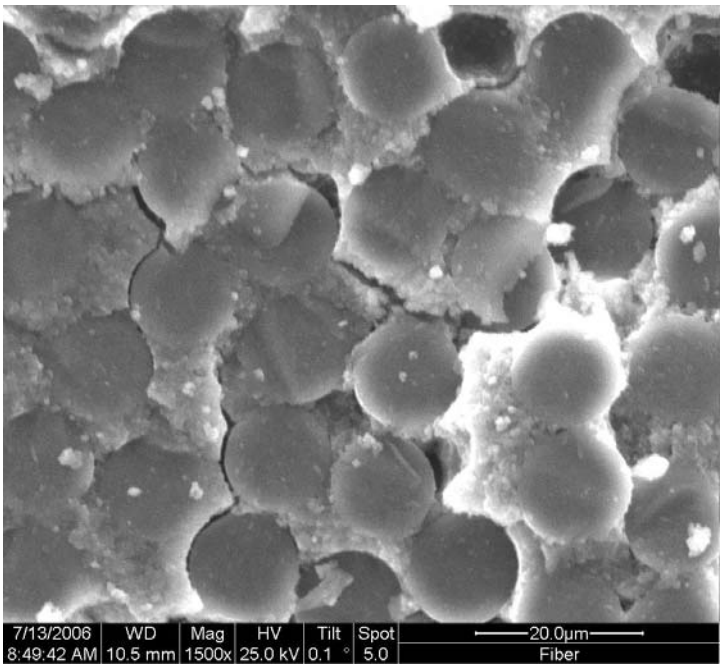

Figure 123. Specimen S80- 1500x

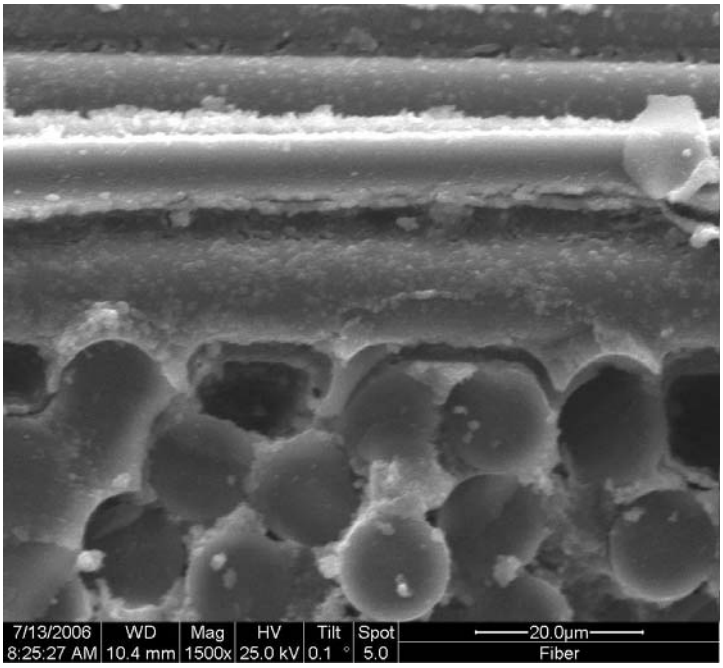

Figure 124. Specimen S80- 1500x

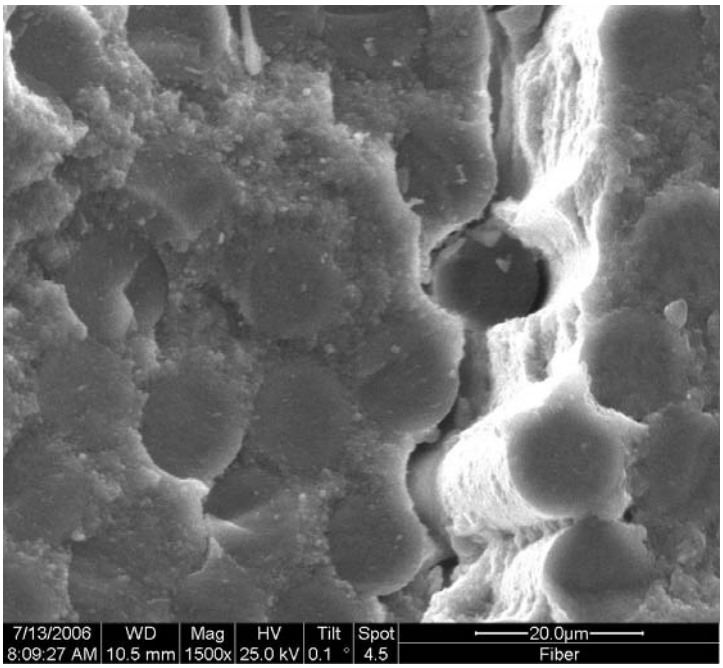

Figure 125. Specimen S80- 1500x

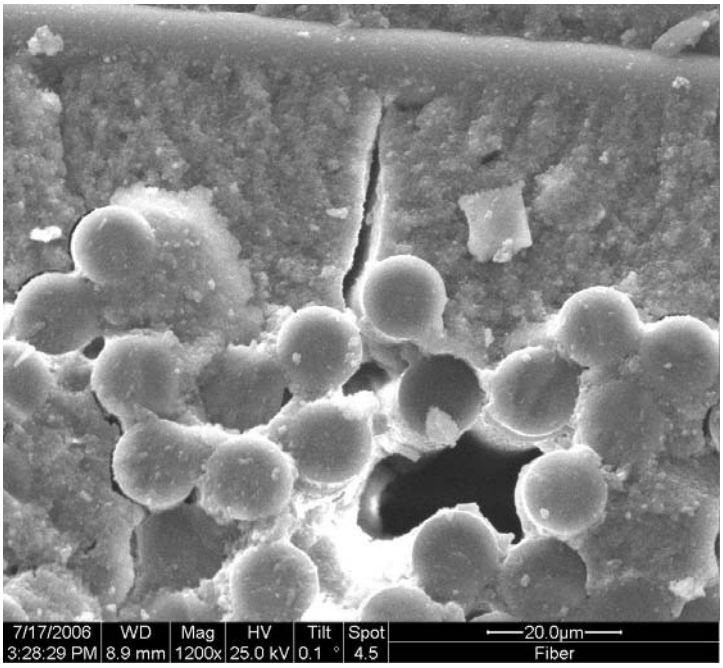

Figure 126. Specimen S80- 1200x

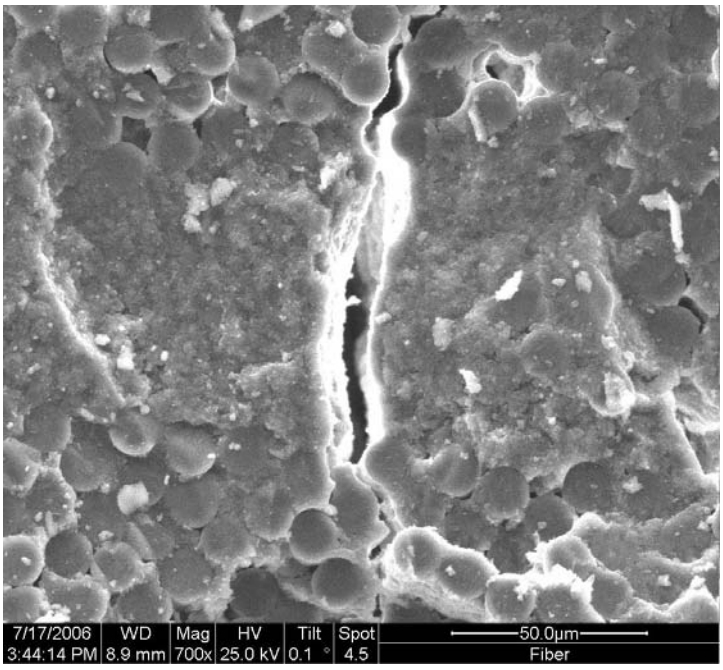

Figure 127. Specimen S80- 700x

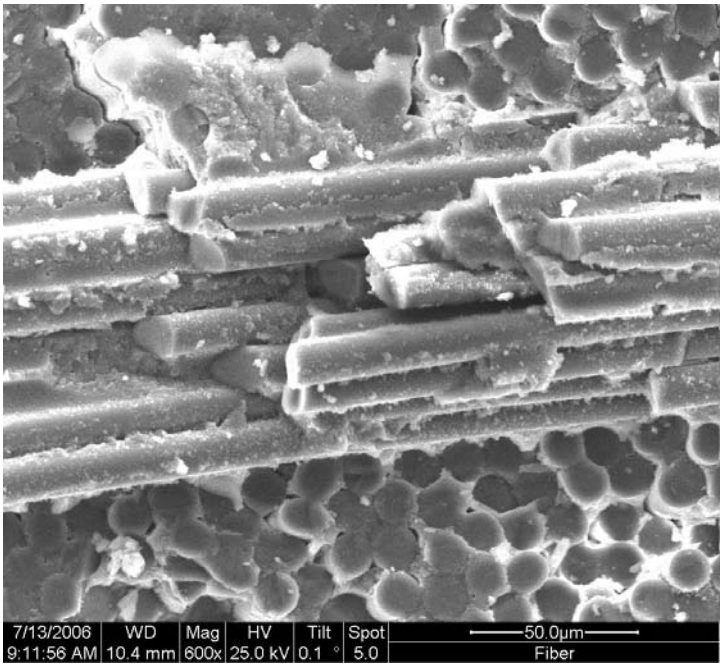

Figure 128. Specimen S80- 600x

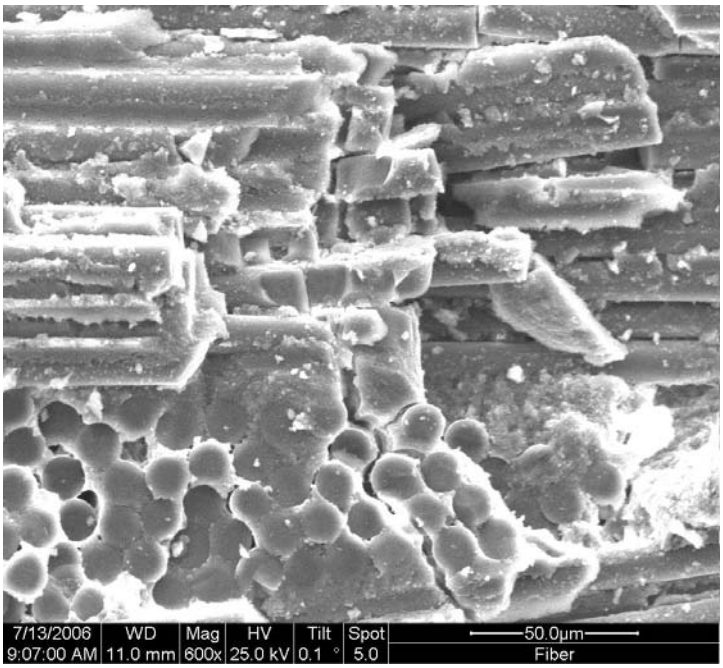

Figure 129. Specimen S80- 600x

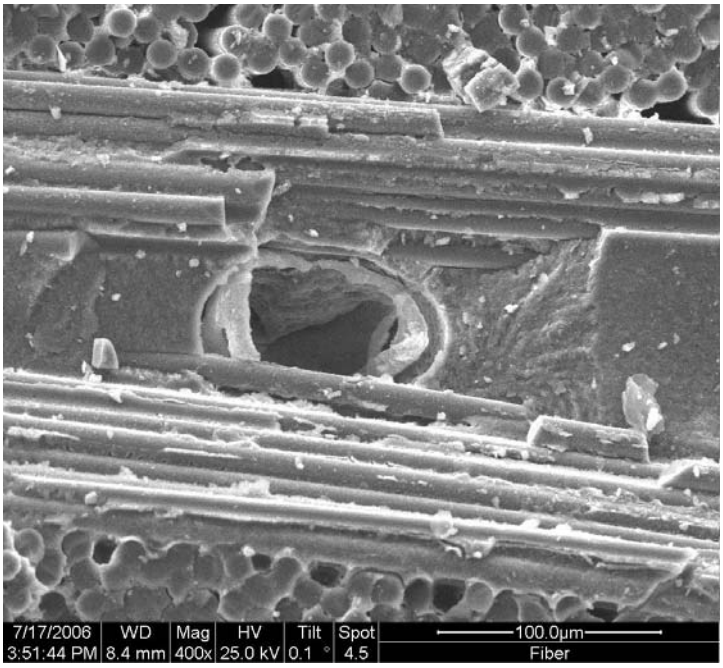

Figure 130. Specimen S80- 400x

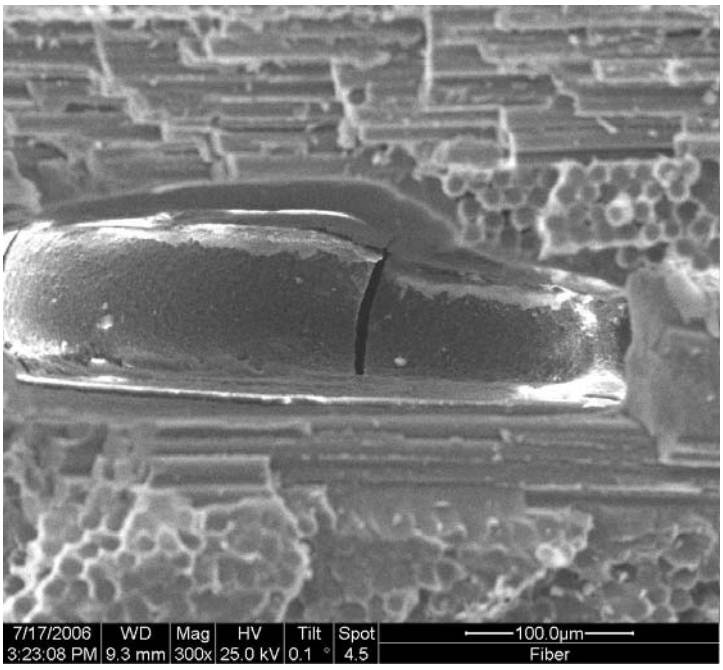

Figure 131. Specimen S80- 300x

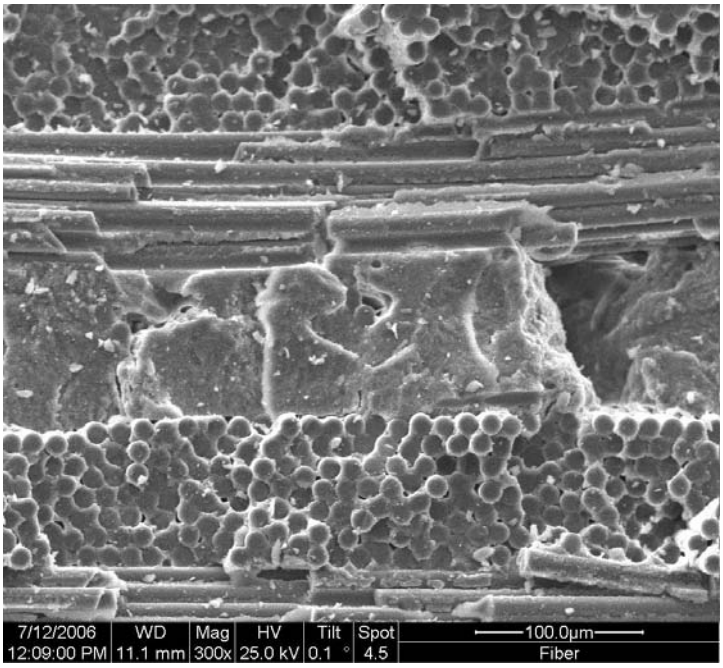

Figure 132. Specimen S80- 300x

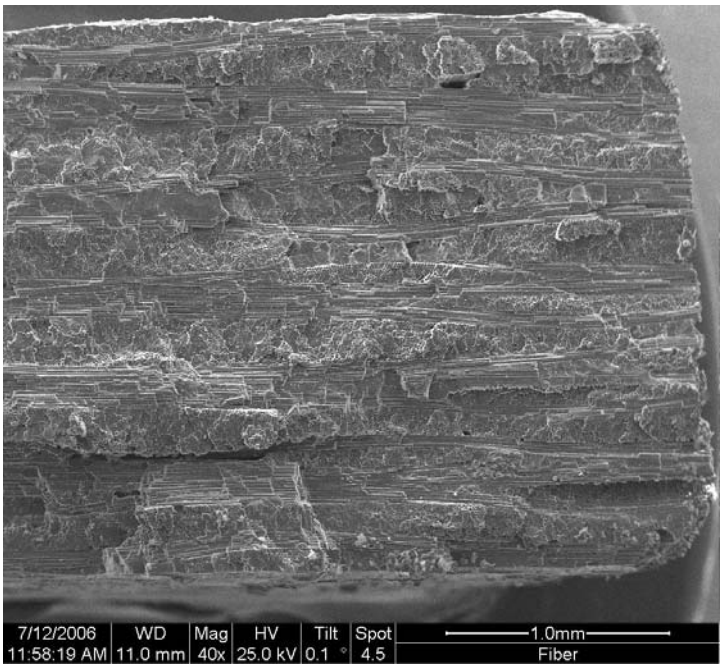

Figure 133. Specimen S80- 40x

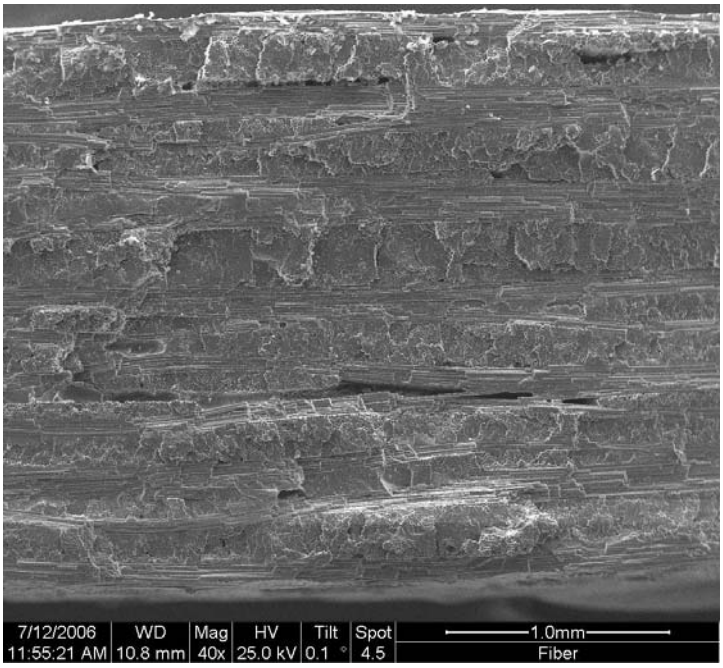

Figure 134. Specimen S80- 40x

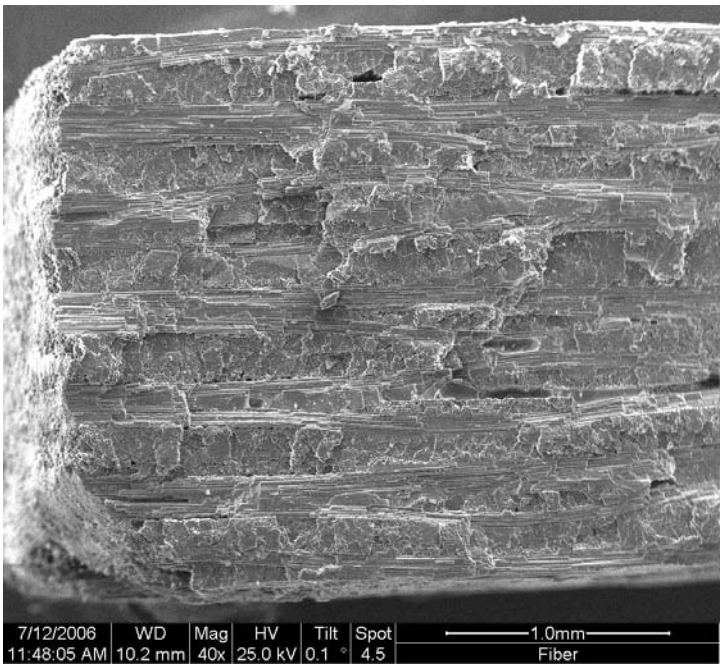

Figure 135. Specimen S80- 40x

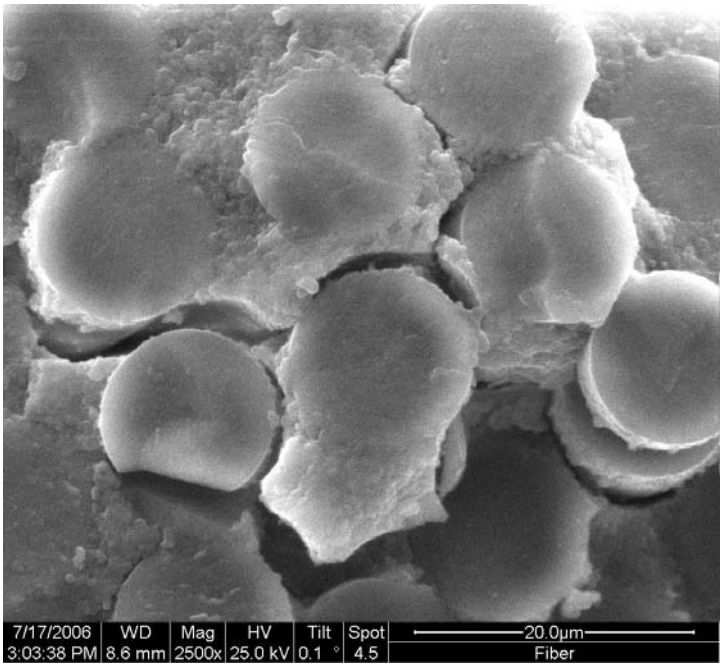

Figure 136. Specimen S80- 2500x

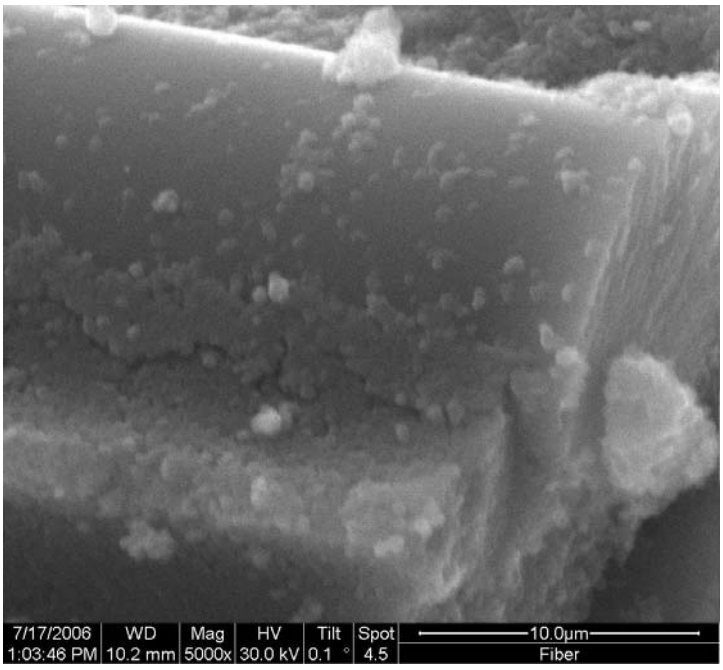

Figure 137. Specimen S100- 5000x

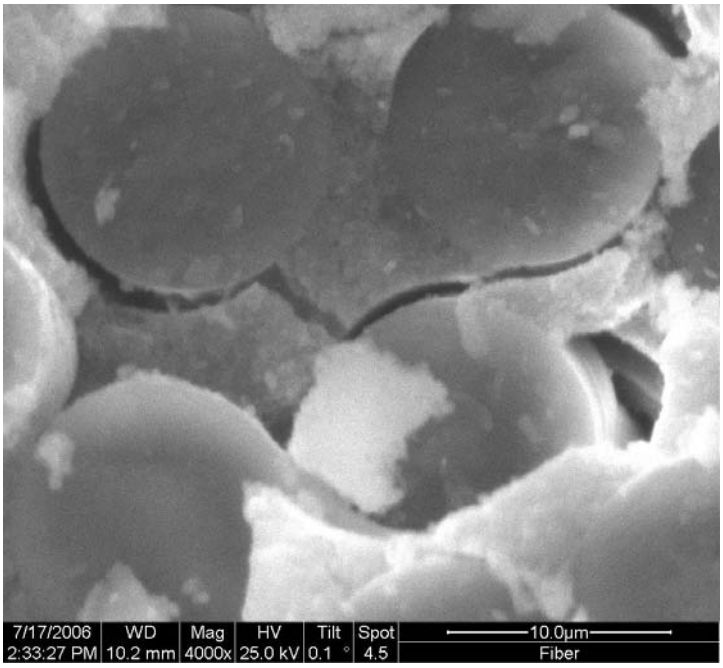

Figure 138. Specimen S100- 4000x

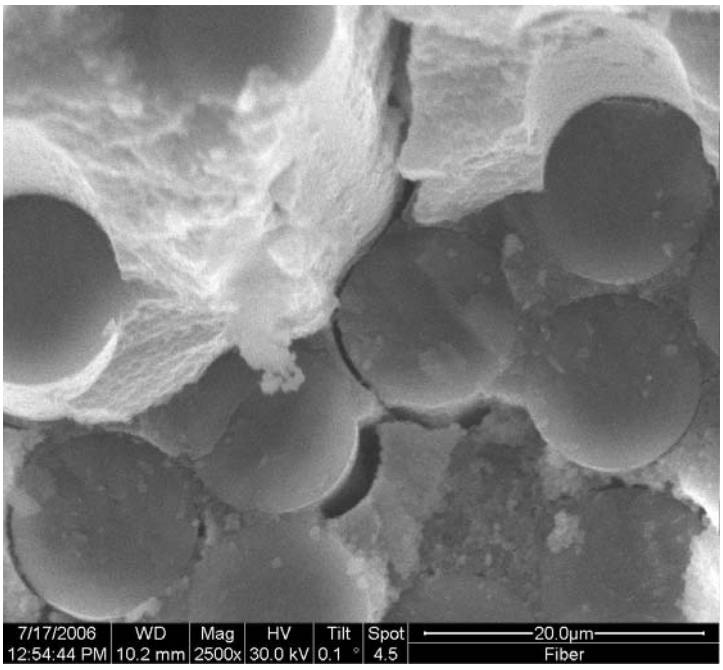

Figure 139. Specimen S100- 2500x

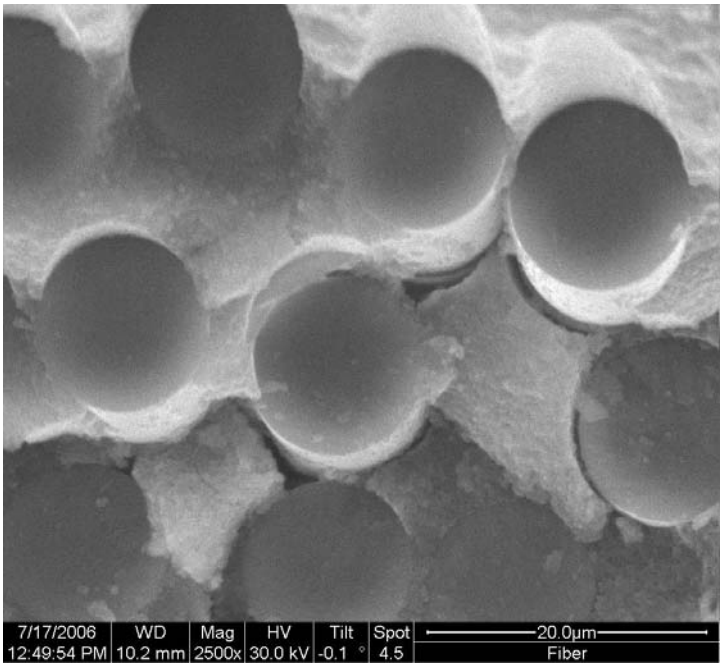

Figure 140. Specimen S100- 2500x

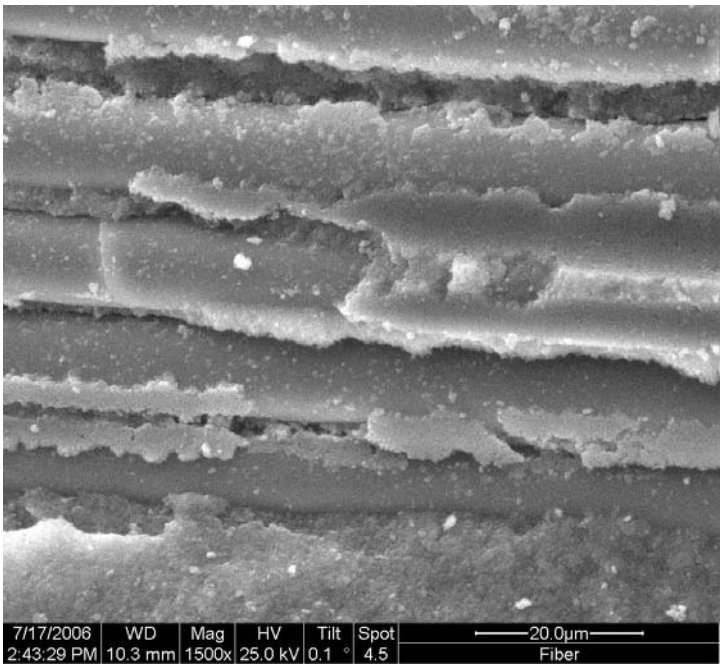

Figure 141. Specimen S100- 1500x

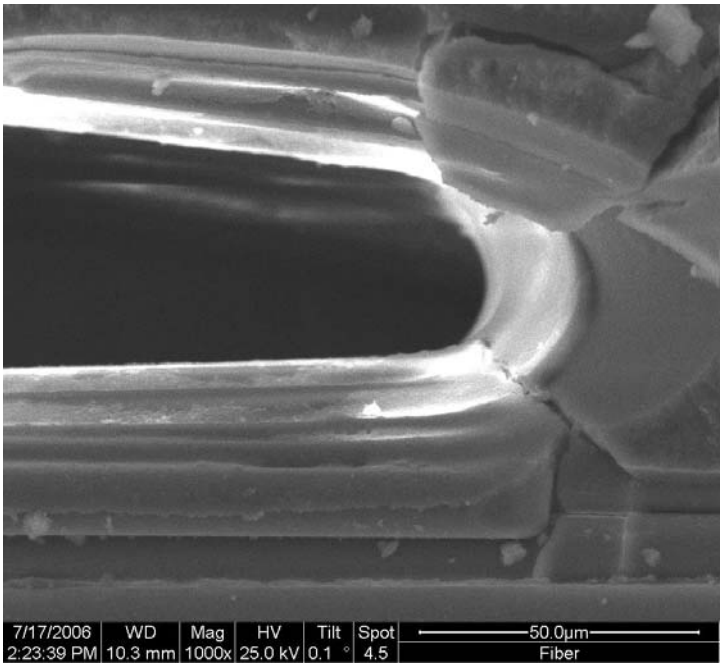

Figure 142. Specimen S100- 1000x

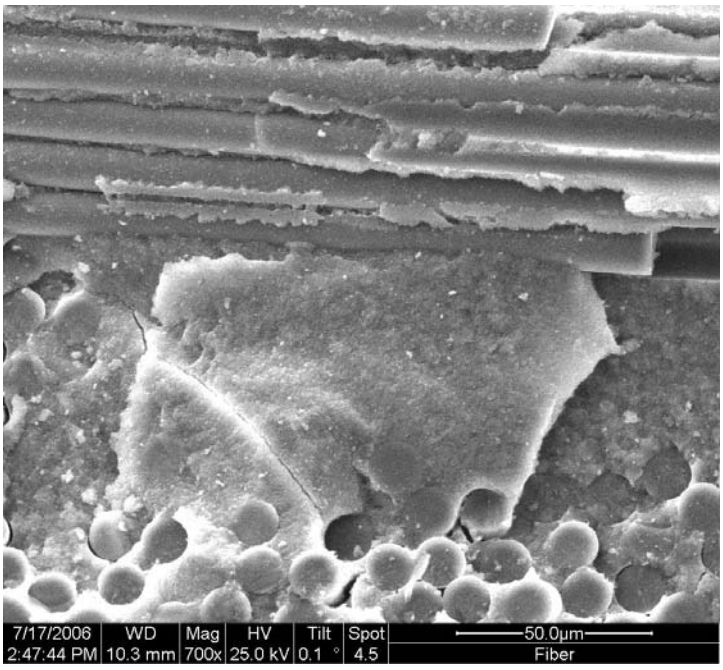

Figure 143. Specimen S100- 700x

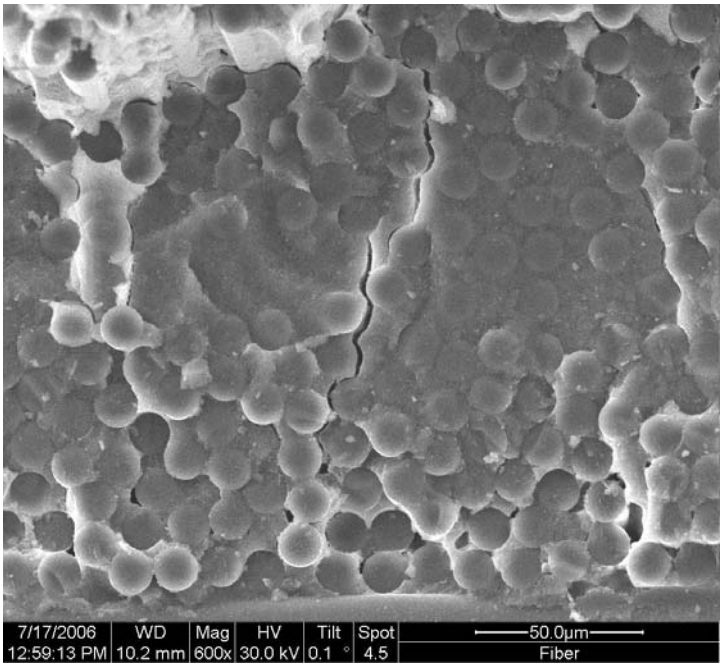

Figure 144. Specimen S100- 600x

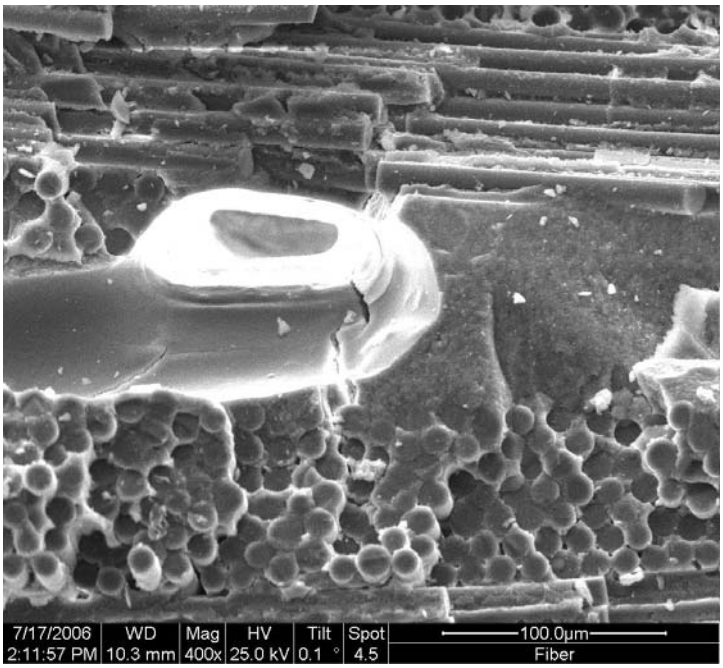

Figure 145. Specimen S100- 400x

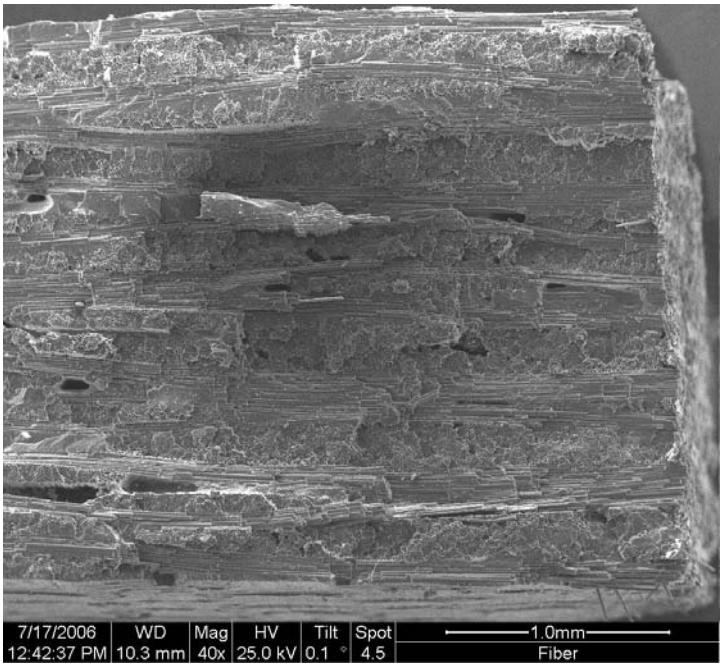

Figure 146. Specimen S100- 40x

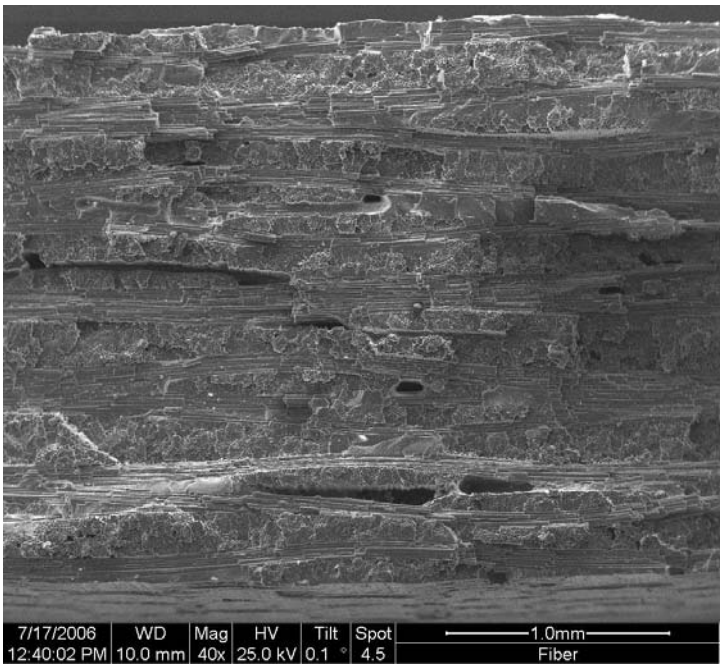

Figure 147. Specimen S100- 40x

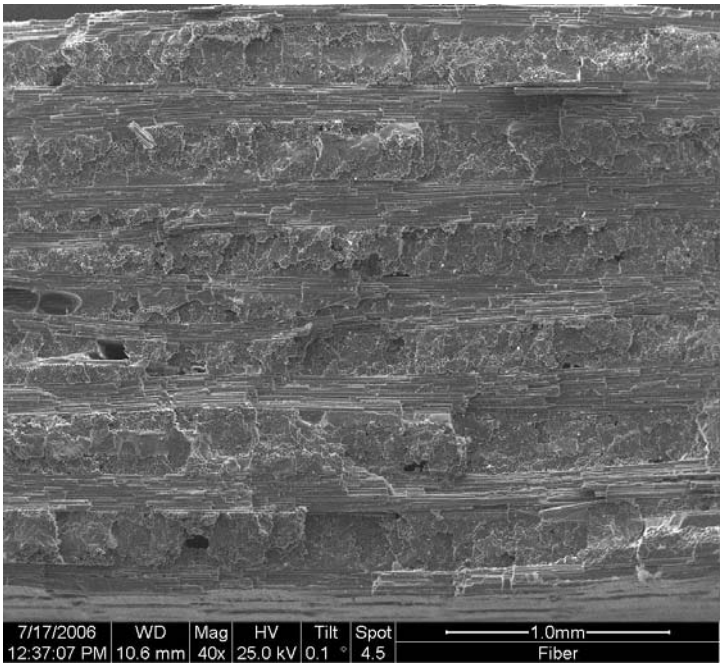

Figure 148. Specimen S100- 40x

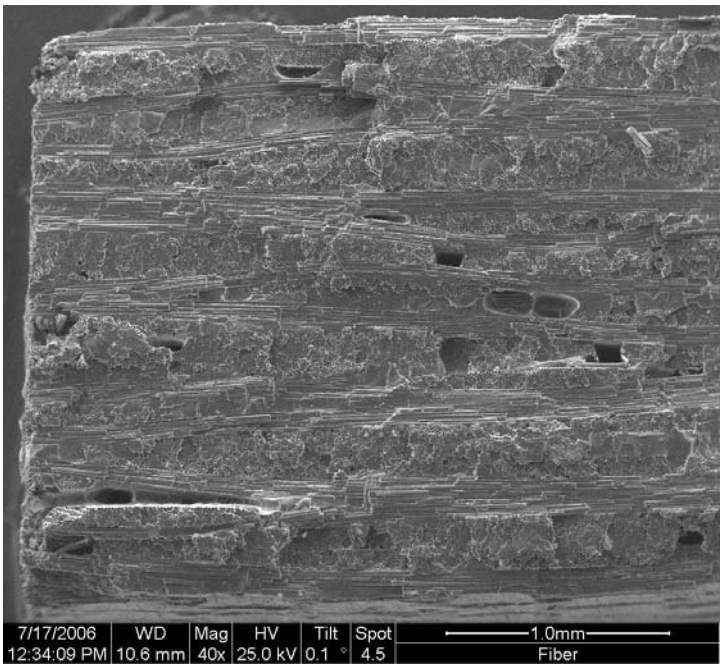

Figure 149. Specimen S100- 40x

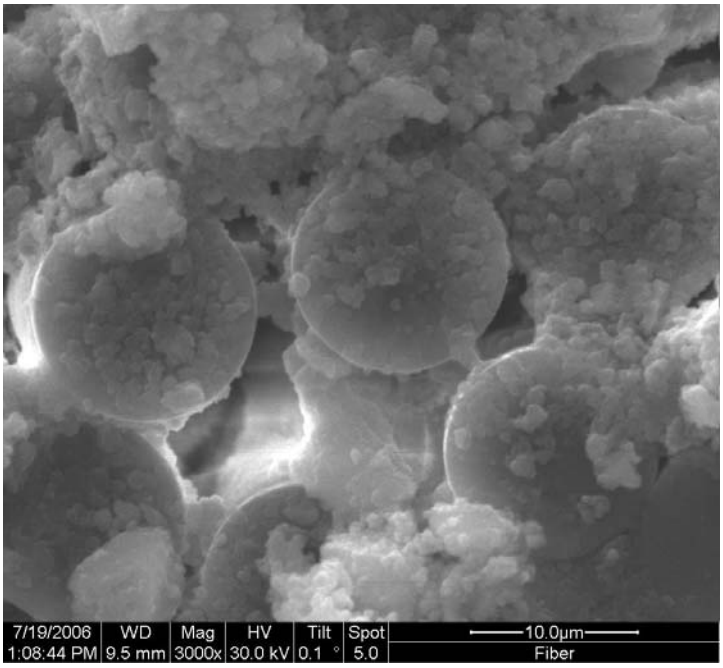

Figure 150. Specimen S125- 3000x

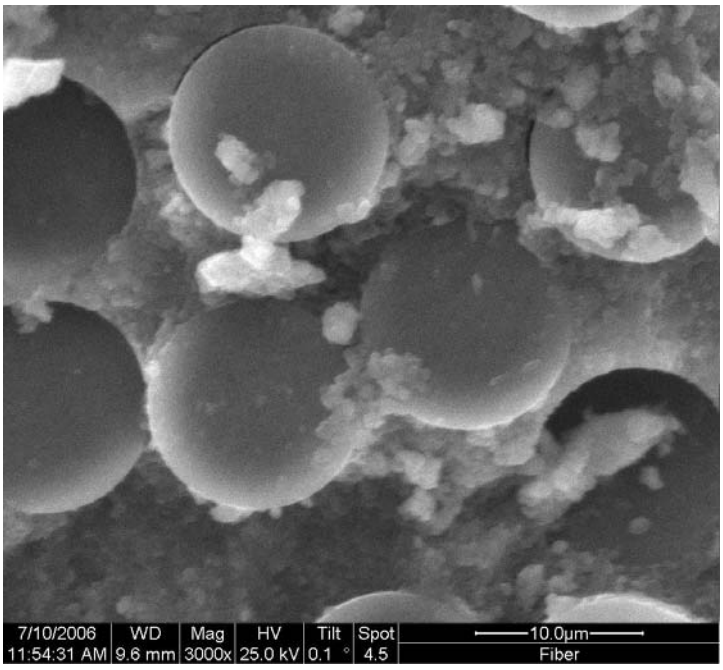

Figure 151. Specimen S125- 3000x

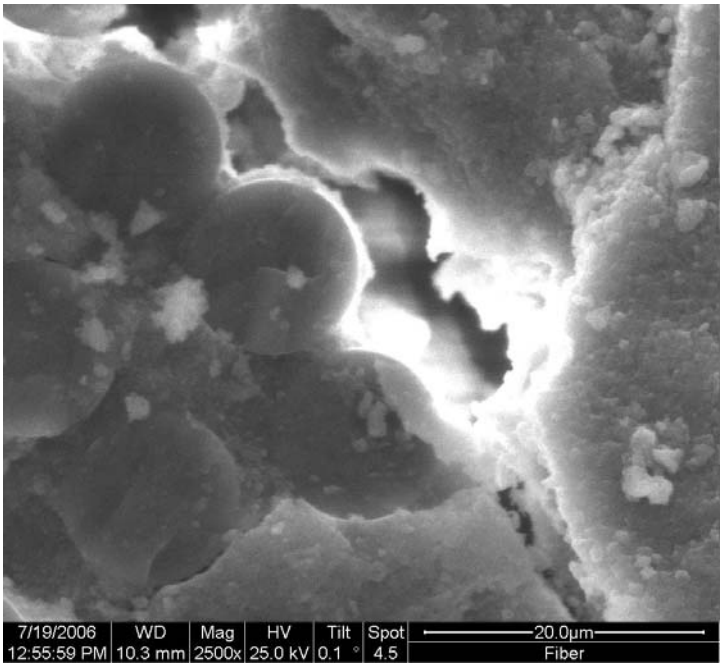

Figure 152. Specimen S125- 2500x

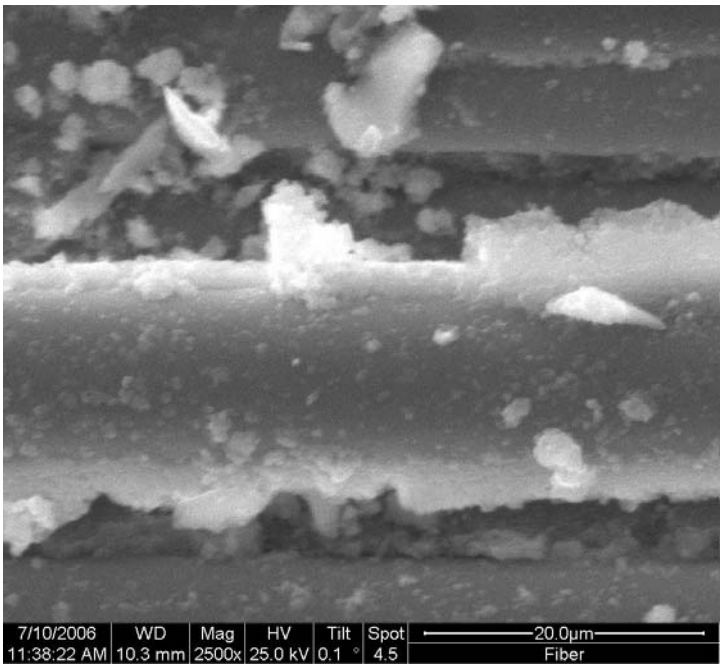

Figure 153. Specimen S125- 2500x

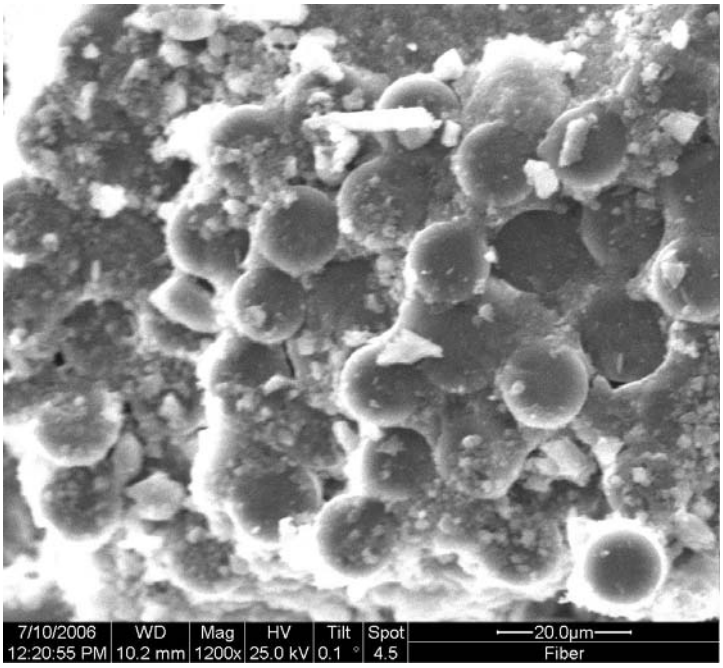

Figure 154. Specimen S125- 1200x

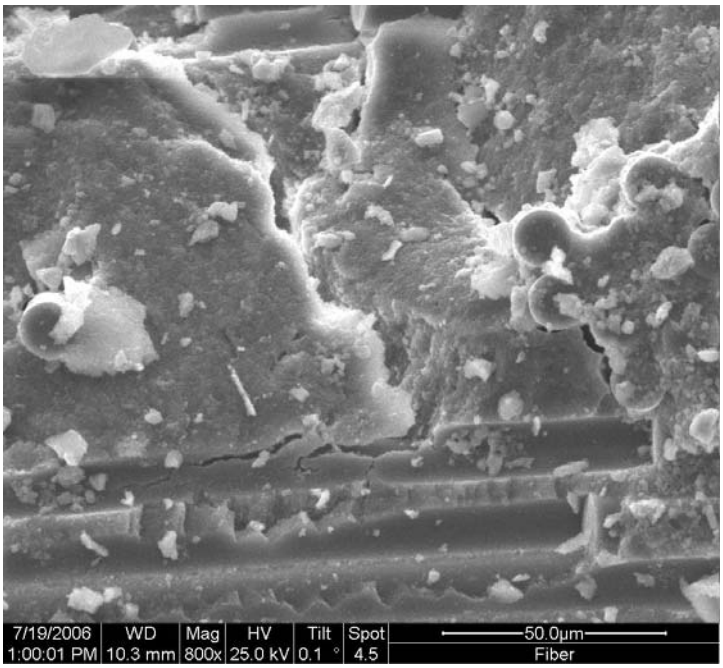

Figure 155. Specimen S125- 800x

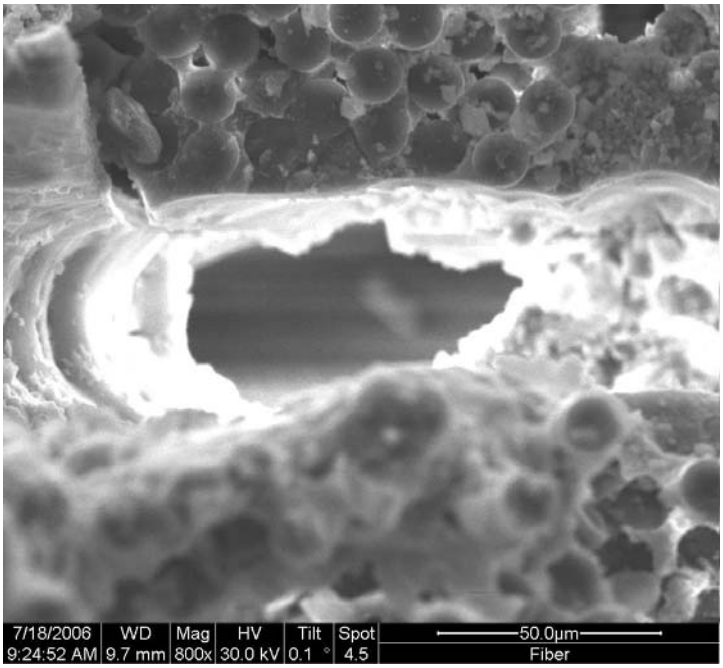

Figure 156. Specimen S125- 800x

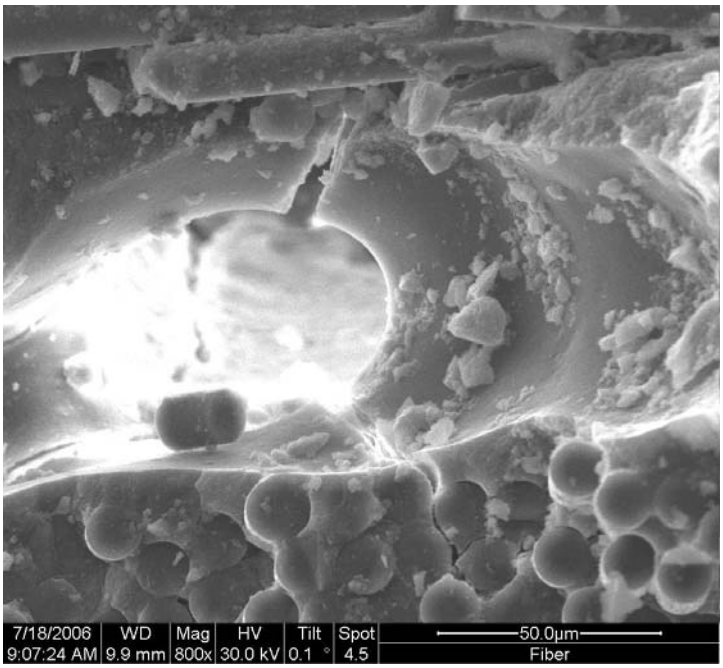

Figure 157. Specimen S125- 800x

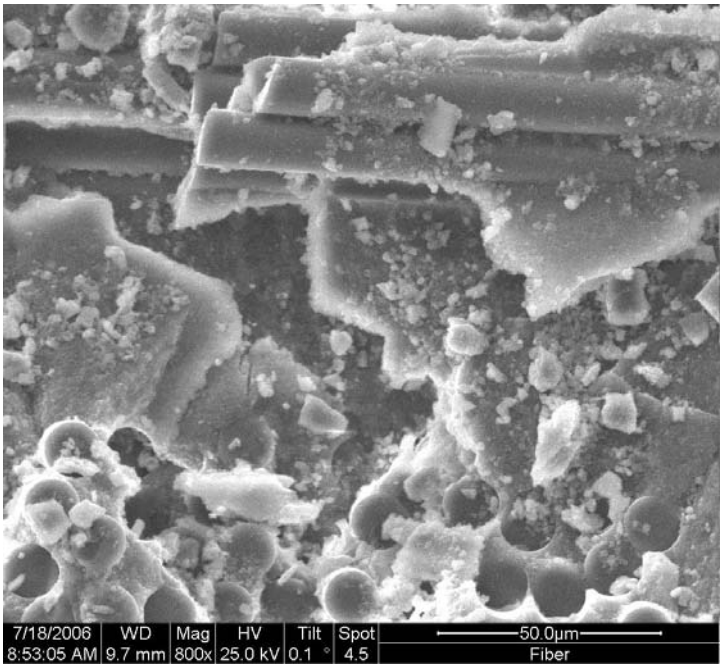

Figure 158. Specimen S125- 800x

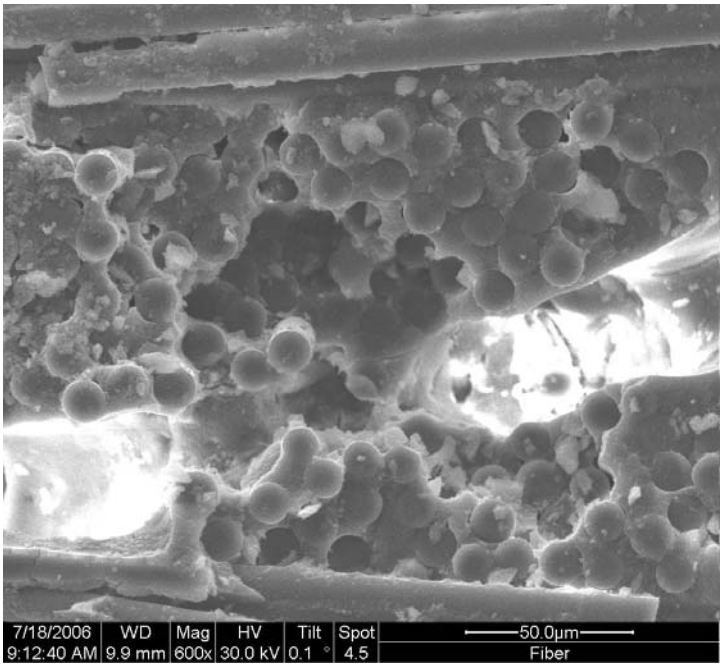

Figure 159. Specimen S125- 600x

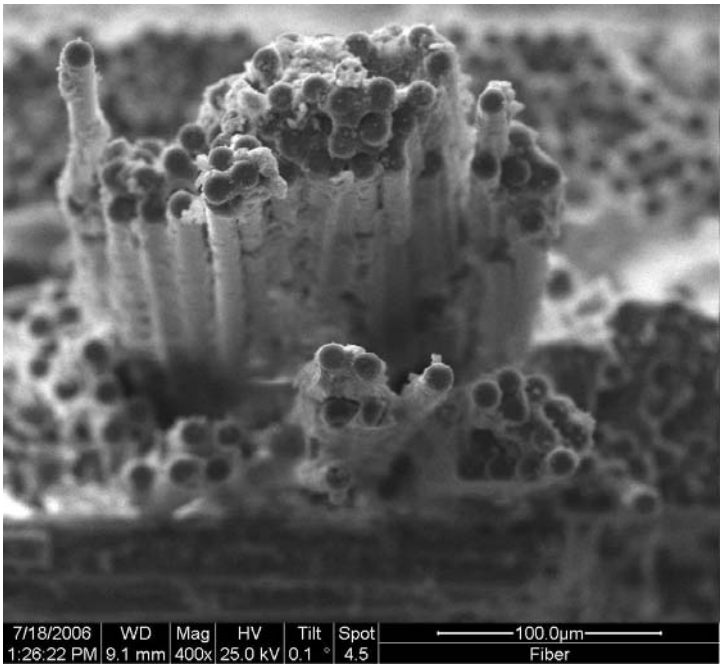

Figure 160. Specimen S125- 400x

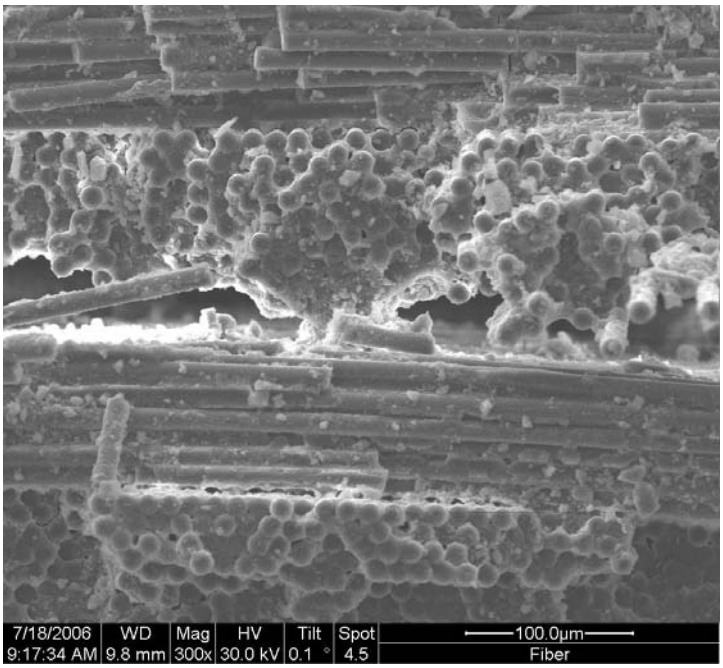

Figure 161. Specimen S125- 300x

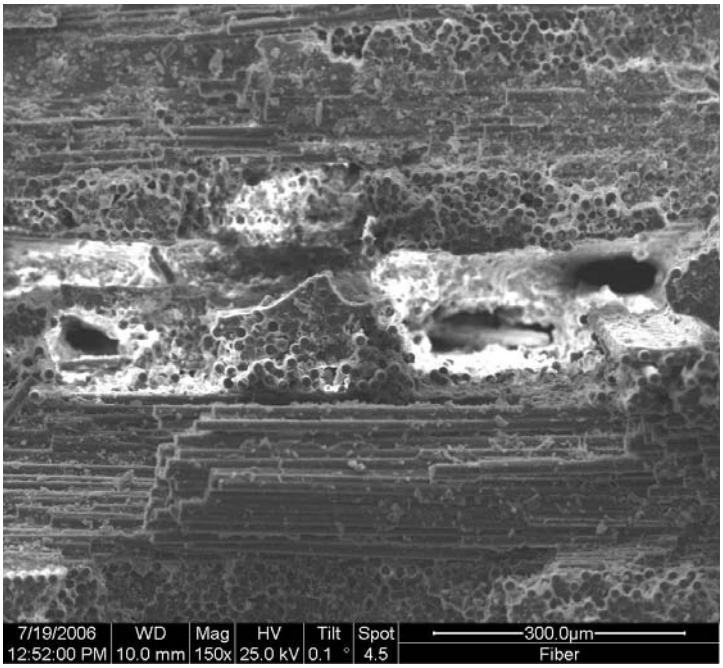

Figure 162. Specimen S125- 150x

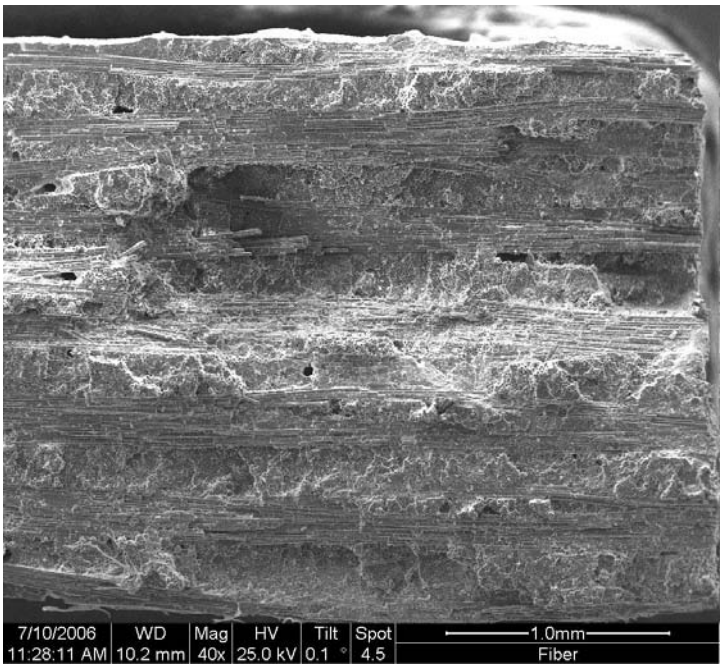

Figure 163. Specimen S125- 40x

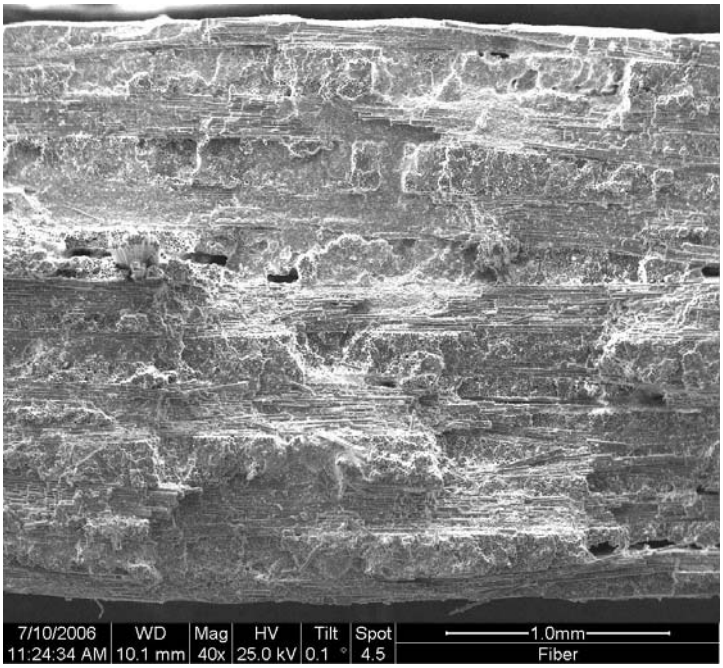

Figure 164. Specimen S125- 40x

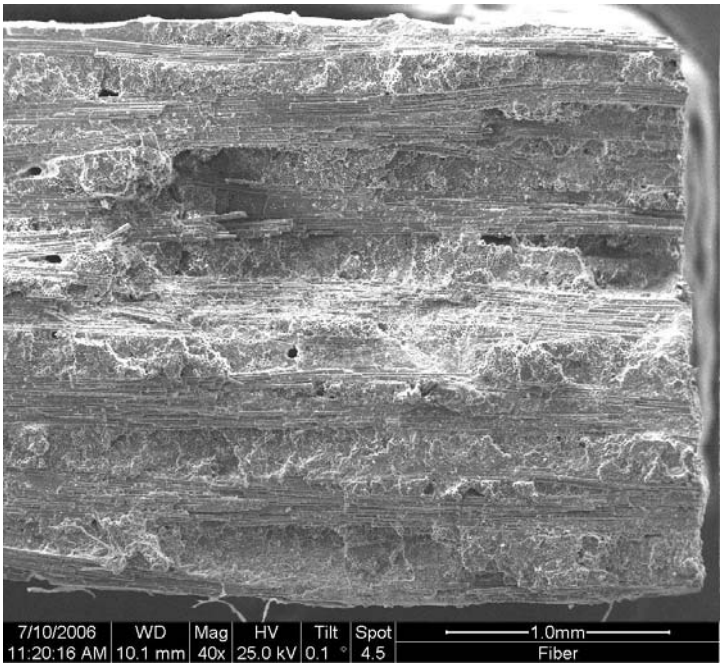

Figure 165. Specimen S125- 40x

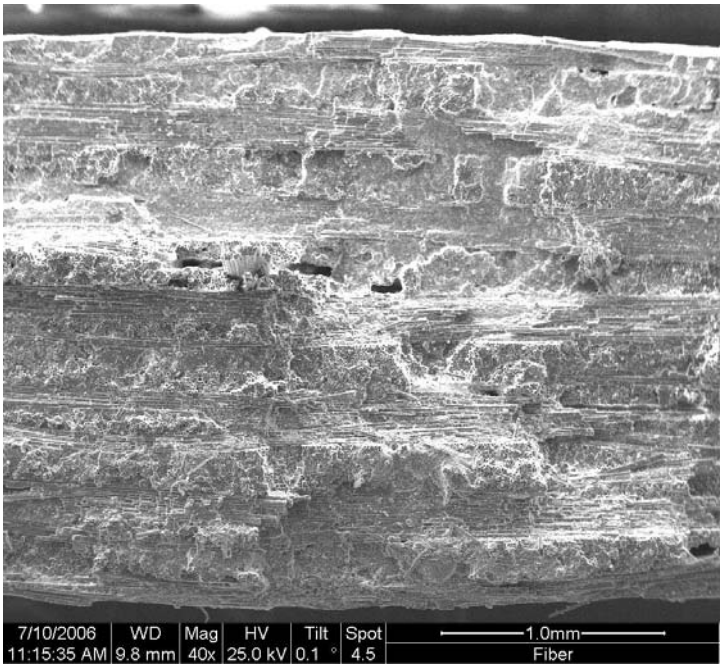

Figure 166. Specimen S125- 40x

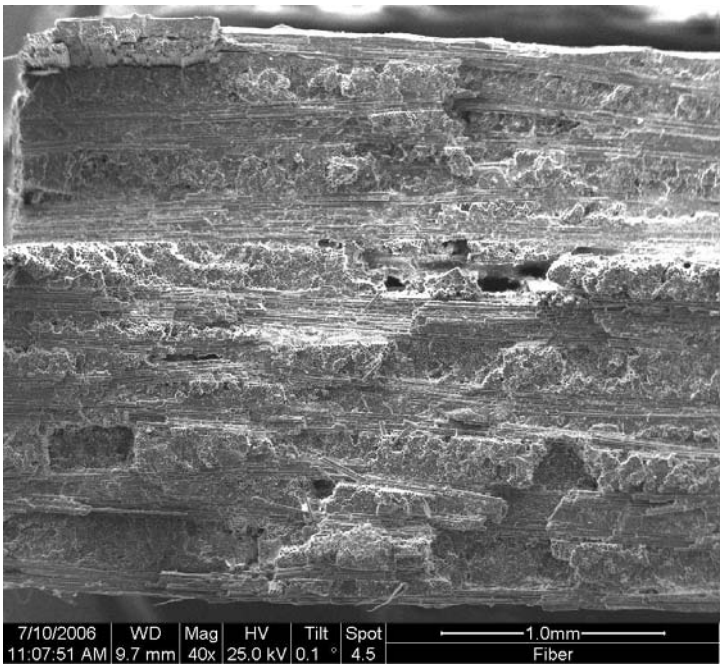

Figure 167. Specimen S125- 40x

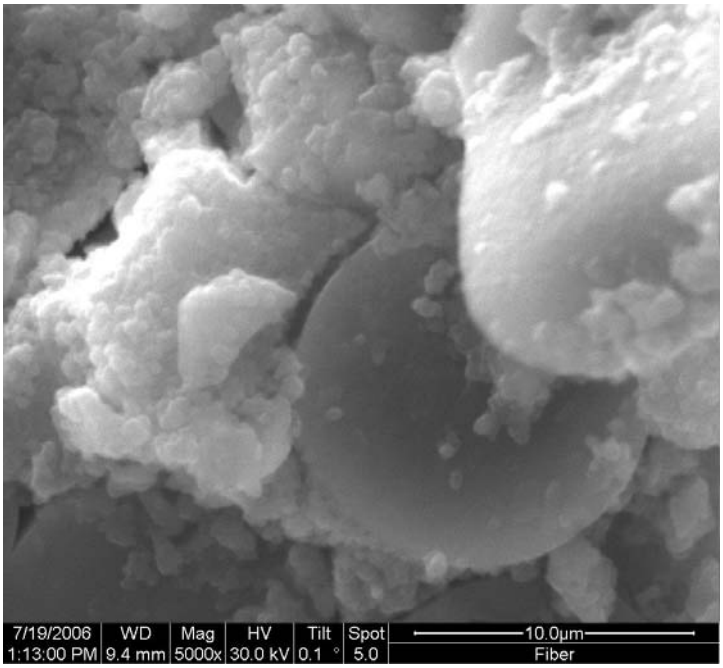

Figure 168. Specimen S150- 5000x

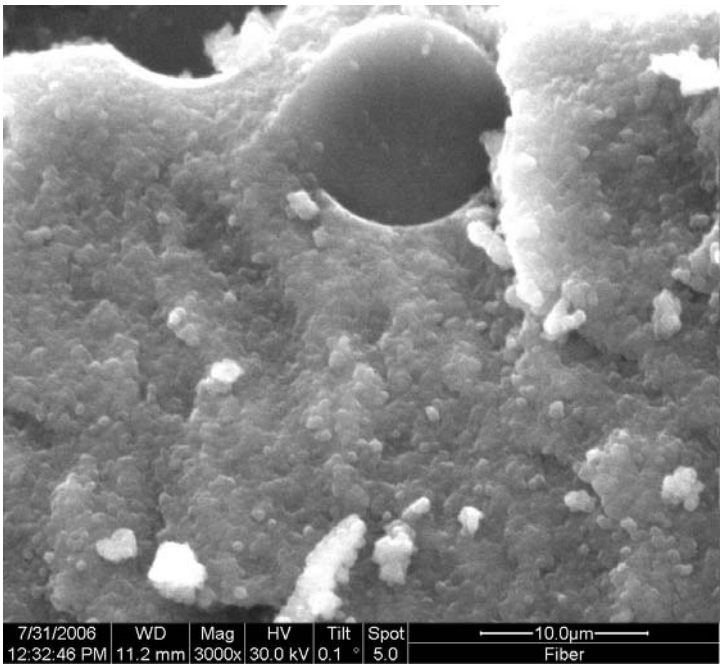

Figure 169. Specimen S150- 3000x

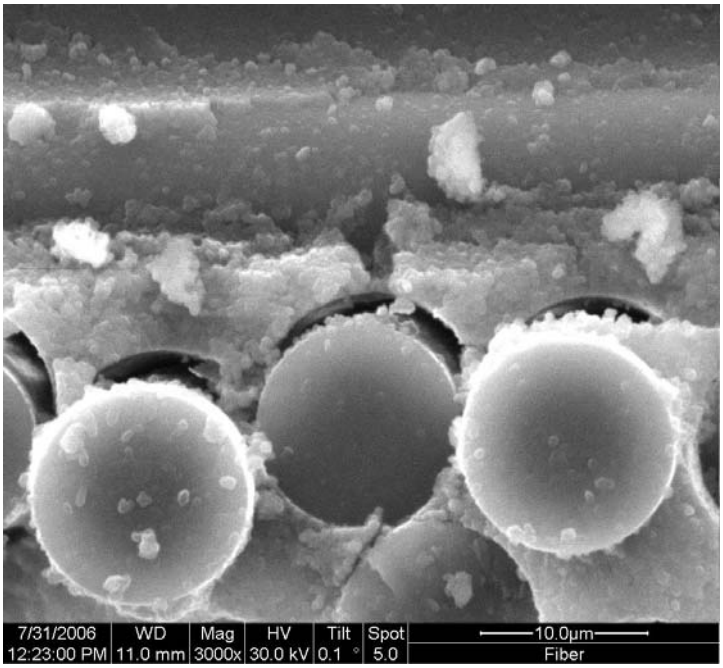

Figure 170. Specimen S150- 3000x

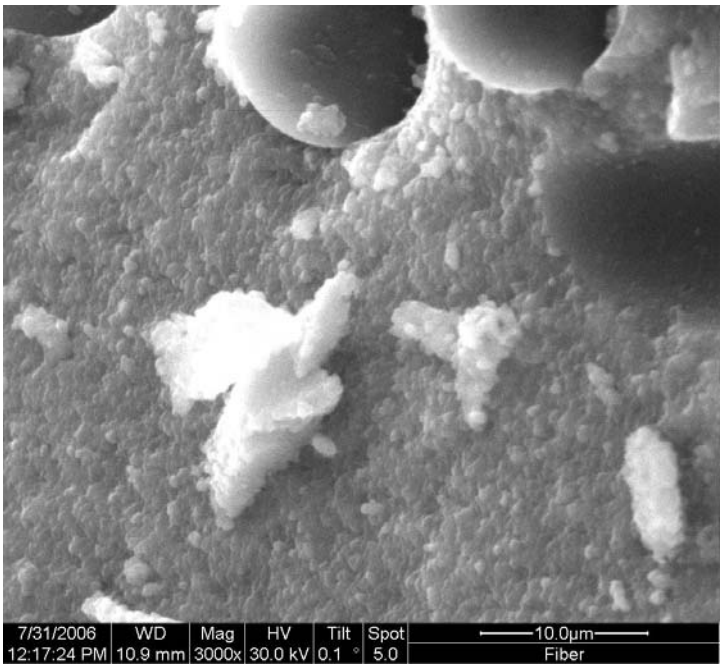

Figure 171. Specimen S150- 3000x

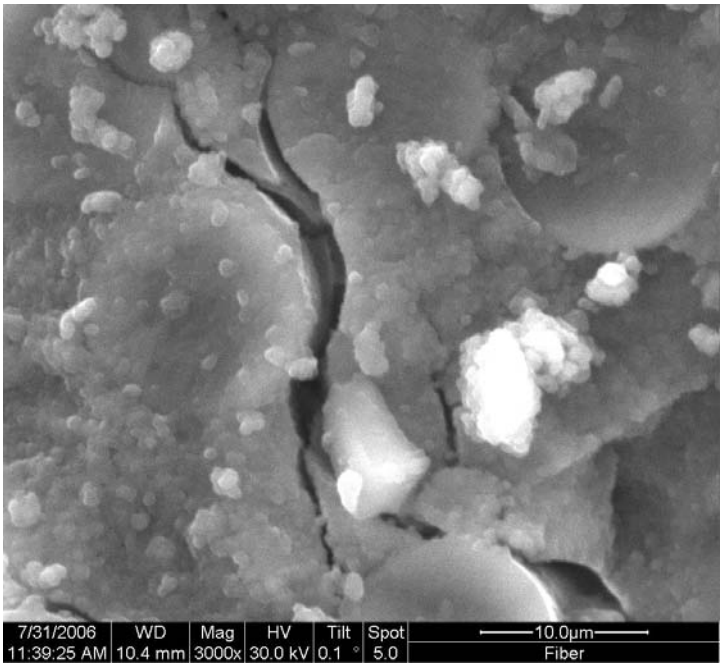

Figure 172. Specimen S150- 3000x

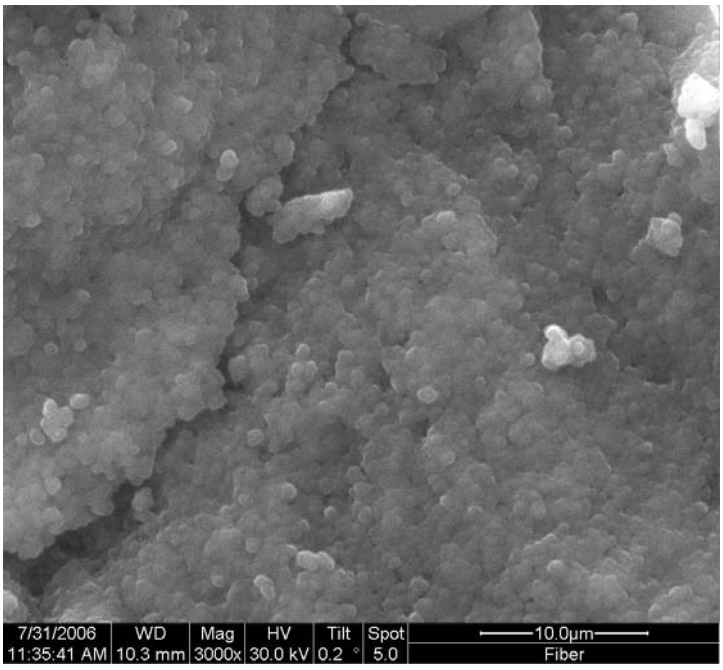

Figure 173. Specimen S150- 3000x

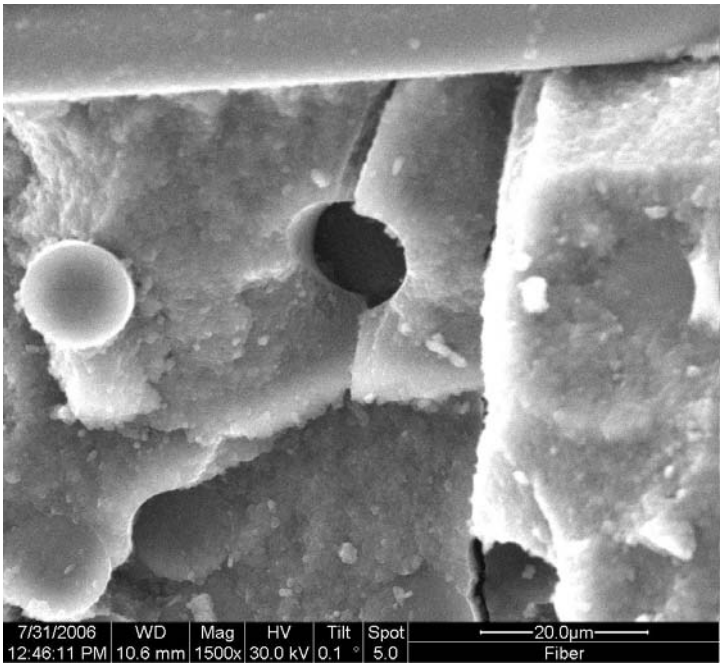

Figure 174. Specimen S150- 1500x

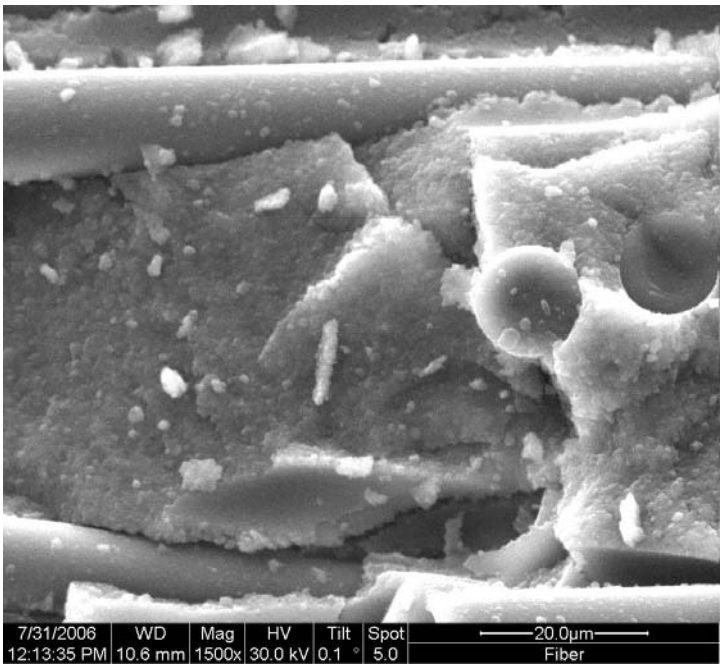

Figure 175. Specimen S150- 1500x

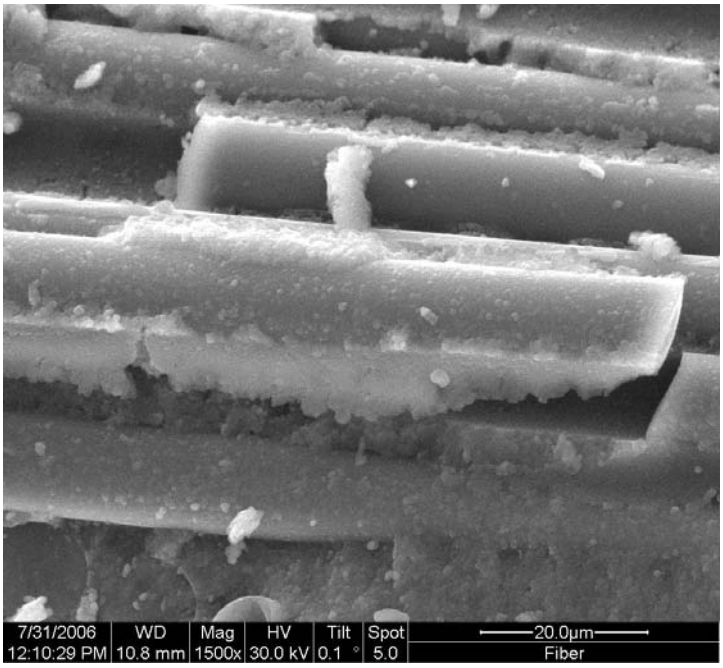

Figure 176. Specimen S150- 1500x

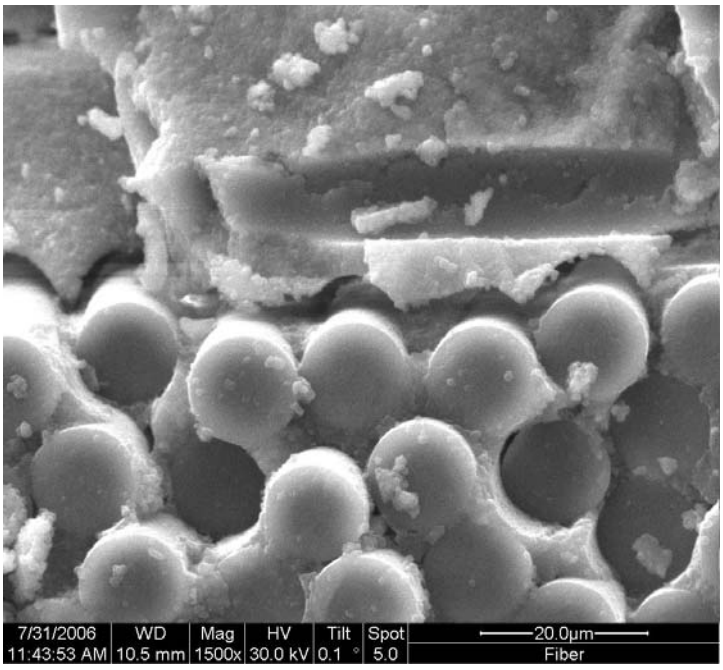

Figure 177. Specimen S150- 1500x

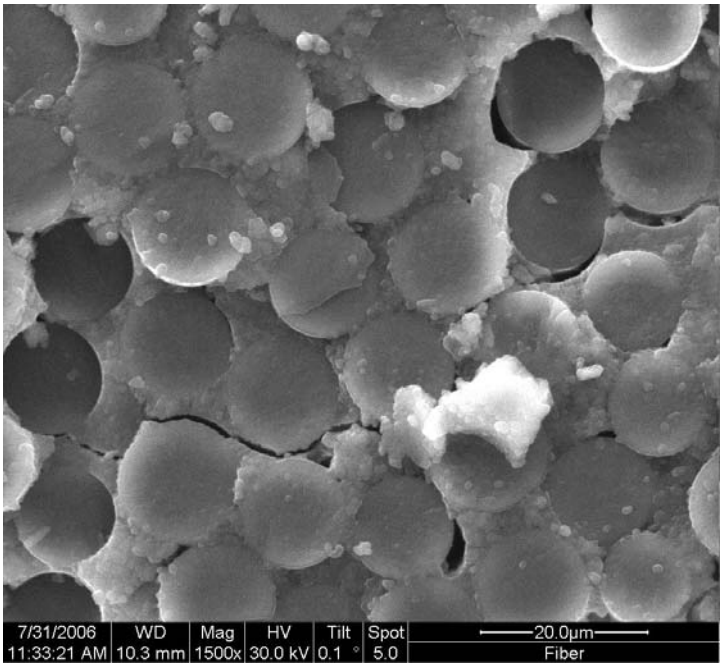

Figure 178. Specimen S150- 1500x

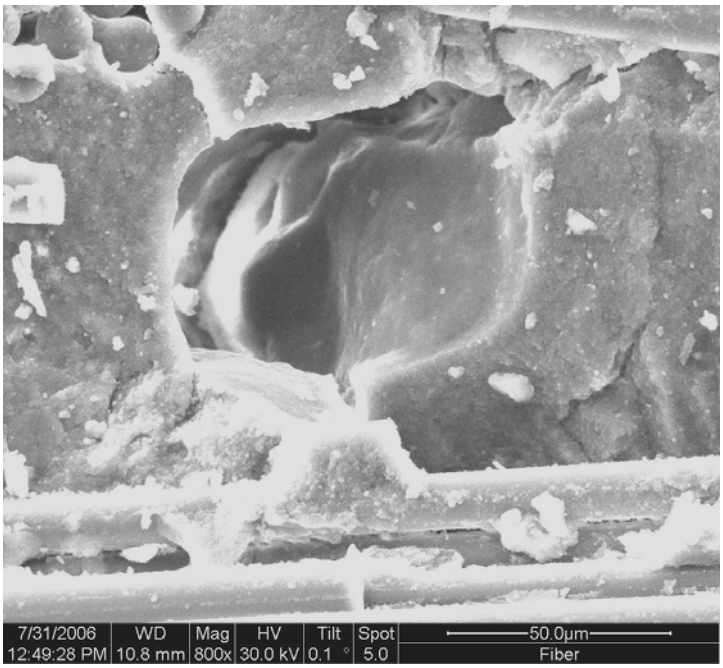

Figure 179. Specimen S150- 800x

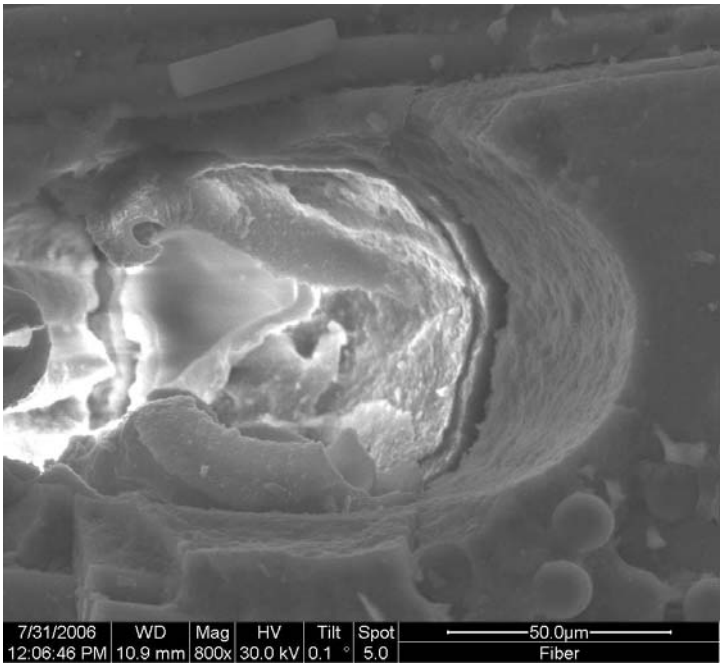

Figure 180. Specimen S150- 800x

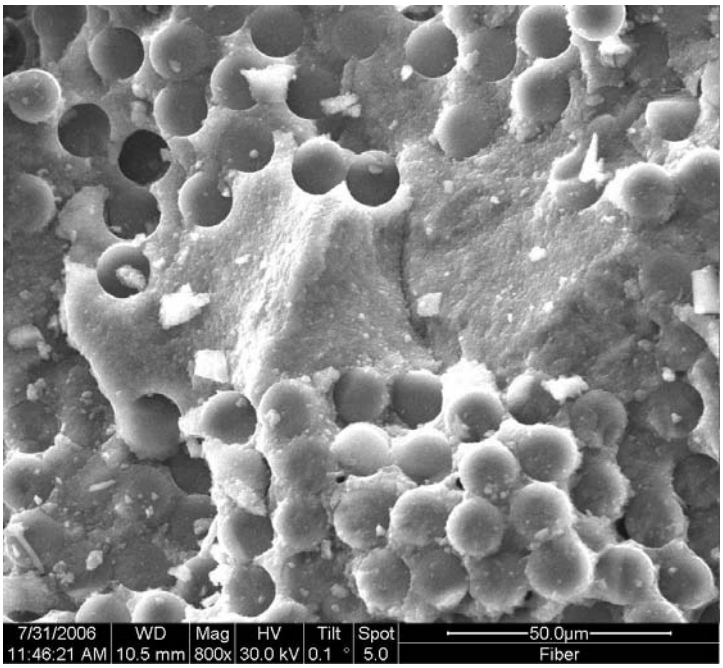

Figure 181. Specimen S150- 800x

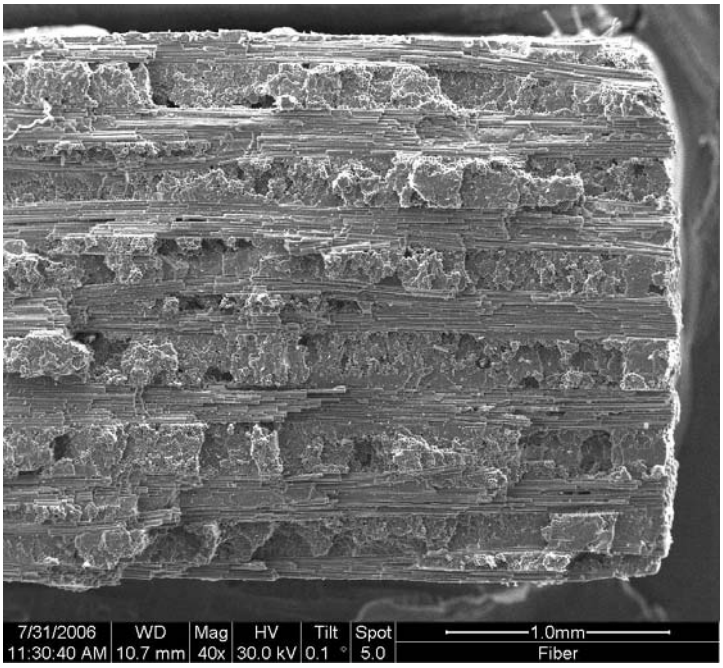

Figure 182. Specimen S150- 40x

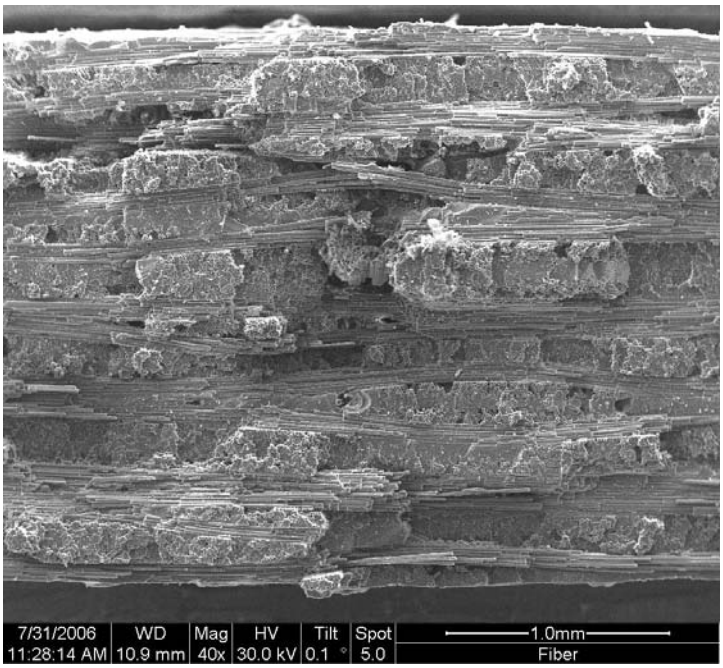

Figure 183. Specimen S150- 40x

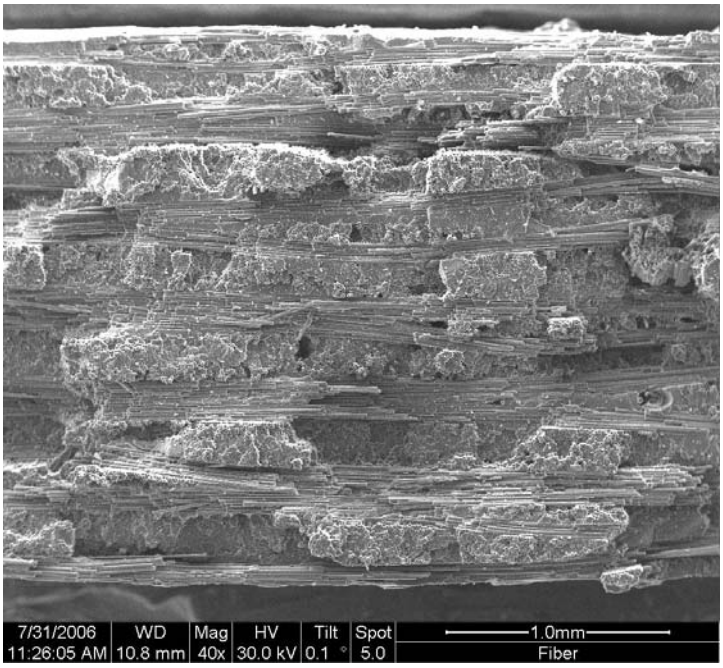

Figure 184. Specimen S150- 40x

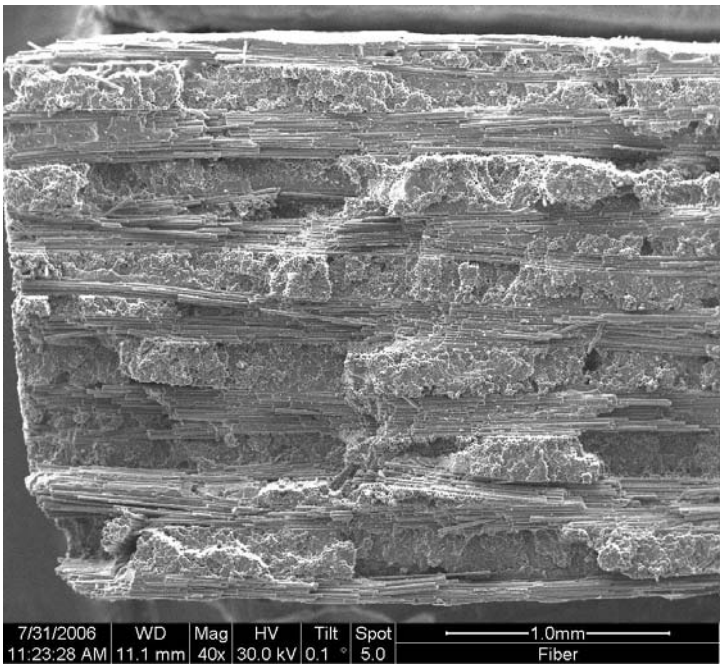

Figure 185. Specimen S150- 40x

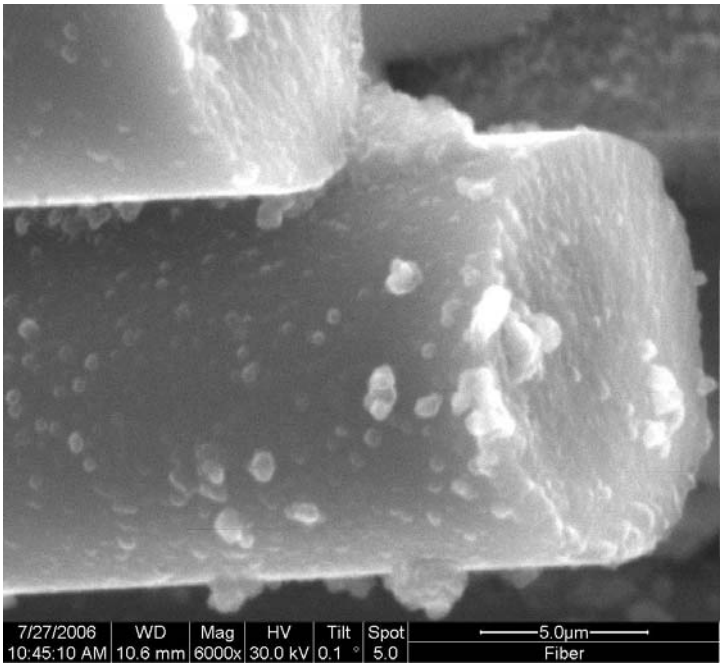

Figure 186. Specimen AsAr80- 6000x

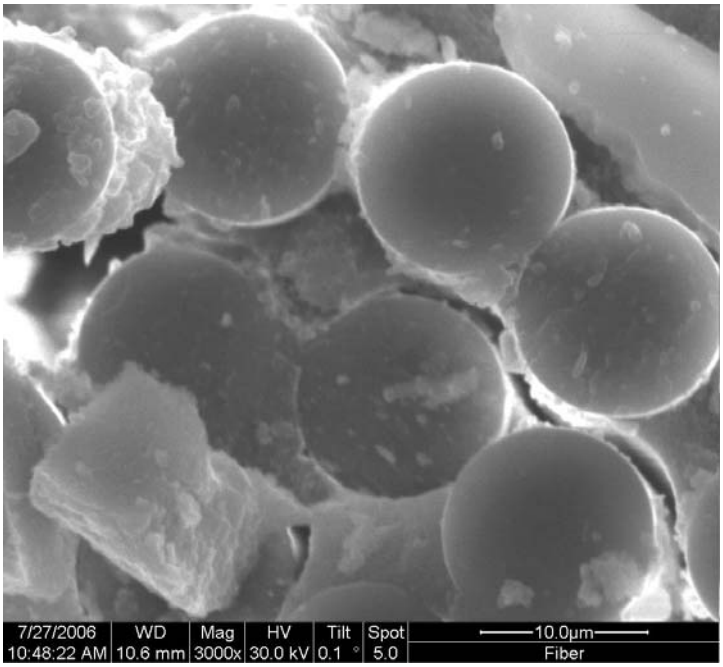

Figure 187. Specimen AsAr80- 3000x

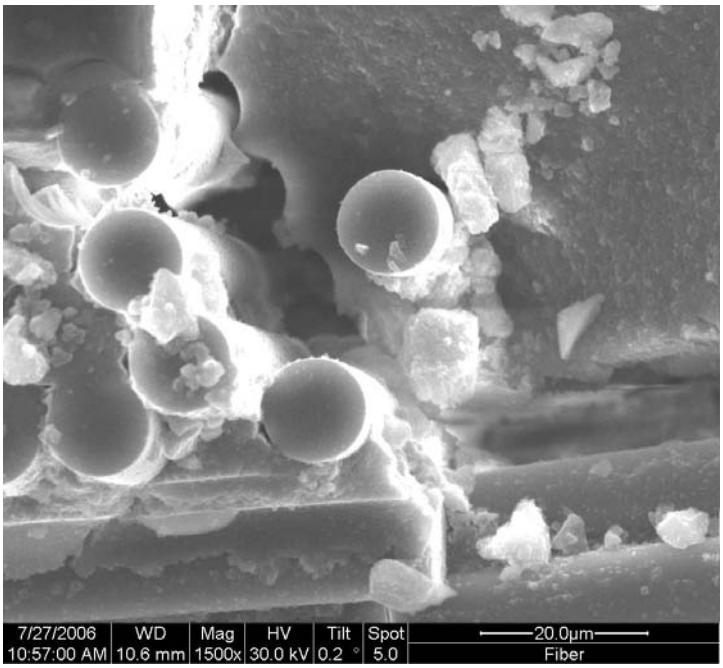

Figure 188. Specimen AsAr80- 1500x

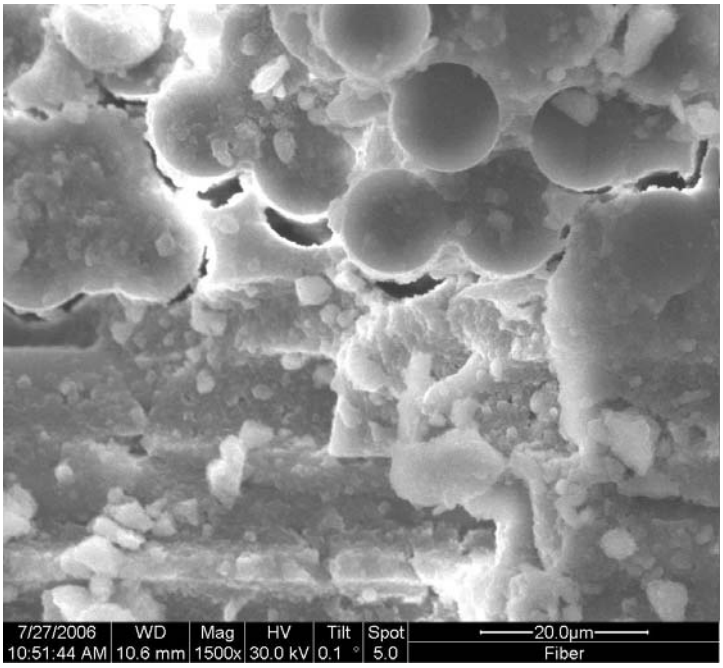

Figure 189. Specimen AsAr80- 1500x

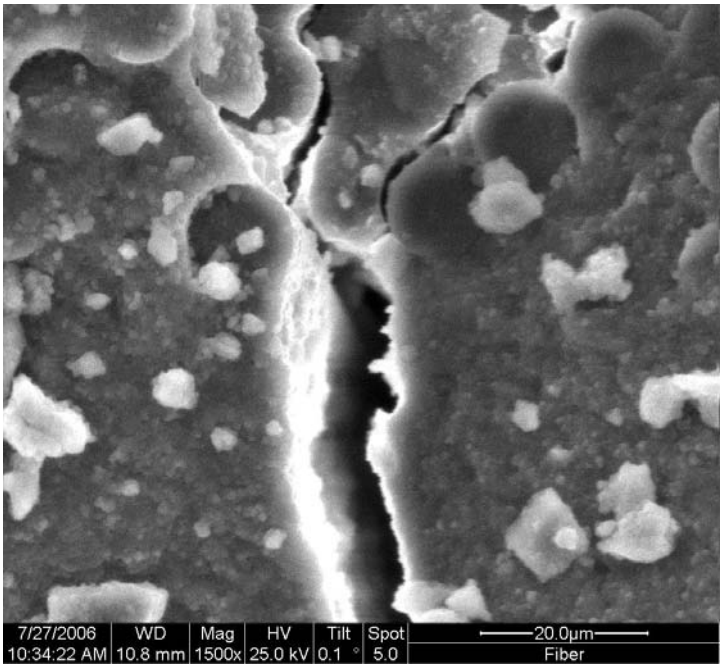

Figure 190. Specimen AsAr80- 1500x

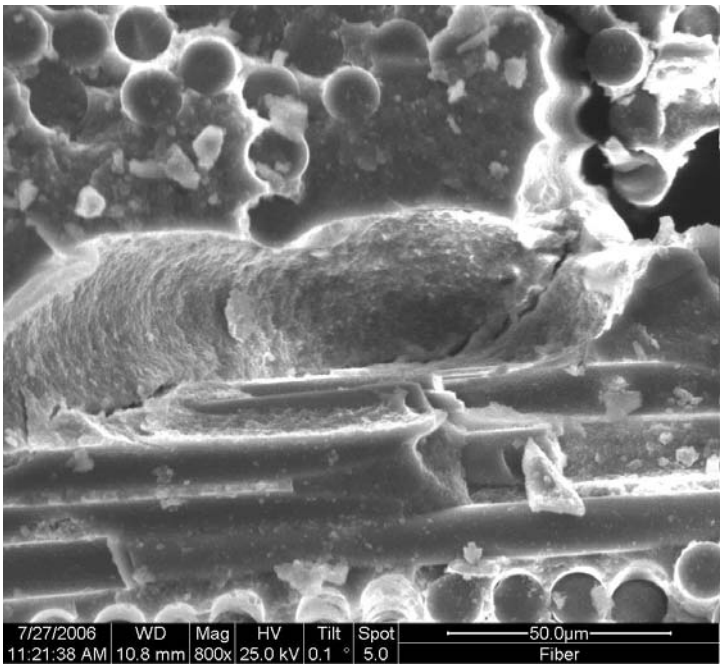

Figure 191. Specimen AsAr80- 800x

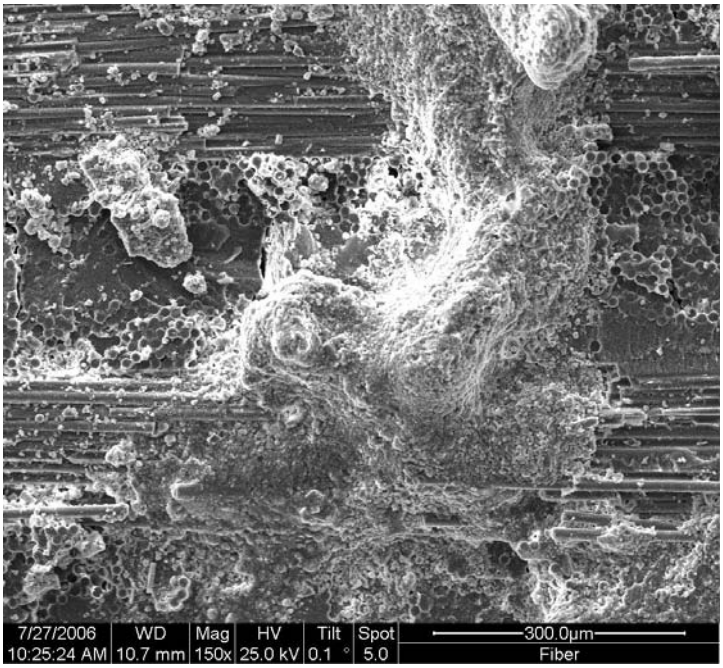

Figure 192. Specimen AsAr80- 150x

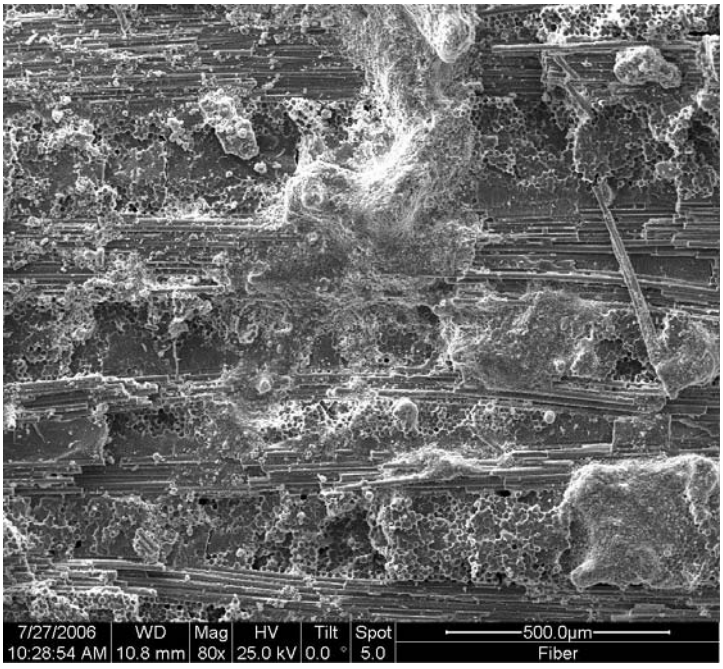

Figure 193. Specimen AsAr80- 80x

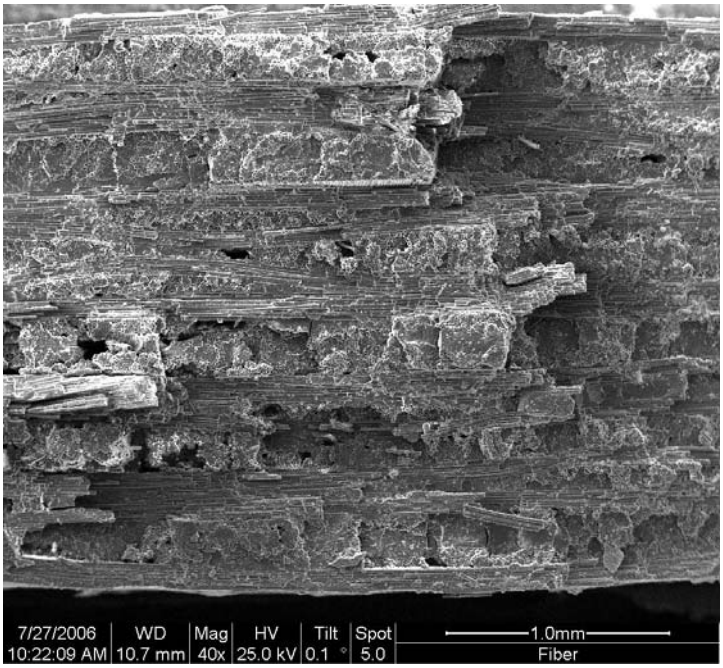

Figure 194. Specimen AsAr80- 40x

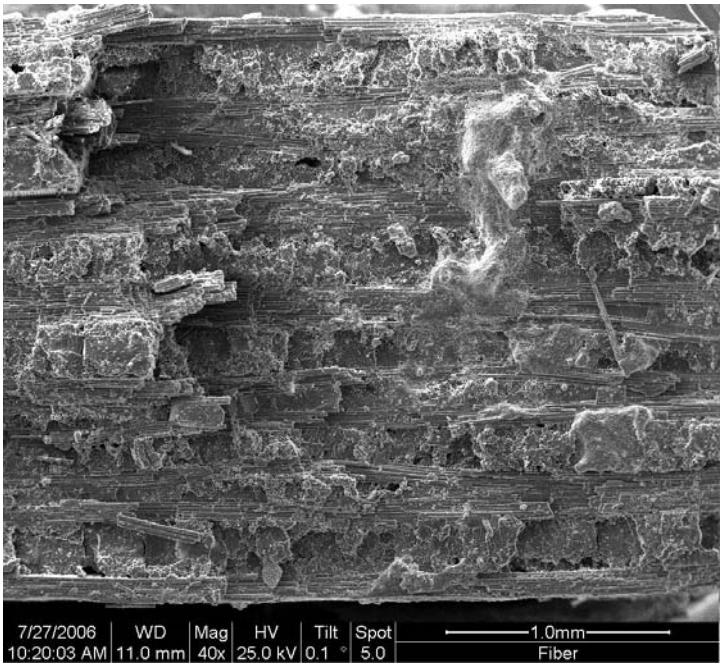

Figure 195. Specimen AsAr80- 40x

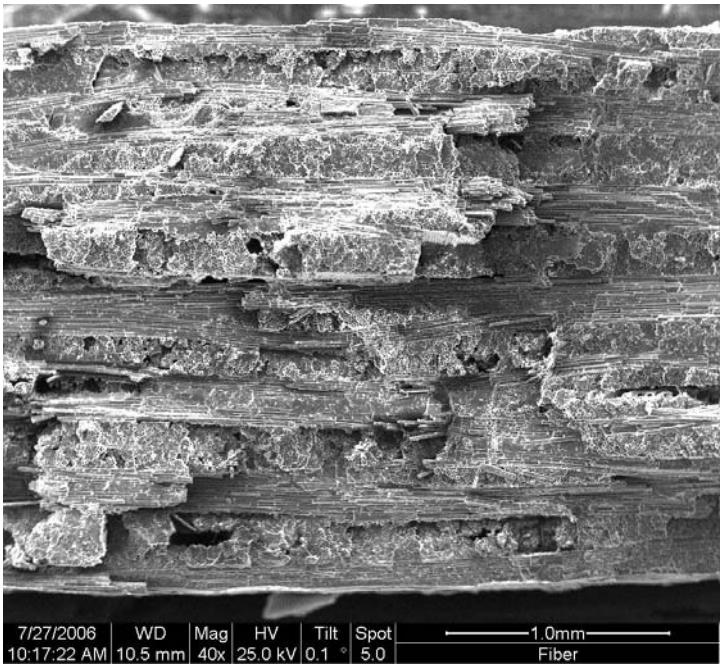

Figure 196. Specimen AsAr80- 40x

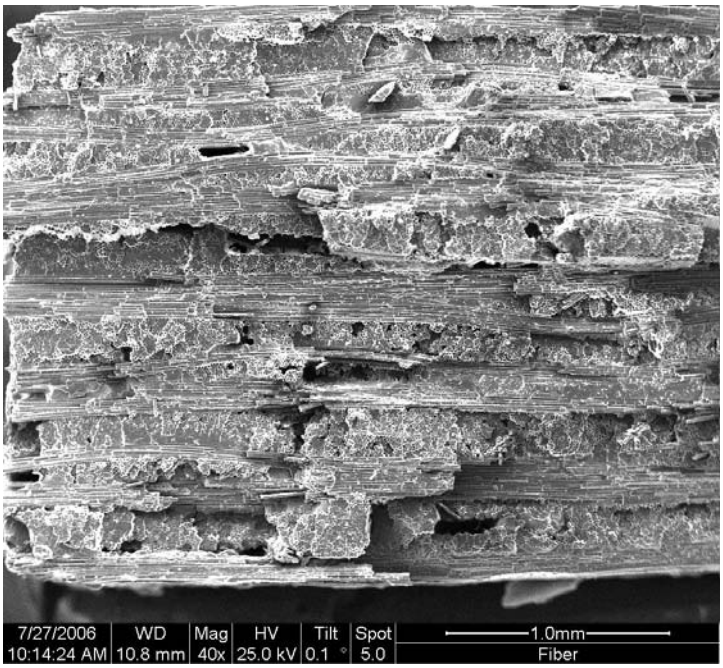

Figure 197. Specimen AsAr80- 40x

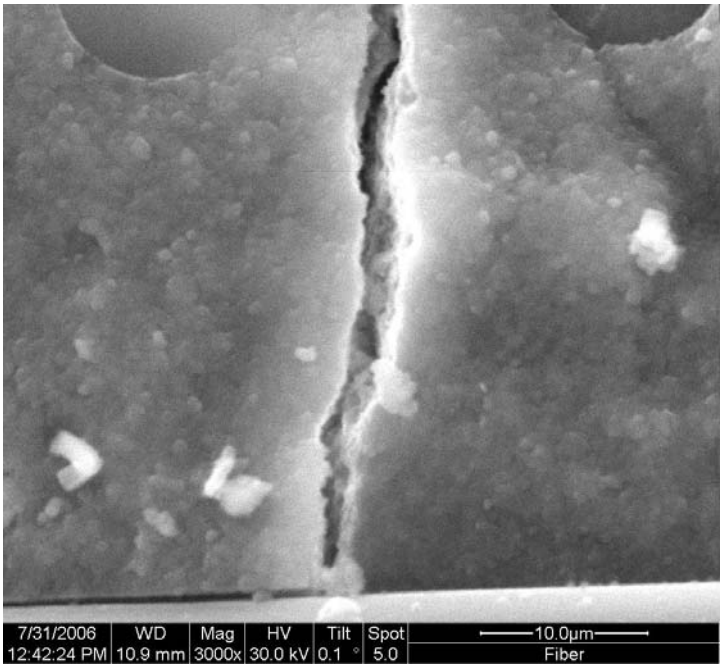

Figure 198. Specimen AsAr100- 3000x

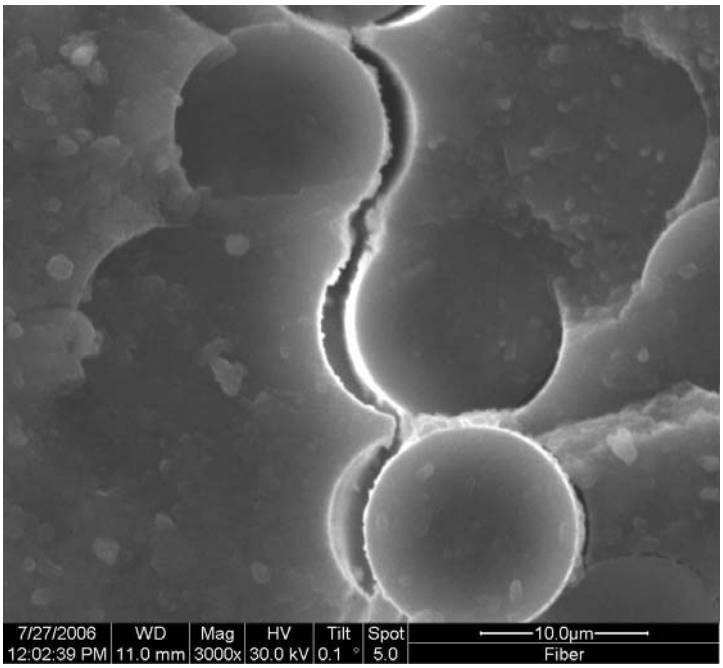

Figure 199. Specimen AsAr100- 3000x

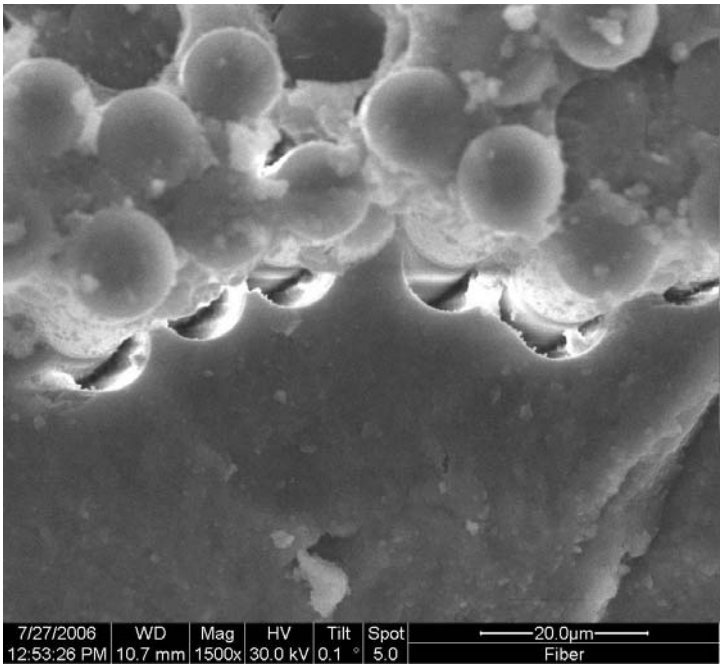

Figure 200. Specimen AsAr100- 1500x

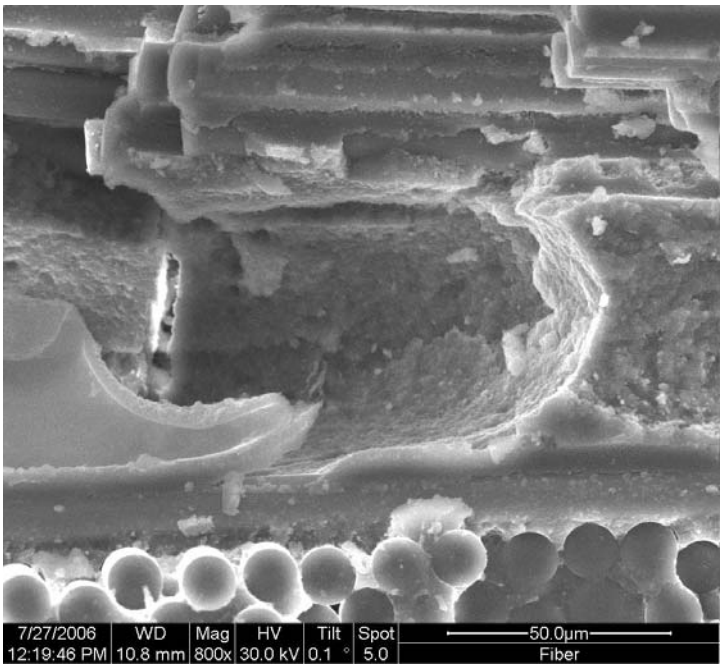

Figure 201. Specimen AsAr100- 800x

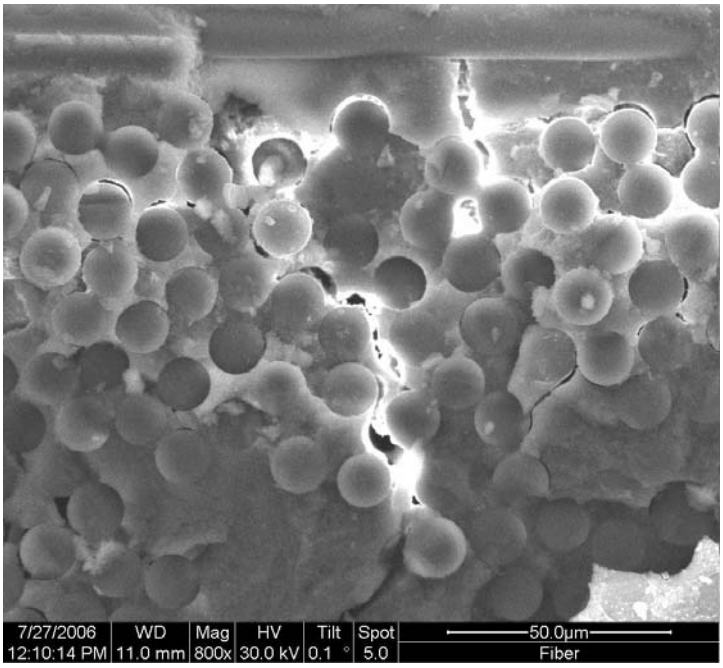

Figure 202. Specimen AsAr100- 800x

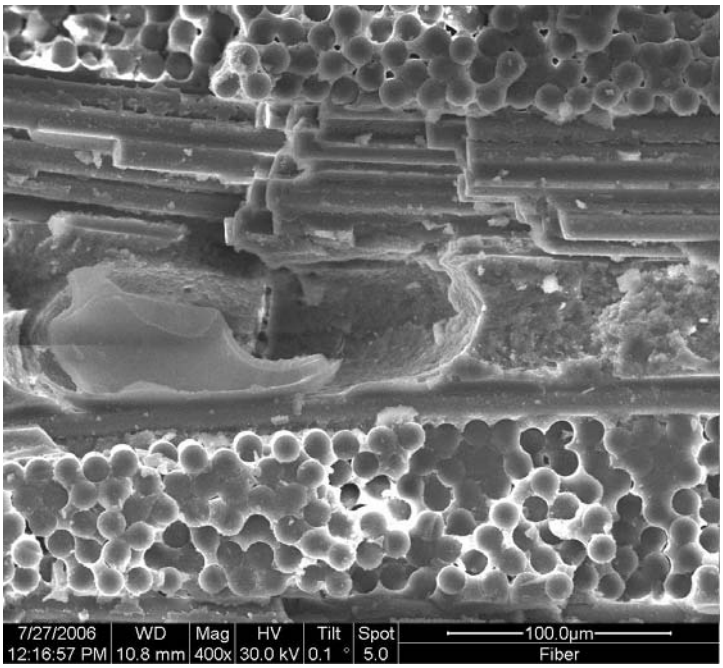

Figure 203. Specimen AsAr100- 400x

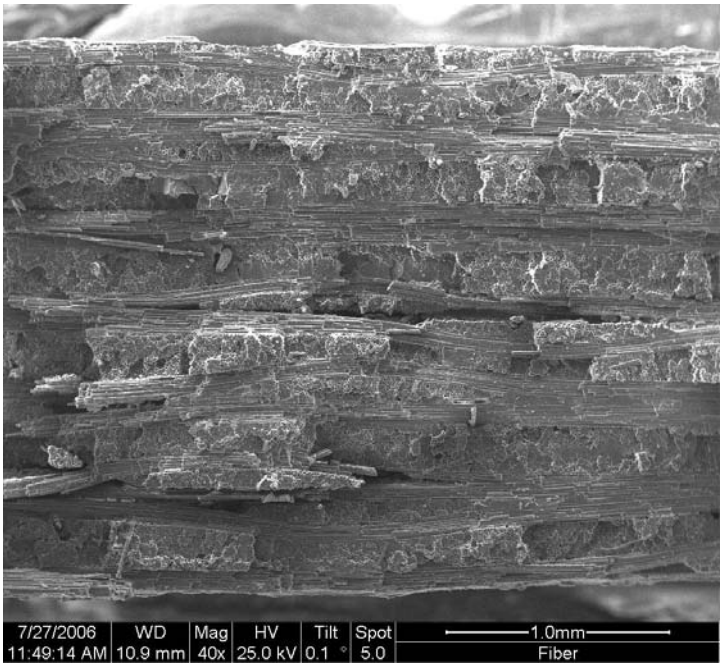

Figure 204. Specimen AsAr100- 40x

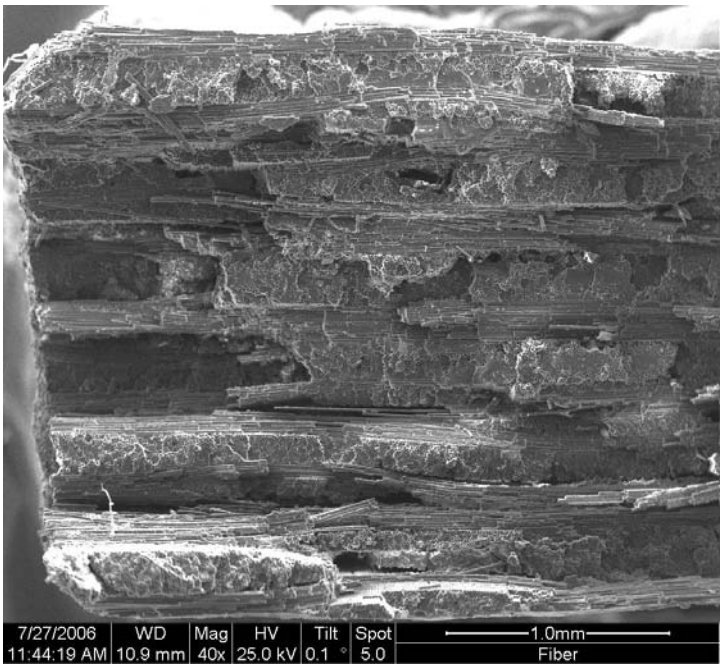

Figure 205. Specimen AsAr100- 40x

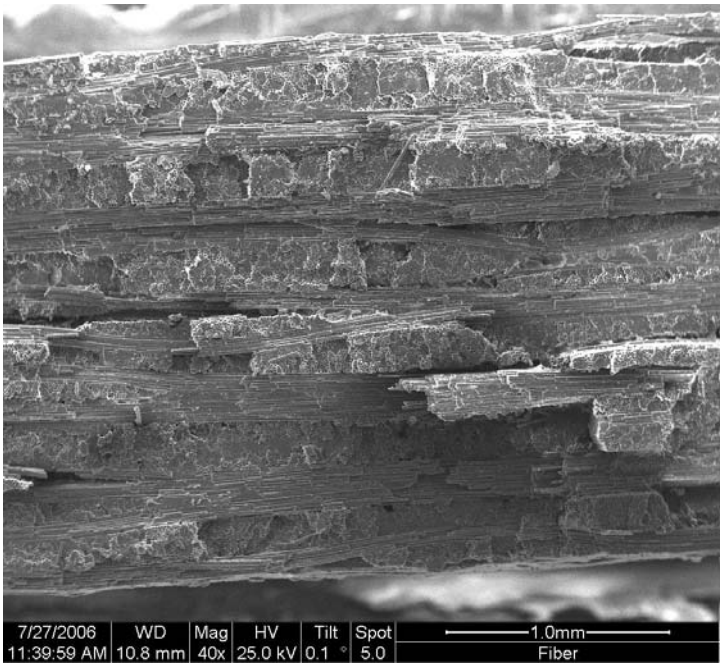

Figure 206. Specimen AsAr100- 40x

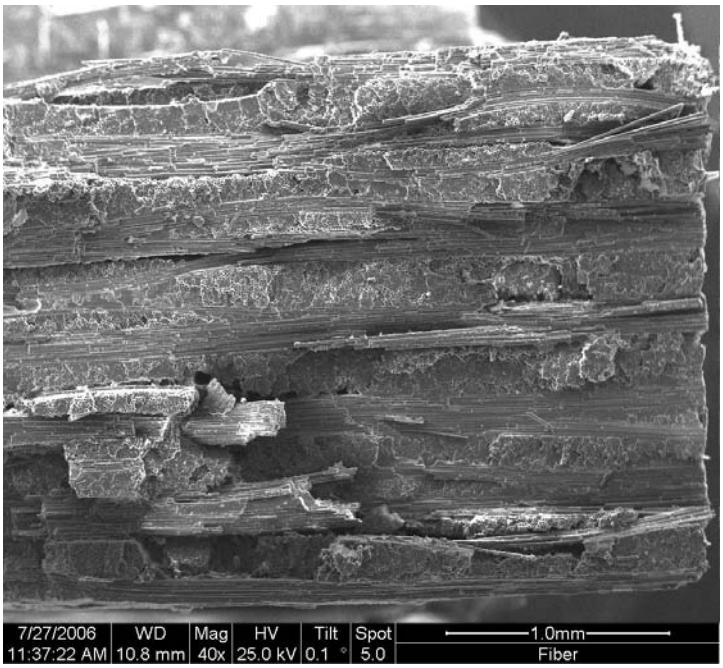

Figure 207. Specimen AsAr100- 40x

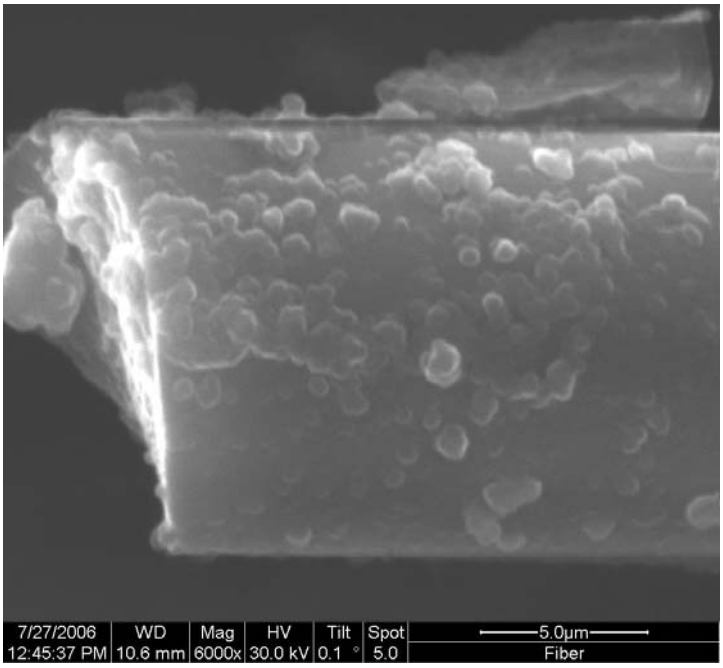

Figure 208. Specimen AsAr125-6000x

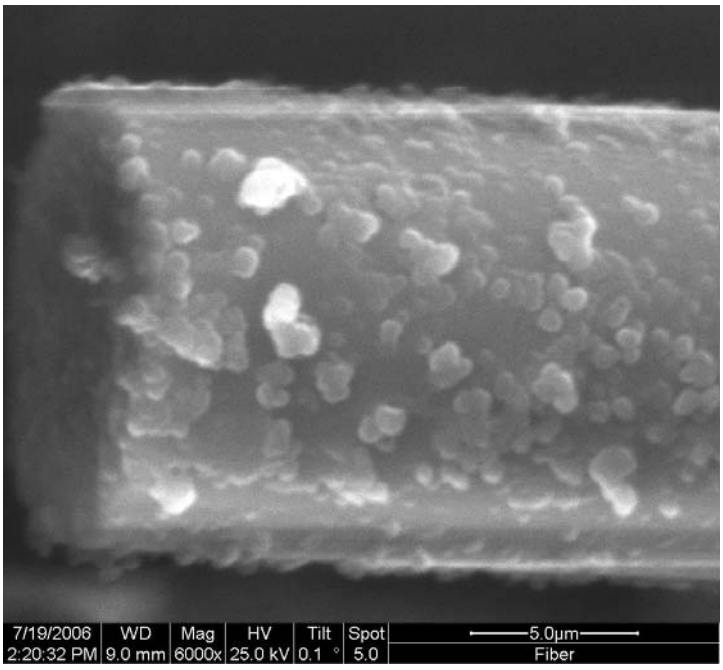

Figure 209. Specimen AsAr125-6000x

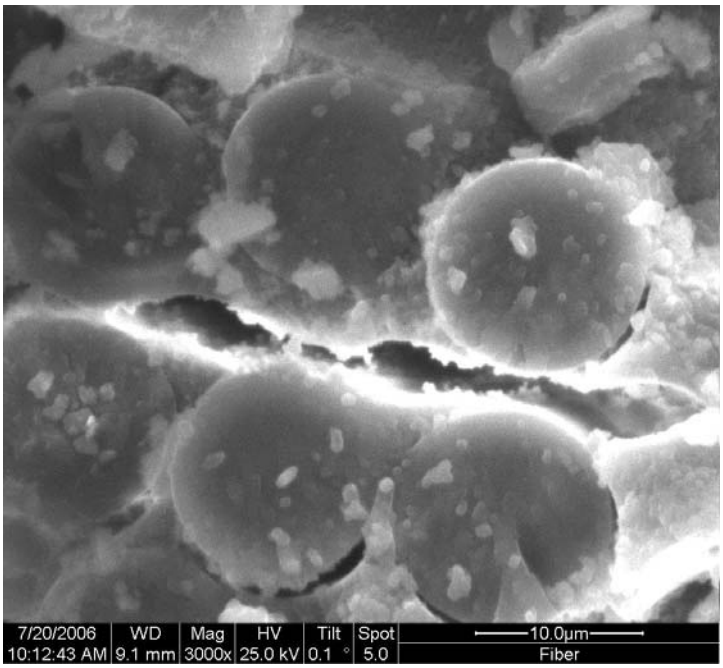

Figure 210. Specimen AsAr125-6000x

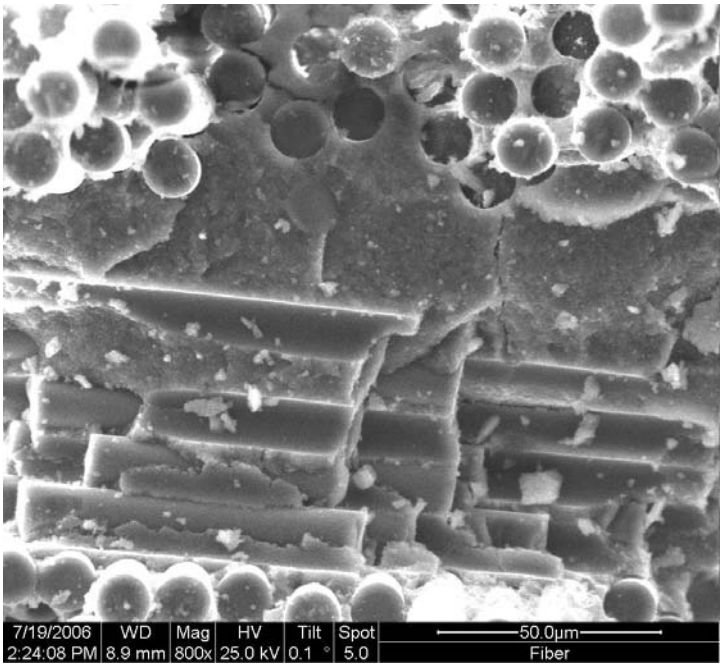

Figure 211. Specimen AsAr125-800x

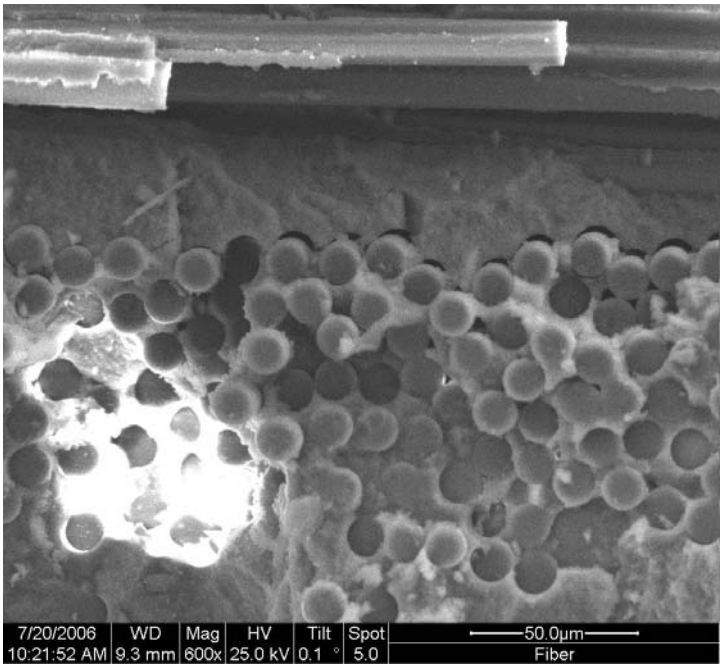

Figure 212. Specimen AsAr125-600x

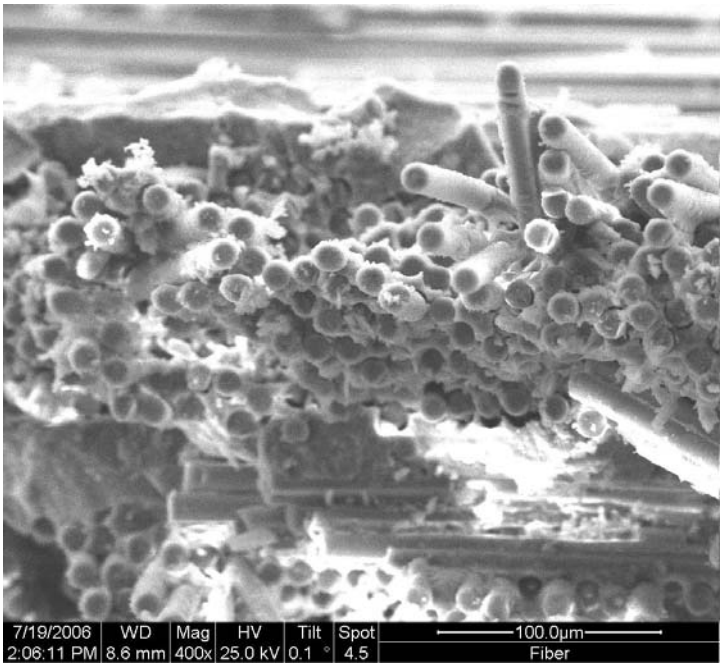

Figure 213. Specimen AsAr125-400x

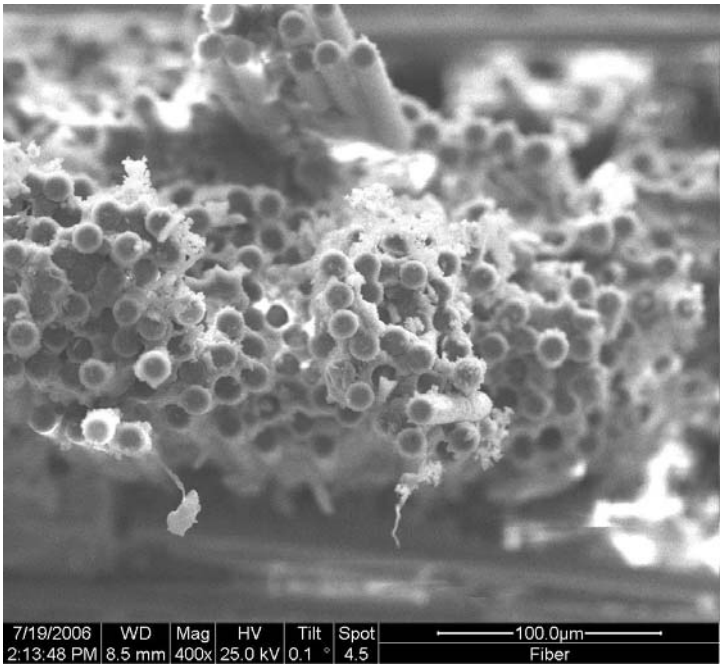

Figure 214. Specimen AsAr125-400x

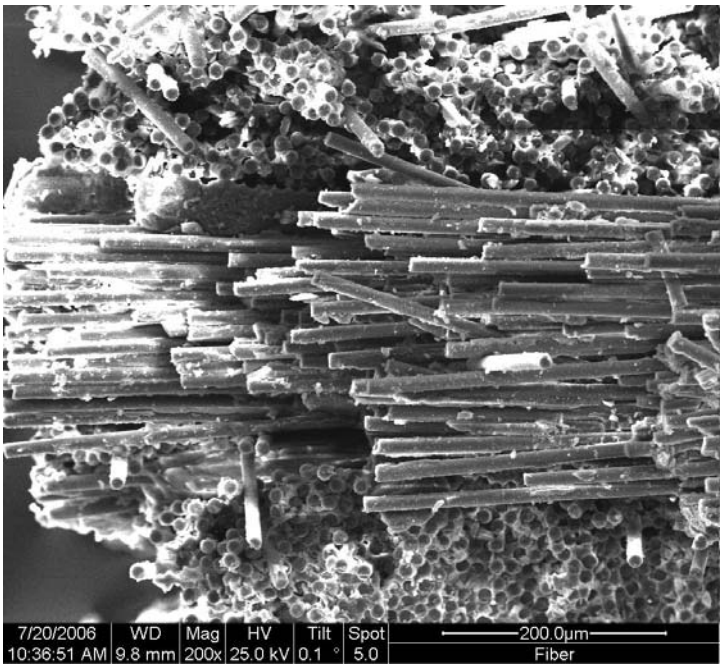

Figure 215. Specimen AsAr125-200x

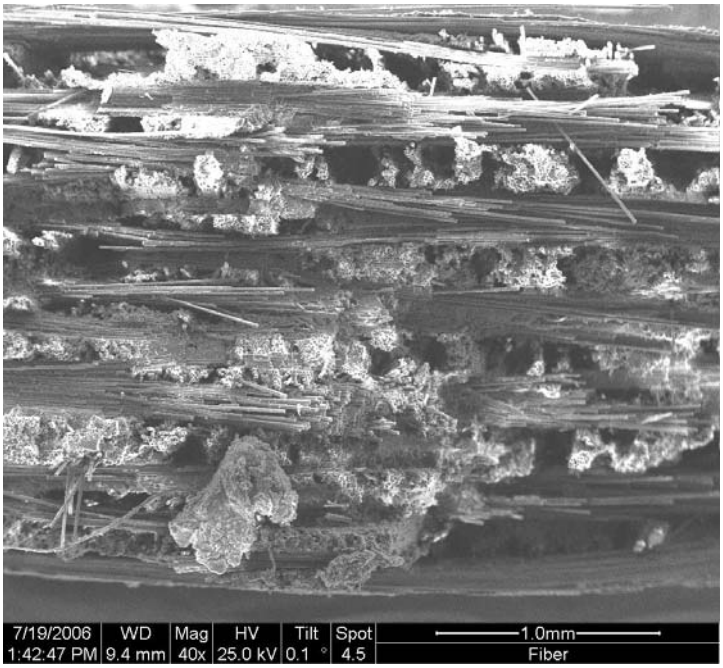

Figure 216. Specimen AsAr125-40x

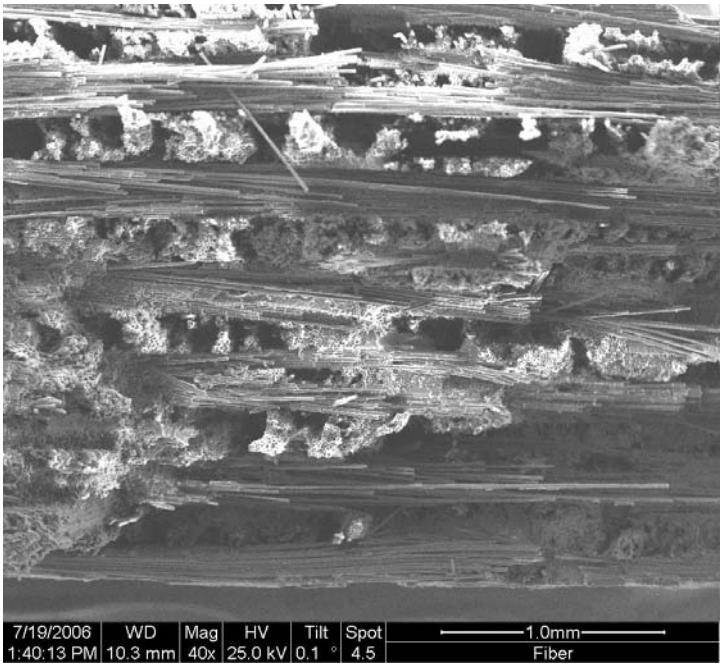

Figure 217. Specimen AsAr125-40x

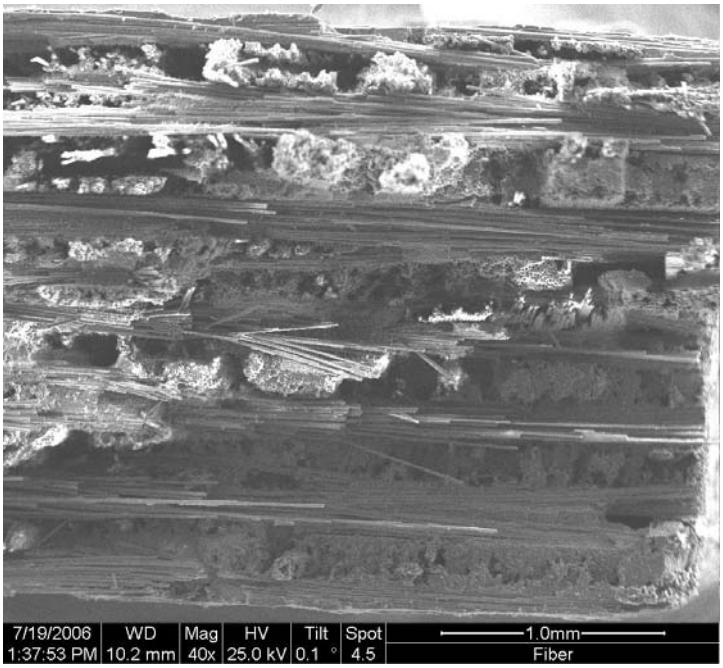

Figure 218. Specimen AsAr125-40x

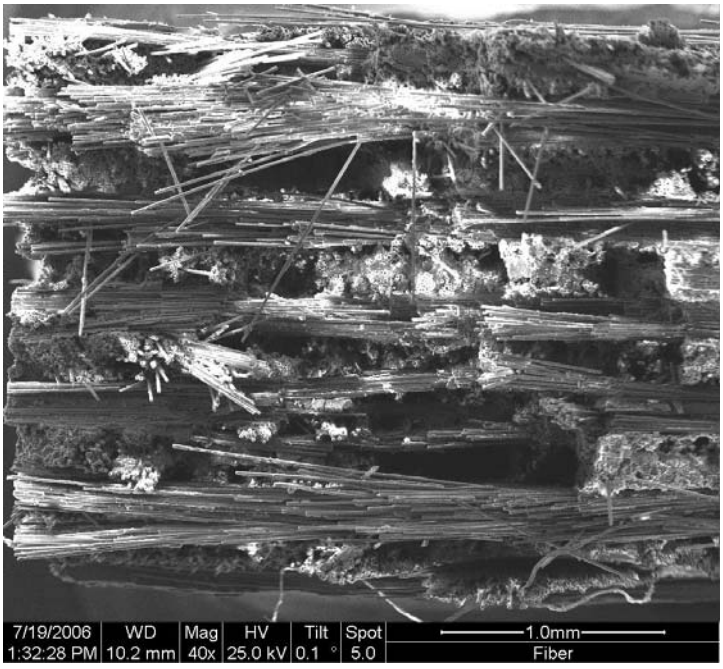

Figure 219. Specimen AsAr125-40x

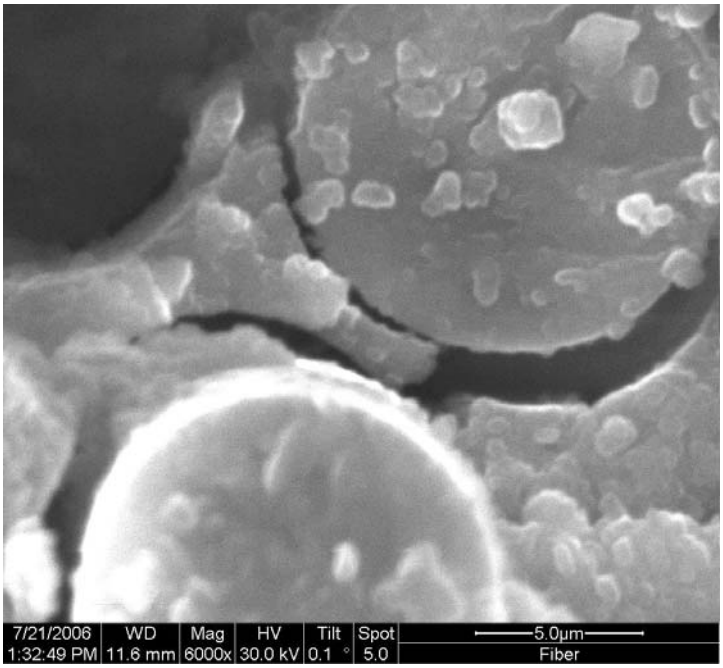

Figure 220. Specimen AsAr150-6000x

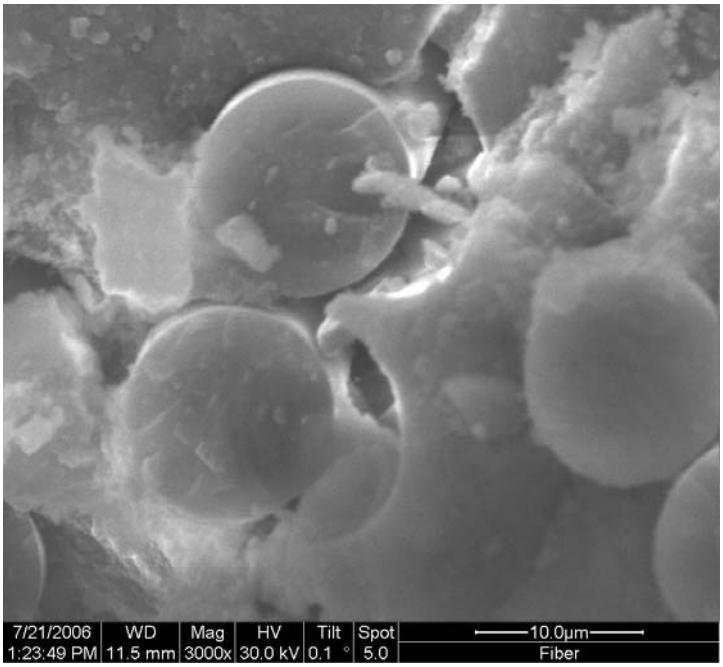

Figure 221. Specimen AsAr150-3000x

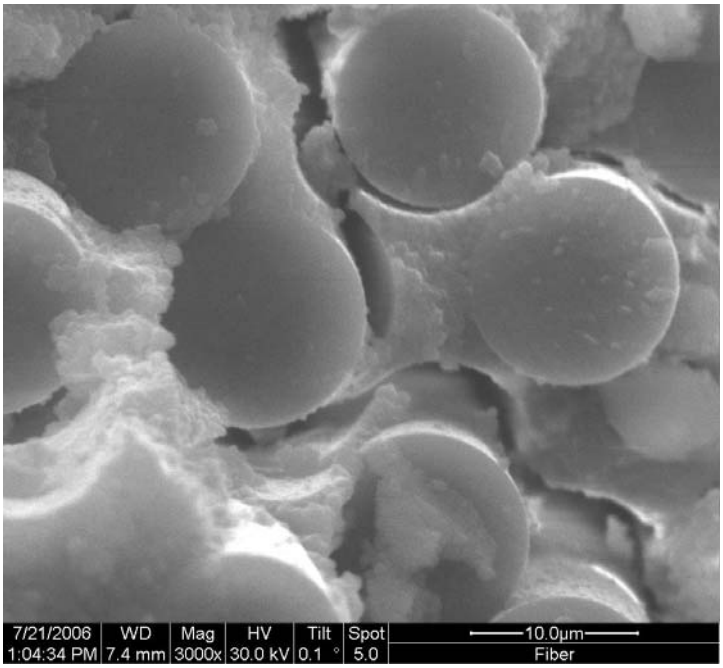

Figure 222. Specimen AsAr150-3000x

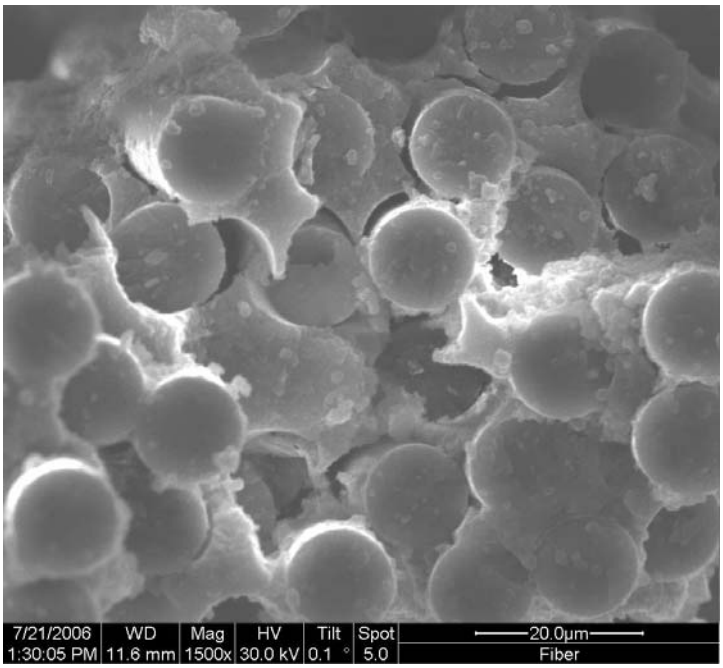

Figure 223. Specimen AsAr150-1500x

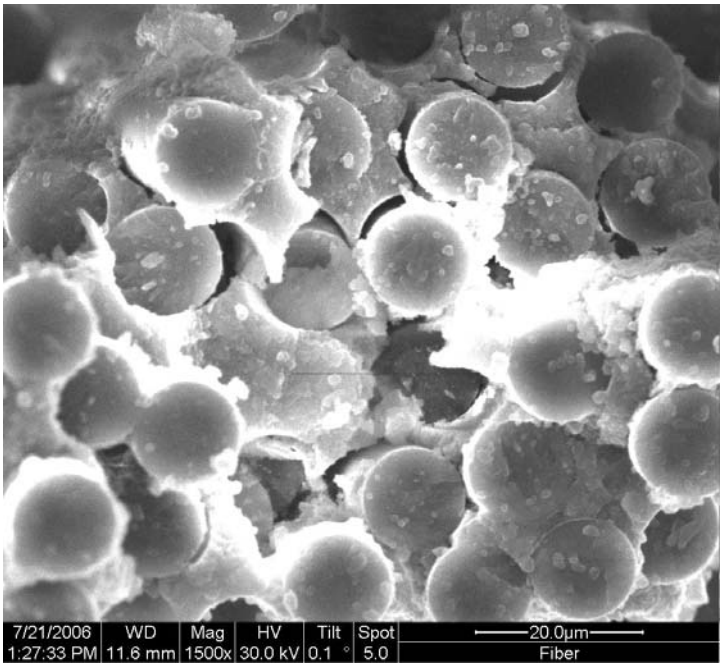

Figure 224. Specimen AsAr150-1500x

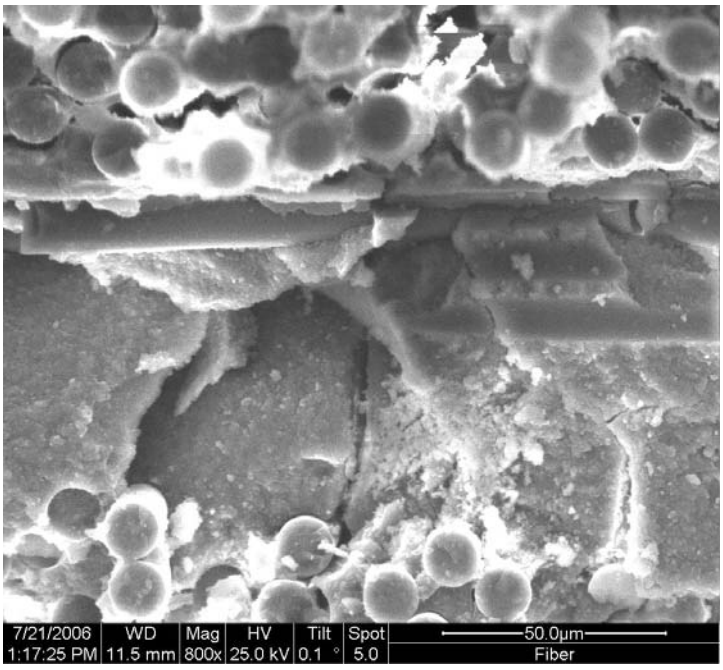

Figure 225. Specimen AsAr150-800x

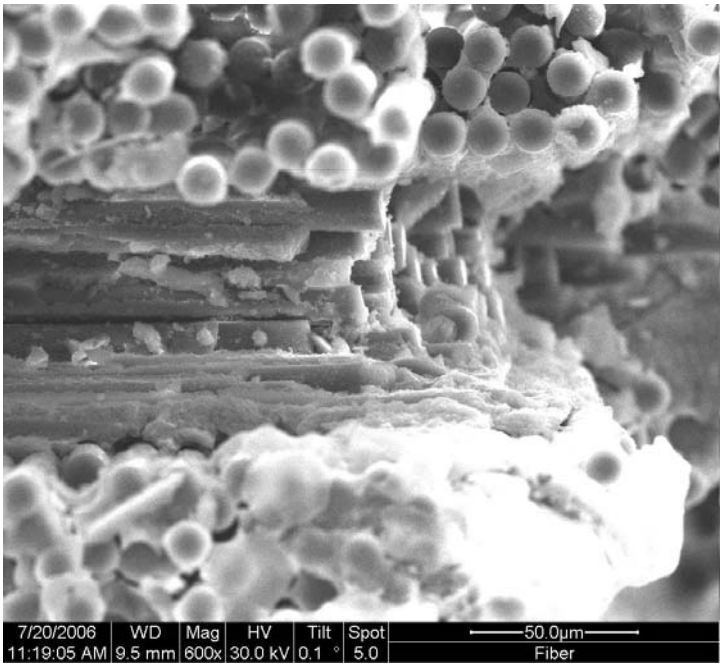

Figure 226. Specimen AsAr150-1500x

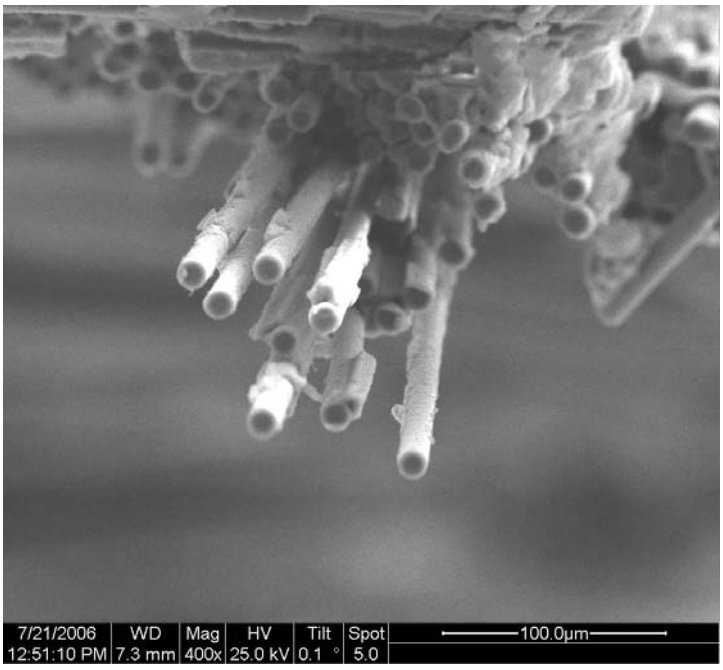

Figure 227. Specimen AsAr150-400x

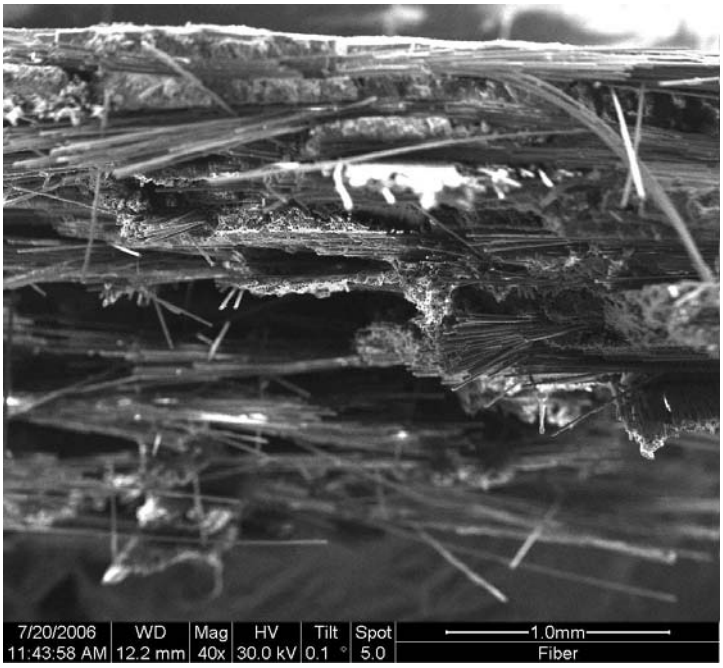

Figure 228. Specimen AsAr150-40x

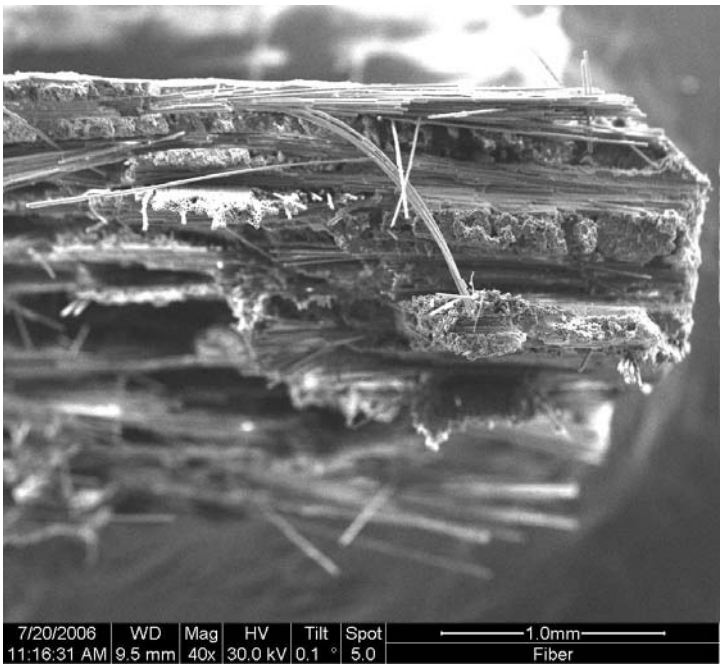

Figure 229. Specimen AsAr150-40x

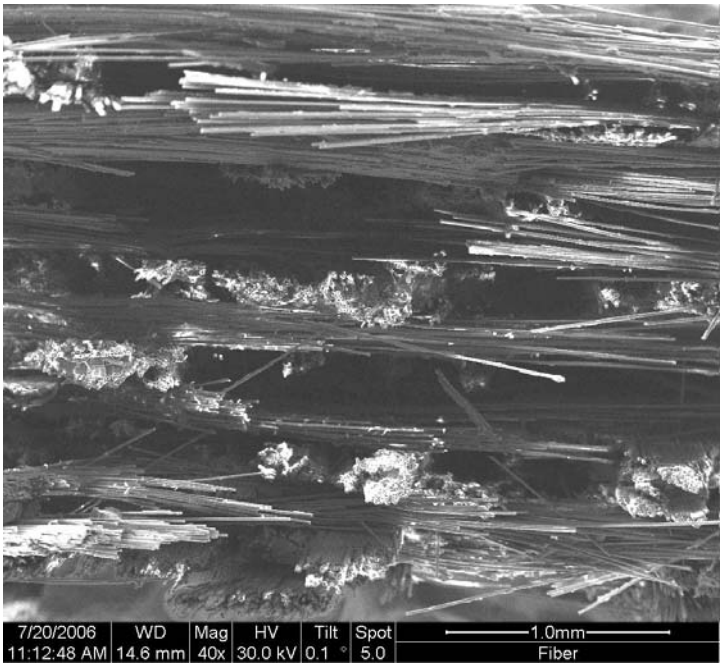

Figure 230. Specimen AsAr150-40x

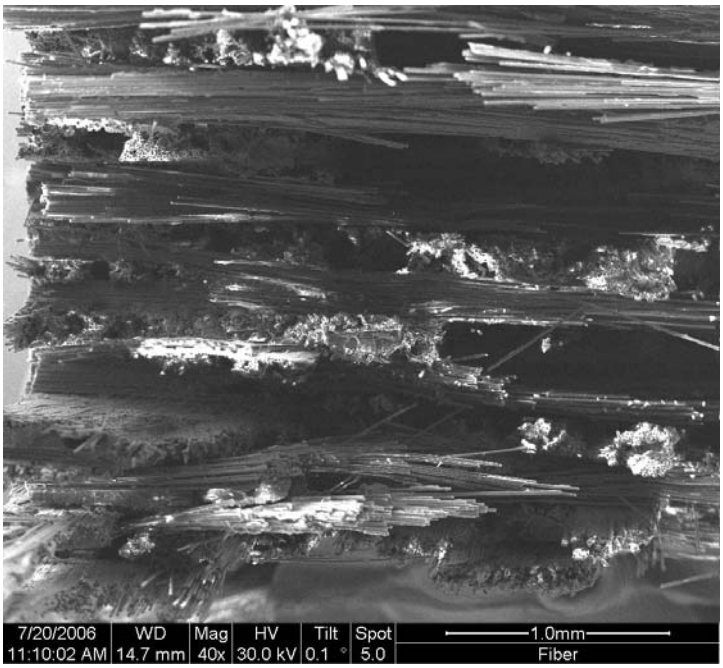

Figure 231. Specimen AsAr150-40x

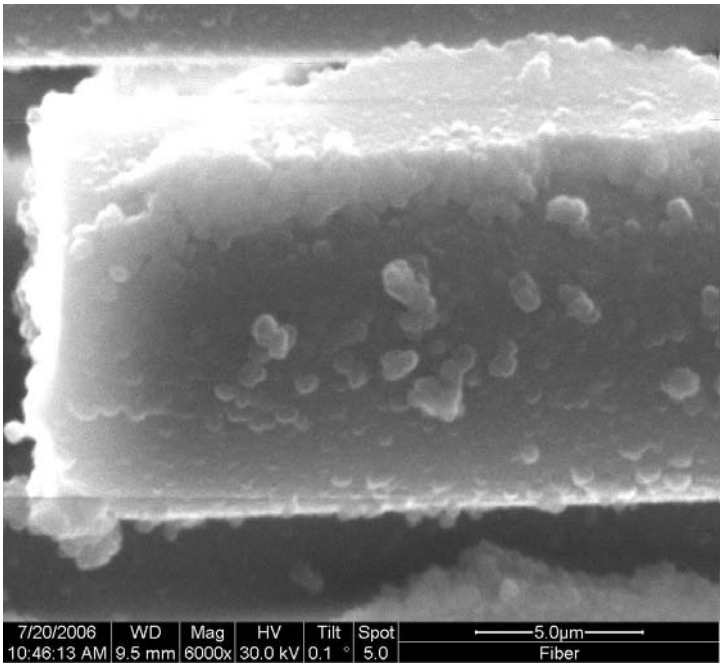

Figure 232. Specimen AAr125-6000x

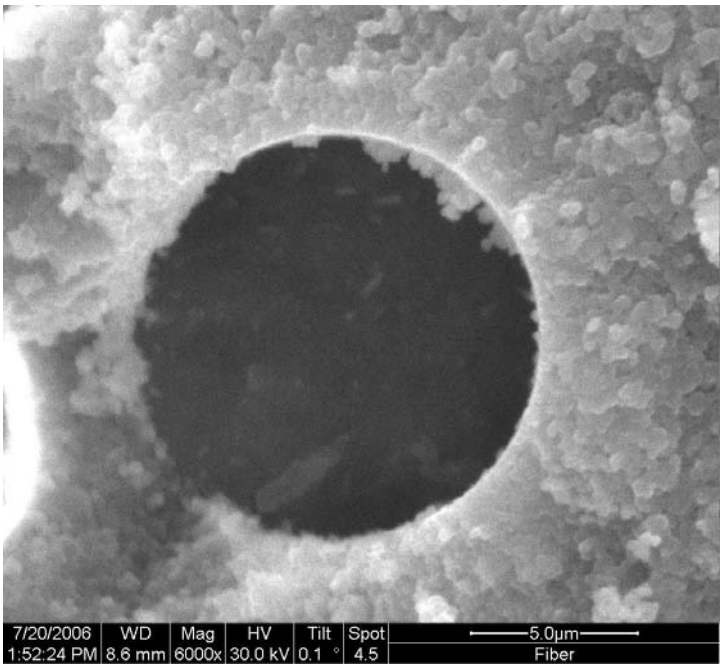

Figure 233. Specimen AAr125-6000x

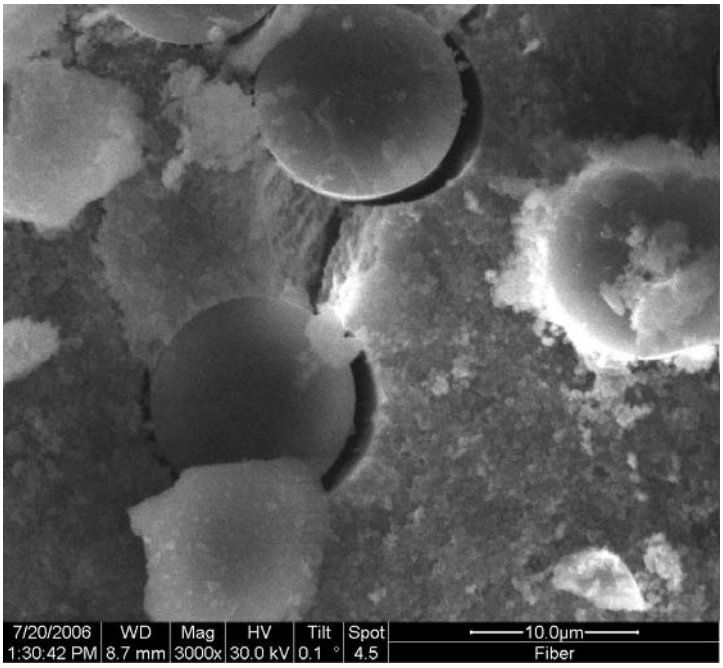

Figure 234. Specimen AAr125-3000x

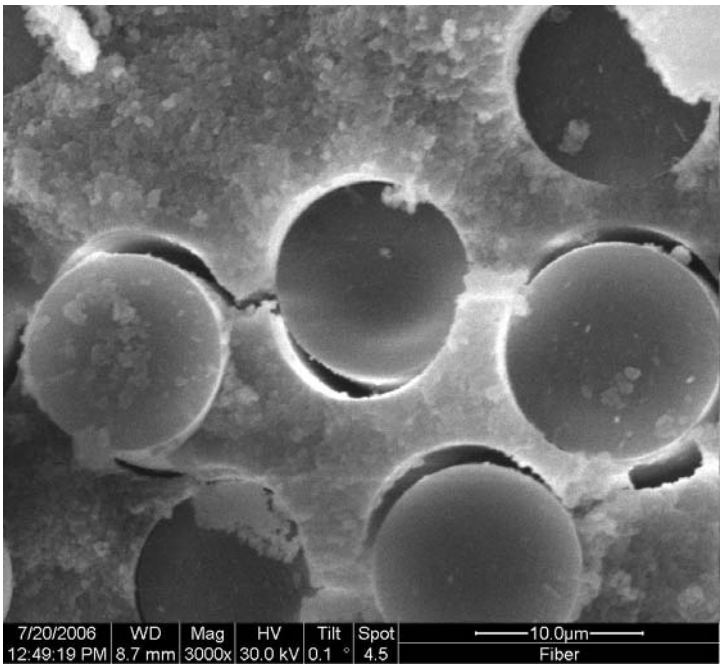

Figure 235. Specimen AAr125-3000x

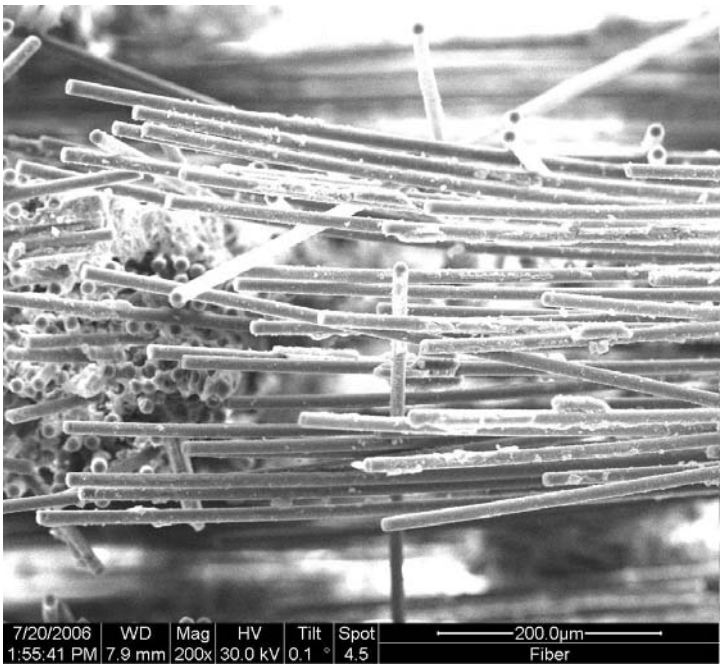

Figure 236. Specimen AAr125-200x

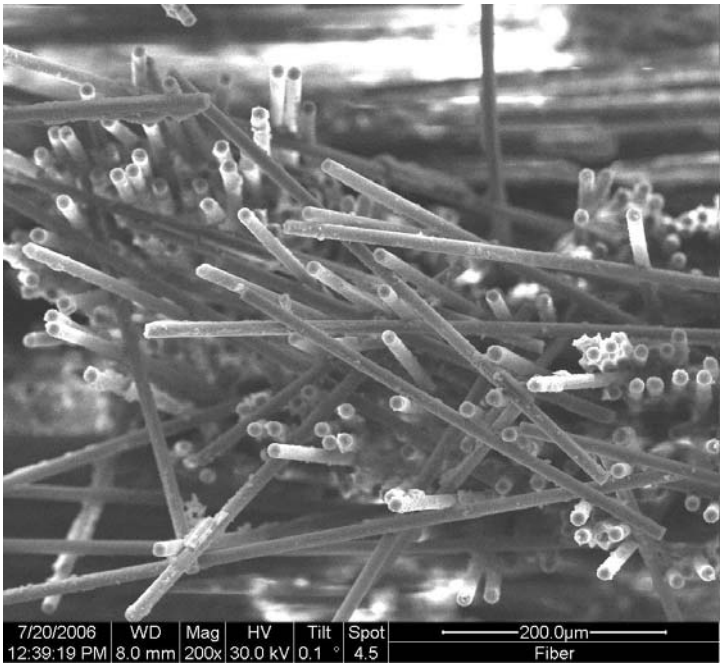

Figure 237. Specimen AAr125-200x

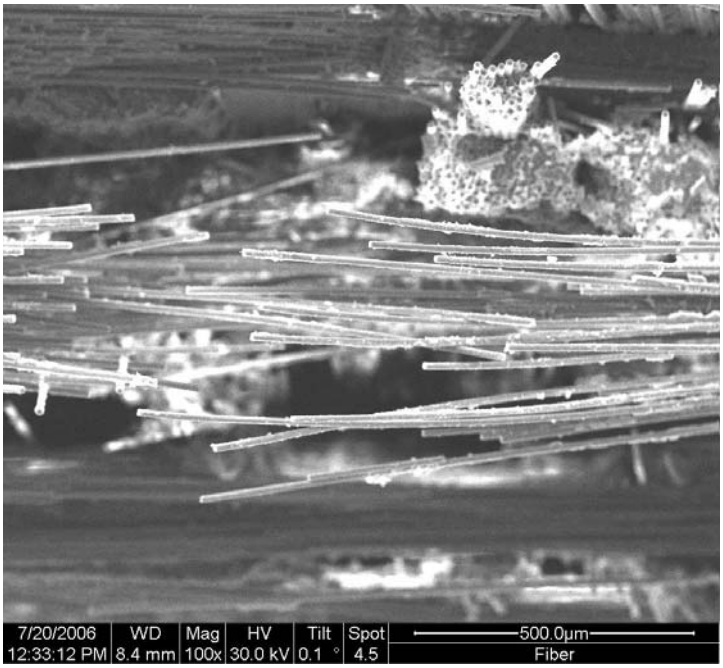

Figure 238. Specimen AAr125-100x

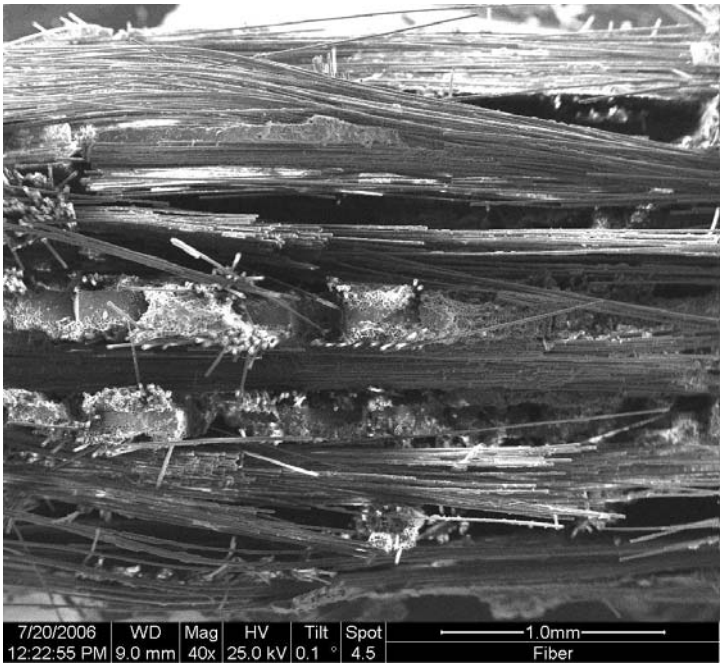

Figure 239. Specimen AAr125-40x

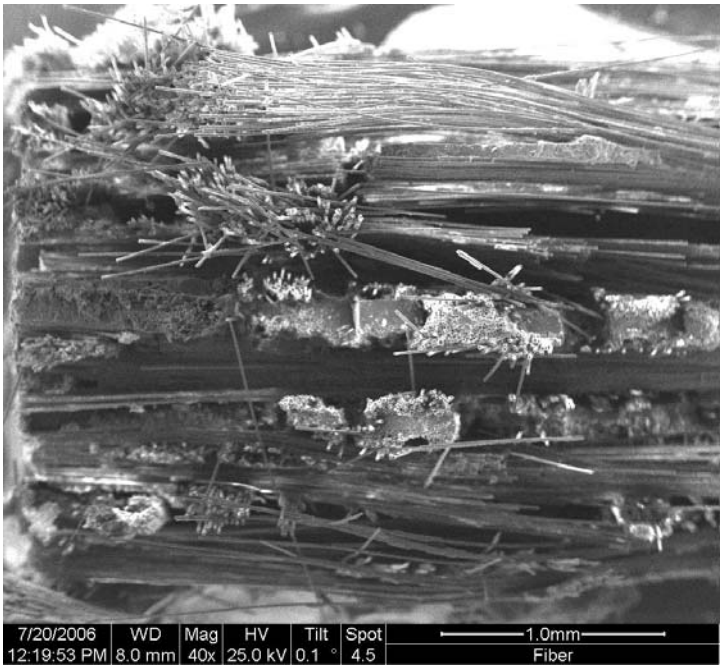

Figure 240. Specimen AAr125-40x

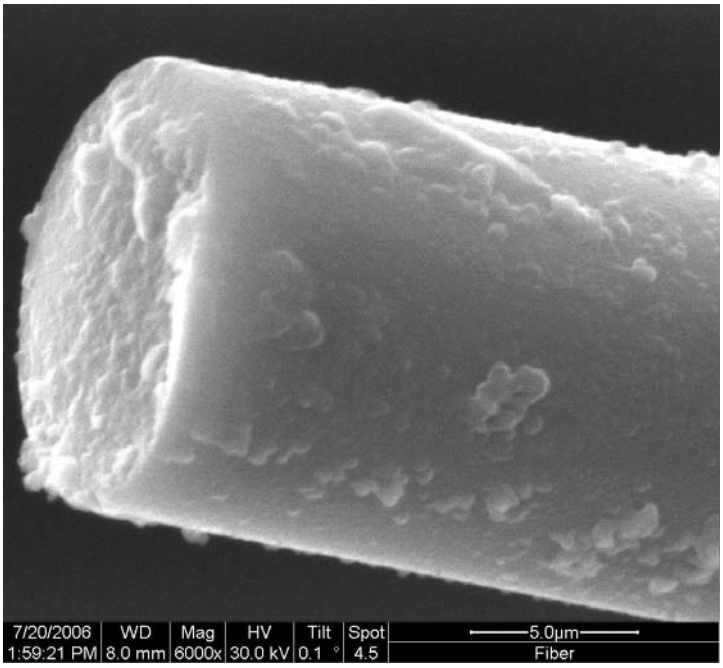

Figure 241. Specimen AAr150-6000x

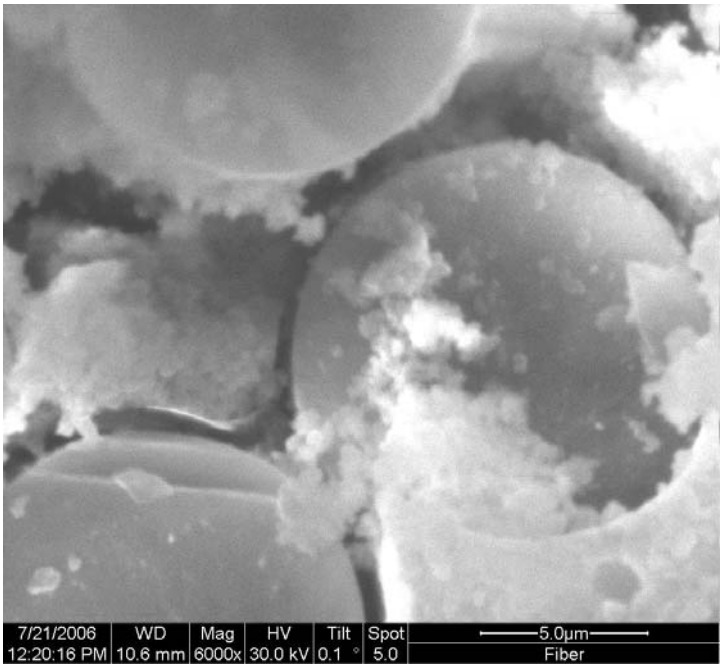

Figure 242. Specimen AAr150-6000x

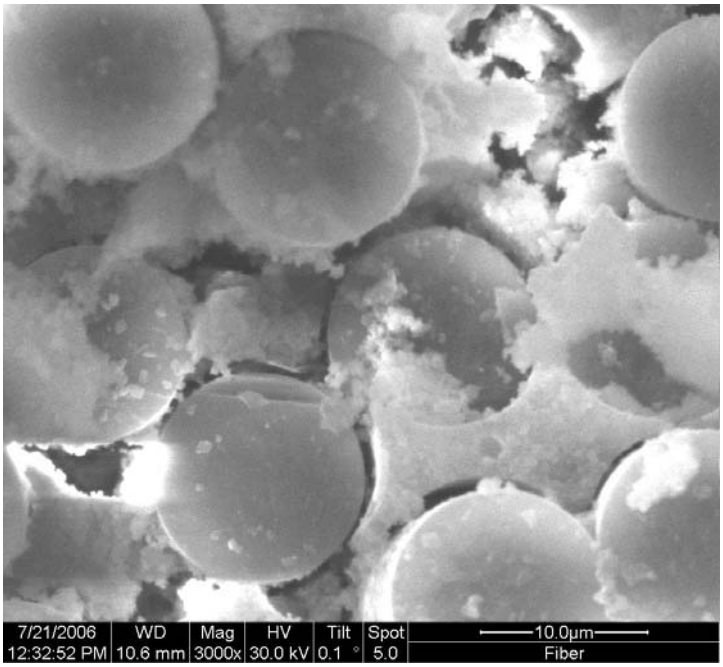

Figure 243. Specimen AAr150-3000x

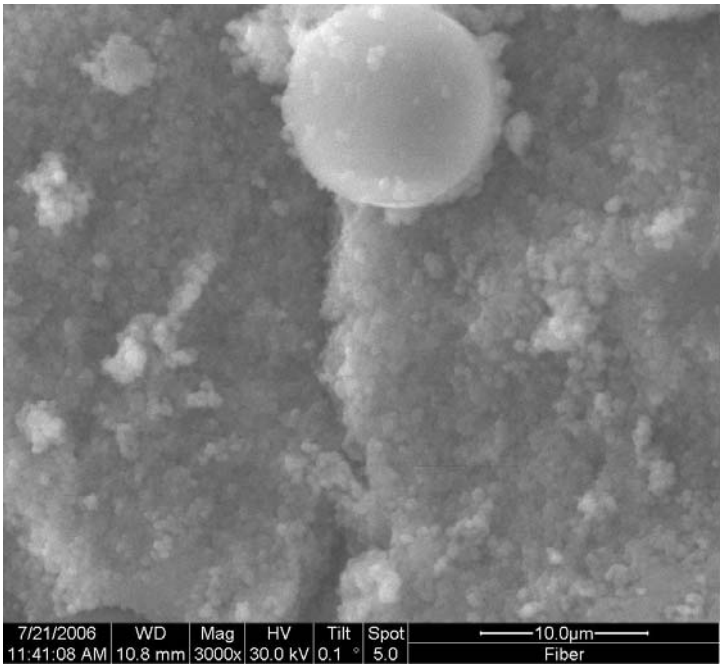

Figure 244. Specimen AAr150-3000x

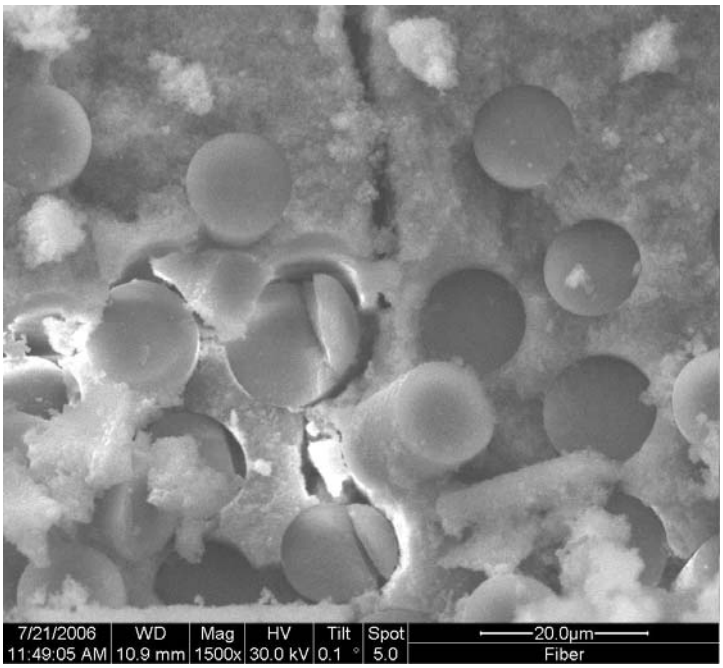

Figure 245. Specimen AAr150-1500x

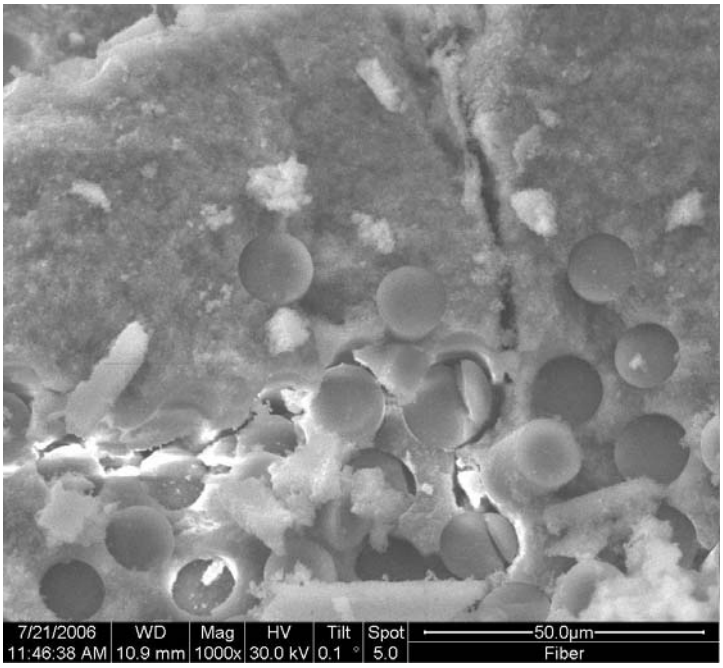

Figure 246. Specimen AAr150-1000x

Figure 247. Specimen AAr150-300x

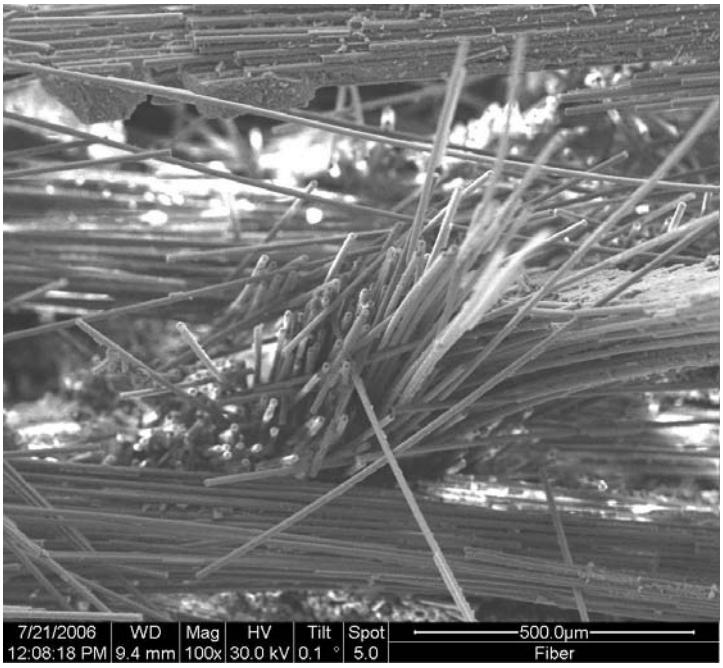

Figure 248. Specimen AAr150-100x

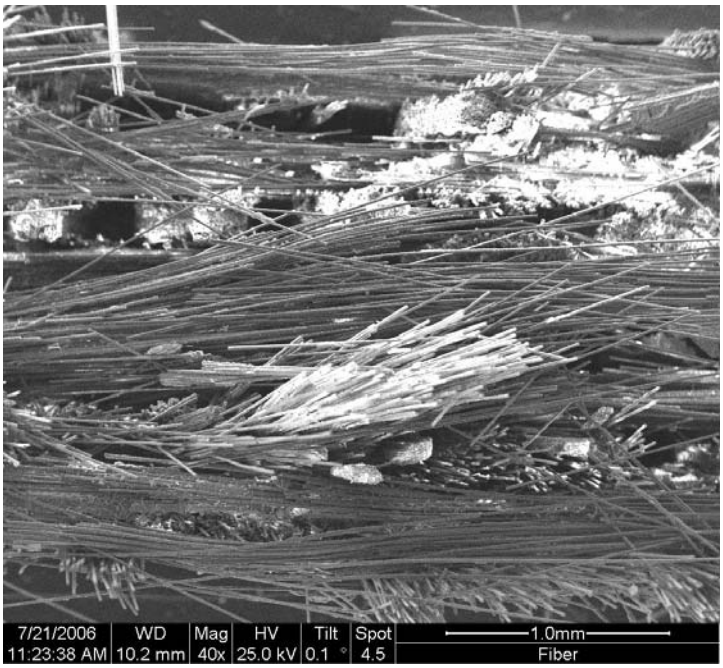

Figure 249. Specimen AAr150-40x

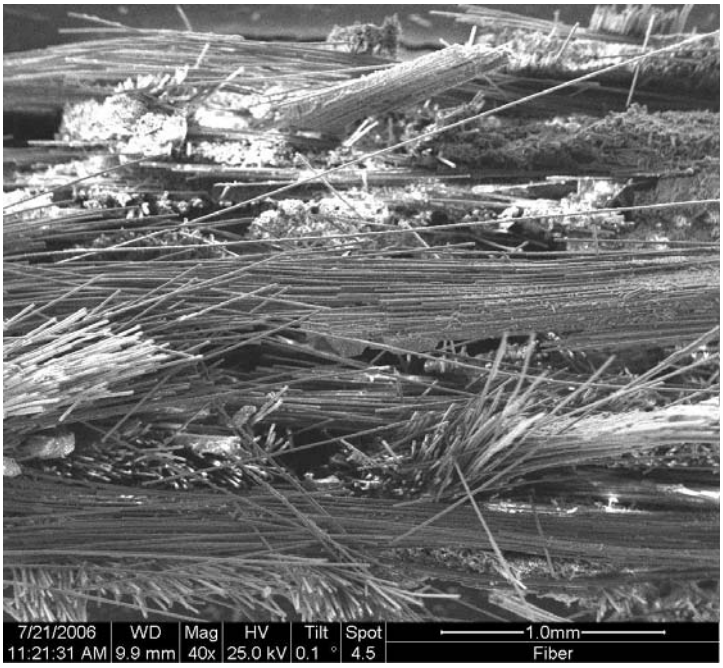

Figure 250. Specimen AAr150-40x

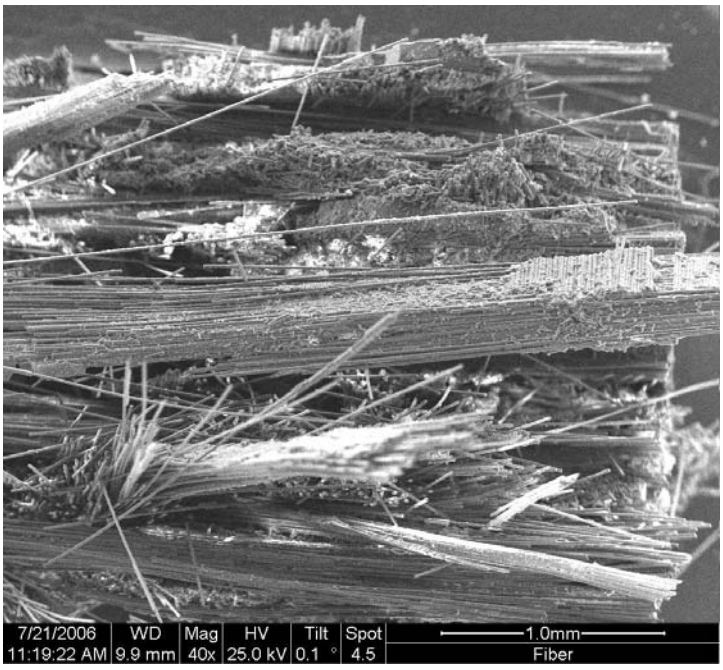

Figure 251. Specimen AAr150-40x

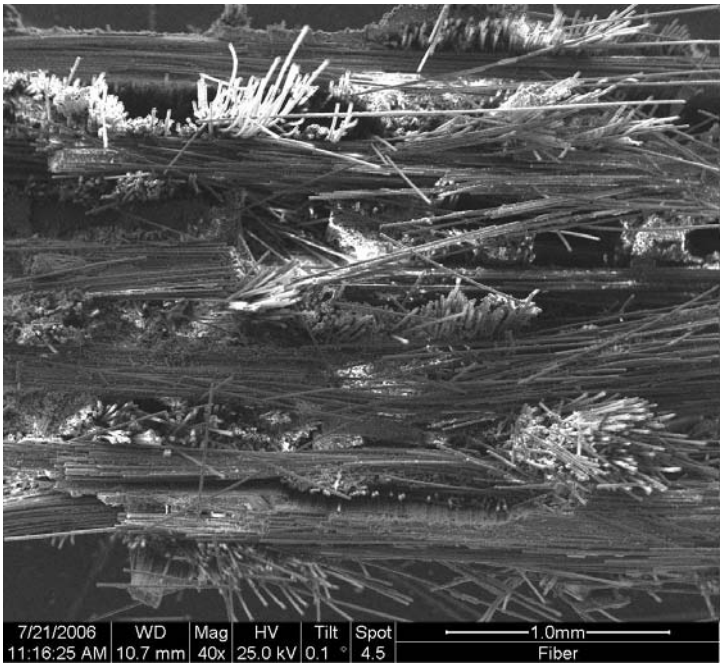

Figure 252. Specimen AAr150-40x

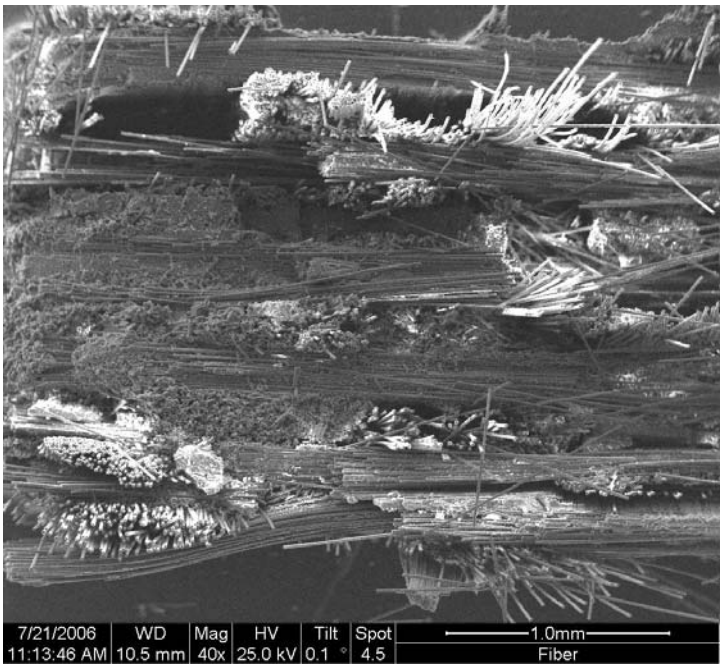

Figure 253. Specimen AAr150-40x

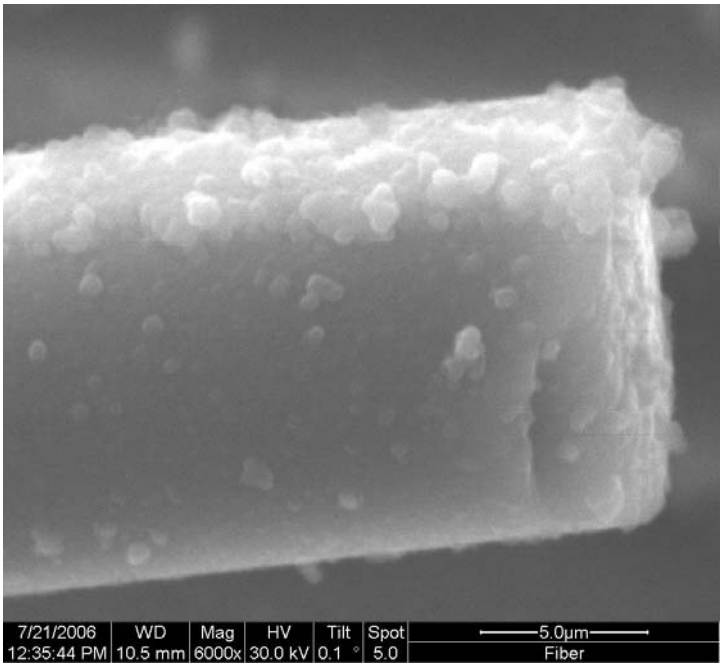

Figure 254. Specimen Virgin AS -6000x

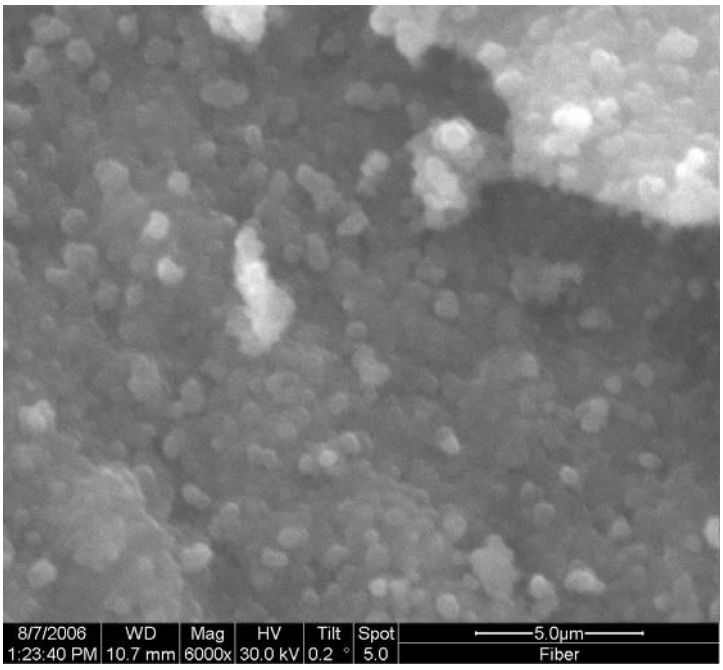

Figure 255. Specimen Virgin AS -6000x

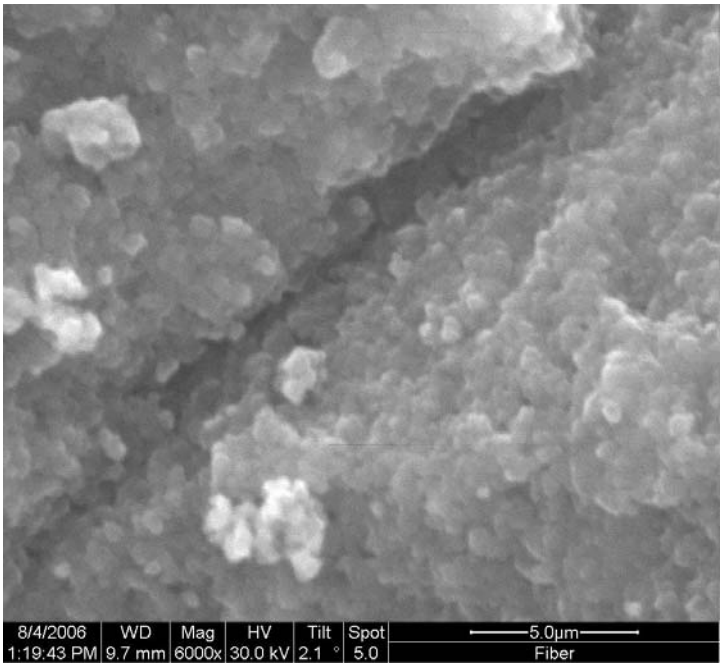

Figure 256. Specimen Virgin AS -6000x

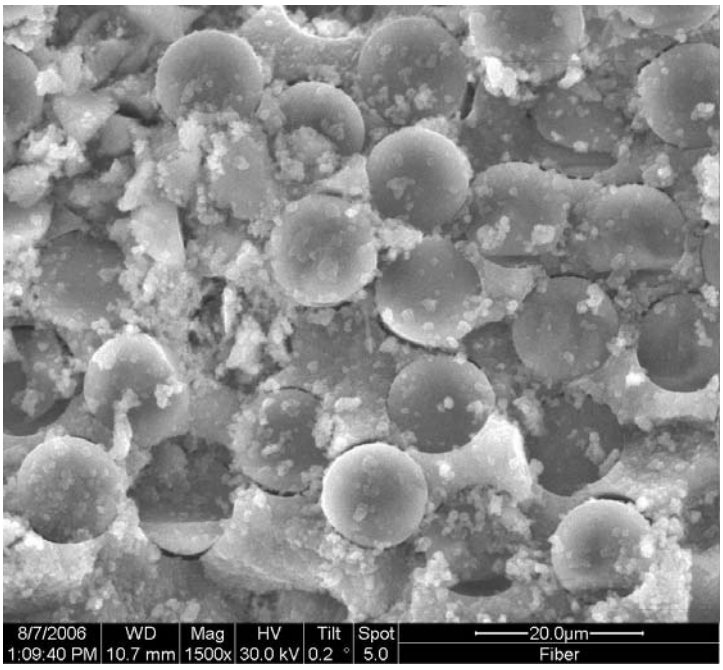

Figure 257. Specimen Virgin AS -1500x

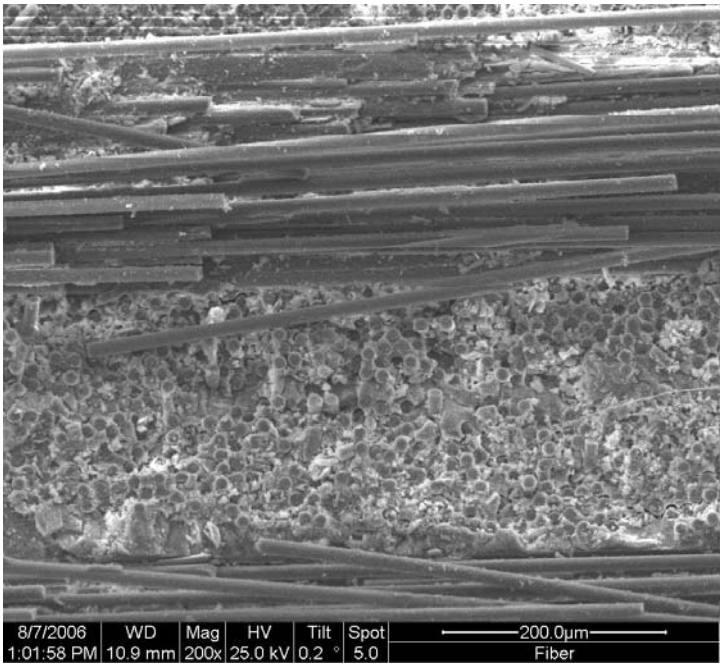

Figure 258. Specimen Virgin AS - 200x

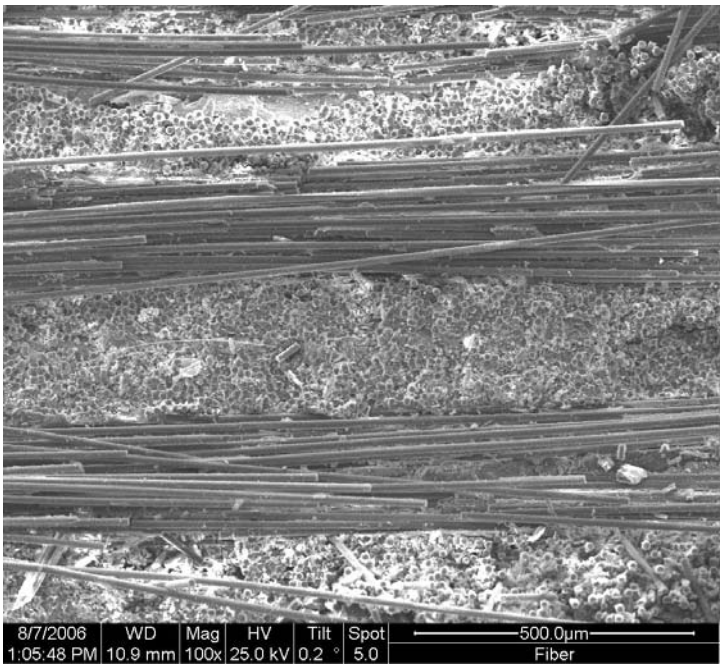

Figure 259. Specimen Virgin AS - 200x

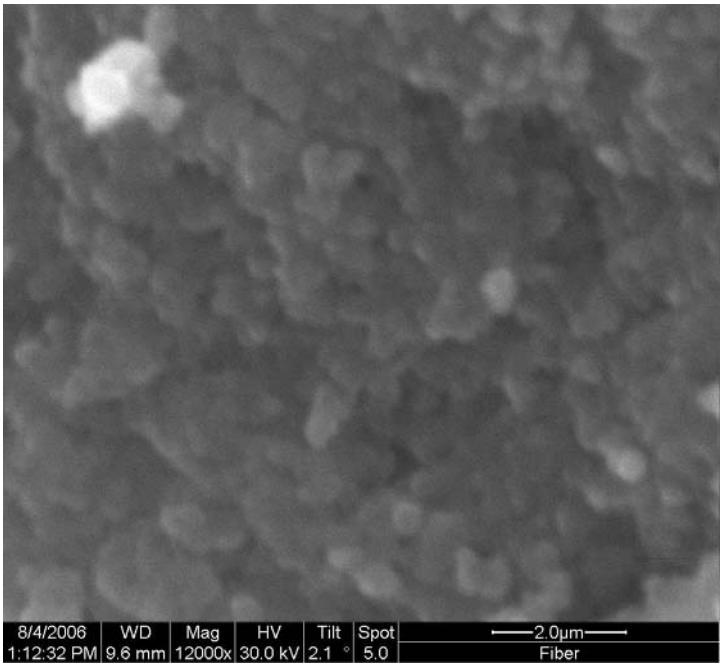

Figure 260. Specimen Virgin A - 12000x

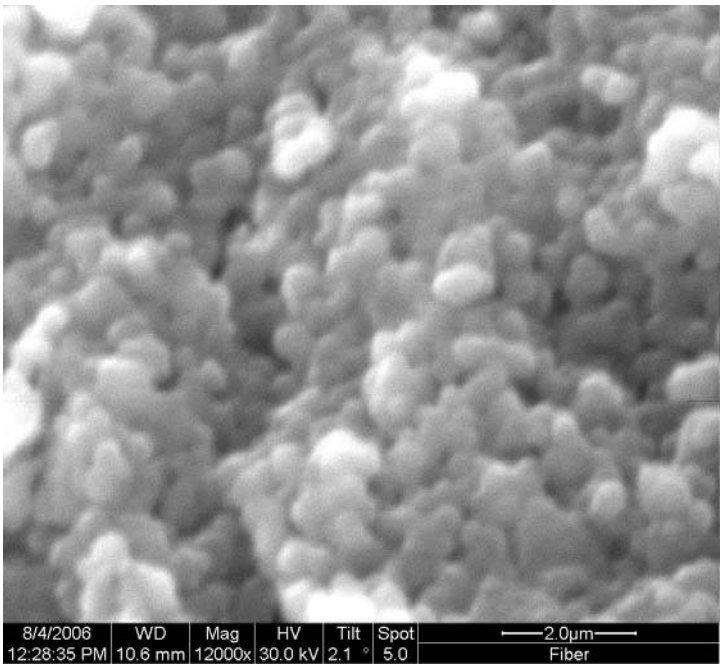

Figure 261. Specimen Virgin A - 12000x

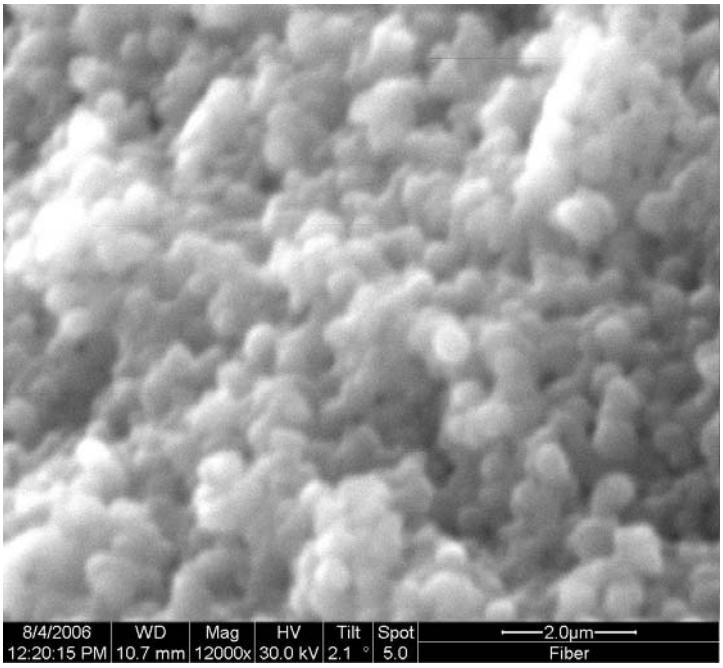

Figure 262. Specimen Virgin A - 12000x

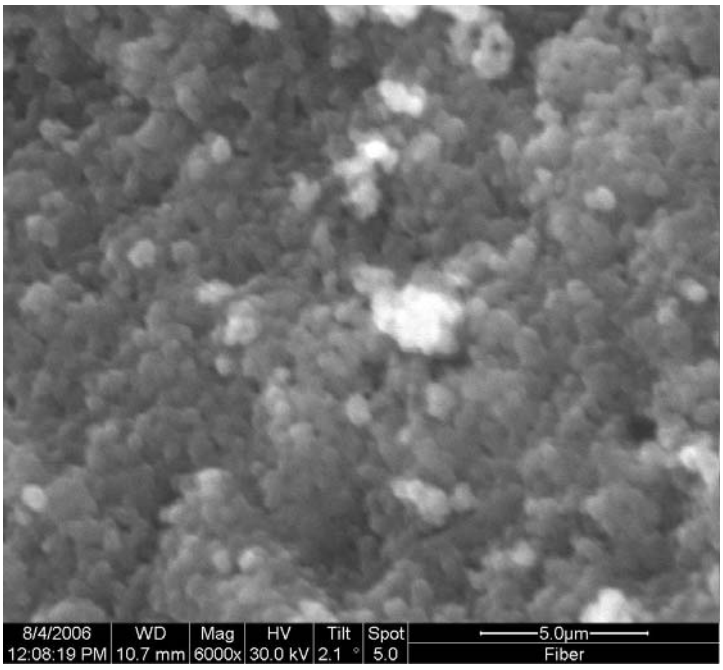

Figure 263. Specimen Virgin A - 6000x

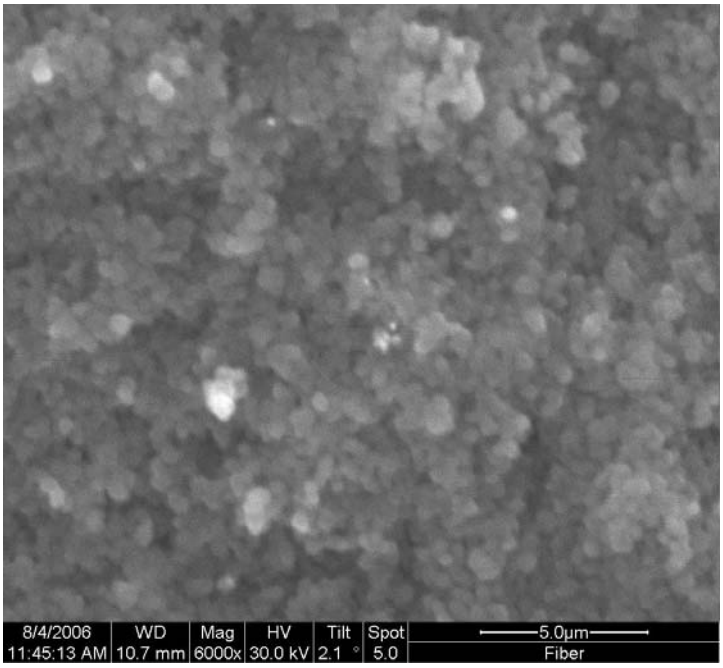

Figure 264. Specimen Virgin A - 6000x

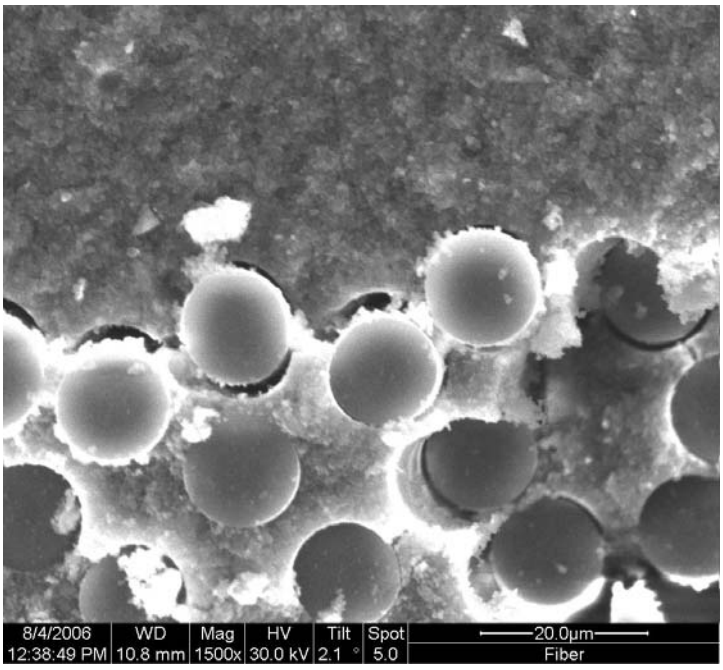

Figure 265. Specimen Virgin A - 1500x

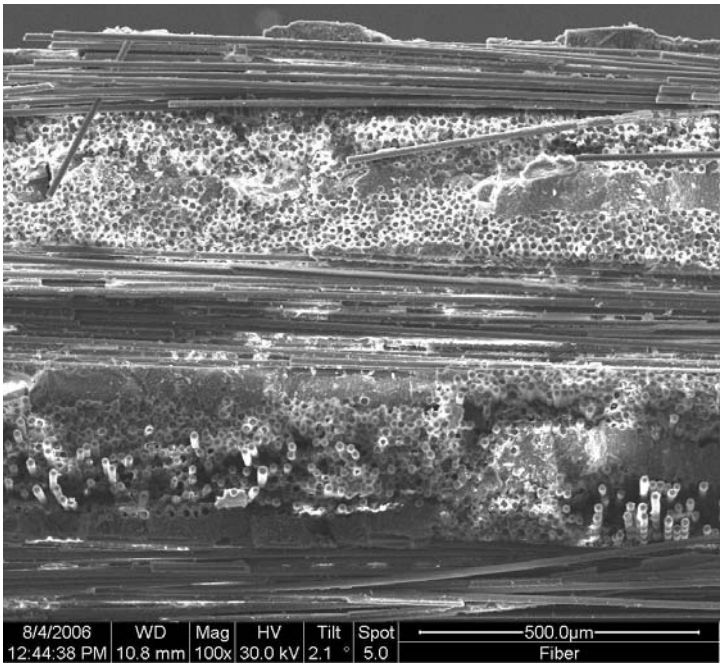

Figure 266. Specimen Virgin A - 100x

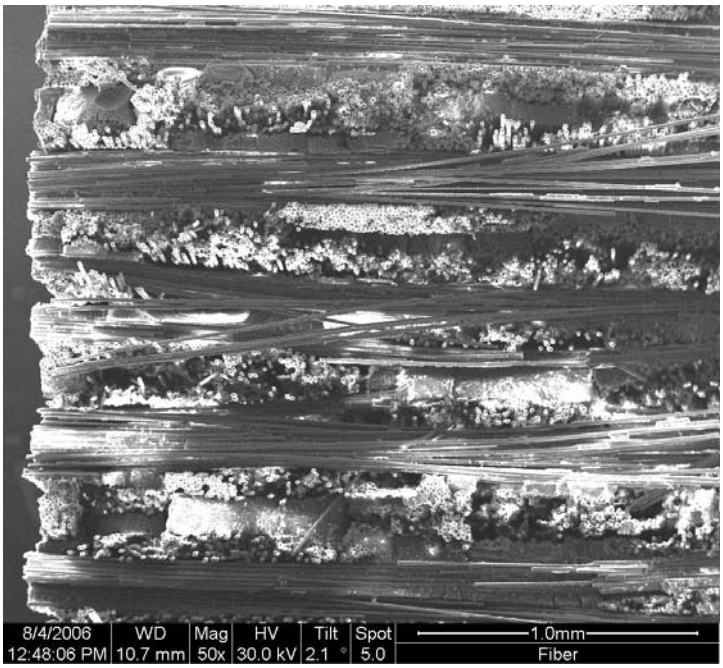

Figure 267. Specimen Virgin A - 50x

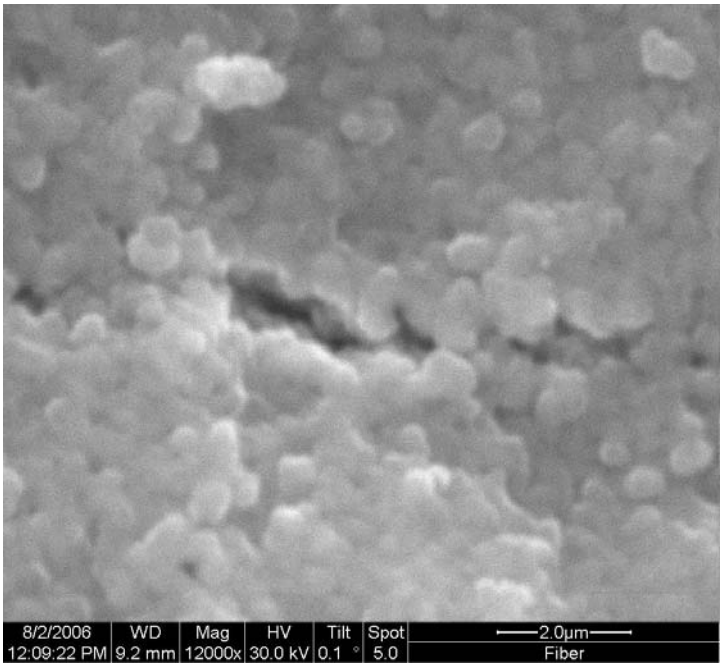

Figure 268. Specimen Steam Aged - 12000x

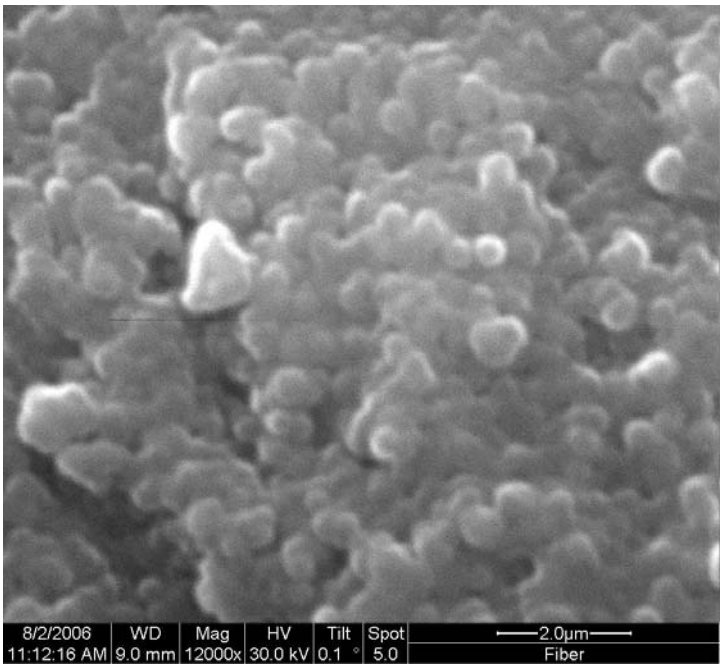

Figure 269. Specimen Steam Aged - 12000x

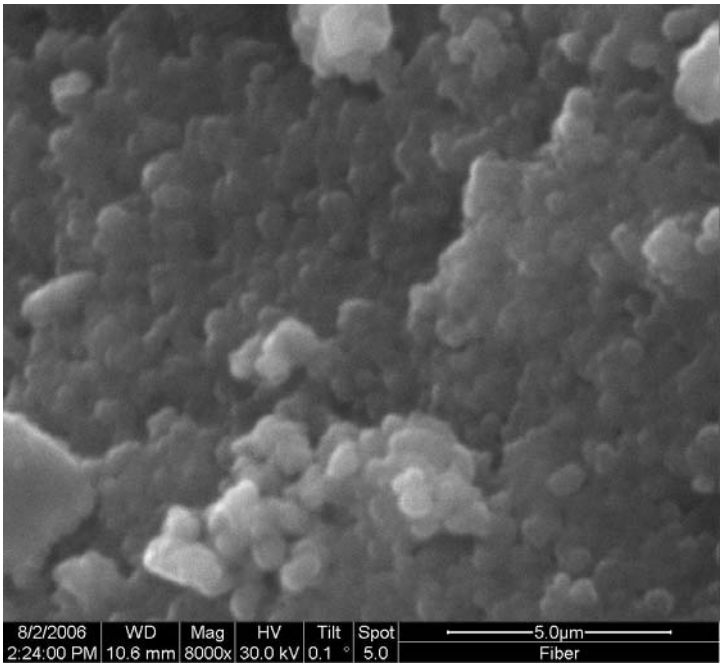

Figure 270. Specimen Steam Aged - 8000x

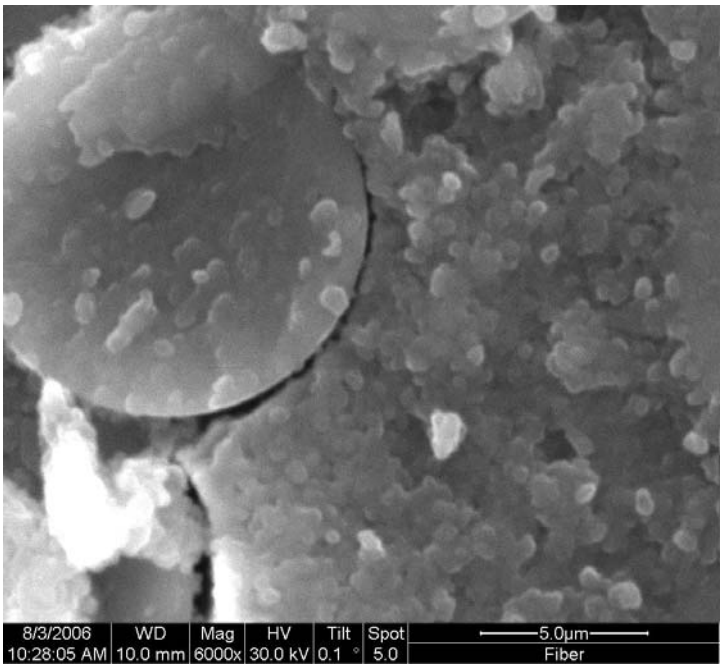

Figure 271. Specimen Steam Aged - 6000x

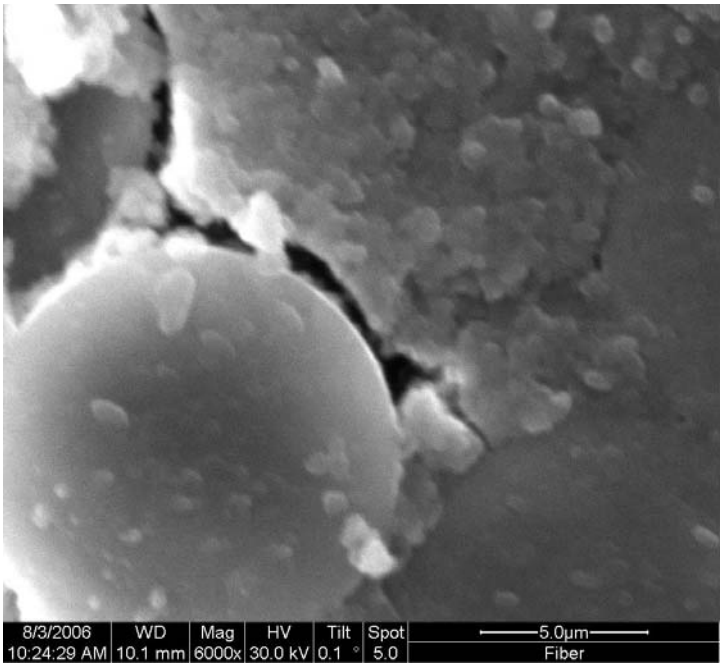

Figure 272. Specimen Steam Aged - 6000x

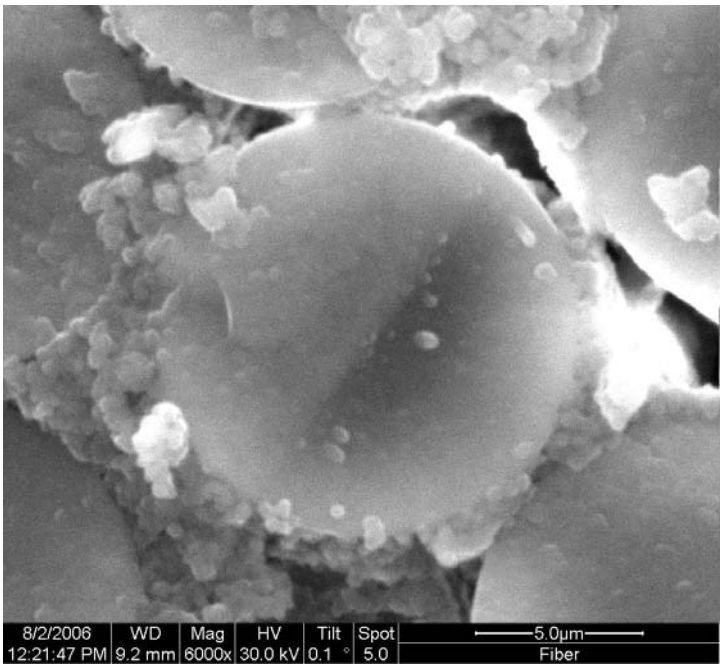

Figure 273. Specimen Steam Aged - 6000x

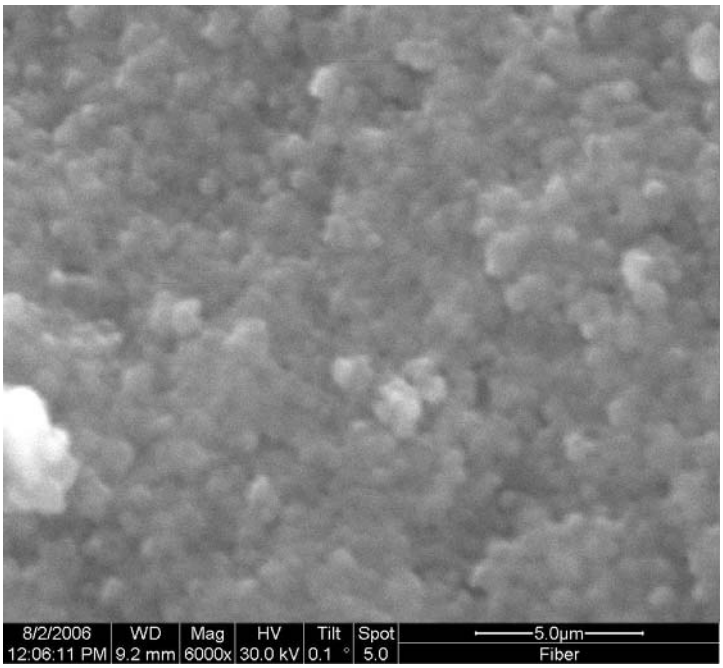

Figure 274. Specimen Steam Aged - 6000x

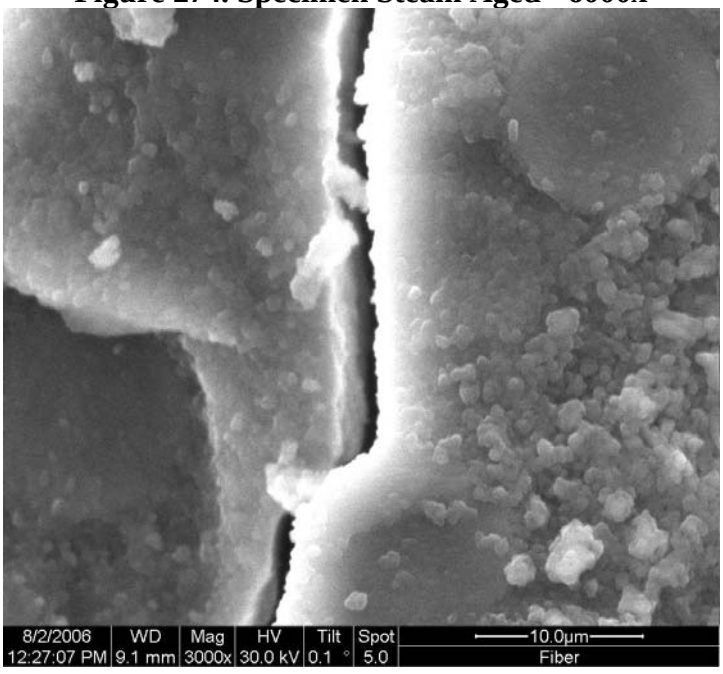

Figure 275. Specimen Steam Aged - 3000x

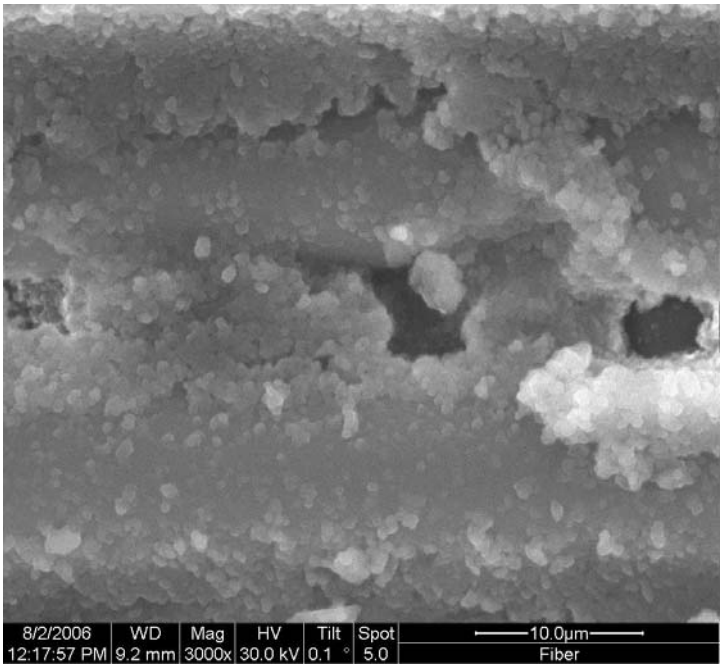

Figure 276. Specimen Steam Aged - 3000x

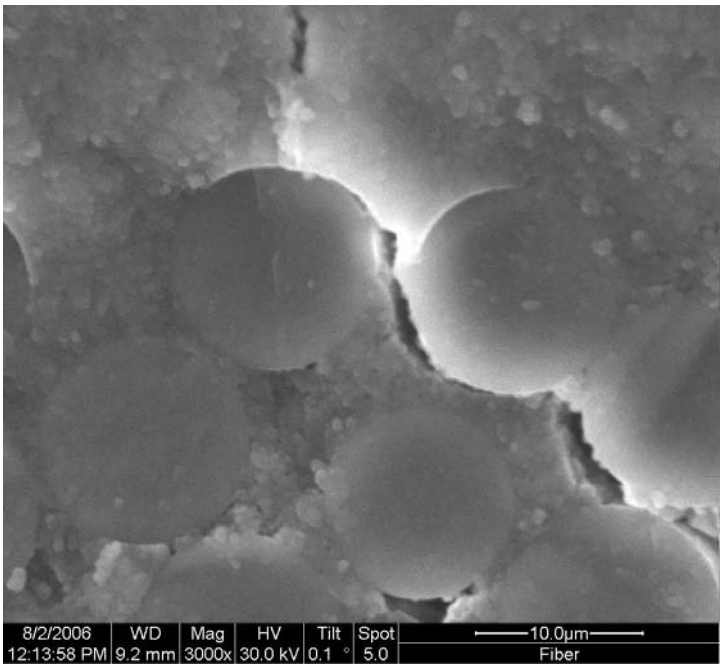

Figure 277. Specimen Steam Aged - 3000x

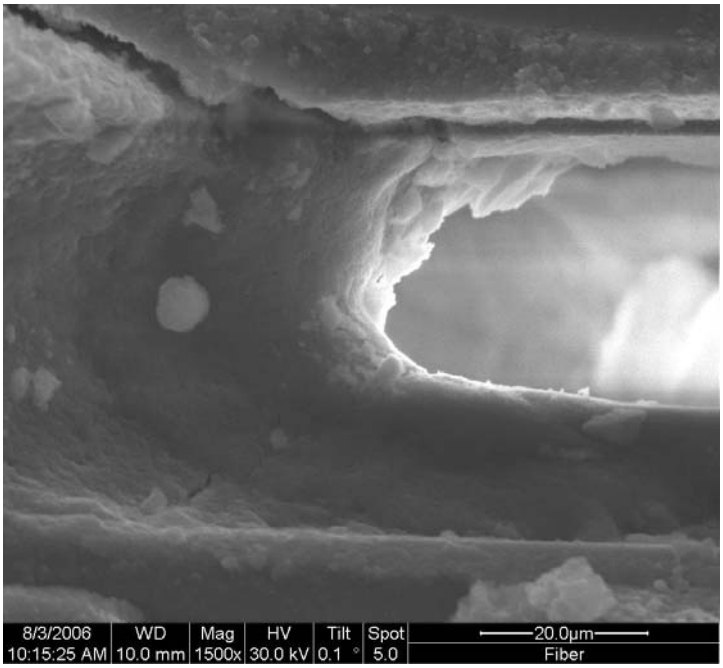

Figure 278. Specimen Steam Aged - 1500x

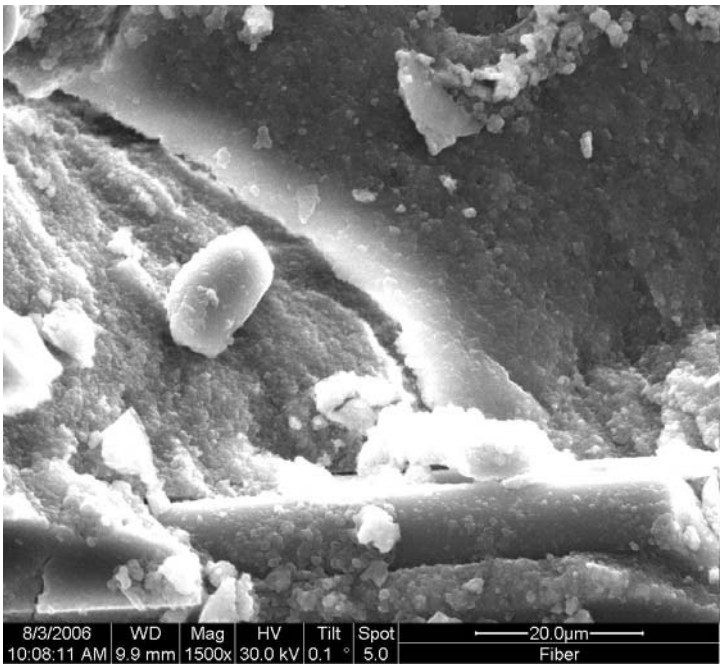

Figure 279. Specimen Steam Aged - 1500x

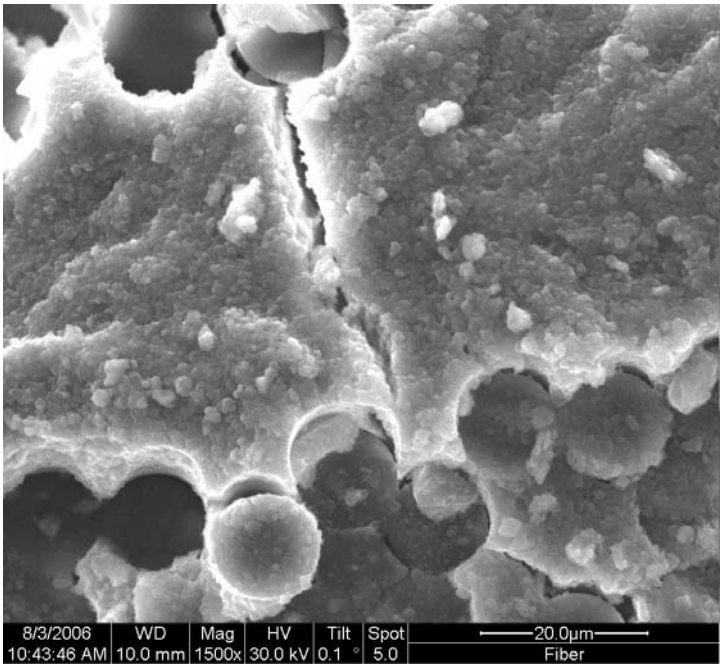

Figure 280. Specimen Steam Aged - 1500x

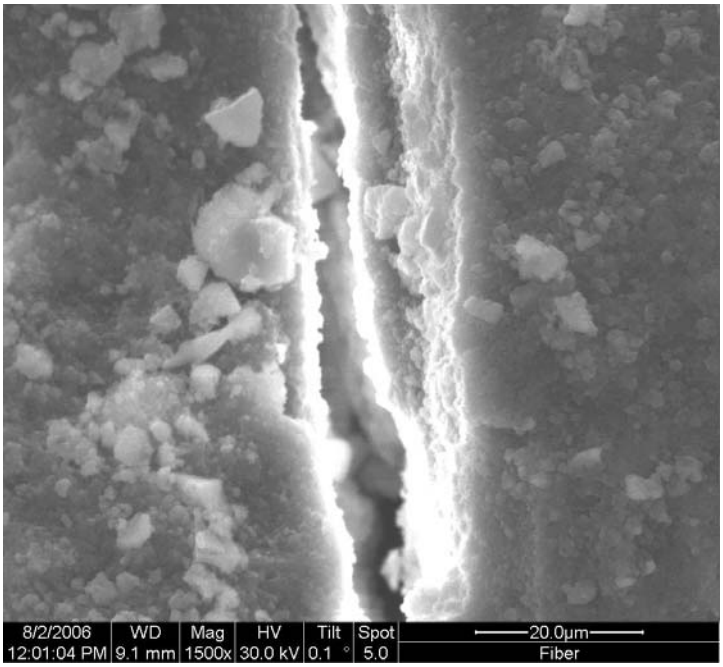

Figure 281. Specimen Steam Aged - 1500x

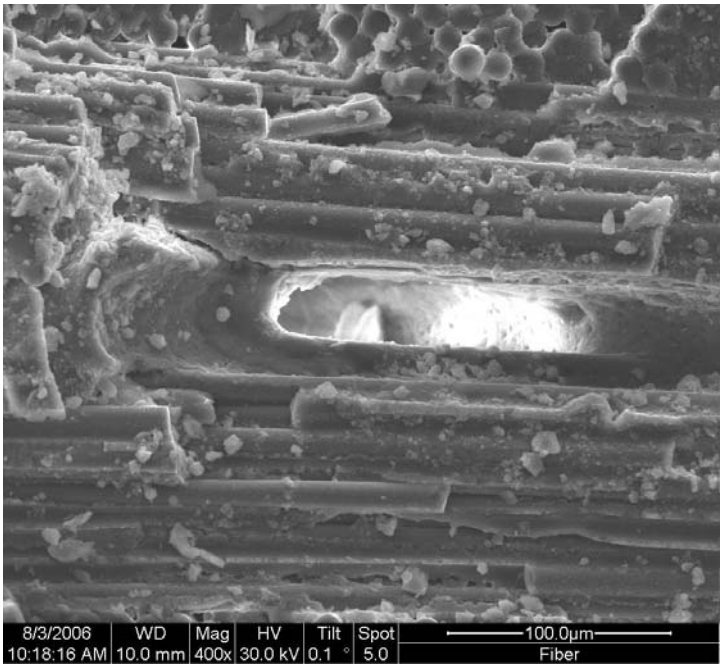

Figure 282. Specimen Steam Aged - 1500x

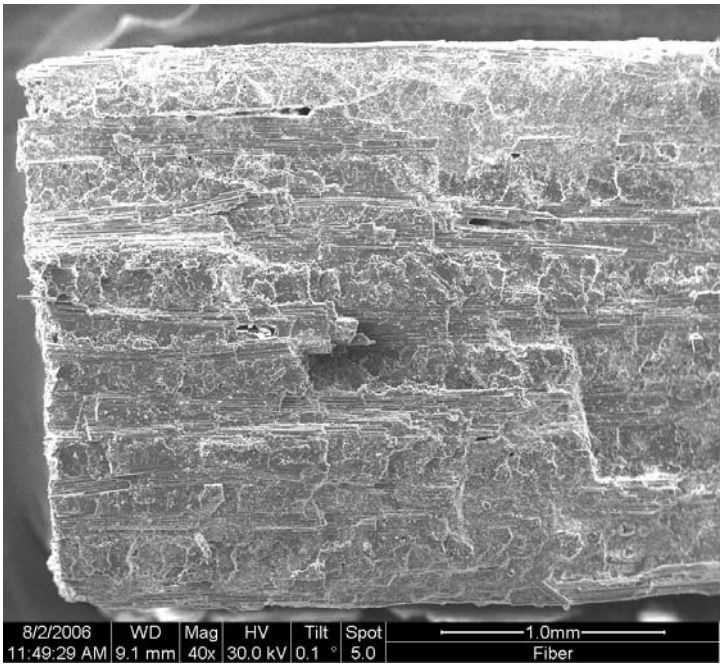

Figure 283. Specimen Steam Aged - 40x

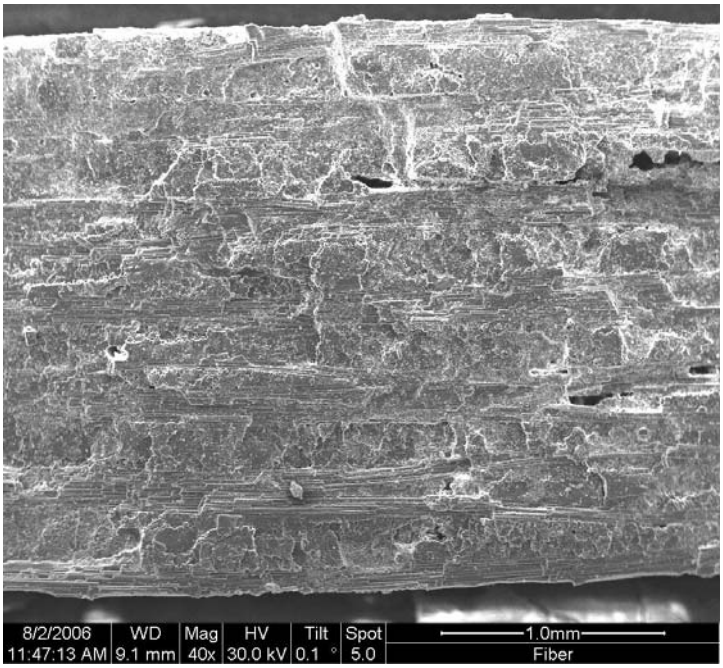

Figure 284. Specimen Steam Aged - 40x

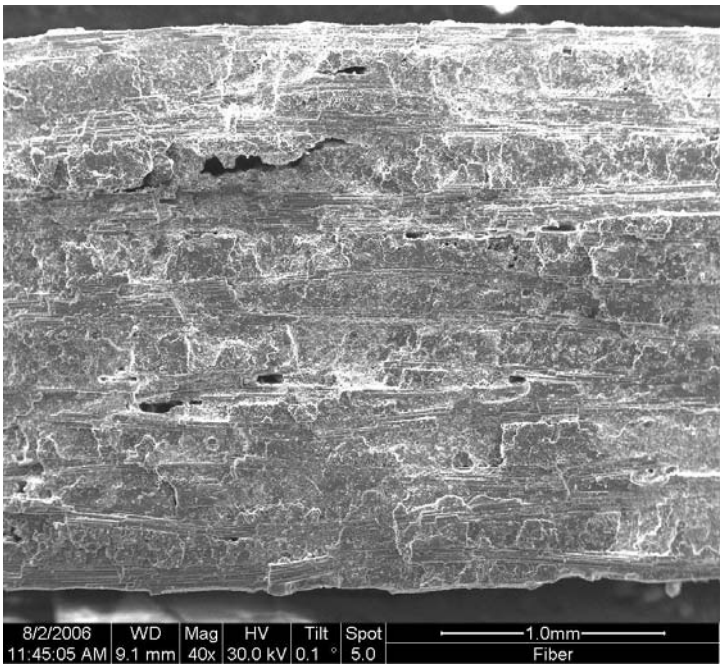

Figure 285. Specimen Steam Aged - 40x

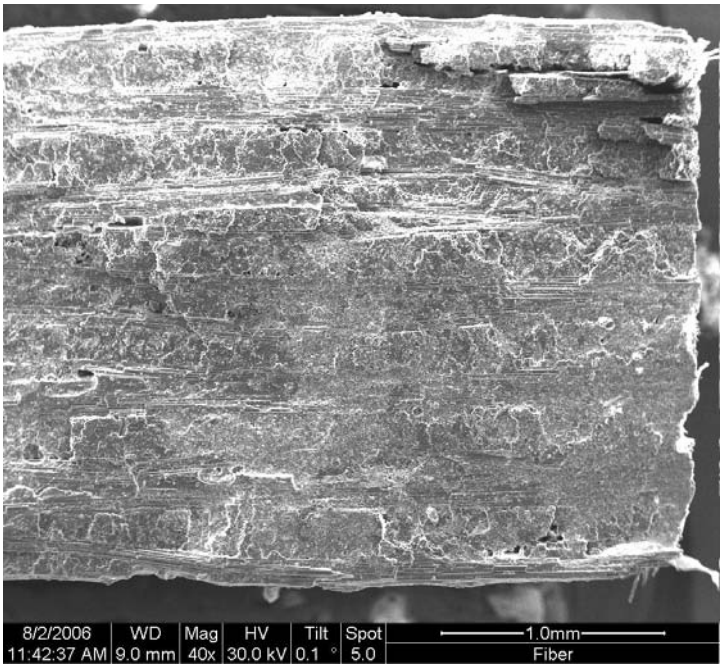

Figure 286. Specimen Steam Aged - 40x

Bibliography

1. 3M Company, *Nextel Textiles, Ceramic Fiber Products for Outerspace Applications* , Brochure

2. Antii M-L, Lara-Curzio E, Warren R. *Thermal Degradation of an Oxide Fibre (Nextel 720)/ Aluminosilicate Composite* Journal of the European Ceramic Society 24 565-578 2004

3. Casas L, J.M. Martinez-Esnaola, *Microstructural characterization of an alumina/mullite composite tested in creep*

4. Chawla, K. K. *Ceramic Matrix Composites.* London: Chapman and Hall, 1993

5. Daniel, I.M., Ishai, O., *Engineering Mechanics of Composite Materials*. New York: Oxford University Press, 1994

6. D.M. Wilson, *New High Temperature Oxide Fibers*, 3M Company, St Paul, MN

7. Eurofighter Tychoon Materials and production http://www.eurofighter.com/Typhoon/Production

8. Harlan, Lee B. *Creep-Rupture Behavior of an Oxide/Oxide Ceramic Matrix Composite at Elevated Temperatures in Air and Steam Environments.* MS thesis, AFIT/GA/ENY/05-M05. School of Engineering and Management, Air Force Institute of Technology (AU), Wright-Patterson AFB, OH, March 2005.

9. Gregory T Siegert *Effect of Environment on Creep Behavior of an Oxide/Oxide CFCC with +-45^0 Fiber Orientation*, MS thesis, AFIT/GAE/ENY/06-J15. School of Engineering and Management, Air Force Institute of Technology (AU), Wright-Patterson AFB, OH, June 2006.

10. Jurf, R.A and Butner,S.C., *Advantages in oxide-oxide CMC. In:Proc. Int. Gas Turbine and Aeroengine Congress and Exhibition*, Indianapolis,IN,1999.

11. J.J Haslam,., Berroth, K.E., Lange, F.F. "Processing and Properties of an all-oxide composite with a porous matrix," *Journal of the European Ceramic Society*, 20:607-618 (2000).

12. Mehrman John M. *Effects of Hold Times on Fatigue Behavior of Nextel 720/Alumina Ceramic Matrix Composite at 1200^{0}C in Air and in Steam Environment*. MS Thesis,AFIT/GA/ENY/06-M23. School of Engineering and Management, Air Force Institute of Technology(AU), Wright-Patterson AFB OH, March 2006.

Vita

Captain Pavlos Koutsoukos graduated from Hellenic Air Force Academy (HAFA), in Tatoi, Athens in July 1996 with a Bachelor of Science degree in Aeronautical Engineering.

His first assignment was at 116 FQ, Patras as a Quality Assurance Officer.

In September 2004 he entered the Graduate School of Engineering and Management, Air Force Institute of Technology (AFIT).

Upon graduation, he will be assigned to the Center of Research and Technology of Hellenic Air Force, Glyfada, Athens.

REPORT DOCUMENTATION PAGE			*Form Approved OMB No. 074-0188*
The public reporting burden for this collection of information is estimated to average 1 hour per response, including the time for reviewing instructions, searching existing data sources, gathering and maintaining the data needed, and completing and reviewing the collection of information. Send comments regarding this burden estimate or any other aspect of the collection of information, including suggestions for reducing this burden to Department of Defense, Washington Headquarters Services, Directorate for Information Operations and Reports (0704-0188), 1215 Jefferson Davis Highway, Suite 1204, Arlington, VA 22202-4302. Respondents should be aware that notwithstanding any other provision of law, no person shall be subject to an penalty for failing to comply with a collection of information if it does not display a currently valid OMB control number. **PLEASE DO NOT RETURN YOUR FORM TO THE ABOVE ADDRESS.**			
1. REPORT DATE *(DD-MM-YYYY)* 07 Sep 06	**2. REPORT TYPE** **Master's Thesis**		**3. DATES COVERED** *(From – To)* Jan 2006 – Mar 2006
4. TITLE AND SUBTITLE Effects of Environment on Creep Behavior of Two Oxide-Oxide Ceramic Matrix Composites at 1200°C			**5a. CONTRACT NUMBER** **5b. GRANT NUMBER** **5c. PROGRAM ELEMENT NUMBER**
6. AUTHOR(S) Pavlos Koutsoukos., Captain, HAF			**5d. PROJECT NUMBER** **5e. TASK NUMBER** **5f. WORK UNIT NUMBER**
7. PERFORMING ORGANIZATION NAMES(S) AND ADDRESS(S) Air Force Institute of Technology Graduate School of Engineering and Management (AFIT/EN) 2950 Hobson Way WPAFB OH 45433-7765			**8. PERFORMING ORGANIZATION REPORT NUMBER** AFIT/GAE/ENY/06-S05
9. SPONSORING/MONITORING AGENCY NAME(S) AND ADDRESS(ES) AFRL/PRTC Attn: Dr. Ruth Sikorski and Dr Joseph Zelina 1950 5th Street WPAFB OH 45433-7251 DSN: 785-7268			**10. SPONSOR/MONITOR'S ACRONYM(S)** **11. SPONSOR/MONITOR'S REPORT NUMBER(S)**
12. DISTRIBUTION/AVAILABILITY STATEMENT APPROVED FOR PUBLIC RELEASE; DISTRIBUTION UNLIMITED.			
13. SUPPLEMENTARY NOTES			
14. ABSTRACT Previous studies by the advisor and graduate students examined creep behavior of the Nextel720/Alumina CMC in air and in 100% steam environments at 1200 and 1330°C. Results showed that while this oxide/oxide system exhibits an exceptionally high fatigue limit at 1200°C it also experiences substantial strain accumulation under sustained loading conditions. Furthermore, these earlier investigations revealed a significant degrading effect of 100%-steam environment on material performance under both static and cyclic loadings. The present effort will investigate creep rupture behavior of Nextel720/Alumina composite in the inert gas environment. In addition, creep rupture behavior of Nextel720/Aluminosilicate CMC will be investigated in both inert gas and in 100% steam environments. Combined with existing data, results of this research will fully reveal effects of progressively more oxidizing environment on creep resistance of these CMCs. In addition, degradation of Nextel720 fibers under load in oxidizing environments will be assessed. The study followed a systematic plan. Baseline tensile tests were performed to verify the at-temperature basic properties and to guide selection of the creep stress levels. Creep-rupture tests were carried out at different stress levels at 1200°C. In order to examine combined effects of temperature and exposure to oxidizing environment on the creep response, creep-rupture tests were performed in the inert gas and in 100% steam environments. For selected creep stress levels, creep tests in laboratory air were performed as well. As a result of this effort creep-rupture curves, as well as families of creep curves were established. Degradation of creep resistance due to increasing moisture exposure were assessed. Composite microstructure, as well as damage and failure mechanisms were examined. The results will establish the boundaries of mechanical behavior and determine the suitability as well as limitations of these materials for use in aerospace applications. The test results will contribute to the basis for future material development and processing.			
15. SUBJECT TERMS Ceramic Matrix Composite (CMC), Nextel ™ 720 fiber, Alumina, Aluminosilicate, Oxide-Oxide, Tension, Creep			

16. SECURITY CLASSIFICATION OF:			**17. LIMITATION OF ABSTRACT**	**18. NUMBER OF PAGES**	**19a. NAME OF RESPONSIBLE PERSON**
REPORT **U**	**ABSTRACT** **U**	**c. THIS PAGE** **U**	**UU**	201	Dr. Marina Ruggles-Wrenn **19b. TELEPHONE NUMBER** *(Include area code)* (937) 255-3636, ext 4641; e-mail: Marina.Ruggles-Wrenn@afit.edu

Standard Form 298 (Rev: 8-98)
Prescribed by ANSI Std. Z39-18